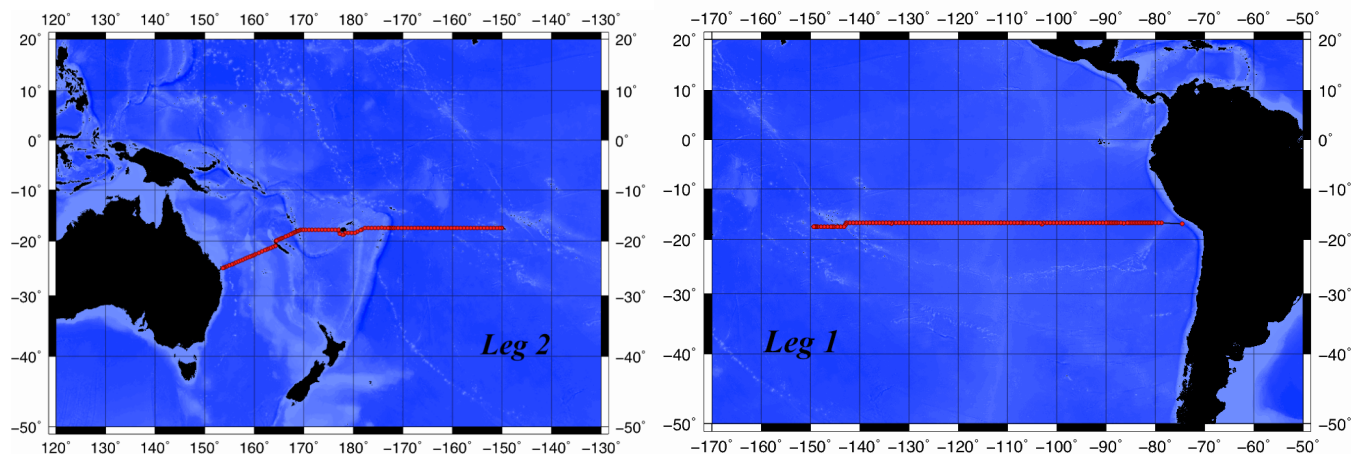


Cruise Report: P21

(Updated NOV 2011)



HIGHLIGHTS

CRUISE SUMMARY INFORMATION

WOCE Section Designation	P21 leg 1	P21 leg 2
Expedition designation (ExpoCodes)	49NZ20090410	49NZ20090521
Chief Scientists	Akihiko Murata/JAMSTEC	Hiroshi Uchida/JAMSTEC
Dates	2009 APR 10 - 2009 MAY 19	2009 MAY 21 - 2009 JUN 19
Ship	<i>R/V Mirai</i>	<i>R/V Mirai</i>
Ports of call	Valparaiso, Chile - Papeete, Tahiti	Papeete, Tahiti - Brisbane, Australia
Geographic Boundaries	153° 44.52'E	15° 29.52'S 75° 09.86'W 24° 59.81'S
Stations	140	117
Floats and drifters deployed	5 Argo floats	0
Moorings deployed or recovered	0	0

Recent Contact Information:

Akihiko Murata
 akihiko.murata@jamstec.go.jp

Hiroshi Uchida
 huchida@jamstec.go.jp

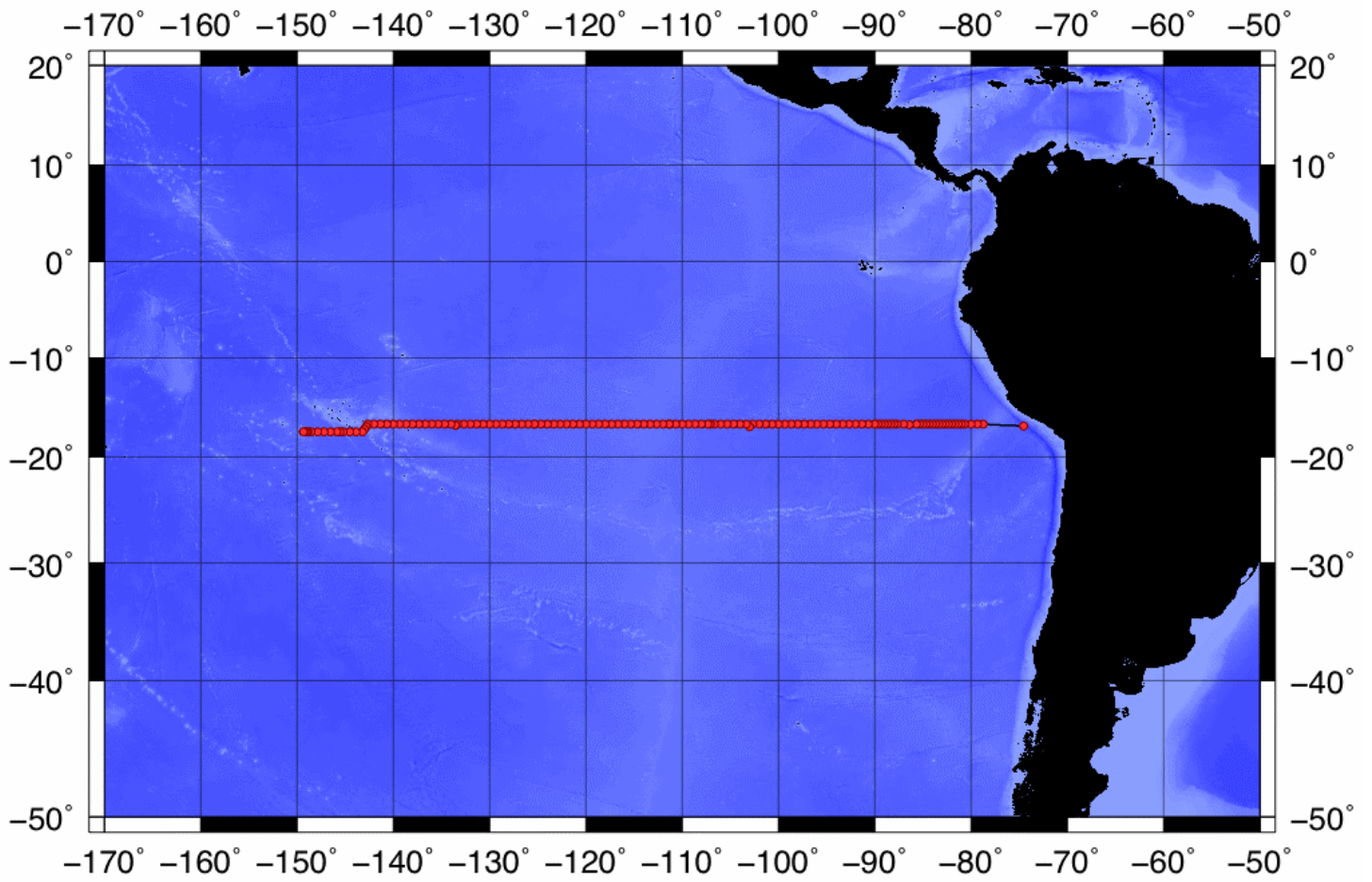
Ocean Climate Change Research Program
 Research Institute for Global Change (RIGC)
 Japan Agency for Marine-Earth Science and Technology (JAMSTEC)
 2-15 Natsushima, Yokosuka, Kanagawa, Japan 237-0061
 Fax: +81-46-867-9455

LINKS TO SELECT TOPICS

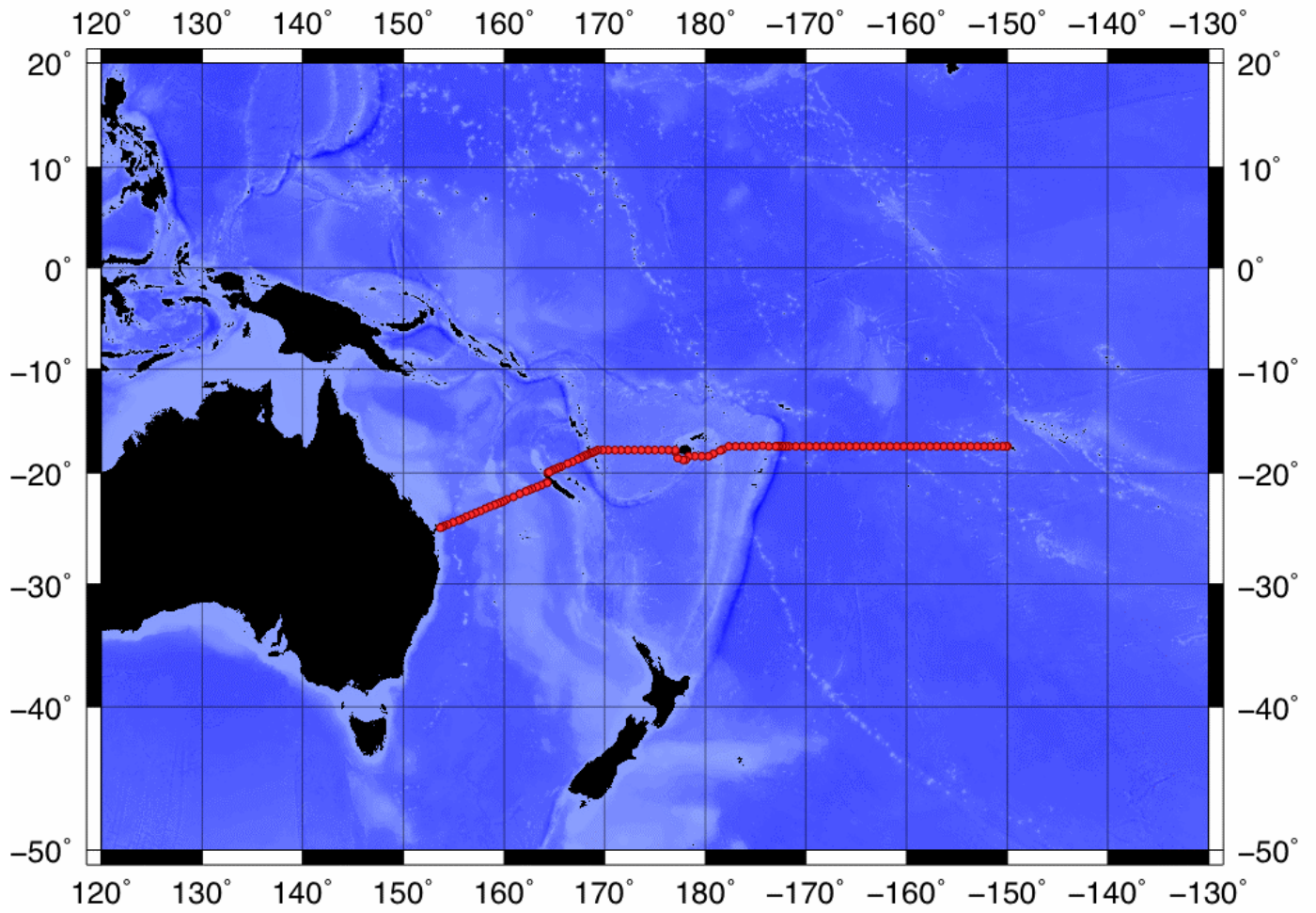
Shaded sections are not relevant to this cruise or were not available when this report was compiled.

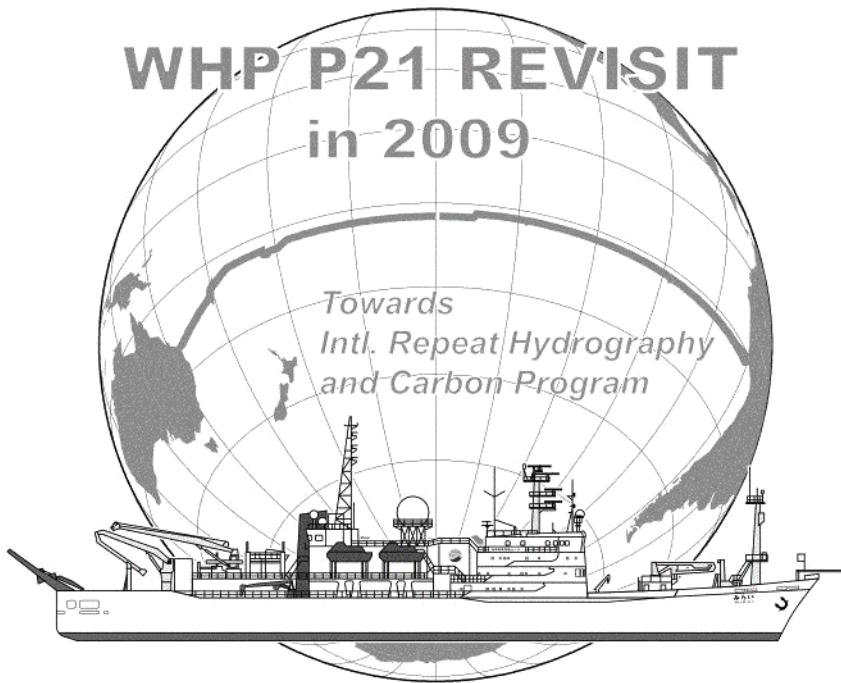
Cruise Summary Information	Hydrographic Measurements
Description of Scientific Program	CTD Data:
Geographic Boundaries	Acquisition
Cruise Track (Figure): PI CCHDO	Processing
Description of Stations	Calibration
Description of Parameters Sampled	Temperature Pressure
Bottle Depth Distributions (Figure)	Salinities Oxygens
Floats and Drifters Deployed	Bottle Data
Moorings Deployed or Recovered	Salinity
	Oxygen
Principal Investigators	Nutrients
Cruise Participants	Carbon System Parameters
	CFCs
Problems and Goals Not Achieved	Helium / Tritium
Other Incidents of Note	Radiocarbon
Underway Data Information	References
Navigation Bathymetry	
Acoustic Doppler Current Profiler (ADCP)	
Thermosalinograph	
XBT and/or XCTD	
Meteorological Observations	Acknowledgments
Atmospheric Chemistry Data	
Data Processing Notes	

P21 • Leg 1 • Murata/JAMSTEC • R/V *Mirai* • 2009



P21 • Leg 2 • Uchida/JAMSTEC • *R/V Mirai* • 2009





WHP P21 REVISIT DATA BOOK

*Edited by Hiroshi Uchida (JAMSTEC)
Akihiko Murata (JAMSTEC)
Toshimasa Doi (JAMSTEC)*

WHP P21 REVISIT DATA BOOK

March 25, 2011 Published

Edited by Hiroshi Uchida (JAMSTEC), Akihiko Murata (JAMSTEC) and Toshimasa Doi (JAMSTEC)

Published by © JAMSTEC, Yokosuka, Kanagawa, 2011
Japan Agency for Marine-Earth Science and Technology
2-15 Natsushima, Yokosuka, Kanagawa. 237-0061, Japan
Phone +81-46-867-9474, Fax +81-46-867-9455

Printed by Aiwa Enterprise, Ltd.

3-22-4 Takanawa, Minato-ku, Tokyo 108-0074, Japan

Contents

Preface	viii
<i>M Fukasawa (JAMSTEC)</i>	
Documents	
1. Cruise Narrative	1
<i>A. Murata, H. Uchida and K Sasaki (JAMSTEC)</i>	
2. Underway Measurements	
2.1 Navigation and Bathymetry	10
<i>S. Okumura (GODI) et al., T Matsumoto (Univ. Ryukyu) et al.</i>	
2.2 Surface Meteorological Observation	17
<i>K Yoneyama (JAMSTEC) et al.</i>	
2.3 Thermo-Salinograph and Related Measurements	23
<i>Y Kumamoto (JAMSTEC) et al.</i>	
2.4 Underway pCO ₂	27
<i>A. Murata (JAMSTEC) et al.</i>	
2.5 Acoustic Doppler Current Profiler	29
<i>S. Kouketsu (JAMSTEC) et al.</i>	
2.6 XCTD	30
<i>H. Uchida (JAMSTEC) et al.</i>	
3. Hydrographic Measurement Techniques and Calibrations	
3.1 CTDO ₂ Measurements	33
<i>H. Uchida (JAMSTEC) et al.</i>	
3.2 Bottle Salinity	52
<i>T Kawano (JAMSTEC) et al.</i>	
3.3 Oxygen	55
<i>Y Kumamoto (JAMSTEC) et al.</i>	
3.4 Nutrients	60
<i>M Aoyama (MRI/JMA) et al.</i>	
3.5 Chlorofluorocarbons (CFCs)	75
<i>K Sasaki (JAMSTEC) et al.</i>	
3.6 Dissolved Inorganic Carbon (C _T)	77
<i>A. Murata (JAMSTEC) et al.</i>	
3.7 Total Alkalinity (A _T) ..	80
<i>A. Murata (JAMSTEC) et al.</i>	
3.8 pH (pH _T)	82
<i>A. Murata (JAMSTEC) et al.</i>	
3.9 LADCP	84
<i>S. Kouketsu (JAMSTEC) et al.</i>	

Figures

<i>Figure captions</i>	89
<i>Station locations</i>	91
<i>Bathymetry</i>	91
<i>Surface wind</i>	96
<i>Sea surface temperature</i>	97
<i>Sea surface salinity</i>	98
ΔpCO_2	99
<i>Surface current</i>	100

Cross-sections

<i>Potential temperature</i>	101
<i>CTD salinity</i>	102
<i>Absolute salinity</i>	103
<i>Density (σ_0)</i>	104
<i>Density (σ_4)</i>	105
<i>Density (γ^n)</i>	106
<i>CTD oxygen</i>	107
<i>Bottle sampled oxygen</i>	108
<i>Silicate</i>	109
<i>Nitrate</i>	110
<i>Nitrite</i>	110
<i>Phosphate</i>	111
<i>Dissolved inorganic carbon (C_T)</i>	112
<i>Total alkalinity (A_T)</i>	113
<i>pH (pH_T)</i>	114
<i>CFC-11</i>	115
<i>CFC-12</i>	116
<i>CFC -113</i>	117
<i>Velocity</i>	118

Difference between WOCE and the revisit

<i>Potential temperature</i>	119
<i>Salinity</i>	120
<i>CTD oxygen</i>	121

CCHDO Data Processing Notes	121
------------------------------------	-----

Preface

P21 was the WOCE one time survey line located slightly in the south of the boundary between two gyre systems of the Equatorial Counter Current and the South Equatorial Current. In 1994, WOCE hydrographic observations were carried out by United States along the line. After this cruise, P21 was not revisited though there is a great possibility that repeat observations along this line could detect decadal or long-time scale variability of low latitudinal gyre system.

In 2008, the research system of JAMSTEC was re-organized. As the result, Institute of Observational Research for Global Change (IORGC) and Frontier Research Center for Global Change (FRCGC) were merged to form a new research organization of Research Institute for Global Change (RIGC). The General Ocean Circulation Research Program of former IORGC, which had been the main driver of CLIVAR Carbon Repeat Hydrography (CCRH) in Japan, was also developed into the Ocean Climate Change Research Program of new RIGC including Argo Group of former IORGC and Ocean assimilation Group of former FRCGC together.

P21 revisit cruise reported in this data book was the first CCRH cruise carried out under the new program of the Ocean Climate Change Research Program of RIGC. Also, it may be better to note here that this revisit-cruise was planned and proposed by bio-geochemical oceanographer in the program. One of distinct scientific outcomes from bio-geochemical researchers in the program was the discovery of the considerable acceleration in the CO₂ up-taking ratio and rapid increase in CO₂ accumulation of the South Pacific during these decades. P01, P02, P03, P10, P06 and P14 data were analyzed comprehensively but the Equator-ward extent of the CO₂ related issues mentioned above were left to be examined. So, this is the biggest reason why P21 was selected to be revisited in spite of the fact that P21 was not included in the recommended repeat line in the strategy of the Global Ocean Ship-Based Hydrographic Investigation Program (GOSHIP).

After OceanObs09 in Venice, quite a few discussions were held on the sustainability of ocean observation and many proposals were published. GOSHIP strategy, which had been discussed since 2008 and was adopted in 2010 finally, is one of answers to those discussions and proposals. The basic and important concept of the strategy is to maintain some of WOCE hydrographic lines by repeat observations along them as a strong tool of ocean monitoring to detect decadal changes in the global oceanic conditions especially in the Meridional Overturn Circulation System. We, ocean climate researchers in JAMSTEC, have carried out revisit cruises along eight WOCE one-time lines so far. However, as long as our activity concerns, P01 is the only line where we repeated observations twice. I strongly hope and believe that we will be able to have repeat observation along all of eight lines in near future to make the strategy of GO-SHIP real and effective.

On the day of Japan Northern Territory*

Masao Fukasawa
Research Director of RIGC/JAMSTEC

* On 7th February 1855, The Japan-Russia Treaty of Peace and Amity was ratified in which Etorofu, Kunashiri, Sikotan and Habomai islands are defined as Japan territory.

1 Cruise Narrative

1.1 Highlight

GHPO Section Designation: P21

Cruise code: MR09-01

Expedition Designation: 49NZ20090410
49NZ20090521

Chief Scientists and Affiliation:

Leg.1: *Akihiko Murata*
akihiko.murata@jamstec.go.jp

Leg.2: *Hiroshi Uchida*
huchida@jamstec.go.jp

Leg.3: *Kenichi Sasaki*
ksasaki@jamstec.go.jp
Ocean Climate Change Research Program
Research Institute for Global Change (RIGC)
Japan Agency for Marine-Earth Science and Technology (JAMSTEC)
2-15 Natsushima, Yokosuka, Kanagawa, Japan 237-0061
Fax: +81-46-867-9455

Ocean Climate Change Research Program
Research Institute for Global Change (RIGC)
Japan Agency for Marine-Earth Science and Technology (JAMSTEC)
2-15 Natsushima, Yokosuka, Kanagawa, Japan 237-0061
Fax: +81-46-867-9455

Ship: R/V Mirai

Ports of Call: Leg 1: Valparaiso, Chile - Papeete, Tahiti
Leg 2a: Papeete, Tahiti - Papeete, Tahiti
Leg 2b: Papeete, Tahiti - Brisbane, Australia
Leg 3: Brisbane, Australia - Moji, Japan

Cruise Dates: Leg 1: April 10, 2009 - May 19, 2009
Leg 2a: May 21, 2009 - May 24, 2009
Leg 2b: May 25, 2009 - June 19, 2009
Leg 3: June 20, 2009 - July 3, 2009

Number of Stations: 257 stations for CTD/Carousel Water Sampler
(Leg 1: 140, Leg 2a: 8, Leg 2b: 109)

Geographic Boundaries (for hydrographic stations): 24° 59.81' S - 15° 29.52' S
153° 44.52' E - 75° 09.86' W

Floats and Drifters Deployed: 5 Argo floats

Mooring Deployed or Recovered Mooring: None

1.2 Cruise Summary

(1) Station occupied

A total of 257 stations was occupied using a Sea-Bird Electronics 36 position carousel equipped with 12 liter Niskin-X water sample bottles, a SBE 9/11plus equipped with SBE35 deep ocean standards thermometer, SBE43 oxygen sensor, AANDERAA Optode 3830 and 4330F oxygen sensors, JFE Alec RINKO oxygen sensor, Seapoint Sensors fluorometer, WET labs C-Star transmissometer, Benthos altimeter, and RDI ADCP. XCTDs were deployed at 23 stations. XMPs (eXpendable Microstructure Profiler) were also deployed at 3 stations. Cruise track and station location are shown in [Figure 1.2.1](#).

(2) Sampling and measurements

Water samples were analyzed for salinity, oxygen, nutrients, CFC-11, -12, -113, total alkalinity, DIC, and pH. The sampling layers are coordinated as so-called staggered mesh. Samples for ^{14}C , ^{13}C , methane, nitrous oxide, carbonyl sulfide, chlorophyll a, PON, POC, ^{15}N -nitrate, ammonia, and a biological study were also collected at the selected stations. The bottle depth diagram is shown in [Figure 1.2.2](#). Underway pCO_2 , temperature, salinity, oxygen, surface current, bathymetry, and meteorological measurements were conducted along the cruise track.

(3) Floats deployment

Five ARGO floats were launched along the cruise track. The launched positions of the ARGO floats are listed in Table 1.2.1.

Table 1.2.1: Launched positions of the ARGO floats.

Float S/N	ARGOS ID	Date and time of reset (UTC)	Date and time of launch (UTC)	Location of launch	CTD station no.
4099	86536	2009/05/01 18:45	2009/05/01 20:03	16-45.21 S 105-20.41 W	P21-080
4042	86510	2009/05/03 08:16	2009/05/03 09:15	16-44.51 S 107-19.90 W	P21-087
4101	86537	2009/05/04 05:54	2009/05/04 06:35	16-45.05 S 109-59.34 W	P21-095
4043	86511	2009/05/05 04:05	2009/05/05 04:52	16-44.99 S 112-41.19 W	P21-099
4102	86538	2009/05/05 18:37	2009/05/05 19:37	16-45.33 S 114-40.55 W	P21-102

1.3 List of Principal Investigators and Persons in Charge on the Ship

The principal investigator (PI) and the person in charge responsible for major parameters measured on the cruise are listed in Table 1.3.1.

Table 1.3.1: List of principal investigator and person in charge on the ship.

Item	Principal Investigator	Person in Charge on the Ship
<i>Underway</i>		
ADCP	Shinya Kouketsu (JAMSTEC) skouketsu@jamstec.go.jp	Shinya Okumura (GODI) (leg 1) Satoshi Okumura (GODI) (leg 2) Souichiro Sueyoshi (GODI) (leg 3)
Bathymetry	Takeshi Matsumoto (Univ. of Ryukyus) tak@sci.u-ryukyu.ac.jp Masao Nakanishi (Chiba Univ.) nakanisi@earth.s.chiba-u.ac.jp	Shinya Okumura (GODI) (leg 1) Satoshi Okumura (GODI) (leg 2) Souichiro Sueyoshi (GODI) (leg 3)
Meteorology	Kunio Yoneyama (JAMSTEC) yoneyamak@jamstec.go.jp	Shinya Okumura (GODI) (leg 1) Satoshi Okumura (GODI) (leg 2) Souichiro Sueyoshi (GODI) (leg 3)
T-S	Yuichiro Kumamoto (JAMSTEC) kumamoto@jamtec.go.jp	Miyo Ikeda (MWJ) (leg 1, 2) Fuyuki Shibata (MWJ) (leg 3)
pCO ₂	Akihiko Murata (JAMSTEC) akihiko.murata@jamstec.go.jp	Minoru Kamata (MWJ) (leg 1, 2) Yasuhiro Arie (MWJ) (leg 3)
<i>Hydrography</i>		
CTD/O ₂	Hiroshi Uchida (JAMSTEC) huchida@jamstec.go.jp	Kenichi Katayama (MWJ) (leg 1) Tomoyuki Takamori (MWJ) (leg 2)
XCTD	Hiroshi Uchida (JAMSTEC) huchida@jamstec.go.jp	Shinya Okumura (GODI) (leg 1) Satoshi Okumura (GODI) (leg 2)
LADCP	Shinya Kouketsu (JAMSTEC) skouketsu@jamstec.go.jp	Shinya Kouketsu (JAMSTEC) (leg 1) Katsuro Katsumata (JAMSTEC) (leg 2)
Salinity	Takeshi Kawano (JAMSTEC) kawanot@jamstec.go.jp	Tatsuya Tanaka (MWJ) (leg 1) Fujio Kobayashi (MWJ) (leg 2)
Oxygen	Yuichiro Kumamoto (JAMSTEC) kumamoto@jamstec.go.jp	Fuyuki Shibata (MWJ) (leg 1) Miyo Ikeda (MWJ) (leg 2)
Nutrients	Michio Aoyama (MRI) maoyama@mri-jma.go.jp	Ayumi Takeuchi (MWJ) (leg 1) Junji Matsushita (MWJ) (leg 2)
DIC	Akihiko Murata (JAMSTEC) akihiko.murata@jamstec.go.jp	Minoru Kamata (MWJ)
Alkalinity	Akihiko Murata (JAMSTEC) akihiko.murata@jamstec.go.jp	Tomonori Watai (MWJ) (leg 1) Yoshiko Ishikawa (MWJ) (leg 2)
pH	Akihiko Murata (JAMSTEC) akihiko.murata@jamstec.go.jp	Tomonori Watai (MWJ) (leg 1) Yoshiko Ishikawa (MWJ) (leg 2)
CFCs	Kenichi Sasaki (JAMSTEC) ksasaki@jamstec.go.jp	Kenichi Sasaki (JAMSTEC)
$\Delta^{14}\text{C}/\delta^{13}\text{C}$	Yuichiro Kumamoto (JAMSTEC) kumamoto@jamstec.go.jp	Yuichiro Kumamoto (JAMSTEC)

N ₂ O/CH ₄	Osamu Yoshida (RGU) yoshida@rakuno.ac.jp	Osamu Yoshida (RGU) (leg 1) Sakae Toyoda (TITECH) (leg 2)
Biology	Ken Furuya (UT) furuya@fs.a.u-tokyo.ac.jp	Taketoshi Kodama (UT)

Floats

ARGO float	Toshio Suga (JAMSTEC) sugat@jamstec.go.jp	Kenichi Katayama (MWJ)
------------	--	------------------------

GODI	Global Ocean Development Inc.
JAMSTEC	Japan Agency for Marine-Earth Science and Technology
MRI	Meteorological Research Institute, Japan Meteorological Agency
MWJ	Marine Works Japan, Ltd.
RGU	Rakuno Gakuen University
TITECH	Tokyo Institute of Technology
UT	The University of Tokyo

1.4 Scientific Program and Methods

(1) Nature and objectives of MR09-01 cruise project

It is well known that climate changes of a timescale more than a decade are influenced by changes of oceanic conditions. Among a lot of oceanic changes, we focus on transport and accumulation of anthropogenic CO₂ and heat in the ocean, both of which are important for global warming. Accordingly we are aimed at clarifying temporal changes of the transport and accumulation quantitatively. In doing so, we pay a special attention to water masses of the Southern Ocean's origin, which play an important role in transporting anthropogenic CO₂ and heat into the ocean's interior. With this purpose, we have so far re-occupied historical observation lines, mainly in the Pacific Ocean.

This cruise is a reoccupation of the hydrographic section called 'WHP-P21', which was observed by an ocean science group of United States of America (USA) in 1994 as a part of World Ocean Circulation Experiment (WOCE). The dataset is included in the data base of Climate Variability and Predictability (CLIVAR) and Carbon Hydrographic Data Office (<http://whpo.ucsd.edu>). We will compare physical and chemical properties along section WHP-P21 with those obtained in 1994 to detect and evaluate long-term changes of the marine environment in the Pacific.

Reoccupations of the WOCE hydrographic sections are now in progress by international cooperation in ocean science community, under the framework of CLIVAR, which is as part of World Climate Research Programme (WCRP) and International Ocean Carbon Coordination Project (IOCCP). Our research is planned as a contribution to this international projects supported by World Meteorological Organization (WMO), International Council for Science (ICSU) / Scientific Committee on Oceanic Research (SCOR) and United Nations Educational, Scientific and Cultural Organization (UNESCO)/Intergovernmental Oceanographic Commission (IOC), and the results and data will be published by 2010 for worldwide use.

The other purposes of this cruise are as follows:

- 1) to observe surface meteorological and hydrological parameters as a basic data of meteorology and oceanography such as studies on flux exchange, air-sea interaction and so on,
- 2) to observe sea bottom topography, gravity and magnetic fields along the cruise track to understand the dynamics of ocean plate and accompanying geophysical activities,
- 3) to observe biogeochemical parameters to study material (carbon, nitrate, etc) cycle in the ocean,

- 4) to observe greenhouse gases in the atmosphere and the ocean to study their cycle from bio-geochemical aspect, and
 5) to estimate diapycnal diffusivity in the deep ocean.

(2) Cruise narrative

R/V Mirai departed Valparaiso, Chile on April 10, 2009. The hydrographic cast was started at the station P21-29 on April 14, since permission of observation in the Peru's EEZ was not yet given. After the CTD station P21-33, R/V Mirai sailed towards the station P21-14 off Peru and waited for a few days in the Peru's EEZ. XCTDs were deployed at stations from P21-29 to P21-33 and the hydrographic cast was restarted at the station P21-41 on April 21.

At Papeete, Tahiti on 21 May, 2009, 34 crews and scientists who came from Japan to embark on R/V Mirai by the same plane were not allowed to embark for 7 days, because one of the scientists developed a fever of 38°C and was suspected as a new type of flu. Therefore, we conducted 8 CTD stations without the 34 crews and scientists during leg 2a from 21 to 24 May. Then R/V Mirai departed Papeete again on May 25 and we conducted the rest of the hydrographic observations in leg 2b. R/V Mirai arrived at Brisbane, Australia on June 19, 2009.

During leg 3 from June 20 to July 3, underway observations were conducted along the cruise track.

1.5 List of Cruise Participants

Table 1.5.1(a): List of cruise participants for leg 1.

Name	Responsibility	Affiliation
Akihiko Murata	Chief scientist/carbon/water sampling	RIGC/JAMSTEC
Hiroshi Uchida	CTD/water sampling	RIGC/JAMSTEC
Sinya Kouketsu	LADCP/ADCP/water sampling	RIGC/JAMSTEC
Yuichiro Kumamoto	DO/thermosalinograph/ $\Delta^{14}\text{C}$	RIGC/JAMSTEC
Kenichi Sasaki	CFCs	MIO/JAMSTEC
Hirokatsu Uno	CTD/water sampling	MWJ
Kenichi Katayama	CTD/water sampling	MWJ
Shinsuke Toyoda	CTD/water sampling	MWJ
Hiroyuki Hayashi	CTD/water sampling	MWJ
Tatsuya Tanaka	Salinity	MWJ
Akira Watanabe	Salinity	MWJ
Fuyuki Shibata	DO/water sampling	MWJ
Miyo Ikeda	DO/water sampling	MWJ
Misato Kuwahara	DO/water sampling	MWJ
Shinichiro Yokogawa	Nutrients	MWJ
Ayumi Takeuchi	Nutrients	MWJ
Kohei Miura	Nutrients	MWJ
Kenichiro Sato	Chief technologist/nutrients/water sampling	MWJ
Ai Ueda	Water sampling	MWJ
Tetsuo Aoki	Water sampling	MWJ
Rui Asakawa	Water sampling	MWJ
Masashi Inose	Water sampling	MWJ
Shinya Iwasaki	Water sampling	MWJ
Masahiro Orui	Water sampling	MWJ
Yuichi Sonoyama	CFCs	MWJ
Katsunori Sagishima	CFCs	MWJ
Shoko Tatamisashi	CFCs	MWJ
Tomonori Watai	pH/total alkalinity	MWJ

Ayaka Hatsuyama	pH/total alkalinity	MWJ
Minoru Kamata	DIC	MWJ
Yoshiko Ishikawa	DIC	MWJ
Shinya Okumura	Meteorology/geophysics/ADCP/XCTD	GODI
Ryo Kimura	Meteorology/geophysics/ADCP/XCTD	GODI
Yosuke Yuki	Meteorology/geophysics/ADCP/XCTD	GODI
Takuhei Shiozaki	Biology/water sampling	UT
Satoshi Kitajima	Biology/water sampling	UT
Taketoshi Kodama	Biology/water sampling	UT
Hiroyuki Kurotori	Biology/water sampling	UT
Osamu Yoshida	CH ₄ and N ₂ O/water sampling	RGU
Sho Imai	CH ₄ and N ₂ O/water sampling	RGU
Chiho Kubota	CH ₄ and N ₂ O/water sampling	RGU
Wolfgang Schneider	CTD/water sampling	COPAS
Lorena Graciela Marquez Ismodes	Observer	Peruvian Navy

COPAS	Center for Oceanographic Research in the eastern South Pacific, University of Concepcion, Chile
GODI	Global Ocean Development Inc.
JAMSTEC	Japan Agency for Marine-Earth Science and Technology
MIO	Mutsu Institute of Oceanography
MWJ	Marine Works Japan, Ltd.
RGU	Rakuno Gakuen University
RIGC	Research Institute for Global Change
UT	The University of Tokyo

Table 1.5.1(b): List of cruise participants for leg 2a.

Name	Responsibility	Affiliation
Hiroshi Uchida	Chief Scientist/CTD/water sampling	RIGC/JAMSTEC
Shinya Kouketsu	LADCP/ADCP/water sampling	RIGC/JAMSTEC
Yuichiro Kumamoto	DO/thermosalinograph / $\Delta^{14}\text{C}$	RIGC/JAMSTEC
Toshimasa Doi	LADCP/water sampling	RIGC/JAMSTEC
Katsuro Katsumata	XMP/LADCP/water sampling	RIGC/JAMSTEC
Kenichi Sasaki	CFCs	MIO/JAMSTEC
Hirokatsu Uno	CTD/water sampling	MWJ
Kenichi Katayama	CTD/water sampling	MWJ
Shinsuke Toyoda	CTD/water sampling	MWJ
Hiroyuki Hayashi	CTD/water sampling	MWJ
Tatsuya Tanaka	Salinity	MWJ
Akira Watanabe	Salinity	MWJ
Fuyuki Shibata	DO/water sampling	MWJ
Miyo Ikeda	DO/water sampling	MWJ
Misato Kuwahara	DO/water sampling	MWJ
Shinichiro Yokogawa	Nutrients	MWJ
Ayumi Takeuchi	Nutrients	MWJ
Kohei Miura	Nutrients	MWJ
Kenichiro Sato	Chief technologist/nutrients/water sampling	MWJ
Ai Ueda	Water sampling	MWJ
Yuichi Sonoyama	CFCs	MWJ
Katsunori Sagishima	CFCs	MWJ
Shoko Tatamisashi	CFCs	MWJ
Tomonori Watai	pH/total alkalinity	MWJ

Ayaka Hatsuyama	pH/total alkalinity	MWJ
Minoru Kamata	DIC	MWJ
Yoshiko Ishikawa	DIC	MWJ
Shinya Okumura	Meteorology/geophysics/ADCP/XCTD	GODI
Ryo Kimura	Meteorology/geophysics/ADCP/XCTD	GODI
Yosuke Yuki	Meteorology/geophysics/ADCP/XCTD	GODI
Takuhei Shiozaki	Biology/water sampling	UT
Satoshi Kitajima	Biology/water sampling	UT
Taketoshi Kodama	Biology/water sampling	UT
Hiroyuki Kurotori	Biology/water sampling	UT
Sho Imai	CH ₄ and N ₂ O/water sampling	RGU
Chiho Kubota	CH ₄ and N ₂ O/water sampling	RGU
Wolfgang Schneider	CTD/water sampling	COPAS
Camillia Pauline Garae	Observer	DGMWR
Harish Pratap	Observer	FMS
DGMWR	Department of Geology Mines and Water Resources, Vanuatu	
FMS	Fiji Meteorological Services, Fiji	

Table 1.5.1(c): List of cruise participants for leg 2b.

Name	Responsibility	Affiliation
Hiroshi Uchida	Chief scientist/CTD/water sampling	RIGC/JAMSTEC
Yuichiro Kumamoto	DO/thermosalinograph/ $\Delta^{14}\text{C}$	RIGC/JAMSTEC
Toshimasa Doi	LADCP/water sampling	RIGC/JAMSTEC
Katsuro Katsumata	XMP/LADCP/water sampling	RIGC/JAMSTEC
Kenichi Sasaki	CFCs	MIO/JAMSTEC
Fujio Kobayashi	Salinity	MWJ
Akira Watanabe	Salinity	MWJ
Miyo Ikeda	DO/water sampling	MWJ
Misato Kuwahara	DO/water sampling	MWJ
Masanori Enoki	DO/water sampling	MWJ
Ayumi Takeuchi	Nutrients	MWJ
Kohei Miura	Nutrients	MWJ
Junji Matsushita	Nutrients	MWJ
Satoshi Ozawa	Chief technologist/CTD/water Sampling	MWJ
Ai Ueda	Water sampling	MWJ
Yuichi Sonoyama	CFCs	MWJ
Katsunori Sagishima	CFCs	MWJ
Shoko Tatamisashi	CFCs	MWJ
Yoshiko Ishikawa	pH/total alkalinity	MWJ
Ayaka Hatsuyama	pH/total alkalinity	MWJ
Minoru Kamata	DIC	MWJ
Yasuhiro Arie	DIC	MWJ
Tomoyuki Takamori	CTD/water sampling	MWJ
Hiroshi Matsunaga	CTD/water sampling	MWJ
Masayuki Fujisaki	CTD/water sampling	MWJ
Shungo Oshitani	CTD/water sampling	MWJ
Tatsuya Ando	Water sampling	MWJ
Tomomi Watanabe	Water sampling	MWJ
Kanako Yoshida	Water sampling	MWJ
Mami Kawai	Water sampling	MWJ
Hideki Yamamoto	Water sampling	MWJ
Satoshi Okumura	Meteorology/geophysics/ADCP/XCTD	GODI

Kazuho Yoshida	Meteorology/geophysics/ADCP/XCTD	GODI
Harumi Ota	Meteorology/geophysics/ADCP/XCTD	GODI
Takuhei Shiozaki	Biology/water sampling	UT
Satoshi Kitajima	Biology/water sampling	UT
Taketoshi Kodama	Biology/water sampling	UT
Hiroyuki Kurotori	Biology/water sampling	UT
Sho Imai	CH ₄ and N ₂ O/water sampling	RGU
Chiho Kubota	CH ₄ and N ₂ O/water sampling	RGU
Wolfgang Schneider	CTD/water sampling	COPAS
Camillia Pauline Garae	Observer	DGMWR
Harish Pratap	Observer	FMS
Sakae Toyoda	CH ₄ and N ₂ O/water sampling	TITECH
Taku Watanabe	CH ₄ and N ₂ O/water sampling	TITECH
TITECH	Tokyo Institute of Technology	

Table 1.5.1(d): List of cruise participants for leg 3.

Name	Responsibility	Affiliation
Kenichi Sasaki	Chief scientist	MIO/JAMSTEC
Fujio Kobayashi	Technician	MWJ
Sinsuke Toyoda	Technician	MWJ
Fuyuki Shibata	Technician	MWJ
Sinichiro Yokogawa	Technician	MWJ
Shoko Tatamisashi	Technician	MWJ
Hideki Yamamoto	Technician	MWJ
Nironori Sato	Technician	MWJ
Yasuhiro Arie	Technician	MWJ
Ryo Kimura	Meteorology/geophysics/ADCP/XCTD	GODI
Soichiro Sueyoshi	Meteorology/geophysics/ADCP/XCTD	GODI
Takuhei Shiozaki	Biology	UT
Satoshi Kitajima	Biology	UT
Taketoshi Kodama	Biology	UT
Hiroyuki Kurotori	Biology	UT
Taku Watanabe	CH ₄ and N ₂ O	TITECH
Sho Imai	CH ₄ and N ₂ O	RGU
Chiho Kubota	CH ₄ and N ₂ O	RGU
Hiroshi Furutani	Air sampling	ORI
Jinyoung Jung	Air sampling	ORI
ORI	Ocean Research Institute, The University of Tokyo	

2 Underway Observation

2.1 Navigation and Bathymetry

September 9, 2009

2.1.1 Navigation

(1) Personnel

<i>Shinya Okumura</i>	<i>(GODI) : Leg 1</i>
<i>Satoshi Okumura</i>	<i>(GODI) : Leg 2</i>
<i>Souichiro Sueyoshi</i>	<i>(GODI) : Leg 3</i>
<i>Ryo Kimura</i>	<i>(GODI) : Leg 1, Leg 3</i>
<i>Yousuke Yuuki</i>	<i>(GODI) : Leg 1</i>
<i>Kazuho Yoshida</i>	<i>(GODI) : Leg 2</i>
<i>Harumi Ota</i>	<i>(GODI) : Leg2</i>

(2) Overview of the equipment

Ship's position, speed and course were provided by Radio Navigation System on R/V MIRAI. The system integrates GPS position, Log speed, Gyro heading and other basic data on a workstation. Ship's course and speed over ground are calculated from GPS position. The workstation clock is synchronized to reference clock using NTP (Network Time Protocol). Navigation data, called "SOJ data", is distributed to client computer every second, and recorded every 60 seconds.

Navigation devices are listed below.

1. GPS receiver (2sets): Trimble DS-4000 9-channel receiver, the antennas are located on Navigation deck, port and starboard side. GPS position from each receiver is converted to the position of radar mast.
2. Doppler log: Furuno DS-30, which use three acoustic beam for current measurement
3. Gyrocompass: Tokimec TG-6000, sperry mechanical gyrocompass
4. Reference clock: Symmetricom TymServ2100, GPS time server
5. Workstation Hewlett-Packard ZX2000 running HP-UX ver.11.22

(3) Data period MR09-01 Leg 1: 17:58 UTC 09 Apr. 2009 to 23:59 UTC 19 May 2009 (UTC)
MR09-01 Leg 2: 00:00 UTC 21 May 2009 to 02:00 UTC 19 Jun. 2009 (UTC)

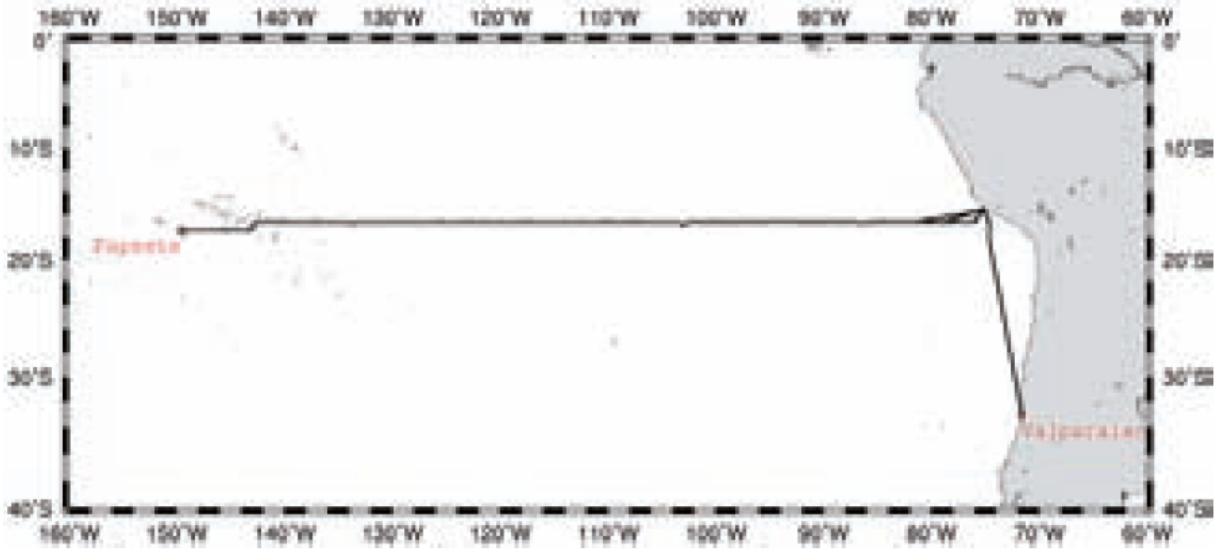


Figure 2.1.1: Cruise Track of MR09-01 Leg 1.

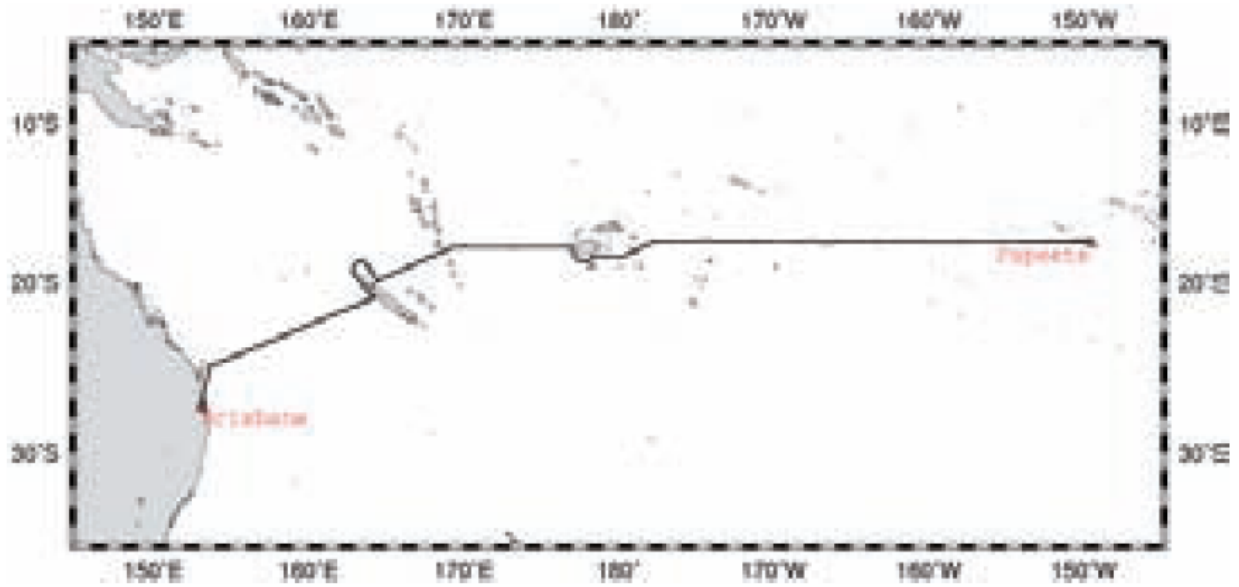


Figure 2.1.2: Cruise Track of MR09-01 Leg 2.

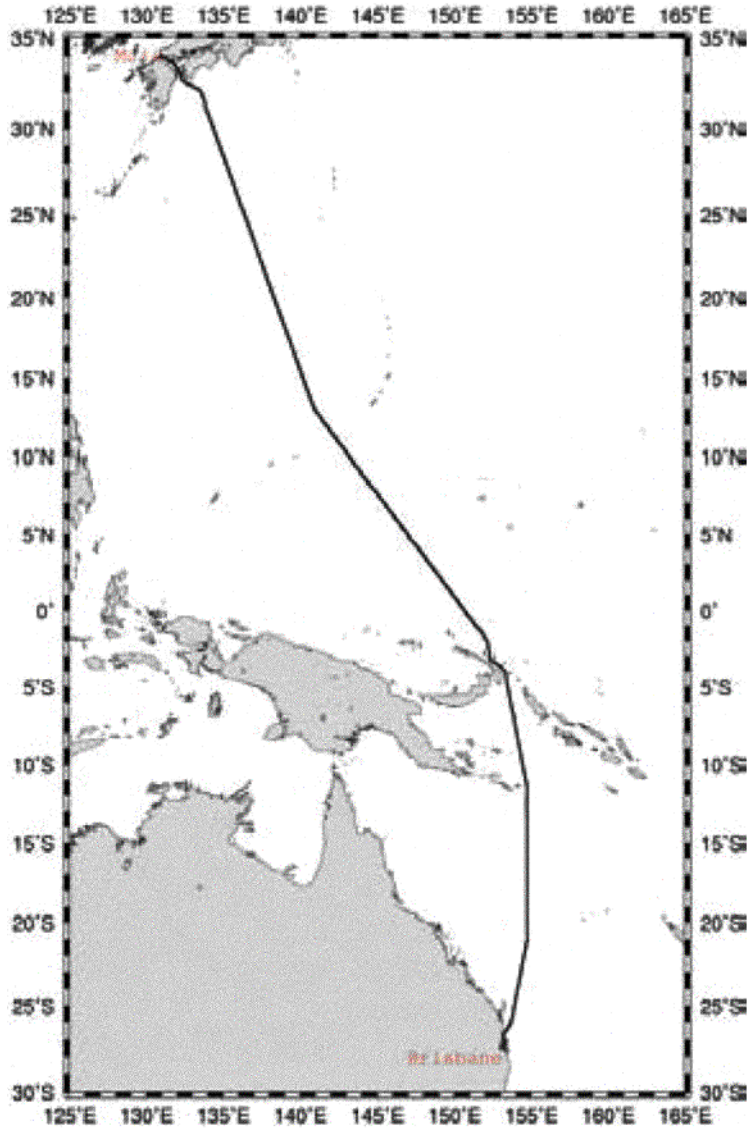


Figure 2.1.3: Cruise Track of MRO9-01 Leg 3.

2.1.2 Bathymetry

(1) Personnel

<i>Takeshi Matsumoto</i>	<i>(University of the Ryukyus)</i>	<i>: Principal investigator/Not on-board</i>
<i>Masao Nakanishi</i>	<i>(Chiba University)</i>	<i>: Principal investigator/Not on-board</i>
<i>Shinya Okumura</i>	<i>(GODI) : Leg1</i>	
<i>Satoshi Okumura</i>	<i>(GODI) : Leg2</i>	
<i>Souichiro Sueyoshi</i>	<i>(GODI) : Leg3</i>	
<i>Ryo Kimura</i>	<i>(GODI) : Leg1, Leg3</i>	
<i>Yousuke Yuuki</i>	<i>(GODI) : Leg1</i>	
<i>Kazuho Yoshida</i>	<i>(GODI) : Leg2</i>	
<i>Harumi Ota</i>	<i>(GODI) : Leg2</i>	

(2) Overview of the equipment

R/V MIRAI equipped with a Multi Beam Echo Sounding system (MBES), SEABEAM 2112.004 (SeaBeam Instruments Inc.) The main objective of MBES survey is collecting continuous bathymetry data along ship's track to make a contribution to geological and geophysical investigations and global datasets. Data interval along ship's track was max 17 seconds at 6,000 m. To get accurate sound velocity of water column for ray-path correction of acoustic multibeam, we used Surface Sound Velocimeter (SSV) data to get the sea surface (6.2 m depth) sound velocity, and the deeper depth profiles were calculated using temperature and salinity profiles from the nearest CTD data by the equation in Mackenzie (1981).

System configuration and performance of SEABEAM 2112.004,

Frequency:	12 kHz
Transmit beam width:	2 degree
Transmit power:	20 kW
Transmit pulse length:	3 to 20 msec.
Depth range:	100 to 11,000 m
Beam spacing:	1 degree athwart ship
Swath width:	150 degree (max) 120 degree to 4,500 m 100 degree to 6,000 m 90 degree to 11,000 m
Depth accuracy:	Within <0.5% of depth or ± 1 m, whichever is greater, over the entire swath. (Nadir beam has greater accuracy; typically within < 0.2% of depth or ± 1 m, whichever is greater)

(3) Data Period

MR09-01 Leg1: P21-029 on 14 April 2009 to P21-033 on 16 April 2009,
P21-014 on 17 April 2009 to P21-156 on 18 May 2009
MR09-01 Leg2: P21-157 on 21 May 2009 to P21-288 on 19 June 2009
MR09-01 Leg3: 20 June 2009 to 1 July 2009
(except for the territorial waters of Papua New Guinea)

(4) Data processing

i. Sound velocity correction

The continuous bathymetry data are split into small areas around each CTD station. For each small area, the bathymetry data are corrected using a sound velocity profile calculated from the CTD data in the area. The equation of Mackenzie (1981) is used for calculating sound velocity. The data processing is carried out using "mbbath" command of MBsystem.

ii. Editing and Gridding

Gridding for the bathymetry data are carried out using the HIPS software version 6.1 Service Pack 2 (CARIS, Canada). Firstly, the bathymetry data during Ship's turning is basically removed before "BASE surface" is made. A spike noise of each swath data is also removed using "swath editor" and "subset editor". Then the bathymetry data are gridded by "Interpolate" function of the software with following parameters.

BASE surface resolution:	50m
Interpolate matrix size:	5 x 5
Minimum number of neighbors for interpolate:	10

Finally, raw data and interpolated data are exported as ASCII data, and converted to 150 m grid data using "xyz2grd" utility of GMT (Generic Mapping Tool) software.

(5) Data Archive

Bathymetry data obtained during this cruise was submitted to the Data Integration and Analysis Group (DIAG) of JAMSTEC, and archived there.

(6) Tectonic history of the Pacific Plate

The Pacific Plate is the largest oceanic lithospheric plate on the Earth. The Pacific Plate was born around 190 Ma, Middle Jurassic (Nakanishi et al., 1992). The tectonic history of the Pacific Plate has been exposed by many studies based on magnetic anomaly lineations. However, the tectonic history in some periods is still obscure because of lack of geophysical data. To reveal the entire tectonic history of the Pacific Plate from Middle Jurassic to the present, increase in geophysical data is indispensable.

Identification of magnetic anomaly lineations has been the most common method for tectonic studies of oceanic plates. After improvement of the multi-narrow beam echo sounder, we become able to describe lineated abyssal hills for the tectonic studies in detail. Abyssal hills are related to the nature of the mid-ocean ridges at which they form (e.g. Goff et al., 1997). For example, abyssal hills heights and widths tend to correlate inversely with spreading rates. Abyssal hills also change morphology depending on crustal thickness and magma supply, factors which can vary within a single ridge segment and/or can vary from one ridge segment to another. Abyssal hills are therefore an off-axis indicator of mid-ocean ridge spreading history.

We collected bathymetric data using SeaBeam 2112 during the cruise. [Figures 2.1.4](#) and [2.1.5](#) show examples of abyssal hills. [Figure 2.1.4](#) is the bathymetric map near the East Pacific Rise (EPR). The crest of the EPR has about 2600 m depth and about 350 m higher than its foot. The depth of the seafloor near the edges of [Figure 2.1.4a](#) is about 3500 m. Most of the abyssal hills have the similar strike as the EPR, but some have different strikes from the EPR. The height of abyssal hills is 50 m near the EPR and is more than 200 m around 114°W.

[Figure 2.1.5](#) is the bathymetric map of the seafloor south of the Manihiki Plateau and crosses the East Manihiki Scarp, which is a remarkably linear feature extending more than 700 km from the northeastern corner of the Manihiki plateau. Previous works (e.g., Viso et al., 2005; Downey et al., 2007) show the existence of the abyssal hills with an E-W strike in this area. The abyssal hills originate from the Pacific-Phoenix Ridge in the mid-Cretaceous. The abyssal hills with an E-W strike exist west of 164°W ([Figure 2.1.5b](#)). The height of the abyssal hills is ~100 m. Several knolls with depression exist around 165°15'W. The height of the knolls is about 600 m. The abyssal hills east of the East Manihiki Scarp (EMS) have an NE-SW strike ([Figure 2.1.5a, c](#)). The height of abyssal hills is more than 100 m. The pattern of the abyssal hills near the EMS is similar to that around 2.5°S reported by Viso et al. (2005). They interpret these abyssal hills as intratransform spreading centers resulting from transtensional strain across the EMS. Thus, the abyssal hills east of the EMS in [Figure 2.1.5\(c\)](#) derive from the same mechanism.

References

- Downey, N.J., J.M. Stock, R.W. Clayton, and S.C. Cande (2007): History of the Cretaceous Osborn spreading center, *J. Geophys. Res.*, 112, B04102, doi:10.1029/2006JB004550.
- Goff, J.A., Y. Ma, A. Shah, J.R. Cochran, and J.-C. Sempere (1997): Stochastic analysis of seafloor morphology on the flank of the Southeast Indian Ridge: The influence of ridge morphology on the formation of abyssal hills, *J. Geophys. Res.*, 102, 15,521-15,534.
- Mackenzie, K.V. (1981): Nine-term equation for the sound speed in the oceans, *J. Acoust. Soc. Am.*, 70 (3), pp 807-812.
- Nakanishi, M., K. Tamaki, and K. Kobayashi (1992): A new Mesozoic isochron chart of the whole western Pacific Ocean: Paleomagnetic and tectonic implications, *Geophys. Res. Lett.*, 19, 693-696.
- Searle, R. (1984): GLORIA survey of the East Pacific Rise Near 3.5°S: Tectonic and volcanic characteristics of a fast spreading mid-ocean rise, *Tectonophysics*, 101, 319-344.
- Viso, R.F., R.L. Larson, and R.A. Pockalny (2005): Tectonic evolution of the Pacific-Phoenix-Farallon triple junction in the South Pacific Ocean, *Earth Planet Sci. Lett.*, 233, 179-194.

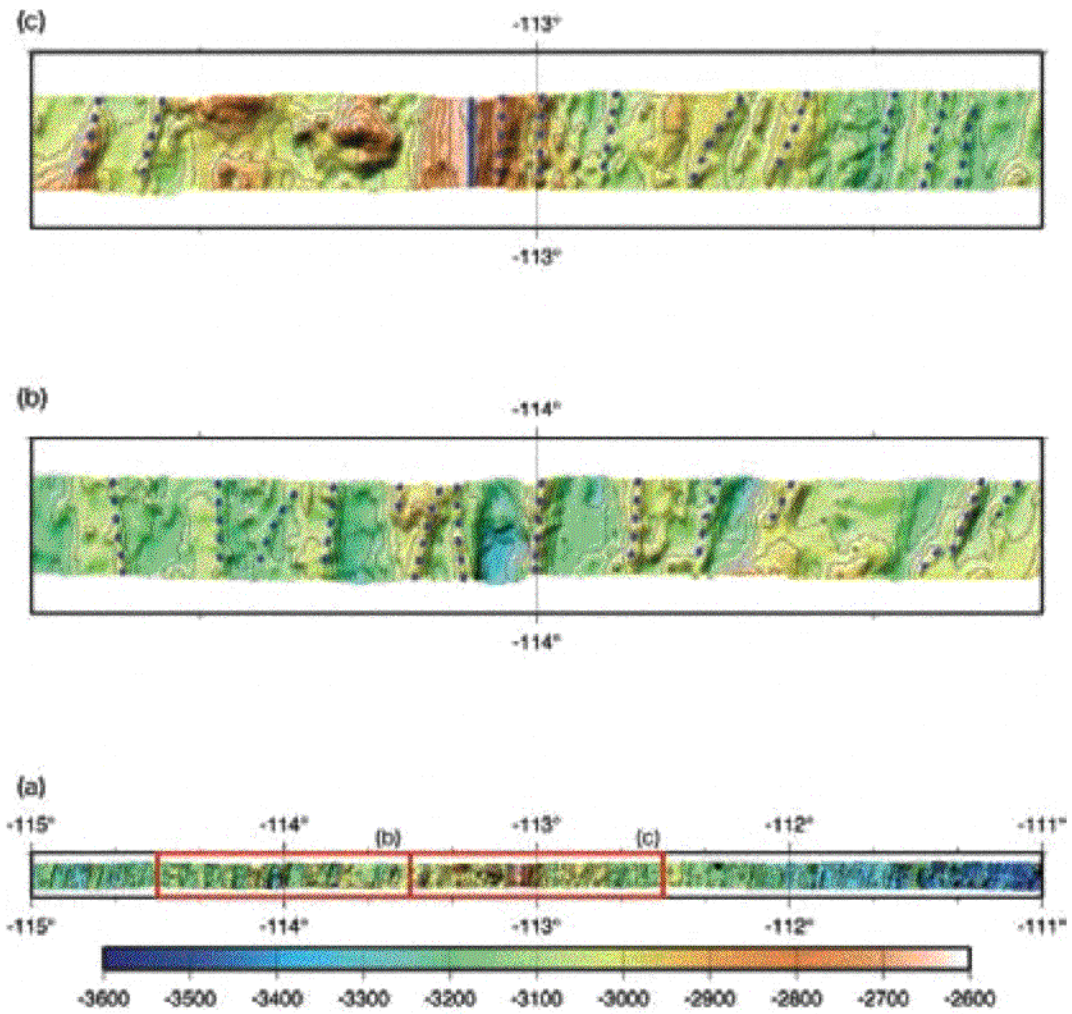


Figure 2.1.4: Bathymetric Map around the East Pacific Rise. Contour interval is 50 m. Bathymetry is illuminated from the northwest. Red rectangles in (a) represent the areas of (b) and (c). Blue dotted lines represent abyssal hills. A blue line shows the crest of the East Pacific Rise.

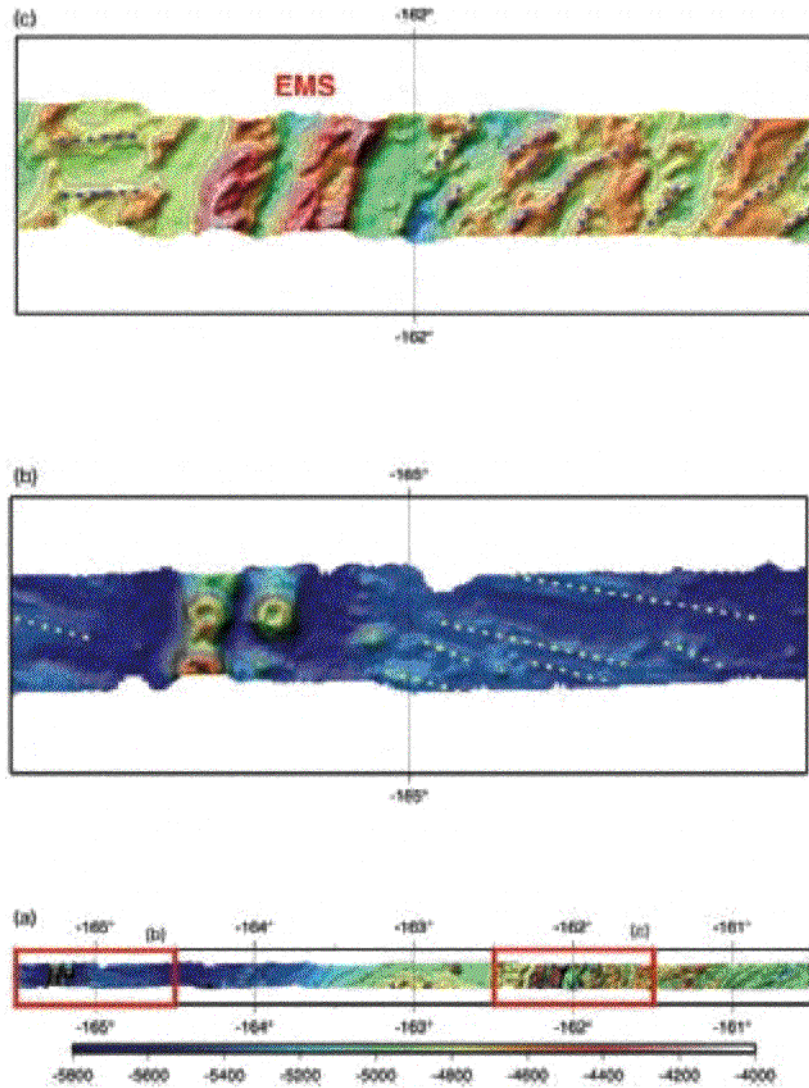


Figure 2.1.5: Bathymetric Map of the seafloor south of the Manihiki Plateau. Contour interval is 50 m. Bathymetry is illuminated from the northwest. Red rectangles in (a) represent the areas of (b) and (c). Yellow and blue dotted lines represent abyssal hills. EMS represents the East Manihiki Scarp.

2.2 Surface Meteorological Observation

January 13, 2010

(1) Personnel

Kunio Yoneyama (JAMSTEC)
Satoshi Okumura (GODI)
Souichiro Sueyoshi (GODI)
Shinya Okumura (GODI)
Ryo Kimura (GODI)
Kazuho Yoshida (GODI)
Harumi Ota (GODI)
Yousuke Yuuki (GODI)

(2) Objective

As a basic dataset that describes weather conditions during the cruise, surface meteorological observation was continuously conducted.

(3) Methods

There are two different surface meteorological measurement systems on board the R/V MIRAI. One is the MIRAI surface meteorological observation system (SMET), and the other is the Shipboard Oceanographic and Atmospheric Radiation measurement system (SOAR).

Instruments of SMET are listed in Table 2.2.1. All SMET data were collected and processed by KOAC-7800 weather data processor made by Koshin Denki, Japan. Note that although SMET contains rain gauge, anemometer and radiometers in their system, we adopted those data from not SMET but SOAR due to the following reasons; 1) Since SMET rain gauge is located near the base of the mast, there is a possibility that its capture rate might be affected, 2) SOAR's anemometer has better starting threshold wind speed (1 m s^{-1}) comparing to SMET's anemometer (2 m^{-1}), and 3) SMET's radiometers record data with 10 W/m^2 resolution while SOAR takes high resolution data of 1 W/m^2 .

SOAR system was designed and constructed by the Brookhaven National Laboratory (BNL), USA, for an accurate measurement of solar radiation on the ship (cf. <http://www.gim.bnl.gov/soar/>). SOAR consist of 1) Portable Radiation Package (PRP) that measures short and long wave downwelling radiation, 2) Zen (meteorological system that measures pressure, air temperature, relative humidity, wind speed/direction and rainfall, and 3) Scientific Computer System (SCS) developed by the National Oceanic and Atmospheric Administration (NOAA), USA, for data collection, management, real-time monitoring, and so on. Information or sensors used here is listed in Table 2.2.2.

Table 2.2.1: Instruments and locations of SMET.

Sensor	Parameter	Manufacturer / type	Location / height from sea level
Thermometer* ¹	air temperature relative humidity	Vaisala, Finland / HMP45A	compass deck* ² / 21 m
Thermometer Barometer	sea temperature pressure	Sea-Bird Electronics, Inc., USA/SBE3S* ³ Setra Systems Inc., USA / 370	4th deck / -5 m captain deck / 13 m

*1 Gill aspirated radiation shield 43408 made by R.M. Young, USA is attached.

*2 There are two thermometers at starboard and port sides.

*3 Sea surface temperature data were taken from EPCS surface water monitoring system.

Table 2.2.2: Instruments and locations of SOAR.

Sensor	Parameter	Manufacturer / type	Location / height from sea level
Anemometer	wind speed/direction	R.M. Young, USA / 05106	foremast / 25 m
Rain gauge	rainfall accumulation	R.M. Young, USA/ 50202	foremast / 24 m
Radiometer	short wave radiation	Eppley, USA/ PSP	foremast / 24 m
	long wave radiation	Eppley, USA/ PIR	foremast / 24 m

(4) Data processing and data format

All raw data were recorded every 6 seconds. Datasets produced here are 1-minute mean values (time stamp at the end of the average). These values are the simple mean of 8 samples, after removing maximum/minimum values from 10 samples to exclude singular/erroneous data. Linear interpolation onto missing values was applied only when their interval is less than 5 minutes.

Since the thermometers are equipped on both starboard/port sides on the deck, we adopted air temperature/relative humidity data taken at upwind side. Dew point temperature was produced from relative humidity and air temperature data.

Any adjustment to a certain height was not applied except pressure data to the sea level.

Data are stored as ASCII format and contains following parameters. Time in UTC expressed as YYYYMMDDHHMM, time in Julian day (1.0000 = January 1, 0000Z), longitude (°E), latitude (°N), pressure (hPa), air temperature (°C), dew point temperature (°C), relative humidity (%), sea surface temperature (°C), zonal wind component (m/sec), meridional wind component (m/sec), precipitation (mm/hr), downwelling shortwave radiation (W/m^2), and downwelling longwave radiation (W/m^2).

Missing values are expressed as "9999".

(5) Data Quality

To ensure the data quality, each sensor was calibrated as follows. Since there is a possibility for fine time resolution data sets to have some noises caused (generated) by turbulence, it is recommended to filter them out (ex. hourly mean) from this 1-minute mean data sets depending on the scientific purpose.

T/RH sensor:

Temperature and humidity probes were calibrated before/after the cruise by the manufacturer. Certificated accuracy of T/RH sensors are better than $\pm 0.2^\circ\text{C}$ and $\pm 2\%$, respectively.

We also checked T/RH values using another calibrated portable T/RH sensor (Vaisala, HIMP45A) before and after the cruise. The results are,

Temperature ($^\circ\text{C}$)

Mean difference between T (SMET) and T (portable) is

-0.08 ± 0.17 ($^\circ\text{C}$) at port side, -0.26 ± 0.33 ($^\circ\text{C}$) at starboard side.

Relative Humidity (%)

Mean difference between RH (SMET) and RH (portable) is

1.3 ± 0.5 (%) at port side, 1.3 ± 1.6 (%) at starboard side.

Sea surface temperature sensor:

Temperature sensor was calibrated before the cruise at the manufacturer. Certificated accuracy is better than $0.002^\circ\text{C}/\text{year}$.

Pressure sensor:

Using calibrated portable barometer (Vaisala, Finland / PTB220, certificated accuracy is better than ± 0.1 hPa), pressure sensor was checked before/after the cruise. Mean difference of SMET pressure sensor and portable sensor is 0.06 ± 0.05 hPa.

Precipitation:

Before the each leg, we checked the linearity of rain gauge value in response to water amount in the gauge. The results are as follows, and data have already been corrected using this relationship.

	Leg-1	Leg-2	Leg-3
minimum input water volume (cc)	0.0	0.0	0.0
maximum input water volume (cc)	505.0	505.7	503.7
minimum measured value (mm)	0.47	0.25	0.47
maximum measured value (mm)	50.23	48.75	49.79

Radiation sensors:

Short wave and long wave radiometers were calibrated by the manufacturer, Remote Measurement and Research Company, USA, prior to the cruise (February 2009).

(6) Data periods

Leg-1 1300 UTC, April 10, 2009 - 0000 UTC, May 20, 2009

Leg-2 0100 UTC, May 21, 2009 - 0100 UTC, June 19, 2009

Leg-3 2300 UTC, June 19, 2009 - 2350 UTC, July 2, 2009

(7) Point of contact

Kunio Yoneyama (yoneyamak@jamstec.go.jp)
Research Institute for Global Change / JAMSTEC
2-15, Natsushima, Yokosuka 237-0061, Japan

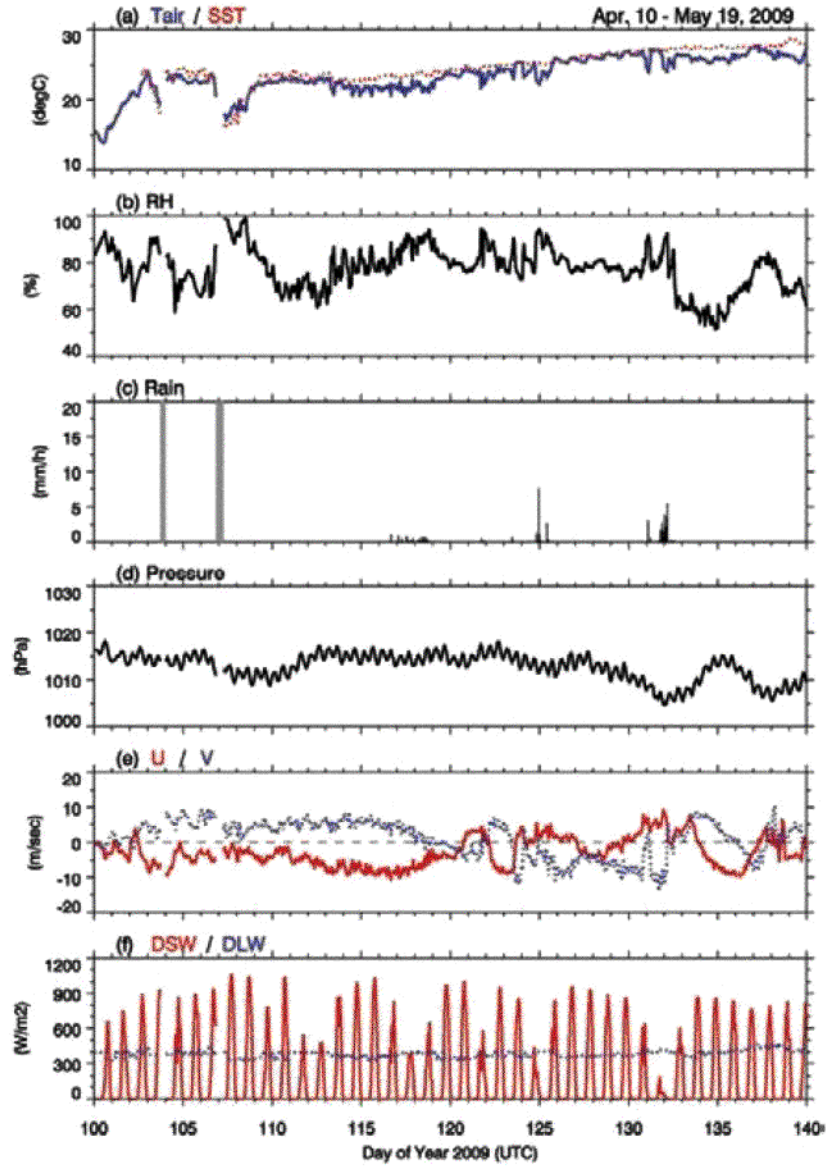


Figure 2.2.1: Time series of surface (a) air/sea temperature, (b) relative humidity, (c) precipitation, (d) pressure, (e) zonal and meridional wind components, and (f) short and long wave radiation for Leg-1. Day 100 corresponds to April 10, 2009.

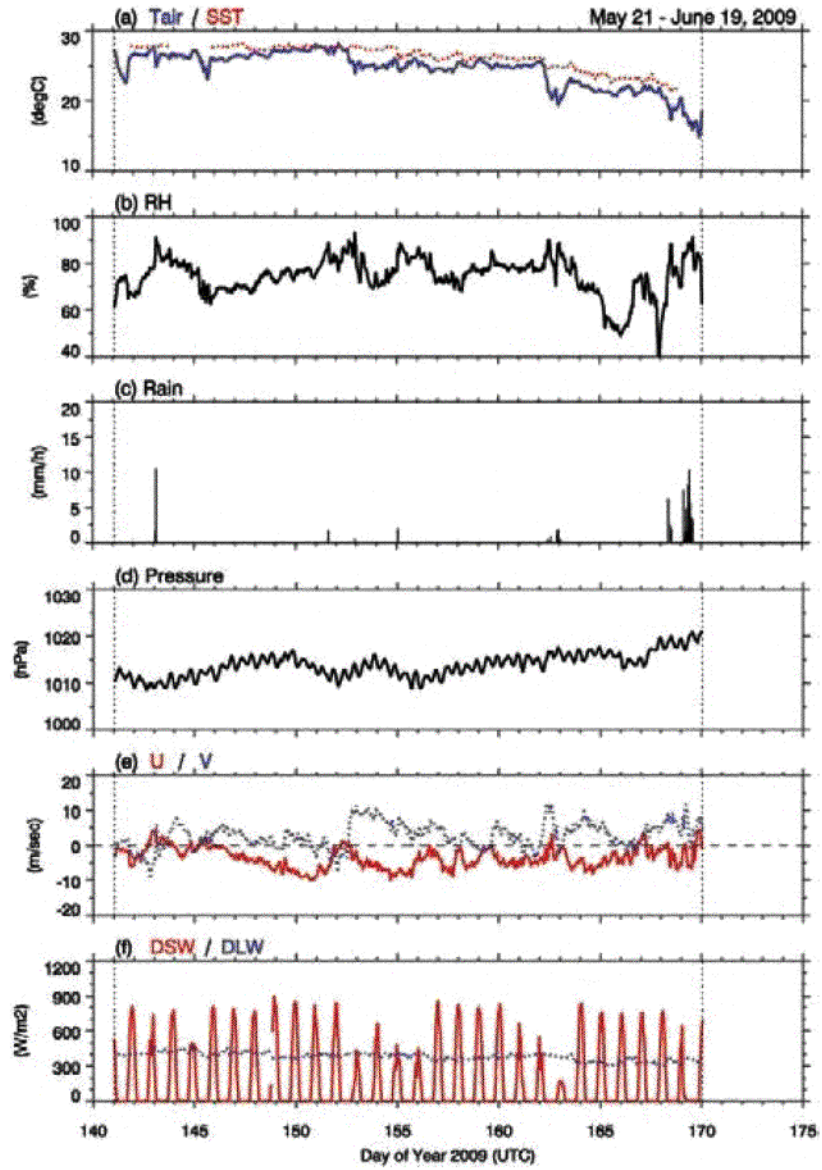


Figure 2.2.2: Same as [Figure 2.2.1](#), but for Leg 2. Day 141 corresponds to May 21, 2009.

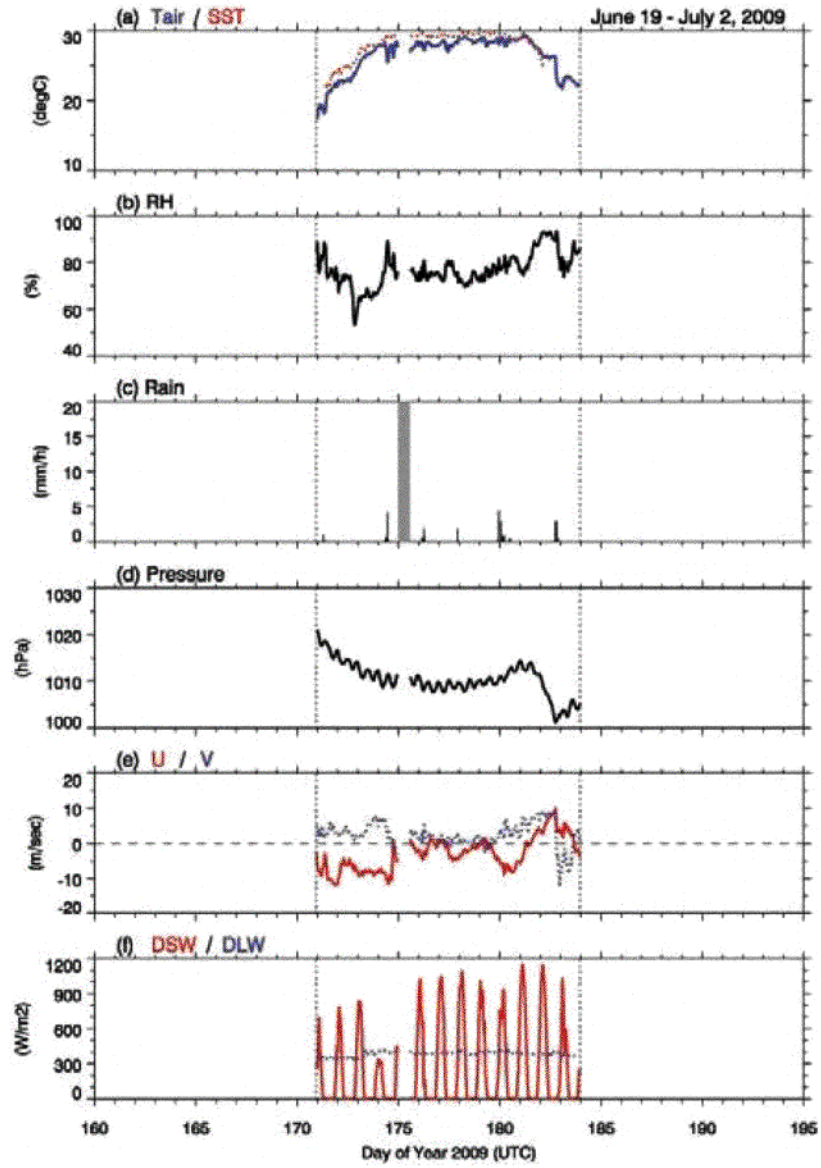


Figure 2.2.3: Same as [Figure 2.2.1](#), but for Leg 3. Day 171 corresponds to June 19, 2009.

2.3 Thermo-Salinograph and Related Measurements

July 31, 2010

(1) Personnel

Yuichiro Kumamoto (JAMSTEC)
Miyo Ikeda (MWJ)
Fuyuki Shibata (MWJ)
Masanori Enoki (MWJ)
Misato Kuwahara (MWJ)

(2) Objective

Our purpose is to obtain salinity, temperature, dissolved oxygen, and fluorescence data continuously in near-sea surface water during MR09-01 cruise.

(3) Methods

The Continuous Sea Surface Water Monitoring System (Nippon Kaiyo Co. Ltd.), including the thermo-salinograph, has five sensors and automatically measures salinity, temperature, dissolved oxygen, and fluorescence in near-sea surface water every one minute. This system is located in the sea surface monitoring laboratory and connected to shipboard LAN system. Measured data, time, and location of the ship were stored in a data management PC (IBM NetVista 6826-CBJ). The near-surface water was continuously pumped up to the laboratory from about 4 m water depth and flowed into the system through a vinyl-chloride pipe. The flow rate of the surface seawater was adjusted to be 12 dm³/min except for a fluorometer (about 0.4 dm³/min). Specifications of the each sensor in this system are listed below.

a) Temperature and salinity sensors

SEACAT THERMOSALINOGRAPH

Model: SBE-21, SEA-BIRD ELECTRONICS, INC.
Serial number: 2126391-3126
Measurement range: Temperature -5 to +35°C (ITS-90), Salinity 0 to 7.0 5 m⁻¹
Accuracy: Temperature 0.01°C 6month⁻¹, Salinity 0.001 5 m⁻¹ month⁻¹
Resolution: Temperatures 0.001°C, Salinity 0.0001 S a⁻¹

b) Bottom of ship thermometer (RMT)

Model: SBE 3S, SEA-BIRD ELECTRONICS, INC.
Serial number: 032175
Measurement range: -5 to +35°C (ITS-90)
Resolution: ±0.001°C
Stability: 0.002°C year⁻¹

c) Dissolved oxygen sensor

Model: 2127A, HACH ULTRA ANALYTICS JAPAN, INC.
Serial number: 61230
Measurement range: 0 to 14 ppm
Accuracy: ± 1% at 5°C of correction range
Stability: 1% month⁻¹

d) Fluorometer

Model: 10-AU-005, TURNER DESIGNS
Serial number: 5562 FRXX
Detection limit: 5 ppt or less for chlorophyll-a
Stability: 0.5% month⁻¹ of full scale

e) Flow meter

Model: EMARG2W, Aichi Watch Electronics LTD.
 Serial number: 8672
 Measurement range: 0 to 30 $l\ min^{-1}$
 Accuracy: $\pm 1\%$
 Stability: $\pm 1\% day^{-1}$

(4) Measurements

Periods of measurement, maintenance, and events during MR09-01 are listed in Table 2.3.1.

Table 2.3.1: Events list of the thermo-salinograph during MR09-01

System Date [UTC]	System Time [UTC]	Events	Remarks
09-Apr.-14	12:47	All the measurements started.	Leg-1 start
09-Apr.-15	23:59	All the measurements stopped due to entering in the Peruvian EEZ.	
09-Apr.-21	00:00		
09-Apr.-22	01:40	Lost of all the data due to reboot of the data management PC.	
09-Apr.-22	02:04		
09-May-18	07:06	All the measurements stopped.	Leg-1 finish
09-May-21	20:18	All the measurements started.	Leg-2a start
09-May-23	20:44	All the measurements stopped.	Leg-2a finish
09-May-25	20:19	All the measurements started.	Leg-2b start
09-Jun.-13	17:07	Lost of all the data due to error on program.	
09-Jun.-13	17:18	Lost of all the data due to error on program.	
09-Jun.-17	19:36	All the measurements stopped.	Leg-2b finish
09-Jun.-20	10:01	All the measurements started.	Leg-3 start
09-Jun.-23	22:59	Lost of all the data	
09-Jun.-24	14:03	Lost of all the data	
09-Jul.-01	04:23	All the measurements stopped.	Leg-3 finish

(5) Calibrations

We collected the surface seawater samples for salinity sensor calibration during Leg-1 and Leg-2 (Table 2.3.2). The seawater was collected approximately twice a day using a 250 ml brown glass bottle. The samples were stored in the sea surface monitoring laboratory and then measured using the Guildline 8400B at the end of the legs after all the measurements of the hydrocast bottle samples.

Table 2.3.2: Comparison of the sensor salinity with the bottle salinity.

Date [UTC]	Time [UTC]	Latitude	Longitude	Sensor salinity [PSS-78]	Bottle salinity [PSS-78]	Difference [Sen. - Bot.]
2009/4/14	13:48	16-44.97580S	078-42.43970W	35.4984	35.4950	0.0034
2009/4/14	21:56	16-45.17830S	079-19.83920W	35.5812	35.5769	0.0043
2009/4/15	8:56	16-44.40370S	080-39.63650W	35.5748	35.5725	0.0023
2009/4/15	22:04	16-40.73990S	080-59.80990W	35.4099	35.4083	0.0016
2009/4/21	8:19	16-44.92050S	080-25.69800W	35.4962	35.4981	-0.0019
2009/4/21	21:10	16-44.52540S	082-00.27190W	35.5029	35.5088	-0.0059
2009/4/22	10:00	16-44.93300S	082-59.85970W	35.5844	35.5889	-0.0045
2009/4/22	10:02	16-44.91210S	082-59.85080W	35.5842	35.5890	-0.0048

Date [UTC]	Time [UTC]	Latitude	Longitude	Sensor salinity [PSS-78]	Bottle salinity [PSS-78]	Difference [Sen. - Bot.]
2009/4/22	21:29	16-45.09040S	083-40.05760W	35.5448	35.5507	-0.0059
2009/4/23	8:51	16-44.56640S	084-20.09390W	35.6529	35.6570	-0.0041
2009/4/23	21:08	16-45.11350S	085-19.65940W	35.5000	35.5058	-0.0058
2009/4/24	9:52	16-49.99990S	086-23.16600W	35.7428	35.7466	-0.0038
2009/4/24	21:11	16-44.71580S	087-40.33490W	35.7371	35.7444	-0.0073
2009/4/25	10:36	16-45.00120S	088-39.82020W	35.7708	35.7750	-0.0042
2009/4/25	10:38	16-45.00260S	088-39.84800W	35.7718	35.7744	-0.0026
2009/4/25	20:55	16-44.78260S	089-20.05120W	35.7637	35.7691	-0.0054
2009/4/26	10:09	16-44.73750S	090-08.14720W	35.7523	35.7574	-0.0051
2009/4/26	21:41	16-44.78340S	091-28.27440W	35.7917	35.7951	-0.0034
2009/4/27	9:19	16-44.80660S	092-49.23870W	35.8304	35.8362	-0.0058
2009/4/27	21:37	16-43.85810S	094-21.16550W	35.8251	35.8318	-0.0067
2009/4/28	9:21	16-45.33650S	095-47.60370W	35.8719	35.8724	-0.0005
2009/4/28	9:23	16-45.34400S	095-48.13740W	35.8679	35.8707	-0.0028
2009/4/28	21:52	16-44.73560S	097-20.31890W	35.8107	35.8161	-0.0054
2009/4/29	9:38	16-44.79350S	098-40.12210W	35.9412	35.9454	-0.0042
2009/4/29	22:07	16-44.05720S	100-00.30900W	36.0435	36.0471	-0.0036
2009/4/30	10:07	16-44.61130S	101-28.24690W	35.9749	35.9805	-0.0056
2009/4/30	10:09	16-44.62880S	101-28.76720W	35.9771	35.9820	-0.0049
2009/4/30	21:57	16-59.19030S	102-58.24090W	35.9857	35.9880	-0.0023
2009/5/1	11:09	16-45.46850S	104-00.09040W	36.0785	36.0822	-0.0037
2009/5/1	23:39	16-45.03880S	106-00.04450W	36.0361	36.0432	-0.0071
2009/5/2	11:08	16-44.97480S	106-54.64000W	36.0931	36.0988	-0.0057
2009/5/3	1:48	16-45.49220S	107-15.05250W	36.1222	36.1272	-0.0050
2009/5/3	10:31	16-44.96970S	107-37.76710W	36.1409	36.1453	-0.0044
2009/5/3	23:03	16-45.14510S	109-19.99040W	36.1931	36.1985	-0.0054
2009/5/3	23:04	16-45.14910S	109-19.98920W	36.1924	36.1974	-0.0050
2009/5/4	11:33	16-45.13740S	110-40.38760W	36.2194	36.2242	-0.0048
2009/5/4	23:32	16-45.29100S	112-00.07440W	36.1544	36.1630	-0.0086
2009/5/5	10:47	16-45.25910S	113-37.45760W	36.3165	36.3205	-0.0040
2009/5/5	21:52	16-45.46490S	115-13.33820W	36.2483	36.2538	-0.0055
2009/5/6	11:27	16-44.98470S	116-42.80650W	36.3767	36.3807	-0.0040
2009/5/6	23:06	16-45.17100S	118-25.21730W	36.2563	36.2622	-0.0059
2009/5/7	11:36	16-45.09820S	120-00.16570W	36.2863	36.2924	-0.0061
2009/5/7	11:38	16-45.10700S	120-00.17050W	36.2868	36.2924	-0.0056
2009/5/8	7:21	16-45.09310S	122-39.65920W	36.2948	36.3001	-0.0053
2009/5/8	11:20	16-44.85160S	122-57.81300W	36.3801	36.3857	-0.0056
2009/5/8	23:17	16-45.11080S	124-39.69490W	36.4907	36.4951	-0.0044
2009/5/9	10:59	16-45.02640S	126-00.21060W	36.3923	36.3965	-0.0042
2009/5/9	23:45	16-45.30990S	127-20.52890W	36.3225	36.3272	-0.0047
2009/5/10	12:35	16-45.01200S	129-05.41100W	36.3609	36.3641	-0.0032
2009/5/10	12:37	16-45.01500S	129-05.91430W	36.3552	36.3591	-0.0039
2009/5/11	2:11	16-45.46310S	130-39.68820W	36.3718	36.3788	-0.0070
2009/5/11	12:12	16-45.05740S	131-59.97770W	36.4767	36.4823	-0.0056
2009/5/12	2:21	16-45.29710S	133-20.19320W	36.3381	36.3432	-0.0051
2009/5/12	11:51	16-45.56450S	134-00.34900W	36.2077	36.2137	-0.0060
2009/5/13	11:58	16-45.31040S	136-39.87070W	36.4252	36.4293	-0.0041
2009/5/13	12:00	16-45.30590S	136-39.85740W	36.4246	36.4307	-0.0061
2009/5/13	17:28	16-44.96630S	137-20.15810W	36.3616	36.3693	-0.0077
2009/5/14	0:08	16-45.09200S	138-22.38950W	36.3073	36.3105	-0.0032
2009/5/14	12:56	16-44.92430S	140-02.89960W	36.3949	36.4020	-0.0071

Date [UTC]	Time [UTC]	Latitude	Longitude	Sensor salinity [PSS-78]	Bottle salinity [PSS-78]	Difference [Sen. - Bot.]
2009/5/15	0:27	16-44.56690S	141-43.14970W	36.2809	36.2862	-0.0053
2009/5/15	14:26	17-18.00390S	143-01.90900W	36.2908	36.2964	-0.0056
2009/5/16	0:40	17-29.56580S	144-09.39550W	36.3152	36.3204	-0.0052
2009/5/16	14:32	17-29.82400S	145-44.07210W	36.3189	36.3234	-0.0045
2009/5/16	14:34	17-29.85300S	145-44.45950W	36.3190	36.3243	-0.0053
2009/5/17	1:06	17-29.80410S	146-55.62150W	36.3267	36.3310	-0.0043
2009/5/17	12:53	17-30.21460S	148-28.58790W	36.2912	36.2957	-0.0045
2009/5/18	2:28	17-30.00190S	149-10.30590W	36.2251	36.2292	-0.0041
2009/5/18	7:03	17-29.95660S	149-19.96200W	36.2223	36.2345	-0.0122
2009/5/22	0:57	17-29.84320S	150-05.34030W	36.1993	36.1916	0.0077
2009/5/22	13:27	17-29.91300S	151-16.85460W	36.1192	36.1159	0.0033
2009/5/23	1:14	17-30.41760S	152-43.27130W	36.038	36.0309	0.0071
2009/5/23	13:20	17-30.39290S	154-03.86520W	35.9694	35.9629	0.0065
2009/5/23	19:06	17-30.73690S	154-19.15890W	35.9772	35.9698	0.0074
2009/5/26	0:33	17-30.27460S	150-56.34070W	36.148	36.1428	0.0052
2009/5/26	7:46	17-28.15840S	152-47.88450W	36.0207	36.0145	0.0062
2009/5/26	7:48	17-28.15860S	152-48.39390W	36.0187	36.0123	0.0064
2009/5/27	2:22	17-29.71150S	155-39.65110W	35.935	35.9279	0.0071
2009/5/27	12:43	17-30.14850S	156-59.98330W	35.9856	35.9789	0.0067
2009/5/28	2:43	17-30.05130S	158-21.80860W	35.6579	35.6521	0.0058
2009/5/28	13:17	17-29.60850S	159-40.16600W	35.7293	35.7217	0.0076
2009/5/29	3:15	17-29.62850S	161-00.53220W	35.7593	35.7527	0.0066
2009/5/29	12:44	17-29.84780S	162-20.19010W	35.5213	35.5153	0.0060
2009/5/29	12:46	17-29.84070S	162-20.19980W	35.5218	35.5148	0.0070
2009/5/30	0:51	17-29.71710S	163-40.22410W	35.5298	35.5240	0.0058
2009/5/30	13:14	17-29.86090S	165-00.09660W	35.658	35.6523	0.0057
2009/5/31	2:37	17-29.50610S	166-20.56290W	35.3233	35.3168	0.0065
2009/5/31	12:34	17-29.75890S	167-19.39840W	35.2629	35.2559	0.0070
2009/6/1	2:10	17-30.02270S	168-57.87450W	35.1326	35.1238	0.0088
2009/6/1	2:12	17-30.01870S	168-58.38400W	35.1286	35.1222	0.0064
2009/6/1	13:19	17-30.12720S	169-57.96900W	35.6192	35.6121	0.0071
2009/6/2	2:06	17-30.09560S	171-19.29490W	35.3532	35.3447	0.0085
2009/6/2	13:53	17-29.47620S	172-09.08020W	35.3759	35.3695	0.0064
2009/6/3	2:19	17-29.86830S	172-39.93180W	35.3979	35.3921	0.0058
2009/6/3	13:42	17-29.76370S	172-59.95610W	35.4848	35.4781	0.0067
2009/6/4	1:57	17-29.15390S	174-53.24790W	35.1388	35.1300	0.0088
2009/6/4	2:00	17-29.24690S	174-54.02150W	35.1391	35.1312	0.0079
2009/6/4	14:06	17-29.84240S	176-29.21680W	35.4266	35.4206	0.0060
2009/6/5	1:48	17-45.08660S	178-15.00220W	35.5201	35.5144	0.0057
2009/6/5	14:08	18-24.86800S	179-39.44760W	35.0543	35.0458	0.0085
2009/6/6	4:37	18-25.14400S	178-19.77450E	34.7175	34.7105	0.0070
2009/6/6	15:05	18-34.43890S	177-15.01060E	34.8111	34.8052	0.0059
2009/6/7	3:07	17-49.80500S	176-20.13720E	34.8422	34.8366	0.0056
2009/6/7	3:09	17-49.80020S	176-20.14540E	34.8446	34.8362	0.0084
2009/6/7	14:51	17-49.96720S	174-30.44490E	34.7476	34.7396	0.0080
2009/6/8	3:29	17-50.20620S	172-57.74250E	34.7886	34.7854	0.0032
2009/6/8	16:16	17-50.03360S	171-00.02810E	34.8332	34.8284	0.0048
2009/6/9	3:14	17-49.98500S	169-39.81200E	34.8549	34.8498	0.0051
2009/6/9	14:51	18-08.76050S	168-35.87720E	34.8734	34.8673	0.0061
2009/6/9	14:54	18-08.72630S	168-35.86890E	34.8733	34.8673	0.0060
2009/6/10	3:33	18-28.98480S	167-48.94890E	34.8825	34.8751	0.0074

Date [UTC]	Time [UTC]	Latitude	Longitude	Sensor salinity [PSS-78]	Bottle salinity [PSS-78]	Difference [Sen. - Bot.]
2009/6/10	15:10	18-41.83330S	167-18.97920E	34.668	34.6618	0.0062
2009/6/11	4:30	19-09.22850S	166-15.30210E	34.6166	34.6111	0.0055
2009/6/11	15:48	19-35.14790S	165-13.44460E	34.8688	34.8621	0.0067
2009/6/12	4:20	19-55.09680S	164-26.87740E	34.7665	34.7596	0.0069
2009/6/12	4:23	19-55.03730S	164-27.09530E	34.7686	34.7604	0.0082
2009/6/12	14:15	18-41.18910S	163-27.76470E	34.7966	34.7912	0.0054
2009/6/13	5:09	20-52.28470S	164-12.34210E	34.9014	34.8964	0.0050
2009/6/13	15:40	20-58.30450S	164-05.86780E	35.1654	35.1531	0.0123
2009/6/14	4:12	21-28.99900S	162-45.98240E	34.894	34.8870	0.0070
2009/6/14	15:44	22-05.92740S	161-12.07260E	35.2426	35.2314	0.0112
2009/6/15	4:55	22-43.07240S	159-39.05030E	35.2074	35.1999	0.0075
2009/6/15	4:57	22-43.07120S	159-39.05450E	35.2077	35.2009	0.0068
2009/6/15	15:44	23-15.94420S	158-15.27150E	35.2435	35.2369	0.0066
2009/6/16	4:18	23-52.07610S	156-43.12080E	35.3243	35.3164	0.0079
2009/6/16	16:06	24-20.93430S	155-30.04440E	35.2284	35.2212	0.0072
2009/6/17	5:24	24-46.82500S	154-19.41980E	35.437	35.4248	0.0122
2009/6/17	18:53	25-02.01130S	153-38.93560E	35.3601	35.3536	0.0065

2.4 Underway pCO₂

December 4, 2010

(1) Personnel

Akihiko Murata (RIGC, JAMSTEC)
 Minoru Kamata (MWJ)
 Yoshiko Ishikawa (MWJ)
 Yasuhiro Arie (MWJ)

(2) Introduction

Concentrations of CO₂ in the atmosphere are now increasing at a rate of 1.9 ppmv y⁻¹ due to human activities such as burning of fossil fuels, deforestation, cement production, etc. It is an urgent task to estimate as accurately as possible the absorption capacity of the ocean against the increased atmospheric CO₂, and to clarify the mechanism of the CO₂ absorption, because the magnitude of the predicted global warming depends on the levels of CO₂ in the atmosphere, and because the ocean currently absorbs 1/3 of the 6 Gt of carbon emitted into the atmosphere each year by human activities.

In the P21 revisit cruise, we were aimed at quantifying how much anthropogenic CO₂ is absorbed in the surface ocean in the Pacific. For the purpose, we measured pCO₂ (partial pressures of CO₂) in the atmosphere and in the surface seawater.

(3) Apparatus and shipboard measurement

Continuous underway measurements of atmospheric and surface seawater pCO₂ were made with the CO₂ measuring system (Nippon ANS, Ltd) installed in the R/V Mirai of JAMSTEC. The system comprises of a non-dispersive infrared gas analyzer (NDIR; BINOS® model 4.1, Fisher-Rosemount), an air-circulation module and a showerhead-type equilibrator. To measure concentrations (mole fraction) of CO₂ in dry air (xCO₂a), air sampled from the bow of the ship (approx. 30 m above the sea level) was introduced into the NDIR through a dehydrating route with an electric dehumidifier (kept at -2°C), a Perma Pure dryer (GL Sciences Inc.), and a chemical desiccant

(Mg(ClO₄)₂). The flow rate of the air was 500 ml min⁻¹. To measure surface seawater concentrations of CO₂ in dry air (xCO_{2s}), the air equilibrated with seawater within the equilibrator was introduced into the NDIR through the same flow route as the dehydrated air used in measuring xCO_{2a}. The flow rate of the equilibrated air was 600 - 800 ml min⁻¹. The seawater was taken by a pump from the intake placed at the approx. 4.5 m below the sea surface. The flow rate of seawater in the equilibrator was 500 - 800 ml min⁻¹.

The CO₂ measuring system was set to repeat the measurement cycle such as 4 kinds of CO₂ standard gases (Table 2.4.1), xCO_{2a} (twice), xCO_{2s} (7 times). This measuring system was run automatically throughout the cruise by a PC control.

(4) Quality control

Concentrations of CO₂ of the standard gases are listed in Table 2.4.1, which were calibrated by the JAMSTEC primary standard gases. The CO₂ concentrations of the primary standard gases were calibrated by C.D. Keeling of the Scripps Institution of Oceanography, La Jolla, CA, USA.

Since differences of concentrations of the standard gases between before and after the cruise were allowable (<0.1 ppmv), the averaged concentrations (Table 2.4.1) were adopted for the subsequent calculations.

In actual shipboard observations, the signals of NDIR usually reveal a trend. The trends were adjusted linearly using the signals of the standard gases analyzed before and after the sample measurements.

Effects of water temperature increased between the inlet of surface seawater and the equilibrator on xCO_{2s} were adjusted based on Gordon and Jones (1973), although the temperature increases were slight, being -0.3°C.

We checked values of xCO_{2a} and xCO_{2s} by examining signals of the NDIR on recorder charts, and by plotting the xCO_{2a} and xCO_{2s} as a function of sequential day, longitude, sea surface temperature and sea surface salinity.

Reference

Gordon, L.I. and L.B. Jones (1973) The effect of temperature on carbon dioxide partial pressure in seawater. Mar. Chem., 1, 317-322.

Table 2.4.1: Concentrations of CO₂ standard gases used during MR09-01 cruise.

Cylinder no.	Concentrations (ppmv)
CQC00742	270.22
CQC00739	330.43
CQC00740	360.04
CQC00741	420.32

2.5 Acoustic Doppler Current Profiler (ADCP)

November 1, 2010

(1) Personnel

<i>Shinya Kouketsu</i>	(JAMSTEC)	
<i>Shinya Okumura</i>	(Global Ocean Development Inc., GODI)	-leg1-
<i>Ryo Kimura</i>	(GODI)	-leg1, 3-
<i>Yousuke Yuki</i>	(GODI)	-leg1-
<i>Satoshi Okumura</i>	(GODI)	-leg2-
<i>Kazuho Yoshida</i>	(GODI)	-leg2-
<i>Harumi Ohta</i>	(GODI)	-leg2-
<i>Souichiro Sueyoshi</i>	(GODI)	-leg3-

(2) Objective

To obtain continuous measurement of the current profile along the ship's track.

(3) Methods

Upper ocean current measurements were made throughout MR09-01 cruise, using the hull mounted Acoustic Doppler Current Profiler (ADCP) system. For most of its operation, the instrument was configured for water-tracking mode recording. Bottom-tracking mode, interleaved bottom-ping with water-ping, was made in shallower water region to get the calibration data for evaluating transducer misalignment angle.

The system consists of following components;

- 1) R/V MIRAI has installed the Ocean Surveyor for vessel-mount (acoustic frequency 75 kHz; Teledyne RD Instruments). It has a phased-array transducer with single ceramic assembly and creates 4 acoustic beams electronically. We mounted the transducer head rotated to a ship-relative angle of 45 degrees azimuth from the keel.
- 2) For heading source, we use ship's gyro compass (Tokimec, Japan), continuously providing heading to the ADCP system directory. Additionally, we have Inertial Navigation System (INS) which provide high-precision heading, attitude information, pitch and roll, are stored in ".N2R" data files with a time stamp.
- 3) GPS navigation receiver (Trimble D54000) provides position fixes.
- 4) We used VmDas version 1.4.2 (TRD Instruments) for data acquisition.
- 5) To synchronize time stamp of ping with GPS time, the clock of the logging computer is adjusted to GPS time every 1 minute.
- 6) The sound speed at the transducer does affect the vertical bin mapping and vertical velocity measurement, is calculated from temperature, salinity (constant value; 35.0 psu) and depth (6.5 m; transducer depth) by equation in Medwin (1975).

The data was configured for 4 m processing bin, 4 m intervals and starting 20 m below the surface. Every ping was recorded as raw ensemble data (.ENR). Also, 60 seconds and 300 seconds averaged data were recorded as short term average (.STA) and long term average (.LTA) data, respectively. We changed the major parameters, and showed the date and time that we changed command file.

(4) Data processing

We processed ADCP data as described below. ADCP-coordinate velocities were converted to the earth-coordinate velocities using the ship heading from the INU. The earth-coordinate currents were obtained by subtracting ship velocities from the earth-coordinate velocities. Corrections of the misalignment and scale factors were made using the bottom track data. The misalignment angle calculated was 0.15, the scale factor was 1.00.

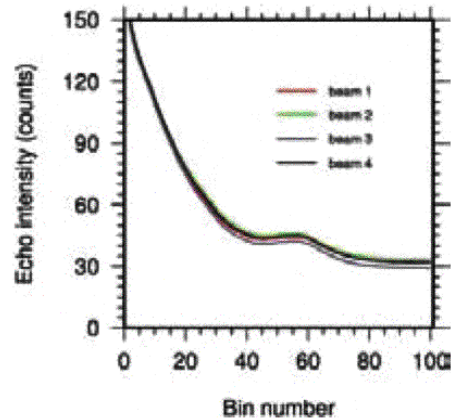


Figure 2.5.1. Cruise-averaged echo intensities.

(5) Remarks

The profile with had quality is included between 200 m in depth and 400 m while in this cruise corresponding to weak echo intensities (Fig. 2.5.1 causes of the weak echo intensity may be considered during data processing after cruise).

2.6 XCTD

February 8, 2011

(1) Personnel

Hiroshi Uchida (JAMSTEC)

Leg 1

Shinya Okumura (GODI)

Ryo Kimura (GODI)

Yosuke Yuki (GODI)

Leg 2

Satoshi Okumura (GODI)

Kazuho Yoshida (GODI)

Harumi Ota (GODI)

(2) Objectives

In this cruise, XCTD (expendable Conductivity, Temperature and Depth profiler) measurements were carried out to examine short-term changes in temperature and salinity profiles, and to evaluate fall rate equations by comparing with CTD (Conductivity, Temperature and Depth profiler) measurements and bottom topography measurements.

(3) Instrument and Method

The XCTDs used were XCTD-1 and XCTD-2 (Tsurumi-Seiki Co., Ltd., Yokohama, Kanagawa, Japan) with an MK-130 deck unit (Tsurumi-Seiki Co., Ltd.). The manufacturer's specifications are listed in [Table 2.6.1](#). In this cruise, seven XCTD-1 probes and twenty-three XCTD-2 probes were deployed by using 8-loading automatic launcher (Tsurumi-Seiki Co., Ltd.) ([Table 2.6.2](#)). Ship's speed was slowed down to 3 knot during the XCTD-2 measurement. For the comparison with CTD, XCTD was deployed at about 5 minutes for XCTD-1 and at about 10 minutes for XCTD-2 after the beginning of the down cast of the CTD.

Table 2.6.1: Manufacturer's specifications of XCTD-1 and XCTD-2.

Parameter	Range	Accuracy
Conductivity	0 - 60 mS cm ⁻¹	±0.03 mS cm ⁻¹
Temperature	-2 - 35°C	±0.02°C
Depth	0 - 1000 m (for XCTD-1)	5 m or 2%, whichever is greater *
	0 - 1850 m (for XCTD-2)	5 m or 2%, whichever is greater *

* Depth error is shown in Kizu et al (2008).

(4) Data Processing and Quality Control

The XCTD data were processed and quality controlled based on a method by Uchida et al. (2011). Thermal bias (+0.016°C) of the XCTD data reported by Uchida et al. (2011) was not corrected. Depth error of the XCTD data was corrected by using the estimated terminal velocity error (-0.0428 m s⁻¹) (Uchida et al., 2011). Salinity biases of the XCTD data were estimated by using temperature and salinity relationships in the deep ocean obtained from the post-cruise calibrated CTD data (Table 2.6.2). For the XCTD data of the station P21291, salinity bias could not be estimated because the maximum depth was too shallow to estimate the salinity bias.

Vertical section of potential temperature is shown in Fig. 2.6.1 for stations between 29 and 33. Comparison with the CTD data shows short-term fluctuation in temperature between the observation periods 6 days apart.

References

Kizu, S., H. Onishi, T. Suga, K. Hanawa, T. Watanabe, and H. Iwamiya (2008): Evaluation of the fall rates of the present and developmental XCTDs. *Deep-Sea Res I*, 55, 571-586.

Uchida, H., K. Shimada, and T. Kawano (2011): A method for data processing to obtain high quality XCTD data. *J. Atmos. Oceanic Technol.*, accepted.

Table 2.6.2: Serial number and probe type of the XCTD. Water depth, ship intake temperature (SST) and salinity (SSS; not corrected), and maximum pressure for the XCTD data are shown. Salinity offset applied to the XCTD data and reference salinity estimated from the CTD data are also shown.

Station	Serial number (type)	Depth [m]	SST [°C]	SSS [PSU]	Max pressure [dbar]	Salinity offset [PSU]	Reference salinity [PSU]
<i>Leg 1</i>							
29_1*	08112315 (2)	3798	23.759	35.444	187**	-	NA
29_2*	08112312 (2)	3816	23.725	35.430	1967	0.009	34.6215 @ 2.5°C
30_1*	08112308 (2)	4462	24.249	35.432	1967	0.021	34.6215 @ 2.5°C
31_1*	08112304 (2)	4441	24.815	35.497	1913	0.022	34.6215 @ 2.5°C
32_1*	08112309 (2)	4713	23.453	35.480	1917	0.007	34.6215 @ 2.5°C
33_1*	08112306 (2)	4442	23.787	35.538	1967	0.014	34.6215 @ 2.5°C
41_1	03022164 (1)	4659	23.975	35.456	1036	0.023	34.5219 @ 4.5°C
41_2	08112305 (2)	4659	23.977	35.455	1967	0.007	34.6215 @ 2.5°C
34_1	08112307 (2)	4536	24.030	35.505	1967	0.012	34.6215 @ 2.5°C
34_2	07022711 (1)***	4537	24.029	35.505	1037	0.000	34.5219 @ 4.5°C
42_1	03022159 (1)	4558	23.544	35.584	1037	-0.017	34.5219 @ 4.5°C
42_2	08112310 (2)	4572	23.547	35.585	1967	0.015	34.6215 @ 2.5°C
96_1	03022156 (1)	3732	25.612	36.217	1036	?0.005	34.5219 @ 4.5°C
96_2	08112311 (2)	3751	25.610	36.218	1967	0.007	34.6215 @ 2.5°C

Station	Serial number (type)	Depth [m]	SST [°C]	SSS [PSU]	Max pressure [dbar]	Salinity offset [PSU]	Reference salinity [PSU]
97_1	03022162 (1)	3462	25.592	36.166	1037	0.012	34.5219 @ 4.5°C
97_2	08112313 (2)	3453	25.591	36.166	1967	0.010	34.6215 @ 2.5°C
98_1	03022157 (1)	3287	25.649	36.149	1037	0.002	34.5219 @ 4.5°C
98_2	08112314 (2)	3297	25.659	36.162	1967	0.010	34.6215 @ 2.5°C
145_1	08112319 (2)	1505	28.117	36.244	1464	0.007	34.5665 @ 3.0°C
146_1	08112316 (2)	1530	27.918	36.291	1520	0.020	34.5665 @ 3.0°C
151_1	08112322 (2)	1531	28.009	36.315	1518	0.005	34.5665 @ 3.0°C
156_1	03022155 (1)	943	28.339	36.223	943	0.008	34.4726 @ 4.5°C

Leg 2

205_1	08112325 (2)	1365	28.097	35.430	1356	0.014	34.4781 @ 3.5°C
206_1	08112317 (2)	1484	27.978	35.548	1470	0.037	34.5512 @ 3.0°C
209_1	08112318 (2)	1924	27.032	35.260	1286 **	0.008	34.4911 @ 3.5°C
213_1	08112327 (2)	991	26.979	35.232	985	0.016	34.4238 @ 4.5°C
221_1	08112320 (2)	1883	26.466	34.783	1911	-0.004	34.6094 @ 2.5°C
250_1	08112321 (2)	1716	25.045	34.938	1700	0.013	34.5710 @ 3.0°C
266_1	08112324 (2)	1638	24.094	34.950	1631	-0.001	34.5860 @ 3.0°C
268_1	08112323 (2)	1562	23.496	35.227	1551	0.014	34.5860 @ 3.0°C

* Not for simultaneous measurements with CTD

** Failure of measurements due to noise or lost contact

*** Relatively large (about 30 minutes) time difference between CTD and XCTD measurements

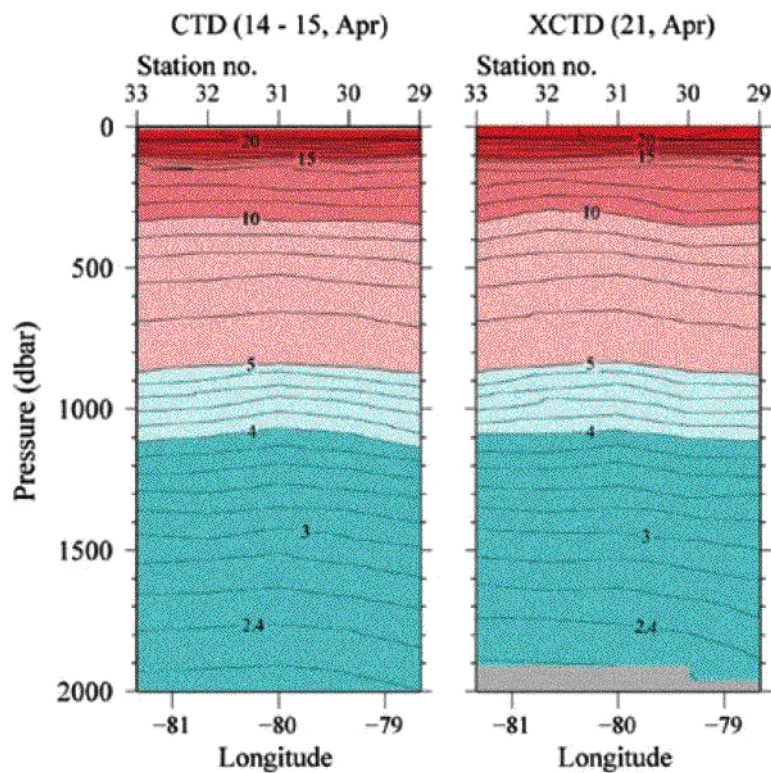


Figure 2.6.1: Vertical sections of potential temperature measured by CTD (left) and XCTD (right).

3 Hydrographic Measurement Techniques and Calibrations

3.1 CTDO₂ Measurements

February 16, 2010

(1) Personnel

Hiroshi Uchida (JAMSTEC)
Wolfgang Schneider (University of Concepcion, Chile)

Leg 1 and leg 2a

Kenichi Katayama (MWJ)
Shinsuke Toyoda (MWJ)
Hirokatsu Uno (MWJ)
Hiroyuki Hayashi (MWJ)

Leg 2b

Tomoyuki Takamori (MWJ)
Hiroshi Matsunaga (MWJ)
Masayuki Fujisaki (MWJ)
Shungo Oshitani (MWJ)
Satoshi Ozawa (MWJ)

(2) Winch arrangements

The CTD package was deployed by using 4.5 Ton Traction Winch System (Dynacon, Inc., Bryan, Texas, USA), which was installed on the R/V Mirai in April 2001 (Fukasawa et al., 2004). Primary system components include a complete CTD Traction Winch System with up to 8000 m of 9.53 mm armored cable (Rochester Wire & Cable).

(3) Overview of the equipment

The CTD system was SBE 911plus system (Sea-Bird Electronics, Inc., Bellevue, Washington, USA). The SBE 911plus system controls 36-position SBE 32 Carousel Water Sampler. The Carousel accepts 12-litre Niskin-X water sample bottles (General Oceanics, Inc., Miami, Florida, USA). The SBE 9plus was mounted horizontally in a 36-position carousel frame. SBE's temperature (SBE 3) and conductivity (SBE 4) sensor modules were used with the SBE 9plus underwater unit. The pressure sensor is mounted in the main housing of the underwater unit and is ported to outside through the oil-filled plastic capillary tube. A modular unit of underwater housing pump (SBE 5T) flushes water through sensor tubing at a constant rate independent of the CTD's motion, and pumping rate (3000 rpm) remain nearly constant over the entire input voltage range of 1218 volts DC. Flow speed of pumped water in standard TC duct is about 2.4 m/s. Two sets of temperature and conductivity modules were used. An SBE's dissolved oxygen sensor (SBE 43) was placed between the primary conductivity sensor and the pump module. Auxiliary sensors, a Deep Ocean Standards Thermometer (SBE 35), an altimeter (PSA-916T; Teledyne Benthos, Inc., North Falmouth, Massachusetts, USA), three oxygen optodes (Oxygen Optode 3830 and 4330F; Aanderaa Data Instruments AS, Bergen, Norway, and a prototype of RINKO-III; JFE Alec Co., Ltd, Kobe Hyogo, Japan), a fluorometer (Seapoint sensors, Inc., Kingston, New Hampshire, USA), and a transmissometer (C-Star Transmissometer; WET Labs, Inc., Philomath, Oregon, USA) were also used with the SBE 9plus underwater unit. To minimize motion of the CTD package, a heavy stainless frame (total weight of the CTD package without sea water in the bottles is about 1000 kg) was used with an aluminum plate (54 x 90 cm).

Summary of the system used in this cruise

Deck unit:

SBE 11plus, S/N 0272

Under water unit:

SBE 9plus, S/N 79511 (Pressure sensor: S/N 0677)

Temperature sensor:

SBE 3plus, S/N 4815 (primary)

SBE 3, S/N 1525 (secondary)

Conductivity sensor:

SBE 4, S/N 2854 (primary)

SBE 4, S/N 1203 (secondary: stations from P21_14_1 to P21_86_1)

SBE 4, S/N 3261 (secondary: stations from P21_87_1 to P21_288_1)

Oxygen sensor:

SBE 43, S/N 0394 (stations from P21_14_1 to P21_76_1)

SBE 43, S/N 0330 (stations from P21_X18_1 to P21_288_1)

AANDERAA Oxygen Optode 3830, S/N 612 (foil batch no. 1707)

AANDERAA Oxygen Optode 4330E S/N 143 (foil batch no. 2808F)

JFE Alec RINKO-III, S/N 006 (foil batch no. 131002A)

Pump:

SBE 5T, S/N 4598 (primary)

SBE 5T, S/N 4595 (secondary)

Altimeter:

PSA-916T, S/N 1100

Deep Ocean Standards Thermometer:

SBE 35, S/N 0045

Fluorometer:

Seapoint Sensors, Inc., S/N 3054

Transmissometer:

C-Star, S/N CST-207RD

Carousel Water Sampler:

SBE 32, S/N 0391

Water sample bottle:

12-litre Niskin-X model 1010X (no TEFLON coating)

* without Oxygen Optode 4330E fluorometer, and transmissometer at station P21_200_1

(4) Pre-cruise calibration

i. Pressure

The Paroscientific series 4000 Digiquartz high pressure transducer (Model 415K-187; Paroscientific, Inc., Redmond, Washington, USA) uses a quartz crystal resonator whose frequency of oscillation varies with pressure induced stress with 0.01 per million of resolution over the absolute pressure range of 0 to 15000 psia (0 to 10332 dbar). Also, a quartz crystal temperature signal is used to compensate for a wide range of temperature changes at the time of an observation. The pressure sensor has a nominal accuracy of 0.015% FS (1.5 dbar), typical stability of 0.0015% FS/month (0.15 dbar/month), and resolution of 0.001% FS (0.1 dbar). Since the pressure sensor measures the absolute value, it inherently includes atmospheric pressure (about 14.7 psi). SEASOFT subtracts 14.7 psi from computed pressure automatically.

Pre-cruise sensor calibrations for linearization were performed at SBE, Inc.

S/N 0677, 4 May 2007

The time drift of the pressure sensor is adjusted by periodic recertification corrections against a dead-weight piston gauge (Model 480DA, S/N 23906; Bundenberg Gauge Co. Ltd., Irlam, Manchester, UK). The corrections are performed at JAMSTEC, Yokosuka, Kanagawa, Japan by Marine Works Japan Ltd. (MWJ), Yokohama, Kanagawa, Japan, usually once in a year in order to monitor sensor time drift and linearity.

S/N 0677, 9 December 2008

slope = 0.99977580
offset = -0.02383

Result of the pre-cruise pressure sensor calibration against the dead-weight piston gauge is shown in Fig. 3.1.1.

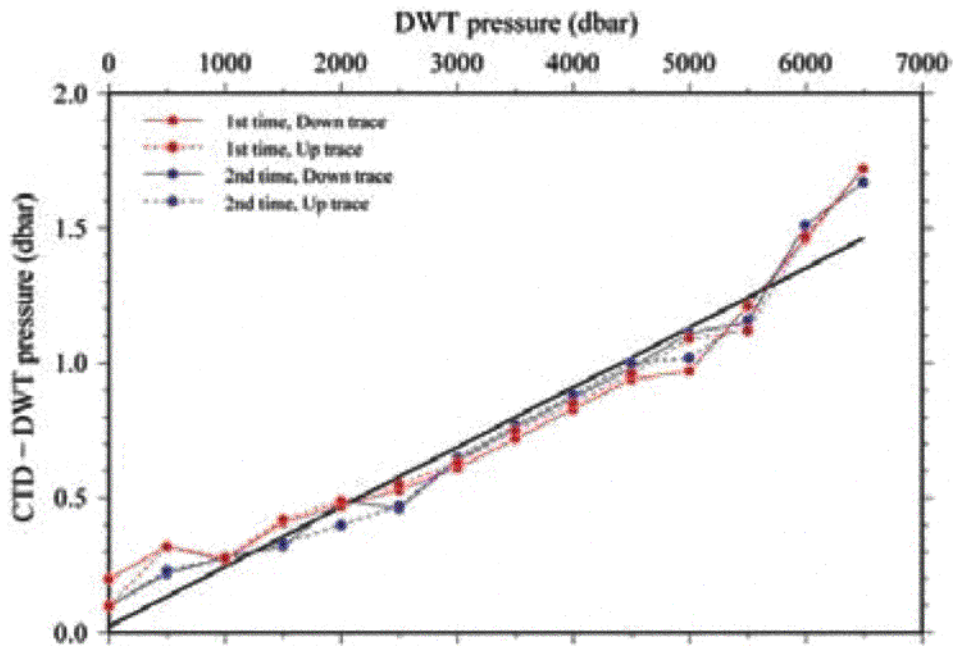


Figure 3.1.1: Difference between the dead-weight piston gauge and the CTD pressure. The calibration line (black line) is also shown.

ii. Temperature (SBE 3)

The temperature sensing element is a glass-coated thermistor bead in a stainless steel tube, providing a pressure-free measurement at depths up to 10500 (6800) m by titanium (aluminum) housing. The SBE 3 thermometer has a nominal accuracy of 1 mK, typical stability of 0.2 mK/month, and resolution of 0.2 mK at 24 samples per second. The premium temperature sensor, SBE 3plus, is a more rigorously tested and calibrated version of standard temperature sensor (SBE 3).

Pre-cruise sensor calibrations were performed at SBE, Inc.

S/N 4815, 26 November 2008
S/N 1525, 25 November 2008

Pressure sensitivity of SBE 3 was corrected according to a method by Uchida et al. (2007), for the following sensor.

S/N 4815, $-3.45974716 \times 10^{-7}$ [°C/dbar]
S/N 1525, 5.92243×10^{-9} [°C/dbar]

Time drift of the SBE 3 temperature sensors based on the laboratory calibrations is shown in Fig. 3.1.2.

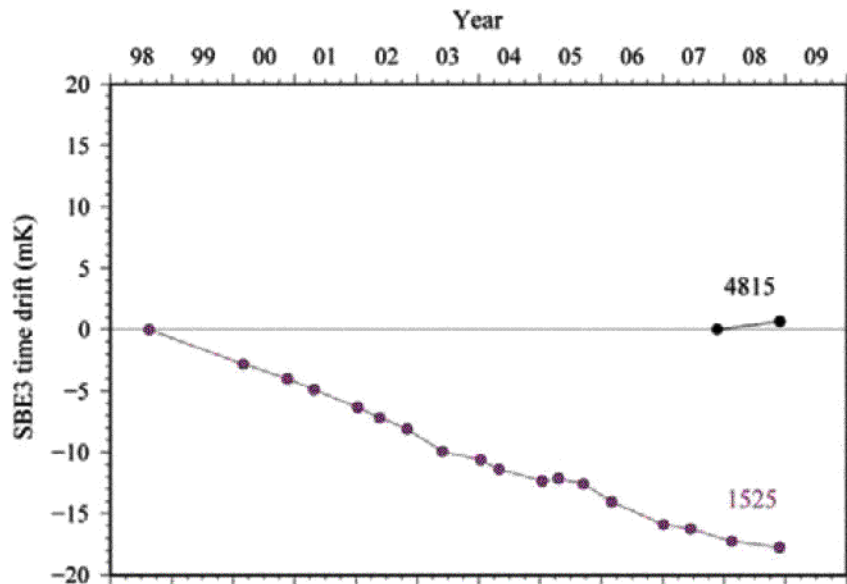


Figure 3.1.2: Time drift of SBE 3 temperature sensors based on laboratory calibrations.

iii. Conductivity (SBE 4)

The flow-through conductivity sensing element is a glass tube (cell) with three platinum electrodes to provide in-situ measurements at depths up to 10500 (6800) m by titanium (aluminum) housing. The SBE 4 has a nominal accuracy of 0.0003 S/m, typical stability of 0.0003 S/m/month, and resolution of 0.00004 S/m at 24 samples per second.

Pre-cruise sensor calibrations were performed at SBE, Inc.

S/N 2954, 25 November 2008 (new cell preventing a stress concentration)
S/N 1203, 12 December 2008 (new cell preventing a stress concentration)
S/N 3261, 17 December 2008 (new cell preventing a stress concentration)

The value of conductivity at salinity of 35, temperature of 15°C (IPTS-68) and pressure of 0 dbar is 4.2914 S/m.

iv. Oxygen (SBE 43)

The SBE 43 oxygen sensor uses a Clark polarographic element to provide in-situ measurements at depths up to 7000 in. The range for dissolved oxygen is 120% of surface saturation in all natural waters, nominal accuracy is 2% of saturation, and typical stability is 2% per 1000 hours.

Pre-cruise sensor calibrations were performed at SBE, Inc. S/N 0394, 20 December 2008 S/N 0330, 20 December 2008

v. Deep Ocean Standards Thermometer

Deep Ocean Standards Thermometer (SBE 35) is an accurate, ocean-range temperature sensor that can be standardized against Triple Point of Water and Gallium Melt Point cells and is also capable of measuring temperature in the ocean to depths of 6800 m. The SBE 35 was used to calibrate the SBE 3 temperature sensors in situ (Uchida et al., 2007).

Pre-cruise sensor linearization was performed at SBE, Inc.

S/N 0045, 27 October 2002

Then the SBE 35 is certified by measurements in thermodynamic fixed-point cells of the TPW (0.01°C) and GaMP (29.7646°C). The slow time drift of the SBE 35 is adjusted by periodic recertification corrections. Pre-cruise sensor calibration was performed at SBE, Inc.

S/N 0045, 23 December 2008 (slope and offset correction)

The time required per sample = 1.1 x NCYCLES + 2.7 seconds. The 1.1 seconds is total time per an acquisition cycle. NCYCLES is the number of acquisition cycles per sample and was set to 4. The 2.7 seconds is required for converting the measured values to temperature and storing average in EEPROM.

When using the SBE 911 system with SBE 35, the deck unit receives incorrect signal from the under water unit for confirmation of firing bottle #16. In order to correct the signal, a module (Yoshi Ver. 1; EMS Co. Ltd., Kobe, Hyogo, Japan) was used between the under water unit and the deck unit.

Time drift of the SBE 35 based on the fixed point calibrations is shown in Fig. 3.1.3.

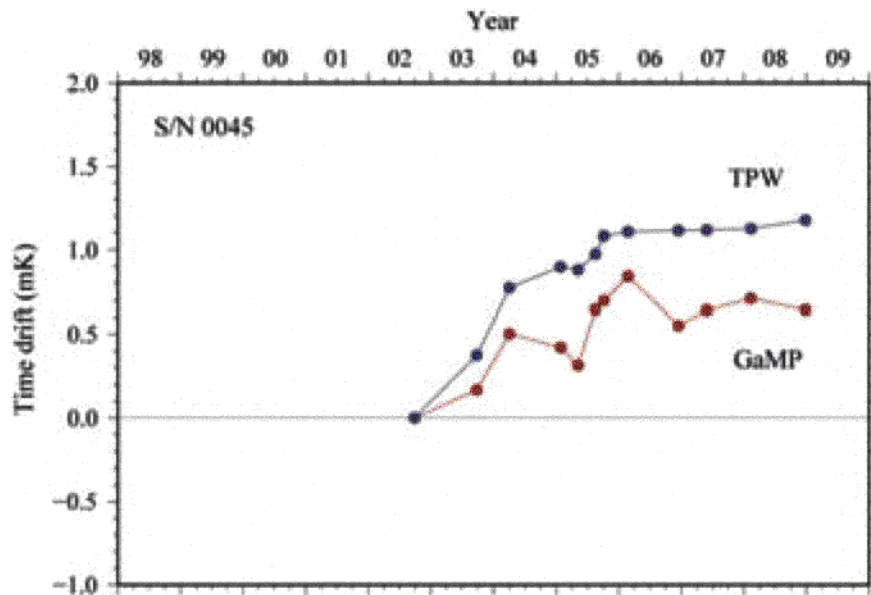


Figure 3.1.3: SBE35 time drift based on laboratory fixed point calibrations (triple point of water, TPW and gallium melt point, GaMP) performed by SBE, Inc.

vi. Altimeter

Benthos PSA-916T Sonar Altimeter (Teledyne Benthos, Inc.) determines the distance of the target from the unit by generating a narrow beam acoustic pulse and measuring the travel time for the pulse to bounce back from the target surface. It is rated for operation in water depths up to 10000 m. The PSA-916T uses the nominal speed of sound of 1500 m/s.

vii. Oxygen Optode

(a) Oxygen Optode 3830

Oxygen Optode 3830 (Aanderaa Data Instruments AS) is based on the ability of selected substances to act as dynamic fluorescence quenchers. In order to use with the SBE 911plus CTD system, an analog adaptor (3966) is connected to the oxygen optode (3830). The analog adaptor is packed into titanium housing made by Alec Electronics Co., Ltd. The sensor is designed to operate down to 6000 m. The range for dissolved oxygen is 120% of surface saturation in all natural waters, nominal accuracy is less than $8 \mu\text{M}$ or 5% of saturation which ever is greater and setting time (63%) is shorter than 25 seconds.

(b) Oxygen Optode 4330F

Oxygen Optode 4330F (Aanderaa Data Instruments AS) is based on the ability of selected substances to act as dynamic fluorescence quenchers. In order to use with the SBE 911plus CTD system, an analog adaptor (3966) with titanium housing for Oxygen Optode 3975 is connected to the oxygen optode (4330F). The sensor is designed to operate down to 6000 m. The range for dissolved oxygen is 150% of surface saturation in all natural waters, nominal accuracy is less than $8 \mu\text{M}$ or 5% of saturation which ever is greater and setting time (63%) is shorter than 8 seconds.

(c) RINKO

RINKO (JFE Alec Co., Ltd.) is based on the ability of selected substances to act as dynamic fluorescence quenchers. RINKO model III is designed to use with a CTD system which accept an auxiliary analog sensor, and is designed to operate down to 7000 m.

Outputs from Optode 3830 and RINKO are the raw phase shift data. Raw phase shift data for Optode 4330F can be back calculated from the outputs (oxygen concentration and temperature). The optode oxygen can be calibrated by the Stern-Volmer equation, according to a method by Uchida et al. (2008) with slight modification:

$$\text{O}_2 (\mu\text{mol/l}) = [(V_0 / V)^2 - 1] / K_{SV}$$

where V is voltage, V_0 is voltage in the absence of oxygen and K_{SV} is Stern-Volmer constant. The V_0 and the K_{SV} are assumed to be functions of temperature as follows.

$$K_{SV} = C_0 + C_1 \times T + C_2 \times T^2$$

$$V_0 = 1 + C_3 \times T$$

$$V = C_4 + C_5 \times V_b$$

where T is CTD temperature ($^{\circ}\text{C}$) and V_b is raw output (volts). V_0 and V are normalized by the output in the absence of oxygen at 0°C . The oxygen concentration is calculated using temperature data from the first responding CTD temperature sensor instead of temperature data from slow responding optode temperature sensor. The pressure-compensated oxygen concentration O_{2c} can be calculated as follows.

$$\text{O}_{2c} = \text{O}_2 (1 + C_p p / 1000)^{1/3}$$

where p is CTD pressure (dbar) and C_p is the compensation coefficient. Since the sensing foil of the optode is permeable only to gas and not to water, the optode oxygen must be corrected for salinity. The salinity-compensated oxygen can be calculated by multiplying the factor of the effect of salt on the oxygen solubility (Garcia and Gordon, 1992). Garcia and Gordon (1992) have recommended the use of the solubility coefficients derived from the data of Benson and Krause.

The calibration coefficients were preliminary determined by using the bottle oxygen data obtained in this cruise, and used during the cruise.

viii. Fluorometer

The Seapoint Chlorophyll Fluorometer (Seapoint Sensors, Inc., Kingston, New Hampshire, USA) provides in-situ measurements of chlorophyll-a at depths up to 6000 m. The instrument uses modulated blue LED lamps and a blue excitation filter to excite chlorophyll-a. The fluorescent light emitted by the chlorophyll-a passes through a red emission filter and is detected by a silicon photodiode. The low level signal is then processed using synchronous demodulation circuitry, which generates an output voltage proportional to chlorophyll-a concentration.

ix. Transmissometer

The C-Star Transmissometer (WET Labs, Inc., Philomath, Oregon, USA) measures light transmittance at a single wavelength over a known path. In general, losses of light propagating through water can be attributed to two primary causes: scattering and absorption. By projecting a collimated beam of light through the water and placing a focused receiver at a known distance away, one can quantify these losses. The ratio of light gathered by the receiver to the amount originating at the source is known as the beam transmittance. Suspended particles, phytoplankton, bacteria and dissolved organic matter contribute to the losses sensed by the instrument. Thus, the instrument provides information both for an indication of the total concentrations of matter in the water as well as for a value of the water clarity.

(5) Data collection and processing

i. Data collection

CTD system was powered on at least 20 minutes in advance of the data acquisition and was powered off at least two minutes after the operation in order to acquire pressure data on the ship's deck.

The package was lowered into the water from the starboard side and held 10 m beneath the surface in order to activate the pump. After the pump was activated, the package was lifted to the surface and lowered at a rate of 1.0 m/s to 200 m (or 300 m when significant wave height is high) then the package was stopped to operate the heave compensator of the crane. The package was lowered again at a rate of 1.2 m/s to the bottom. For the up cast, the package was lifted at a rate of 1.1 m/s except for bottle firing stops. At each bottle firing stop, the bottle was fired after waiting from the stop for 30 seconds (20 seconds from station P21_23_1) and the package was stayed at least 5 seconds for measurement of the SBE 35. At 200 m (or 300 m) from the surface, the package was stopped to stop the heave compensator of the crane.

Water samples were collected using a 36-bottle SBE 32 Carousel Water Sampler with 12-litre Niskin-X bottles. Before a cast taken water for CFCs, the 36-bottle frame and Niskin-X bottles were wiped with acetone.

Data acquisition software

SEASAVE-Win32, version 7.18c

ii. Data collection problems

(a) Temperature and conductivity sensors

Since differences of temperature-salinity relationship calculated from the secondary sensors between downcast and upcast were larger than that calculated from the primary sensors, the secondary conductivity sensor S/N 1203 was replaced with the conductivity sensor S/N 3261 after the station P21_86_1. However, the differences were still larger than that calculated from the primary sensors. The results suggest that the secondary temperature sensor S/N 1525 may have a pressure hysteresis relatively larger than the primary temperature sensor.

At the station P21161, the primary temperature and conductivity data were noisy probably due to jellyfish in the primary TC duct. Therefore, the second cast P21_16_2 was carried out.

At the station P21261, the primary temperature and conductivity data were noisy probably due to jellyfish in the primary TC duct. Since the second cast was not carried out, the secondary temperature and conductivity data must be used for this station.

(b) SBE43 oxygen sensor

Since differences between downcast and upcast profiles near the surface gradually became large, the SBE43 oxygen sensor S/N 0394 was replaced with the oxygen sensor S/N 0330 after the station P21_76_1.

(c) Miss trip and miss fire

Niskin bottles did not trip correctly at the following stations.

Miss trip	Miss fire
P21331, #13	P21611, #14
P21181, #13	P21691, #15
P21361, #15	P211771, #21
	P211851, #21
	P211881, #21
	P212551, #33

(d) Problem of the Niskin bottle #13

Discrepancies between CTD salinity and bottle sampled salinity data for the bottle #13 (about 3000 dbar) were slightly larger (about 0.001) than that obtained from neighboring bottles during leg 1. Bottle salinity data were obtained from a different bottle at the same depth of following stations, and were compared with the bottle salinity data obtained from the bottle #13.

Bottle #2 of P21471

Bottle #3 of P211311, P211321, P211331, P211351, P211371

Bottle #9 of P211361

Mean difference with standard error between CTD salinity and bottle salinity data are -0.0021 ± 0.0002 and -0.0013 ± 0.0001 for the bottle #13 and for the duplicate bottles, respectively. Salinity data from bottle #13 were significantly smaller than the other bottles probably due to slight leakage, although leak was not found for the bottle #13 at the water sampling. Therefore, the Niskin bottle #13 (S/N X12013) was replaced with the Niskin bottle S/N X12014 after the station P21_141_1, and the bottle flags of #13 for stations from P21_29_1 to P21_141_1 were set to 7 (unknown problem). For the other water sampling parameters, significant difference was not detected for the duplicate bottle comparison (#2 and #13) at the station P21471.

(e) Errors of bottle sampled oxygen data from nitrites

During the determination of dissolved oxygen by using the Winkler method, errors from nitrites were introduced at the time the solution was made acidic with sulfuric acid (Wetzel and Gene, 2000). Therefore, the bottle sampled oxygen data were corrected when the nitrite concentration was high ($> 0.5 \mu\text{mol/kg}$) as follows and used for the CTD oxygen calibration.

$$O_{2c} = O_2 - 0.25 \text{ NO}_2$$

If the nitrite concentration was higher than $5 \mu\text{mol/kg}$, the bottle sampled oxygen data was not used, because the error was significantly greater than 0.25 NO_2 .

(f) Other incidents of note

At the station P21_200_1, Oxygen Optode 4330F, fluorometer, and transmissometer were removed from the CTD system, because the maximum pressure (6500 dbar) for the cast was beyond the proof pressure of these sensors (6000 m).

To gain more observation time, the bottle was fired after waiting from the stop for 20 seconds at each bottle firing stops from station P21_23_1. Immediately after the bottle firing stop, water around the instruments can be contaminated by the wake effect (Uchida et al., 2007). Although the wake effect is usually large within the first 20 seconds of the stop, the data may somewhat contaminated by the wake effect.

At the station P21_97_1, the cast was aborted at 285 dbar of the down cast due to a bad condition of the winch system, and the second cast P21_97_2 was carried out. At the station P21_118_1, the cast was aborted at 54 dbar of the down cast due to a mistake of the parameter setting for the LADCP, and the second cast P21_118_2 was carried out.

iii. Data processing

SEASOFT consists of modular menu driven routines for acquisition, display, processing, and archiving of oceanographic data acquired with SBE equipment. Raw data are acquired from instruments and are stored as unmodified data. The conversion module DATCNV uses instrument configuration and calibration coefficients to create a converted engineering unit data file that is operated on by all SEASOFT post processing modules. The following are the SEASOFT and original software data processing module sequence and specifications used in the reduction of CTD data in this cruise.

Data acquisition software

SEASOFT-Win32, version 7.18c

DATCNV converted the raw data to engineering unit data. DATCNV also extracted bottle information where scans were marked with the bottle confirm bit during acquisition. The duration was set to 4.4 seconds, and the offset was set to 0.0 second. The hysteresis correction for the SBE 43 data (voltage) was applied for both profile and bottle information data.

TCORP (original module, version 1.1) corrected the pressure sensitivity of the SBE 3 for both profile and bottle information data.

RINKOCOR (original module, version 1.0) corrected the time-dependent, pressure-induced effect (hysteresis) of the RINKO for both profile data.

RINKOCORROS (original module, version 1.0) corrected the time-dependent, pressure-induced effect (hysteresis) of the RINKO for bottle information data by using the hysteresis-corrected profile data.

BOTTLESUM created a summary of the bottle data. The data were averaged over 4.4 seconds.

ALIGNCTD converted the time-sequence of sensor outputs into the pressure sequence to ensure that all calculations were made using measurements from the same parcel of water. For a SBE 9plus CTD with the ducted temperature and conductivity sensors and a 3000-rpm pump, the typical net advance of the conductivity relative to the temperature is 0.073 seconds. So, the SBE 11plus deck unit was set to advance the primary and the secondary conductivity for 1.73 scans ($1.75/24 = 0.073$ seconds). Oxygen data are also systematically delayed with respect to depth mainly because of the long time constant of the oxygen sensor and of an additional delay from the transit time of water in the pumped plumbing line. This delay was compensated by 5 seconds advancing oxygen sensor output (voltage) relative to the temperature data. Delay of the RINKO data was also compensated by 1 second advancing sensor output (voltage) relative to the temperature data.

WILDEDIT marked extreme outliers in the data files. The first pass of WILDEDIT obtained an accurate estimate of the true standard deviation of the data. The data were read in blocks of 1000 scans. Data greater than 10 standard deviations were flagged. The second pass computed a standard deviation over the same 1000 scans excluding the flagged values. Values greater than 20 standard deviations were marked bad. This process was applied to pressure, temperature, conductivity and SBE 43 output.

CELLTM used a recursive filter to remove conductivity cell thermal mass effects from the measured conductivity. Typical values used were thermal anomaly amplitude $\alpha = 0.03$ and the time constant $1/\beta = 7.0$.

FILTER performed a low pass filter on pressure with a time constant of 0.15 seconds. In order to produce zero phase lag (no time shift) the filter runs forward first then backwards.

WFILTER performed as a median filter to remove spikes in fluorometer and transmissometer data. A median value was determined by 49 scans of the window.

SECTIONU (original module, version 1.1) selected a time span of data based on scan number in order to reduce a file size. The minimum number was set to be the start time when the CTD package was beneath the sea-surface after activation of the pump. The maximum number was set to be the end time when the depth of the package was 1 dbar below the surface. The minimum and maximum numbers were automatically calculated in the module.

LOOPEDIT marked scans where the CTD was moving less than the minimum velocity of 0.0 m/s (traveling backwards due to ship roll).

DESPIKE (original module, version 1.0) removed spikes of the data. A median and mean absolute deviation was calculated in 1-dbar pressure bins for both down- and up-cast, excluding the flagged values. Values greater than 4 mean absolute deviations from the median were marked bad for each bin. This process was performed 2 times for temperature, conductivity, SBE 43, Optode 3830, and RINKO output.

DERIVE was used to compute oxygen (SBE 43).

BINAVG averaged the data into 1-dbar pressure bins. The center value of the first bin was set equal to the bin size. The bin minimum and maximum values are the center value plus and minus half the bin size. Scans with pressures greater than the minimum and less than or equal to the maximum were averaged. Scans were interpolated so that a data record exist every dbar.

OPTBACKCAL (original module, version 1.0) calculated raw phase shift data of the Optode 4330F from the Optode 4330F outputs (oxygen concentration and temperature data). For bottle information data, this module was applied before applying the module BOTTLESUM.

DERIVE was re-used to compute salinity, potential temperature, and density (σ_θ).

SPLIT was used to split data into the down cast and the up cast.

Remaining spikes in the CTD data were manually eliminated from the 1-dbar-averaged data. The data gaps resulting from the elimination were linearly interpolated with a quality flag of 6.

(6) Post-cruise calibration

i. Pressure

The CTD pressure sensor offset in the period of the cruise was estimated from the pressure readings on the ship deck. For best results the Paroscientific sensor was powered on for at least 20 minutes before the operation. In order to get the calibration data for the pre- and post-cast pressure sensor drift, the CTD deck pressure was averaged over first and last one minute, respectively. Then the atmospheric pressure deviation from a standard atmospheric pressure (14.7 psi) was subtracted from the CTD deck pressure. The atmospheric pressure was measured at the captain deck (20 m high from the base line) and sub-sampled one-minute interval as a meteorological data. Time series of the CTD deck pressure is shown in [Fig. 3.1.4](#).

The CTD pressure sensor offset was estimated from the deck pressure obtained above. Mean of the pre- and the post-casts data over the whole period gave an estimation of the pressure sensor offset from the pre-cruise calibration. Mean residual pressure between the dead-weight piston gauge and the calibrated CTD data at 0 dbar of the pre-cruise calibration was subtracted from the mean deck pressure. Estimated mean offset of the pressure data is listed in [Table 3.1.1](#). The post-cruise correction of the pressure data is not deemed necessary for the pressure sensor.

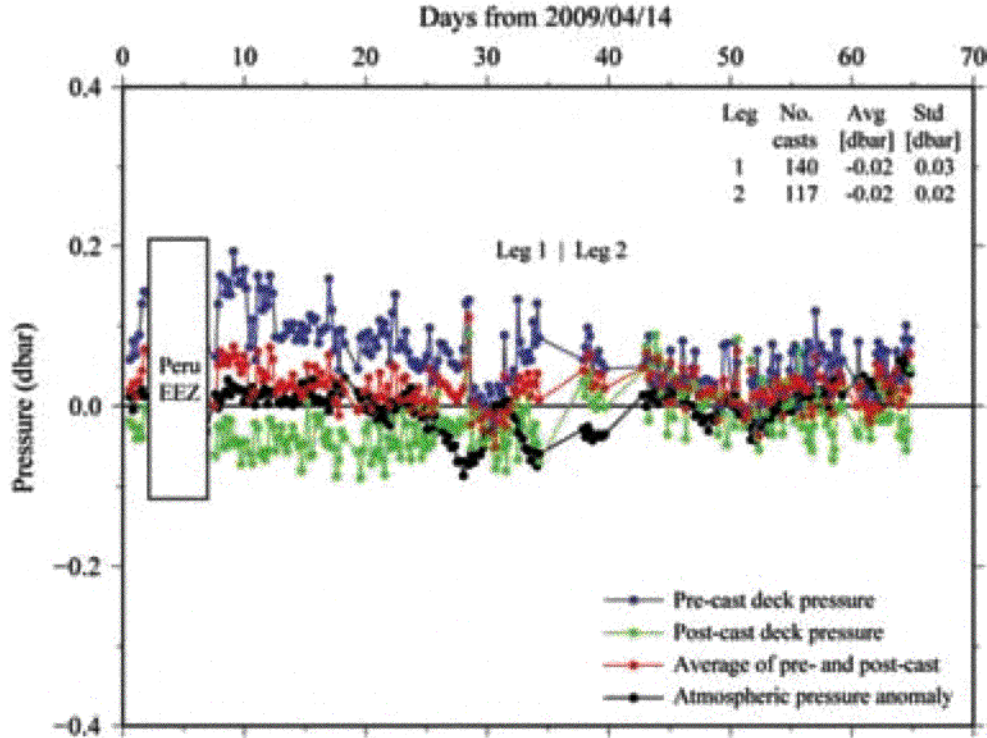


Figure 3.1.4: Time series of the CTD deck pressure. Black dot indicates atmospheric pressure anomaly. Blue and green dots indicate pre- and post-cast deck pressures, respectively. Red dot indicates an average of the pre- and the post-cast deck pressures.

Table 3.1.1: Offset of the pressure data. Mean and standard deviation are calculated from time series of the average of the pre- and the post-cast deck pressures.

	Number of cast	Mean deck pressure [dbar]	Standard deviation [dbar]	Residual pressure [dbar]	Estimated offset [dbar]
Leg 1	140	0.02	0.03	0.13	-0.11
Leg 2	117	0.02	0.02	0.13	-0.11

ii. Temperature

The CTD temperature sensors (SBE 3) were calibrated with the SBE 35 under the assumption that discrepancies between SBE 3 and SBE 35 data were due to pressure sensitivity, the viscous heating effect, and time drift of the SBE 3, according to a method by Uchida et al. (2007).

Post-cruise sensor calibration for the SBE 35 was performed at SBE, Inc.

SIN 0045, 19 August 2009 (2nd step: fixed point calibration)

$$\text{Slope} = 1.000013$$

$$\text{Offset} = -0.001173$$

Offset of the SBE 35 data from the pre-calibration was estimated to be smaller than 0.1 mK for temperature smaller than 4.5°C. So the post-cruise correction of the SBE 35 temperature data was not deemed necessary for the SBE 35.

The CTD temperature was preliminary calibrated as

$$\text{Calibrated temperature} = T - (c_0 \times P + c_1 \times t + c_2)$$

where T is CTD temperature in °C, P is pressure in dbar t is time in days from pre-cruise calibration date of the CTD temperature and c_0 , c_1 , and c_2 are calibration coefficients. The coefficients were determined using the data for the depths deeper than 1950 dbar.

The primary temperature data were basically used for the post-cruise calibration. The secondary temperature sensor was also calibrated and used instead of the primary temperature data for the station P21_26_1. The number of data used for the calibration and the mean absolute deviation from the SBE 35 are listed in Table 3.1.2 and the calibration coefficients are listed in Table 3.1.3. The results of the post-cruise calibration for the CTD temperature are summarized in Table 3.1.4 and shown in Figs. 3.1.6 and 3.1.7.

Table 3.1.2: Number of data used for the calibration (pressure \geq 1950 dbar) and mean absolute deviation between the CTD temperature and the SBE 35.

Leg	Serial number	Number	Mean absolute deviation	Note
1	4815	1315	0.1 mK	
1	1525	1315	0.1 mK	for station P21_26_1
2	4815	834	0.1 mK	
2	1525	834	0.1 mK	Not used

Table 3.1.3: Calibration coefficients for the CTD temperature sensors.

Leg	Serial number	c_0 (°C/dbar)	c_1 (°C/day)	c_2 (°C)
1	4815	1.03996e-8	2.23793e-6	-0.0000
1	1525	-7.61078e-9	1.76847e-6	0.0005
2	4815	-4.16502e-8	3.67354e-7	-0.0003
2	1525	1.76844e-8	-1.01065e-5	0.0024

Table 3.1.4: Difference between the CTD temperature and the SBE 35 after the post-cruise calibration. Mean and standard deviation (Sdev) are calculated for the data below and above 1950 dbar Number of data used is also shown.

Serial number	Pressure \geq 1950 dbar			Pressure < 1950 dbar		
	Number	Mean (mK)	Sdev (mK)	Number	Mean (mK)	Sdev (mK)
<i>Leg 1</i>						
4815	1315	-0.01	0.2	2647	-0.03	8.7
1525	1315	-0.01	0.2	2647	0.46	9.8
<i>Leg 2</i>						
4815	834	-0.00	0.3	2171	-0.42	4.8
1525	834	-0.02	0.5	2171	-0.00	5.2

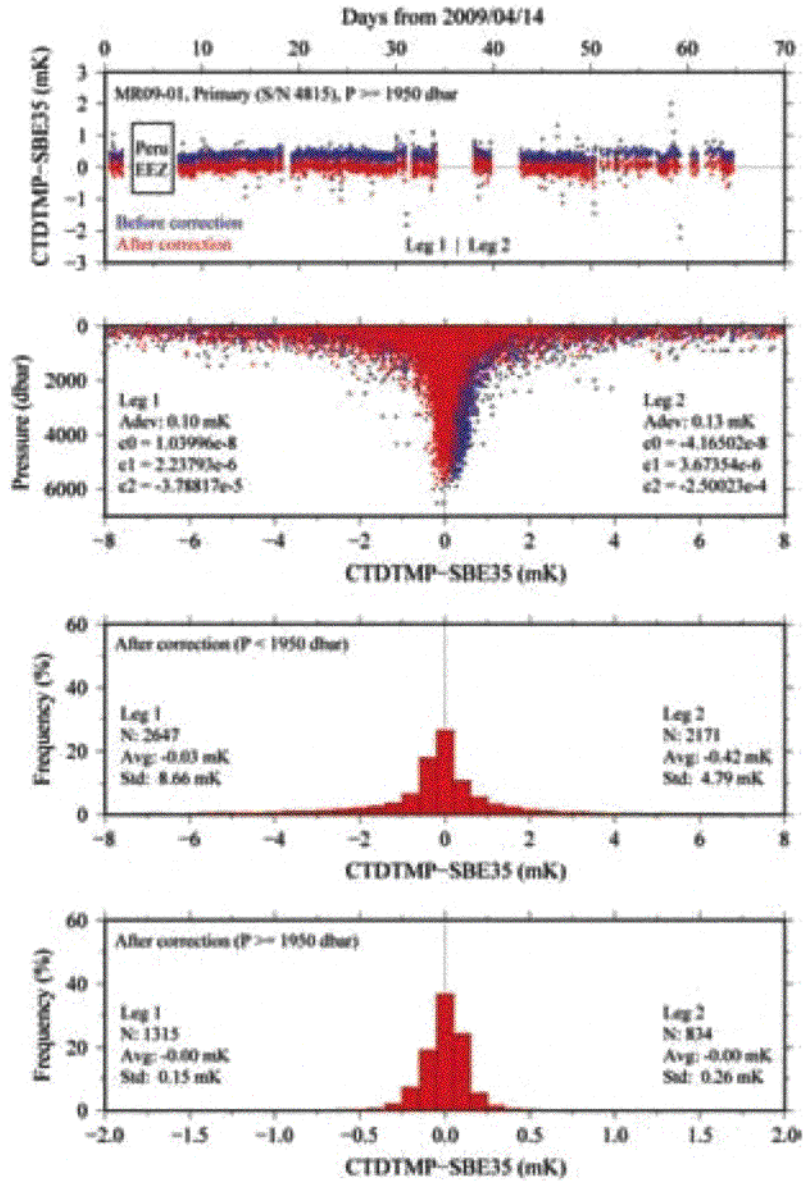


Figure 3.1.5: Difference between the CTD temperature and the SBE 35. Blue and red dots indicate before and after the post-cruise calibration using the SBE 35 data, respectively. Lower two panels show histogram of the difference after the calibration. Results from the primary temperature sensor (S/N 4815) are shown.

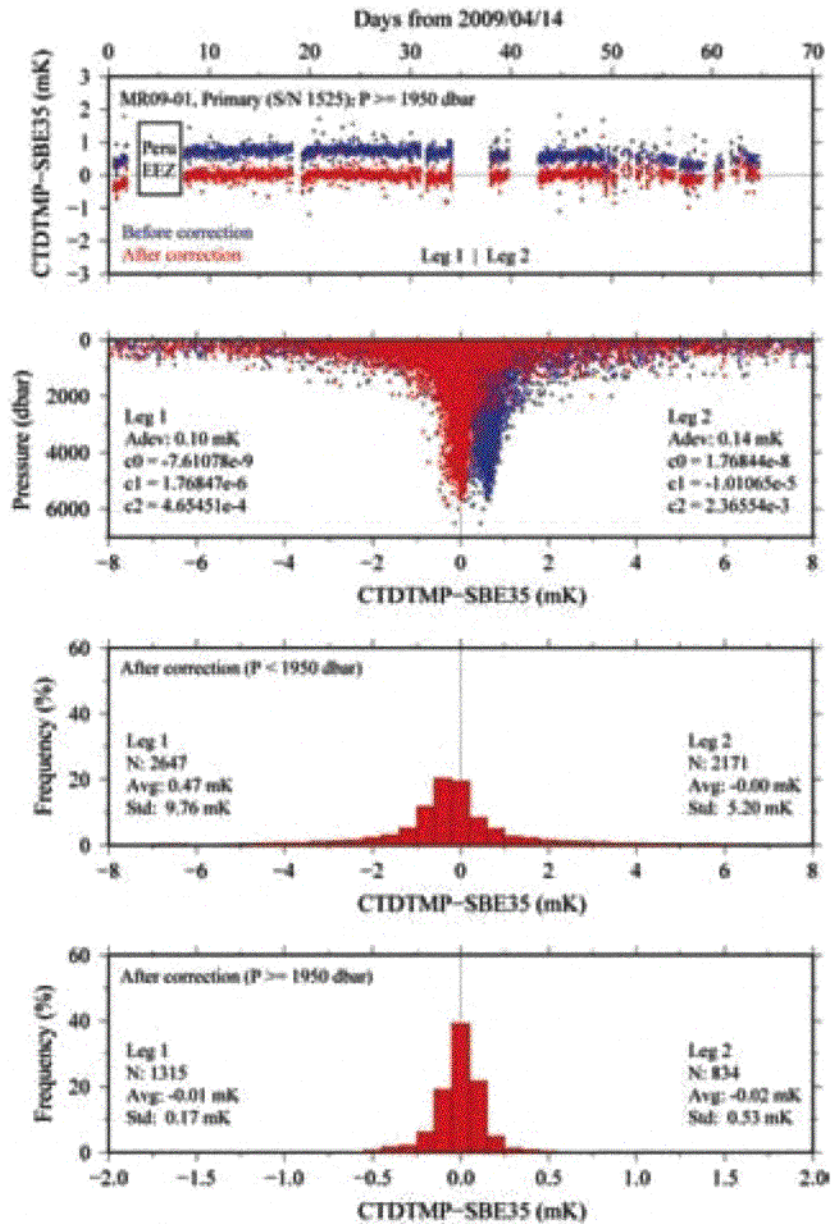


Figure 3.1.6: Same as Fig. 3.1.5, but for the secondary temperature sensor (S/N 1525).

iii. Salinity

The discrepancy between the CTD conductivity and the conductivity calculated from the bottle salinity data with the CTD temperature and pressure data is considered to be a function of conductivity, pressure and time. The CTD conductivity was calibrated as

$$\text{Calibrated conductivity} = c_0 \times C + c_1 \times P + c_2 \times C \times P + c_3 \times t + c_4$$

where C is CTD conductivity in S/m, P is pressure in dbar, t is time in days from 14 April 2009 and c_0 , c_1 , c_2 , c_3 and c_4 are calibration coefficients. The best fit sets of coefficients were determined by a weighted least square technique to minimize the deviation from the conductivity calculated from the bottle salinity data. The revised quasi-Newton method (FORTRAN subroutine DMINF1 from the Scientific Subroutine Library

II, Fujitsu Ltd., Kanagawa, Japan) was used to determine the sets. The weight was given as a function of pressure as

$$\text{Weight} = \min[100, \exp\{\log(100) \times P / \text{PR}\}]$$

where PR is threshold of the pressure (950 dbar). When pressure is large (small), the weight is large (small) at maximum (minimum) value of 100 (1).

The primary conductivity data created by the software module ROSSUM were basically used after the post-cruise calibration for the temperature data. For the station P21_26_1, the secondary conductivity data was used, because the primary conductivity data was not able to be used for the station. Data from the station P21_14_1 to P21_27_1 were used for the calibration of the secondary conductivity. The coefficients were determined for each leg. The calibration coefficients are listed in Table 3.1.5. The results of the post-cruise calibration for the CTD salinity are summarized in Table 3.1.6 and shown in Fig. 3.1.7.

Table 3.1.5: Calibration coefficients for the CTD conductivity sensors.

Number	c_0	c_1 [S/(m dbar)]	c_2 (1/dbar)	c_3 [S/(m day)]	c_4 (S/m)	Note
<i>Leg 1</i>						
3743	1.00015	3.00883e-8	-9.60863e-8	4.24710e-6	-4.86614e-4	S/N 2854
330	0.999985	1.87529e-7	-6.74291e-8	5.33449e-5	-9.41355e-5	S/N 1203
<i>Leg 2</i>						
2849	1.00021	-3.50016e-8	5.62948e-9	-1.22961e-6	-4.63040e-4	S/N 2854

Table 3.1.6: Difference between the CTD salinity and the bottle salinity after the post-cruise calibration. Mean and standard deviation (Sdev) (in 1 σ) are calculated for the data below and above 950 dbar. Number of data used is also shown.

Leg (Serial no.)	Pressure \geq 950 dbar			Pressure < 950 dbar		
	Number	Mean	Sdev	Number	Mean	Sdev
Leg 1 (2854)	1933	-0.02	0.42	1810	0.15	5.57
Leg 1 (1203)	163	-0.00	0.40	167	0.13	3.20
Leg 2 (2854)	1347	0.00	0.39	1502	0.05	4.58

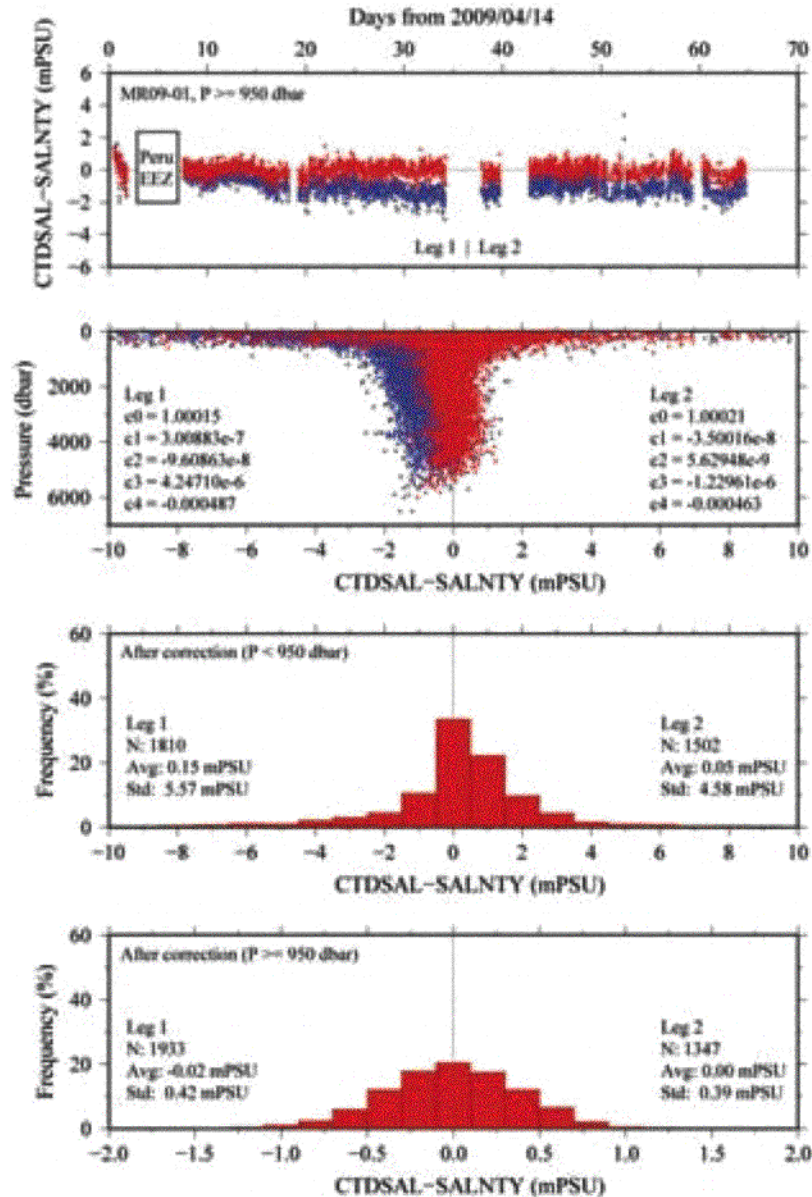


Figure 3.1.7: Difference between the CTD salinity and the bottle salinity. Blue and red dots indicate before and after the post-cruise calibration, respectively. Lower two panels show histogram of the difference after the calibration. Results from the primary conductivity sensor (S/N 2854) are shown.

iv. Oxygen

The RINKO oxygen optode was calibrated and used as the CTD oxygen data, since the RINKO has a fast time response. However, the time-dependent, pressure-induced effect on the sensing foil was large for the RINKO, as was observed for the SBE 43. Data from the RINKO was corrected for the time-dependent, pressure-induced effect by means of the same method as that developed for the SBE 43 (Sea-Bird Electronics, 2009). The calibration coefficients, H1 (amplitude of hysteresis correction), H2 (curvature function for hysteresis), and H3 (time constant for hysteresis) were determined empirically as:

$$H1 = 0.0065$$

$$H2 = 5000 \text{ dbar}$$

$$H3 = 2000 \text{ seconds.}$$

Difference between the up and down cast oxygen was quite small for the pressure-hysteresis corrected RINKO data (Fig. 3.1.8).

The pressure-hysteresis corrected RINKO data was calibrated by the Stern-Volmer equation, basically according to a method by Uchida et al. (2008) with modification:

$$[O_2] (\mu\text{mol/l}) = [(V_0 / V)^2 - 1] / K_{SV}$$

and

$$K_{SV} = C_0 + C_1 \times T + C_2 \times T^2$$

$$V_0 = 1 + C_3 \times T$$

$$V = C_4 + C_5 \times V_b + C_6 \times t + C_7 \times t \times V_b$$

where V_b is the RINKO output (voltage), V_0 is voltage in the absence of oxygen, T is temperature in °C, and t is exciting time (days) integrated from the first CTD cast. Time drift of the RINKO output was corrected. The pressure-compensation coefficient (C_p) was estimated to be 0.058. The coefficient for the V_0 ($C_3 = -0.00076$) was estimated from laboratory experiments on August 6, 2009. The remaining seven coefficients ($C_0, C_1, C_2, C_4, C_5, C_6,$ and C_7) were determined by minimizing the sum of absolute deviation with a weight from the bottle oxygen data. The revised quasi-Newton method (DMINF1) was used to determine the sets. The weight was given as a function of pressure as

$$\text{Weight} = \min[20, \exp\{\log(20) \times P / PR\}], \text{ when } [O_2] \geq 5 \mu\text{mol/kg}$$

$$\text{Weight} = 20, \text{ when } [O_2] < 5 \mu\text{mol/kg},$$

where PR is threshold of the pressure (950 dbar).

The post-cruise calibrated temperature and salinity data were used for the calibration. The coefficients were determined for some groups of the CTD stations. The calibration coefficients are listed in Table 3.1.7. The results of the post-cruise calibration for the RINKO oxygen are summarized in Table 3.1.8 and shown in Fig. 3.1.9.

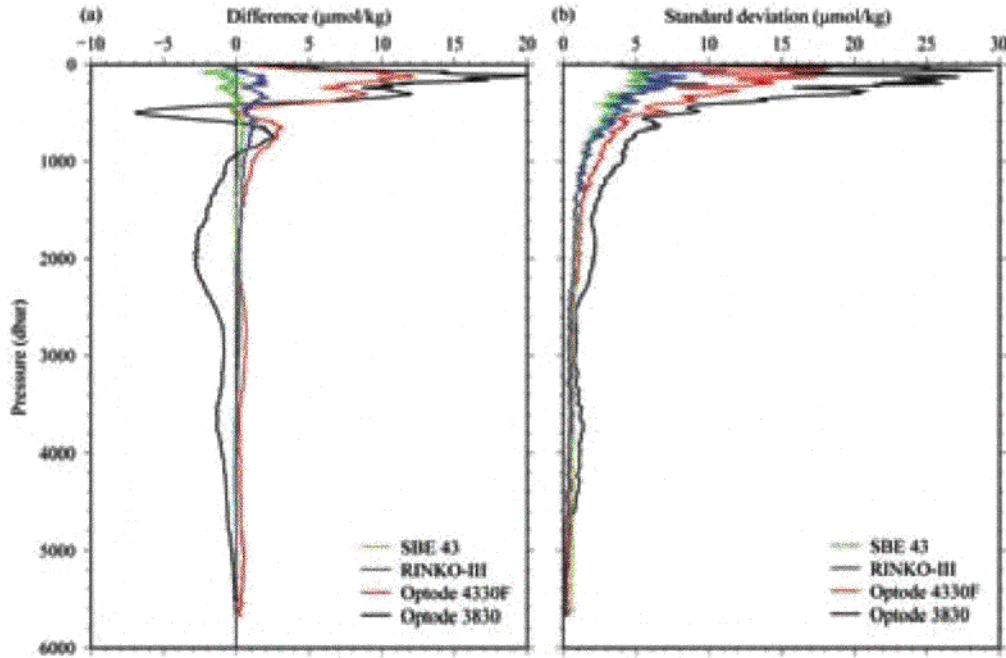


Figure 3.1.8: Difference between the up and down cast oxygen profiles from RINKO, SBE 43, Optode 4330E and Optode 3830. (a) mean and (b) standard deviation calculated from all CTD data.

Table 3.1.7: Calibration coefficients for the RINKO oxygen sensor.

Group	C ₀	C ₁	C ₂	C ₄	C ₅	C ₆	C ₇
Leg 1							
A	6.689376e-3	1.762279e-4	4.882030e-6	8.338279e-2	0.2267409	-4.196177e-3	3.326666e-3
B	6.782221e-3	1.365800e-4	6.972649e-6	7.467877e-2	0.2304436	-2.522455e-3	2.283958e-3
C	6.422881e-3	2.150534e-4	2.960990e-6	8.887120e-2	0.2285794	-7.967244e-5	8.759761e-4
D	6.707974e-3	2.692866e-4	1.586005e-6	7.623816e-2	0.2298613	-1.307925e-4	8.577014e-4
E	7.702781e-3	3.032778e-4	3.319508e-6	3.659057e-2	0.2395650	-3.795239e-4	5.390385e-4
F	8.815933e-3	3.357220e-4	4.934811e-6	2.385302e-2	0.2267504	-1.456302e-3	1.483800e-3
Leg 2							
G	8.751177e-3	3.336450e-4	4.553403e-6	-4.679584e-2	0.2673914	2.997944e-3	-9.971862e-4
H	8.835125e-3	3.345906e-4	5.044742e-6	1.583165e-2	0.2399865	-9.708137e-4	6.960351e-4

Group of CTD stations A: 291-331, B: 141-281, C: 411-681, D: 691-861,
E: 871-1481, F: 1491-1561, G: 1641-1721, H: 1731-2881

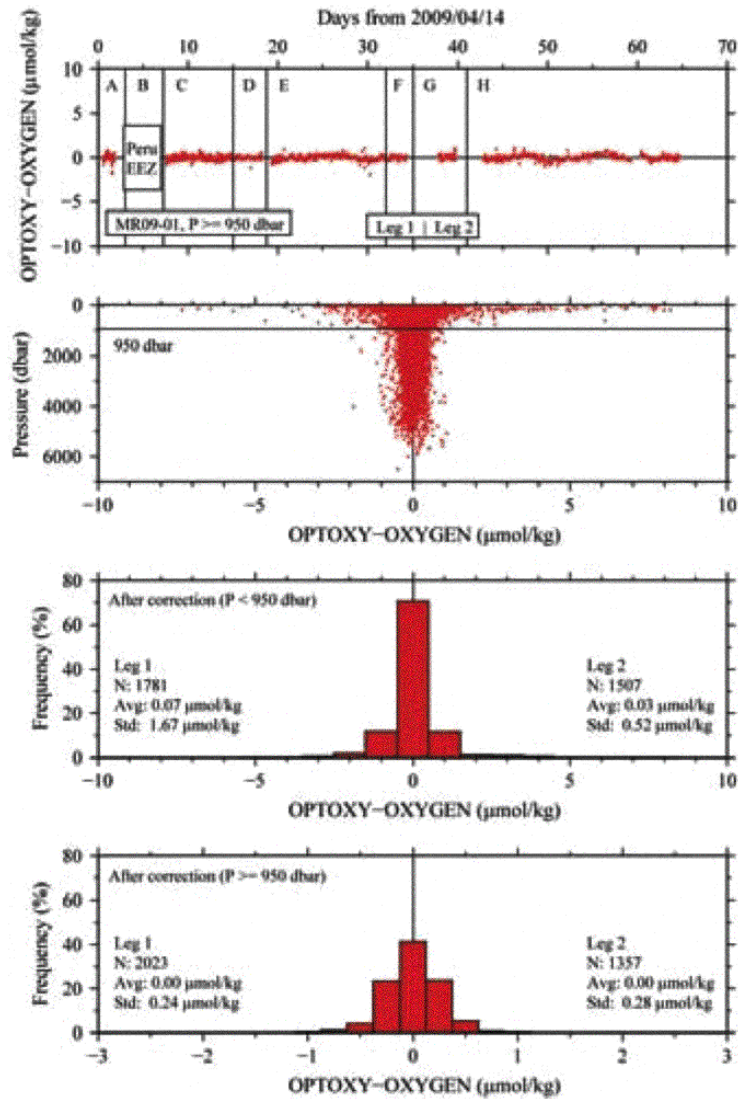


Figure 3.1.9: Difference between the RINKO oxygen and the bottle oxygen after the post-cruise calibration. Lower two panels show histogram of the difference.

Table 3.1.8: Difference between the RINKO oxygen and the bottle oxygen after the post-cruise calibration. Mean and standard deviation (Sdev) are calculated for the data below and above 950 dbar Number of data used is also shown.

Leg	Pressure \geq 950 dbar			Pressure $<$ 950 dbar		
	Number	Mean ($\mu\text{mol/kg}$)	Sdev ($\mu\text{mol/kg}$)	Number	Mean ($\mu\text{mol/kg}$)	Sdev ($\mu\text{mol/kg}$)
Leg 1	2023	0.00	0.24	1781	0.07	1.67
Leg 2	1357	0.01	0.28	1507	0.03	0.52

(7) Estimation of tripped depth for the bottle #13 of stations P21_33_1 and P21_18_1

True tripped depths for the following miss tripped bottles were estimated by using post-cruise calibrated CTD salinity and oxygen data compared to the bottle sampled salinity and oxygen data (Table 3.1.9).

Table 3.1.9: Estimated pressure of tripped depth for miss tripped bottles. The CTD temperature, salinity and oxygen data at the estimated pressure are also shown.

Bottle	Estimated pressure (dbar)			CTDTMP (ITS-90)	CTDSAL (PSS-78)	CTDOXY ($\mu\text{mol/kg}$)
	by CTDSAL	by CTDOXY	Average			
P21_33_1#13	2403.0	2388.6	2395.8	1.9394	34.6628	134.45
P21_18_1#13	762.2	763.2	762.7	5.6999	34.5179	28.86

References

Fukasawa, M., T. Kawano and H. Uchida (2004): Blue Earth Global Expedition collects CTD data aboard Mirai, BEAGLE 2003 conducted using a Dynacon CTD traction winch and motion-compensated crane, *Sea Technology*, 45, 14-18.

Garcia, H.E. and L.I. Gordon (1992): Oxygen solubility in seawater: Better fitting equations. *Limnol. Oceanogr.*, 37 (6),1307-1312.

Sea-Bird Electronics (2009): SBE 43 dissolved oxygen (DO) sensor - hysteresis corrections, Application note no. 64-3, 7 pp.

Uchida, H., K. Ohyama, S. Ozawa, and M. Fukasawa (2007): In situ calibration of the Sea-Bird 9plus CTD thermometer, *J. Atmos. Oceanic Technol.*, 24, 1961-1967.

Uchida, H., T. Kawano, I. Kaneko, and M. Fukasawa (2008): In situ calibration of optode-based oxygen sensors, *J. Atmos. Oceanic Technol.*, 25,2271-2281.

Wetzel, R.G. and G.E. Likens (2000): *Limnological Analysis*, 429 pp., Springer, New York, USA.

3.2 Bottle Salinity

September 9, 2009

(1) Personnel

Takeshi Kawano (JAMSTEC)
Fuji Kobayashi (MWJ)
Tatsuya Tanaka (MWJ)
Akira Watanabe (MWJ)
Kenichi Katayama (MWJ)

(2) Objectives

Bottle salinities were measured to compare with CTD salinities for calibrating CTD salinities and for identifying leaking bottles.

(3) Instrument and Method

i. Salinity Sample Collection

The bottles in which the salinity samples are collected and stored are 250 ml Phoenix brown glass bottles with screw caps. Each bottle was rinsed three times with sample water and was filled to the shoulder of the bottle. The caps were also thoroughly rinsed. Salinity samples were stored more than 12 hours in the same laboratory as the salinity measurement was made.

ii. Instruments and Method

The salinity analysis was carried out on Guildline Autosal salinometer model 8400B (S/N 62556), which was modified by adding an Ocean Scientific International Ltd. peristaltic-type sample intake pump and two Guildline platinum thermometers model 9450. One thermometer monitored an ambient temperature and the other monitored a bath temperature. The resolution of the thermometers was 0.001°C. The measurement system was almost same as Aoyama et al. (2002). The salinometer was operated in the air-conditioned laboratory of the ship at a bath temperature of 24°C.

An ambient temperature varied from approximately 20°C to 24°C, while a bath temperature is very stable and varied within $\pm 0.002^\circ\text{C}$ on rare occasion. A measure of a double conductivity ratio of a sample is taken as a median of 31 readings. Data collection was started after 10 seconds and it took about 10 seconds to collect 31 readings by a personal computer. Data were sampled for the sixth and seventh filling of the cell. In case where the difference between the double conductivity ratio of this two fillings is smaller than 0.00002, the average value of the two double conductivity ratios is used to calculate the bottle salinity with the algorithm for practical salinity scale, 1978 (UNESCO 1981). If the difference is greater than or equal to the 0.00003, we measure another additional filling of the cell. In case where the double conductivity ratio of the additional filling does not satisfy the criteria above, we measure other additional fillings of the cell within 10 fillings in total. In case where the number of fillings is 10 and those fillings do not satisfy the criteria above, the median of the double conductivity ratios of five fillings are used to calculate the bottle salinity.

The measurement was conducted about from 12 to 20 hours per day and the cell was cleaned with soap after the measurement of the day. We measured more than 8,500 samples in total.

(4) Preliminary Result

i. Standard Seawater

Leg1 and Leg2a

Standardization control was set to 649 during Leg1 and Leg2a. The value of STANDBY was 5491 ± 0002 and that of ZERO was 0.00000 ± 0.00001 . We used IAPSO Standard Seawater batch P150 which conductivity ratio was 0.99978 (double conductivity ratio is 1.99956) as the standard for salinity. We measured 219 bottles of P150 during

routine measurement. Fig.3.2.1 shows the history of double conductivity ratio of the Standard Seawater batch P150 during Leg1 and Leg2a.

Drifts were calculated by fitting data from P150 to the equation obtained by the least square method (solid lines). Correction for the double conductivity ratio of the sample was made to compensate for the drift. After correction, the average of double conductivity ratio became 1.99956 and the standard deviation was 0.00001, which is equivalent to 0.0002 in salinity.

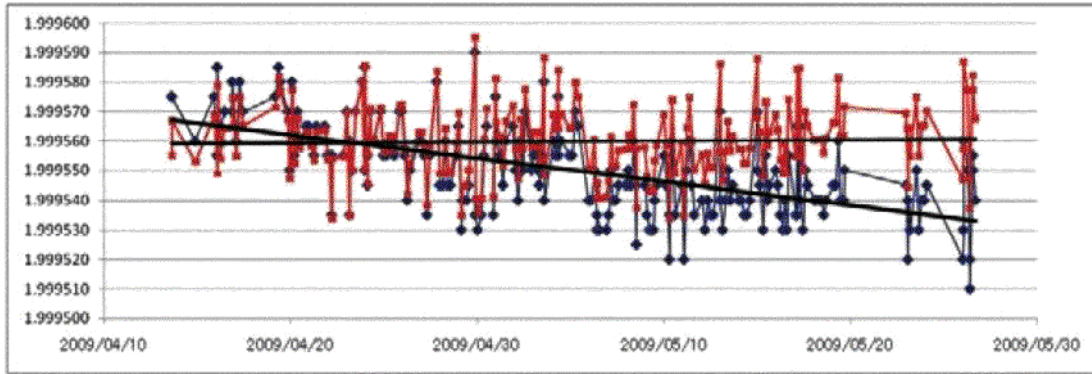


Figure 3.2.1: History of Double conductivity ratio of P150 during Leg1 and Leg2a. X and Y axes represents date and double conductivity ratio, respectively. Blue diamond is raw data and red rectangular is corrected data.

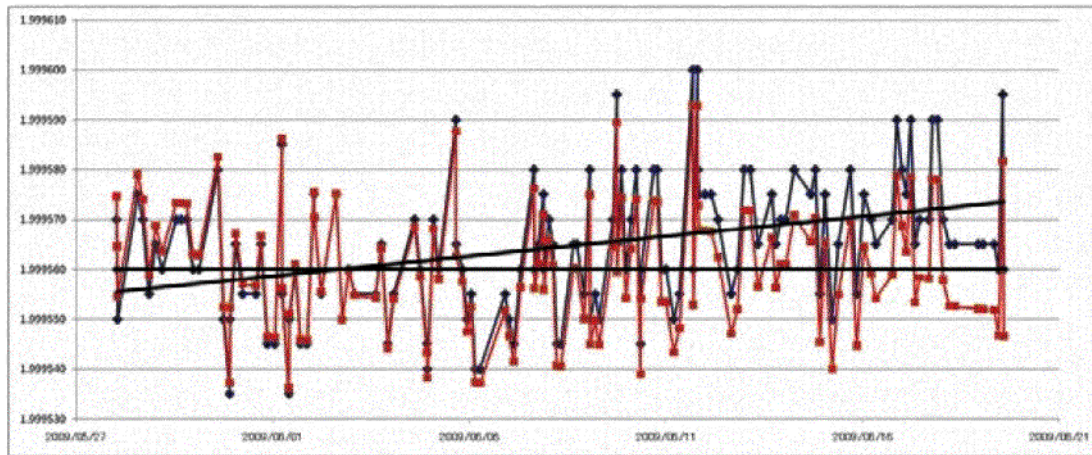


Figure 3.2.2: History of Double conductivity ratio of P150 during Leg2b. X and Y axes represents date and double conductivity ratio, respectively. Blue diamond is raw data and red rectangular is corrected data.

Leg2b

As the drift of this salinometer had been significant, the re-standardization was done on 27 May, and standardization control was set to 652 during Leg2b. The value of STANDBY was 5492 ± 0001 and that of ZERO was $.00000 \pm 0.00001$. We used IAPSO Standard Seawater batch P150 which conductivity ratio was 0.99978 (double conductivity ratio is 1.99956) as the standard for salinity. We measured 137 bottles of P150 during routine measurement. Fig.3.2.2 shows the history of double conductivity ratio of the Standard Seawater batch P150 during Leg2b.

Drifts were calculated by fitting data from P150 to the equation obtained by the least square method (solid lines). Correction for the double conductivity ratio of the sample was made to compensate for the drift. After correction,

the average of double conductivity ratio became 1.99956 and the standard deviation was 0.00001, which is equivalent to 0.0002 in salinity.

ii. Sub-Standard Seawater

We also used sub-standard seawater which was deep-sea water filtered by pore size of 0.45 micrometer and stored in a 20 liter cubitainer made of polyethylene and stirred for at least 24 hours before measuring. It was measured every six samples in order to check the possible sudden drift of the salinometer. During the whole measurements, there was no detectable sudden drift of the salinometer.

iii. Replicate Samples

Leg1

We took 819 pairs of replicate during Leg1. Fig.3.2.3 shows the histogram of the absolute difference between replicate samples. There was 1 bad measurement of replicate samples. Excluding these bad measurements, the standard deviation of the absolute difference of 818 pairs of replicate samples was 0.00023 in salinity.

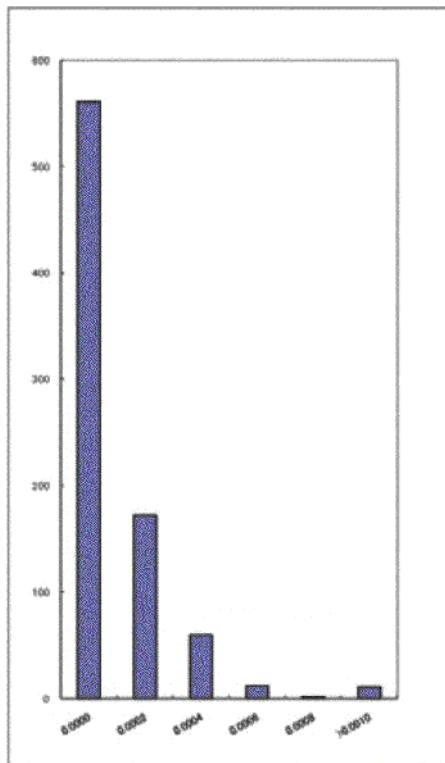


Figure 3.2.3: The histogram of the absolute difference between replicate samples in Leg1. X axis is absolute difference in salinity and Y axis is frequency.

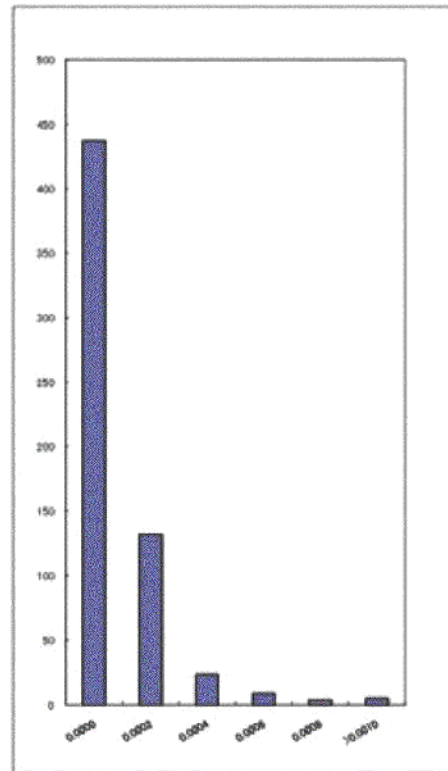


Figure 3.2.4: The histogram of the absolute difference between replicate samples in Leg2. X axis is absolute difference in salinity and Y axis is frequency.

Leg2

We took 613 pairs of replicate during Leg₂. Fig.3.2.4 shows the histogram of the absolute difference between replicate samples. There was 1 bad measurement of replicate samples. Excluding these bad measurements, the standard deviation of the absolute difference of 612 pairs of replicate samples was 0.00019 in salinity.

(5) Further data quality check

All the data will be checked once again in detail with other parameters such as dissolved oxygen and nutrients.

References

Aoyama, M., T. Joyce, T. Kawano and Y. Takatsuki (2002): Standard seawater comparison up to P129. Deep-Sea Research, I, Vol. 49, 1103-1114.

UNESCO (1981): Tenth report of the Joint Panel on Oceanographic Tables and Standards. UNESCO Tech. Papers in Mar. Sci., 36, 25 pp.

3.3 Oxygen

July 31, 2010

(1) Personnel

Yuichiro Kumamoto (JAMSTEC)

Miyo Ikeda (MWJ)

Fuyuki Shibata (MWJ)

Masanori Enoki (MWJ)

Misato Kuwahara (MWJ)

(2) Objectives

Dissolved oxygen is one of good tracers for the ocean circulation. Recent studies indicated that the oxygen minimum layers in the tropical region have expanded (Stramma et al., 2008). Climate models predict a decline in oceanic dissolved oxygen concentration and a consequent expansion of the oxygen minimum layers under the global warming, which results mainly from decreased interior advection and ongoing oxygen consumption by remineralization. The mechanism of the decrease, however, is still unknown. During MR09-01, we measured dissolved oxygen concentration from surface to bottom layers at all the hydrocast stations along approximately 18°S in the tropical South Pacific. These stations reoccupied the WOCE Hydrographic Program (WHP) P21 stations in 1994. Our purpose is to evaluate temporal change in dissolved oxygen concentration in the tropical South Pacific between the 1994 and 2009.

(3) Reagents

Pickling Reagent I: Manganous chloride solution (3M)

Pickling Reagent II: Sodium hydroxide (8M) / sodium iodide solution (4M)

Sulfuric acid solution (5M)

Sodium thiosulfate (0.025M)

Potassium iodate (0.001667M)

CSK standard of potassium iodate: Lot T5K3592, Wako Pure Chemical Industries Ltd., 0.0100N

(4) Instruments

Burette for sodium thiosulfate and potassium iodate: APB-510 manufactured by Kyoto Electronic Co. Ltd. / 10 cm³ of titration vessel

Detector: Automatic photometric titrator, DOT-01 manufactured by Kimoto Electronic Co. Ltd.

(5) Seawater sampling

Following procedure is based on an analytical method, entitled by "Determination of dissolved oxygen in sea water by Winkler titration", in the WHP Operations Manual (Dickson, 1996). Seawater samples were collected from 12-liters Niskin sampler bottles attached to the CTD-system. Seawater for bottle oxygen measurement was transferred from the Niskin sampler bottle to a volume calibrated glass flask (ca. 100 cm³). Three times volume of the flask of seawater was overflowed. Sample temperature was measured by a thermometer during the overflowing. Then two reagent solutions (Reagent I, II) of 0.5 cm³ each were added immediately into the sample flask and the stopper was inserted carefully into the flask. The sample flask was then shaken vigorously to mix the contents and to disperse the precipitate finely throughout. After the precipitate has settled at least halfway down the flask, the flask was shaken again to disperse the precipitate. The sample flasks containing pickled samples were stored in a laboratory until they were titrated.

(6) Sample measurement

At least two hours after the re-shaking, the pickled samples were measured on board. A magnetic stirrer bar and 1 cm³ sulfuric acid solution were added into the sample flask and stirring began. Samples were titrated automatically by sodium thiosulfate solution whose molarity was determined by standard solution of potassium iodate (see section 7). Temperature of sodium thiosulfate during titration was recorded by a thermometer. We measured dissolved oxygen concentration using two sets of the titration apparatus, named DOT-1 and DOT-2.

Dissolved oxygen concentration ($\mu\text{mol}/\text{kg}^{-1}$) was calculated by the sample temperature during the sampling, CTD salinity, flask volume, and the titrant concentration and volume corrected with burette-volume calibration. When we measured suboxic samples (oxygen concentration less than about 40 $\mu\text{mol}/\text{kg}^{-1}$), titration procedure was adjusted manually. In case of anoxic sample measurements (oxygen concentration less than about 6 $\mu\text{mol}/\text{kg}^{-1}$), titration volume of sodium thiosulfate titrant was not corrected with the burette-volume calibration.

(7) Standardization

Concentration of sodium thiosulfate titrant (ca. 0.025M) was determined by potassium iodate solution. Pure potassium iodate (Lot TSK3592, Wako Pure Chemical Industries Ltd., 99.96±0.01%) was dried in an oven at 130°C. 1.7835 g potassium iodate weighed out accurately was dissolved in deionized water and diluted to final volume of 5 dm³ in a calibrated volumetric flask (0.001667M). 10 cm³ of the standard potassium iodate solution was added to a flask using a volume-calibrated dispenser. Then 90 cm³ of deionized water, 1 cm³ of sulfuric acid solution, and 0.5 cm³ of pickling reagent solution II and I were added into the flask in order. Amount of titrated volume of sodium thiosulfate (usually 5 times measurements average) gave the molarity of the sodium thiosulfate titrant (Table 3.3.1). Error (C.V.) of the standardization was 0.02±0.01%, or c.a. 0.05 $\mu\text{mol}/\text{kg}^{-1}$.

(8) Determination of the blank

The oxygen in the pickling reagents 1(0.5 cm³) and 11(0.5 cm³) was assumed to be 3.8 x 10⁸ mol (Murray et al., 1968). The blank due to other than oxygen was determined as follows. 1 and 2 cm³ of the standard potassium iodate solution were added to two flasks respectively. Then 100 cm³ of deionized water, 1 cm³ of sulfuric acid solution, and 0.5 cm³ of pickling reagent solution II and I each were added into the two flasks in order. The blank was determined by difference between the two times of the first (1 cm³ of KIO₃) titrated volume of the sodium thiosulfate and the second (2 cm³ of KIO₃) one. The results of 3 times blank determinations were averaged (Table 3.3.1). The averaged blank values for DOT-1 and DOT-2 were -0.002±0.001 (S.D., n=27) and -0.000±0.001 (S.D., n=27) cm³, respectively. The blank determined here can cancel a sum of errors due to oxidants or reductants in the reagents, differences between the measured end-point and the equivalence point, and oxidation of iodide to iodate

with the atmospheric O₂ during the titration. However, blank due to redox species other than oxygen in seawater sample, called "seawater blank", still remains in the Winkler oxygen concentration.

Table 3.3.1: Results of the standardization and the blank determinations during MRO9-01.

Date (UTC)	#	KIO ₃ standard	Na ₂ S ₂ O ₃	DOT-1		DOT-2		Stations
		ID No.		E.P.	blank	E.P.	blank	
2009/4/13	11	20081203-11-02	20080704-2-1	3.957	-0.001	3.957	-0.001	029,030,031,032,040,033
2009/4/18		20081203-11-03	20080704-2-1	3.958	0.001	3.959	0.003	-
2009/4/18		20081203-11-04	20080704-2-2	3.958	-0.002	3.957	-0.002	-
2009/4/21		20081203-11-05	20080704-2-2	3.956	-0.001	3.956	0.001	041,034,042,035
2009/4/22		20081203-11-07	20080704-3-1	3.960	-0.002	3.960	-0.001	043,036,044,037,045,038,046,039
2009/4/24	12	20081203-12-02	20080704-3-1	3.962	-0.002	3.962	-0.001	047,X19,049,050
2009/4/25		20081203-12-03	20080704-3-2	3.961	-0.002	3.964	0.001	054,051,055,056,053,057,058,059,060,061,062,063,064,065
2009/4/26		20081203-12-04	20080704-3-2	3.962	-0.002	3.961	0.000	052
2009/4/28		20081203-12-06	20080704-4-1	3.963	-0.002	3.962	0.000	066,067,068,069,070,071,072,073,074,075,076,X18,077,078
2009/5/1		20081203-12-08	20080704-4-2	3.963	-0.002	3.964	-0.001	079,080,085,086,087,088,089,090,095,096,097-2,098,099,100
2009/5/5	13	20081203-12-10	20080704-5-1	3.964	-0.002	3.964	0.000	101,102,103,104,105,106
2009/5/6		20081203-13-01	20080704-5-1	3.962	-0.001	3.962	0.000	107,108,109,110,111,112,113,114
2009/5/8		20081203-13-02	20080704-5-2	3.965	-0.002	3.964	-0.001	115,116,117,118,119,120,121,122,123,124,125,126,127
2009/5/11		20081203-13-04	20080704-6-1	3.964	-0.001	3.964	0.000	128,129,130,X17,131,132,133,134,135,136,137
2009/5/14		20081203-13-06	20080704-6-2	3.964	-0.002	3.964	-0.001	138,139,140,141,142,143,144,145,146,147,148,149,150,151,152
2009/5/16	14	20081203-13-08	20080704-7-1	3.963	-0.001	3.965	0.000	153,154,155,160,159,158,157,156
2009/5/21		20081203-14-01	20080704-7-2	3.963	-0.003	3.965	-0.003	164,165,X16,167,168,169,170,171,172
2009/5/26		20081203-14-03	20080704-8-1	3.968	-0.001	3.971	0.001	173,174,175,176,177,178,179,180,181,182,183
2009/5/29		20081203-14-05	20080704-8-2	3.968	-0.001	3.969	-0.001	184,185,186,187,188,189,190,191,192
2009/6/1		20081203-14-07	20080704-9-1	3.965	-0.001	3.965	-0.001	193,194,195,196,197,198,199,200,201,203,204,205
2009/6/3	15	20081203-14-09	20080704-9-2	3.965	-0.002	3.966	0.000	206,207,208,209,210,211,212,213
2009/6/5		20081203-15-01	20080704-9-2	3.963	-0.002	3.964	0.000	214,215,216,217,218,220,221,222
2009/6/6		20081203-15-03	20080704-10-1	3.975	-0.001	3.976	0.001	223,224,225,226,227,228,229,230,231,232,233
2009/6/9		20081203-15-05	20080704-10-2	3.977	-0.001	3.978	0.002	234,235,236,237,238,239,240,241,243,244,245,246
2009/6/10		20081203-15-07	20080704-11-1	3.965	-0.001	3.965	0.000	247,248,249,250,251,252,253,255,254
2009/6/13	16	20081204-16-01	20080704-11-2	3.967	-0.002	3.968	0.000	260,261,262,263,264,265,266,267,268,269,270,271,272,273,274,275,276
2009/6/16		20081204-16-03	20080704-12-1	3.966	-0.002	3.967	0.000	277,278,279,280,281,282,283,285,287,286,288

Batch number of the KIO₃ standard solution

(9) Replicate sample measurement

Replicate samples were taken from every CTD cast. Total amount of the replicate sample pairs of good measurement (flagged 2) was 656. The standard deviation of the replicate measurement was 0.09 μmol kg⁻¹ that was calculated by a procedure (SOP23) in DOE (1994). The replicate measurements depended on neither measurement date nor sampling depth (Fig.3.3.1). Each set of "good" data from replicate sample pairs were averaged and then flagged 2 (see section 12).

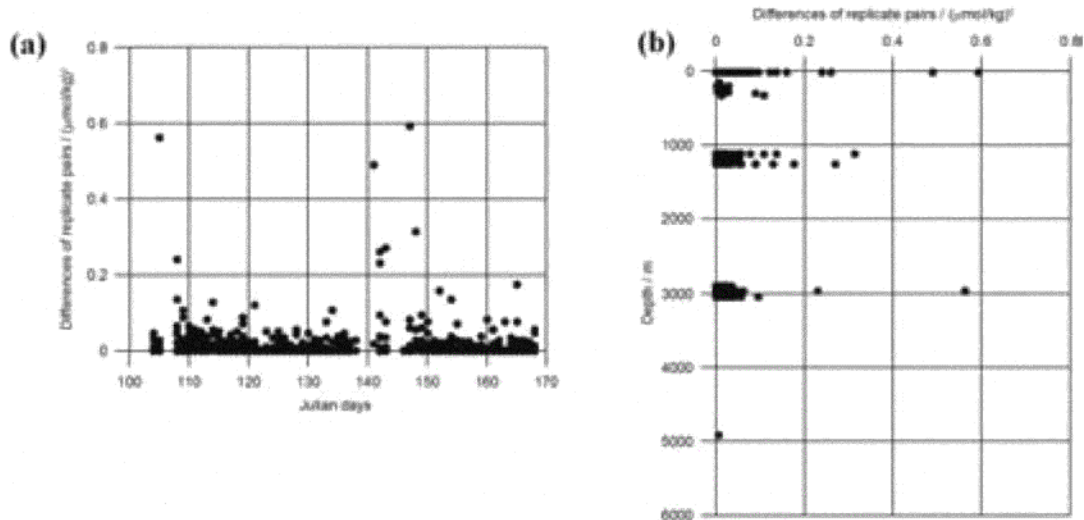


Figure 3.3.1: Differences ($(\mu\text{mol kg}^{-1})^2$) of replicate sample pairs against the Julian days (a) and sampling depth (b).

(10) Duplicate sample measurement

Duplicate samples were taken from 27 CTD casts during this cruise. The standard deviation of the duplicate measurements was calculated to be $0.07 \mu\text{mol kg}^{-1}$ which was equivalent with that of the replicate measurements ($0.09 \mu\text{mol kg}^{-1}$). We concluded that the precision of our oxygen measurement through this cruise, including errors from the seawater sampling, pickling, and the Winkle titration, were about $0.1 \mu\text{mol kg}^{-1}$.

(11) CSK standard measurements

The CSK standard is a commercial potassium iodate solution (0.0100 N) for analysis of dissolved oxygen. Before the cruise, we titrated the CSK standard solutions (Lot TSK3592) against all the six batch series (#11-#16) of our KIO_3 standard solution (see section 7) which had been prepared for this cruise. In addition, the CSK solution was also measured at the beginning, mid, and end of the cruise. The results of the CSK are shown in Table 3.3.2. A good agreement among them confirms that there was no systematic shift in our oxygen analyses on board. We also confirmed that there was not difference in the results between the current (TSK3592) and former (EWL3818) batches of the CSK standard solutions which were applied to this cruise and previous ones in 2007 (MR07-04 and MR07-06), respectively. This agreement indicates comparability in the oxygen data between 2007 and 2009.

Table 3.3.2: Results of the CSK standard (Lot TSK3592) measurements.

Date (UTC)	KIO ₃ ID No.	DOT-3		-	-	Remarks
		Conc. (N)	error (N)			
2008/12/08	20081203-11-12	0.010000	0.000002	-	-	before cruise
2008/12/08	20081203-12-12	0.010001	0.000002	-	-	before cruise
2008/12/08	20081203-13-12	0.010001	0.000002	-	-	before cruise
2008/12/08	20081203-14-12	0.009999	0.000002	-	-	before cruise
2008/12/08	20081203-15-12	0.009999	0.000002	-	-	before cruise
2008/12/09	20081203-16-12	0.010001	0.000003	-	-	before cruise

Date (UTC)	KIO ₃ ID No.	DOT-1		DOT-2		Remarks
		Conc. (N)	error (N)	Conc. (N)	error (N)	
2009/04/10	20081203-11-01	0.010003	0.000002	0.010008	0.000001	MR09-01 Leg-1
2009/05/18	20081203-13-09	0.010008	0.000001	0.010003	0.000003	MR09-01 Leg-1
2009/06/18	20081204-16-04	0.010005	0.000007	0.010002	0.000002	MR09-01 Leg-2

(12) Quality control flag assignment

Quality flag values were assigned to oxygen measurements using the code defined in Table 0.2 of WHP Office Report WHPO 91-1 Rev.2 section 4.5.2 (Joyce *et al.*, 1994). Measurement flags of 2 (good), 3 (questionable), 4 (bad), and 5 (missing) have been assigned (Table 3.3.3). The replicate data were averaged and flagged 2 if both of them were flagged 2. If either of them was flagged 3 or 4, a datum with "younger" flag was selected. Thus we did not use flag of 6 (see section 9). For the choice between 2, 3, or 4, we basically followed a flagging procedure as listed below:

- Bottle oxygen concentration was plotted against sampling pressure. Any points not lying on a generally smooth trend were noted.
- Difference between the bottle oxygen and CTD oxygen was then plotted against sampling pressure. If a datum deviated from a group of plots, it was flagged 3.
- Vertical transections against pressure and potential density were drawn. If a datum was anomalous on the section plots, datum flag was degraded from 2 to 3, or from 3 to 4.
- If there was problem in the measurement, the datum was flagged 4.
- If the bottle flag was 4 (did not trip correctly), a datum was flagged 4 (bad). In case of the bottle flag 3 (leaking) or 7 (unknown problem), a datum was flagged based on steps a, b, c, and d.

Table 3.3.3: Summary of assigned quality control flags.

Flag	Definition	
2	Good	6319
3	Questionable	30
4	Bad	29
5	Not reported (missing)	0
Total		6378

References

- Dickson, A. (1996): Determination of dissolved oxygen in sea water by Winkler titration, in WHPO Pub. 91-1 Rev. 1, November 1994, Woods Hole, Mass., USA.
- DOE (1994): Handbook of methods for the analysis of the various parameters of the carbon dioxide system in seawater; version 2. A.G. Dickson and C. Goyet (eds), ORNL/CDIAC-74.
- Joyce, T., and C. Corry, eds., C. Corry, A. Dessier, A. Dickson, T. Joyce, M. Kenny, R. Key, D. Legler, R. Millard, R. Onken, P. Saunders, M. Stalcup (1994): Requirements for WOCE Hydrographic Programme Data Reporting, WHPO Pub. 90-1 Rev. 2, May 1994 Woods Hole, Mass., USA.
- Murray, C.N., J.P. Riley, and T.R.S. Wilson (1968): The solubility of oxygen in Winkler reagents used for determination of dissolved oxygen, *Deep-Sea Res.*, 15, 237-238.
- Stramma, L., G.C. Johnson, J. Sprintall, and V. Mohrholz (2008): Expanding Oxygen-Minimum Zones in the Tropical Oceans, *Science*, 320, 655-668.

3.4 Nutrients

September 1, 2010

(1) Personnel

Michio Aoyama (Meteorological Research Institute/Japan Meteorological Agency, Principal Investigator)

LEG 1

Ayumi Takeuchi (Department of Marine Science, Marine Works Japan Ltd.)

Shinichiro Yokogawa (Department of Marine Science, Marine Works Japan Ltd.)

Kohei Miura (Marine Works Japan Ltd.)

LEG 2

Junji Matsushita (Department of Marine Science, Marine Works Japan Ltd.)

Ayumi Takeuchi (Department of Marine Science, Marine Works Japan Ltd.)

Kohei Miura (Marine Works Japan Ltd.)

(2) Objectives

The objectives of nutrients analyses during the R/V Mirai MR0901 cruise, WOCE P21 revisited cruise in 2009, in the North Pacific are as follows;

- Describe the present status of nutrients concentration with excellent comparability.
- The determinants are nitrate, nitrite, phosphate and silicate.
- Study the temporal and spatial variation of nutrients concentration based on the previous high quality experiments data of WOCE previous P21 cruises in 1994, GEOSECS, IGY and so on.
- Study of temporal and spatial variation of nitrate: phosphate ratio, so called Redfield ratio.
- Obtain more accurate estimation of total amount of nitrate, phosphate and silicate in the interested area.
- Provide more accurate nutrients data for physical oceanographers to use as tracers of water mass movement.

(3) Summary of nutrients analysis

We made 233 TRAACS800 runs for the samples at 243 stations in MR0901. The total amount of layers of the seawater sample reached up to 6369 for MR0901. We made duplicate measurement at all layers.

(4) Instrument and Method

(4.1) Analytical detail using TRAACS 800 systems (BRAN+LUEBBE)

The phosphate analysis is a modification of the procedure of Murphy and Riley (1962). Molybdic acid is added to the seawater sample to form phosphomolybdic acid which is in turn reduced to phosphomolybdous acid using L-ascorbic acid as the reductant.

Nitrate + nitrite and nitrite are analyzed according to the modification method of Grasshoff (1970). The sample nitrate is reduced to nitrite in a cadmium tube inside of which is coated with metallic copper. The sample stream with its equivalent nitrite is treated with an acidic, sulfanilamide reagent and the nitrite forms nitrous acid which reacts with the sulfanilamide to produce a diazonium ion. N-1-Naphthylethylene-diamine added to the sample stream then couples with the diazonium ion to produce a red, azo dye. With reduction of the nitrate to nitrite, both nitrate and nitrite react and are measured; without reduction, only nitrite reacts. Thus, for the nitrite analysis, no reduction is performed and the alkaline buffer is not necessary. Nitrate is computed by difference.

The silicate method is analogous to that described for phosphate. The method used is essentially that of Grasshoff et al. (1983), wherein silicomolybdic acid is first formed from the silicate in the sample and added molybdic acid; then

the silicomolybdic acid is reduced to silicomolybdous acid, or "molybdenum blue," using ascorbic acid as the reductant. The analytical methods of the nutrients during this cruise are same as the methods used in (Kawano et al. 2009). We, though, changed the rate of NED in channel 2 from WHT/WHT to RED/RED to increase stability of the analysis. We also made slight change in NED reagent that we add Triton(R) X-100 as shown in (4.3) Nitrite Regents. The flow diagrams and reagents for each parameter are shown in Figures 3.4.1 to 3.4.4.

(4.2) Nitrate Reagents

Imidazole (buffer), 0.06 M (0.4% w/v)

Dissolve 4 g imidazole, $C_3H_4N_2$, in ca. 1000 ml DIW; add 2 ml concentrated HCl. After mixing, 1 ml Triton(R) X-100 (50% solution in ethanol) is added.

Sulfanilamide, 0.06 M (1% w/v) in 1.2M HCl

Dissolve 10 g sulfanilamide, $4-NH_2C_6H_4SO_3H$, in 900 ml of DIW, add 100 ml concentrated HCl. After mixing, 2 ml Triton(R)X-100 (50% solution in ethanol) is added.

N-1-Naphthylethylene-diamine dihydrochloride, 0.004 M (0.1% w/v)

Dissolve 1 g NEDA, $C_{10}H_7NHCH_2CH_2NH_2 \cdot 2HCl$, in 1000 ml of DIW and add 10 ml concentrated HCl. After mixing, 1 ml Triton(R)X-100 (50% solution in ethanol) is added. Stored in a dark bottle.

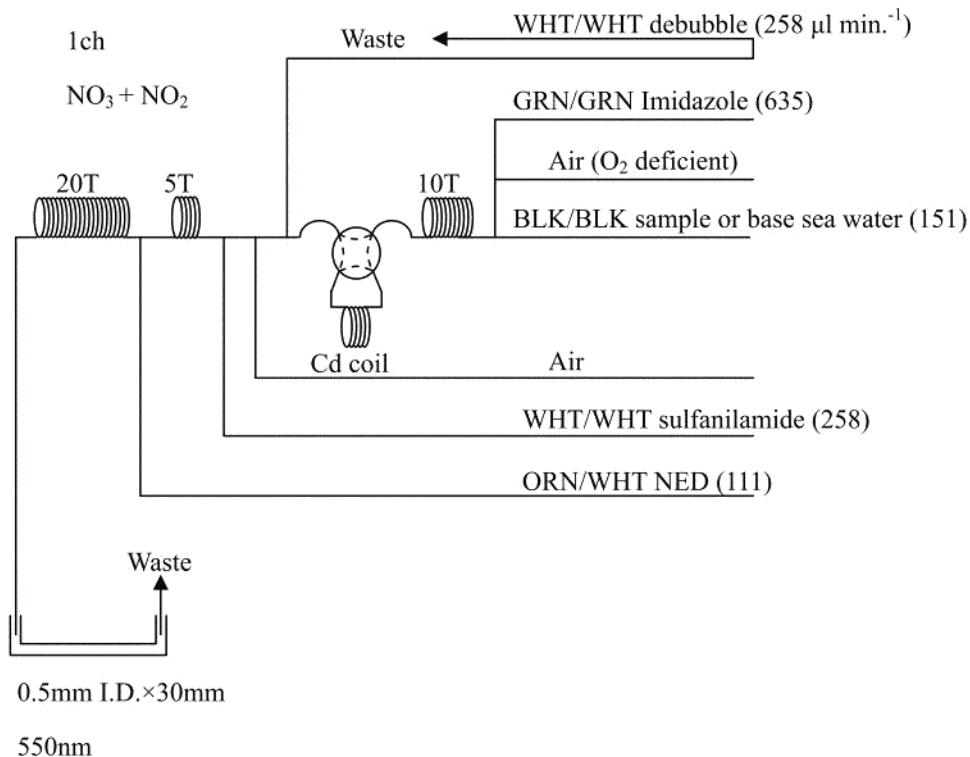


Figure 3.4.1: 1ch. (NO_3+NO_2) Flow diagram

(4.3) Nitrite Reagents

Sulfanilamide, 0.06 M (1% w/v) in 1.2 M HCl

Dissolve 10g sulfanilamide, 4-NH₂C₆H₄SO₃H, in 900 ml of DIW, add 100 ml concentrated HCl. After mixing, 2 ml Triton(R)X-100 (50% solution in ethanol) is added.

N-1-Naphthylethylene-diamine dihydrochloride, 0.004 M (0.1% w/v)

Dissolve 1 g NEDA, C₁₀H₇NHCH₂CH₂NH₂ 2HCl, in 1000 ml of DIW and add 10 ml concentrated HCl. After mixing, 1 ml Triton(R)X-100 (50% solution in ethanol) is added. Stored in a dark bottle.

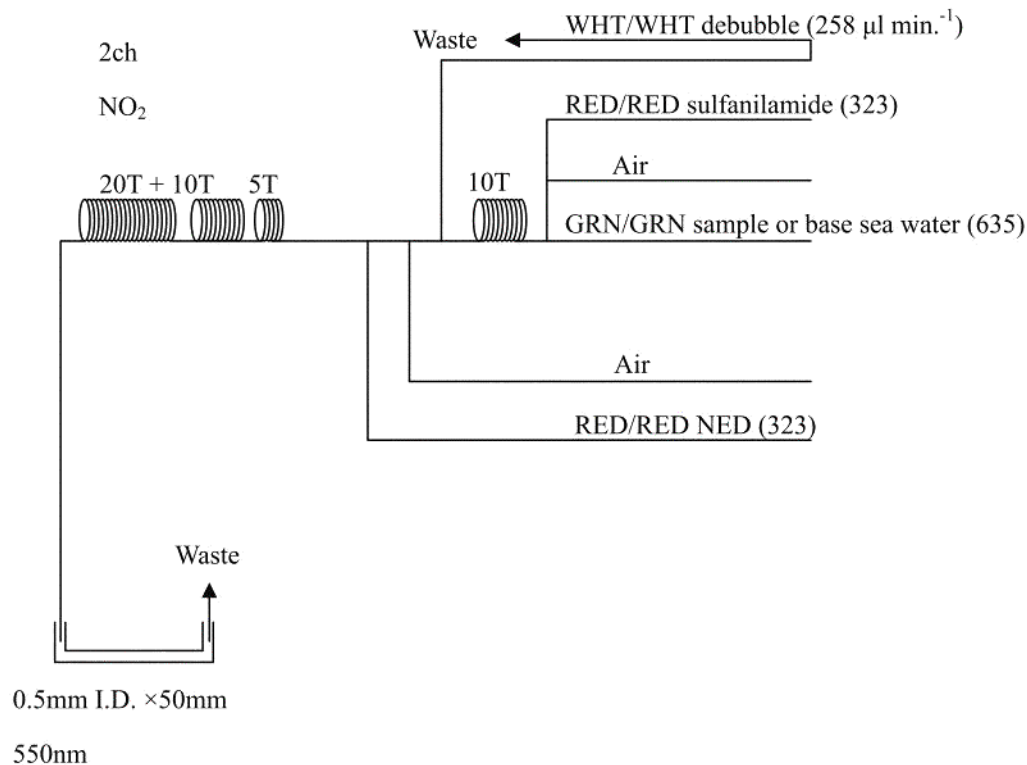


Figure 3.4.2: 2ch. (NO₂) Flow diagram

(4.4) Silicate Reagents Molybdic acid, 0.06 M (2% w/v)

Dissolve 15 g Disodium Molybdate(VI) Dihydrate, Na₂MoO₄ 2H₂O, in 980 ml DIW, add 8 ml concentrated H₂SO₄. After mixing, 20 ml sodium dodecyl sulphate (15% solution in water) is added.

Oxalic acid, 0.6 M (5% w/v)

Dissolve 50 g Oxalic Acid Anhydrous, HOOC: COOH, in 950 ml of DIW.

Ascorbic acid, 0.01 M (3% w/v)

Dissolve 2.5 g L (+)-Ascorbic Acid, C₆H₈O₆, in 100 ml of DIW. Stored in a dark bottle and freshly repaired before every measurement.

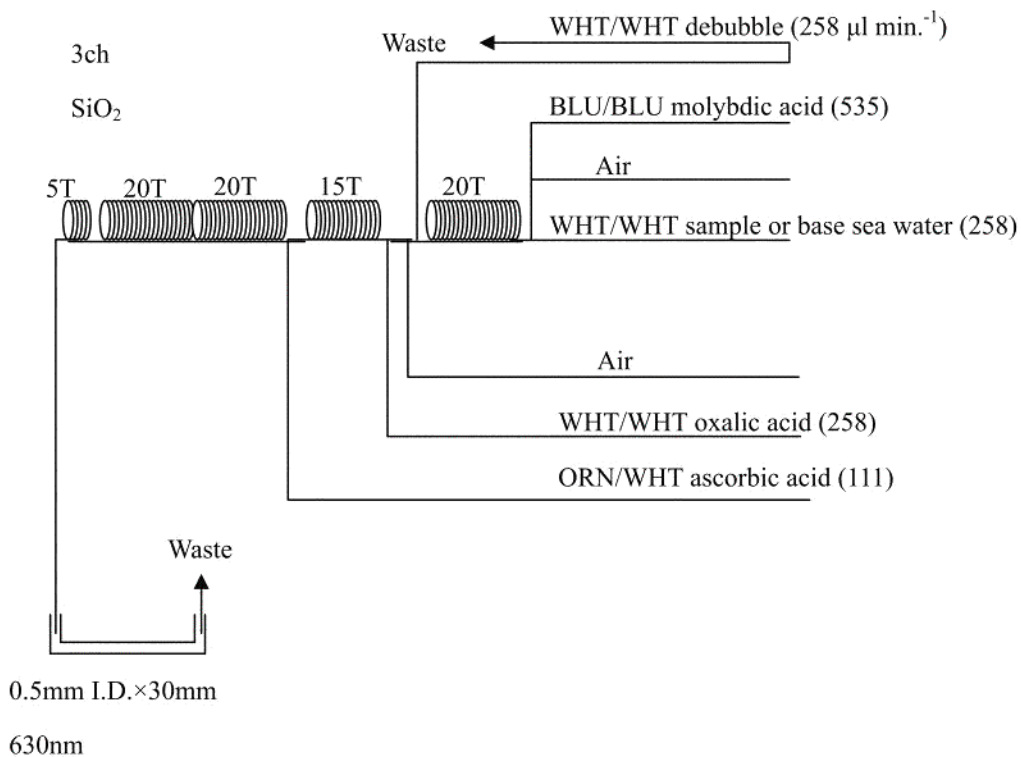


Figure 3.4.3: 3ch. (SiO₂) Flow diagram.

(4.5) Phosphate Reagents

Stock molybdate solution, 0.03 M (0.8% w/v)

Dissolve 8 g Disodium Molybdate(VI) Dihydrate, Na₂MoO₄ · 2H₂O, and 0.17 g Antimony Potassium Tartrate, C₈H₄K₂O₁₂Sb₂ · 3H₂O, in 950 ml of DIW and add 50 ml concentrated H₂SO₄.

Mixed Reagent

Dissolve 0.8 g L (+)-Ascorbic Acid, C₆H₈O₆, in 100 ml of stock molybdate solution. After mixing, 2 ml sodium dodecyl sulphate (15% solution in water) is added. Stored in a dark bottle and freshly prepared before every measurement.

Reagent for sample dilution

Dissolve Sodium Hydrate, NaCl, 10 g in ca. 950 ml of DIW, add 50 ml Acetone and 4 ml concentrated H₂SO₄. After mixing, 5 ml sodium dodecyl sulphate (15% solution in water) is added.

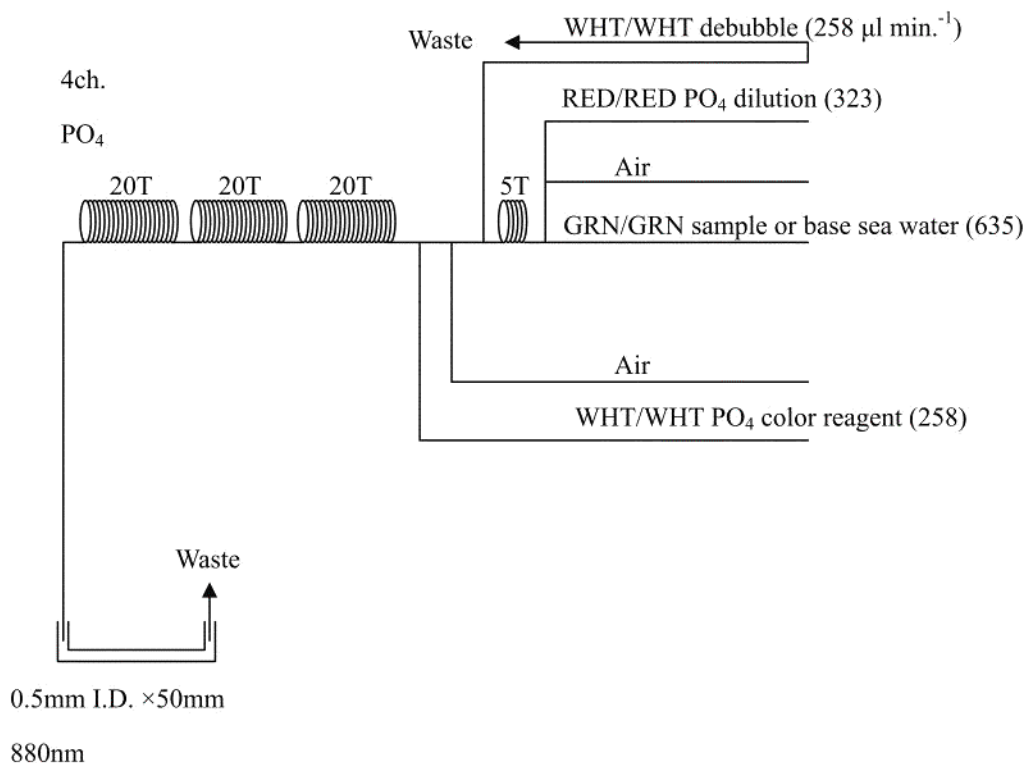


Figure 3.4.4: 4ch. (PO₄) Flow diagram.

(4.6) Sampling procedures

Sampling of nutrients followed that oxygen, trace gases and salinity. Samples were drawn into two of virgin 10 ml polyacrylates vials without sample drawing tubes. These were rinsed three times before filling and vials were capped immediately after the drawing. The vials are put into water bath adjusted to ambient temperature, $25 \pm 1^\circ\text{C}$, in 10 to 20 minutes before use to stabilize the temperature of samples in MR0901.

No transfer was made and the vials were set an auto sampler tray directly. Samples were analyzed after collection basically within 17 hours in MR0901.

(4.7) Data processing

Raw data from TRAACS800 were treated as follows;

- Check baseline shift.
- Check the shape of each peak and positions of peak values taken, and then change the positions of peak values taken if necessary.
- Carry-over correction and baseline drift correction were applied to peak heights of each samples followed by sensitivity correction.
- Baseline correction and sensitivity correction were done basically using liner regression.
- Load pressure and salinity from CTD data to calculate density of seawater.
- Calibration curves to get nutrients concentration were assumed second order equations.

(5) Nutrients standards

(5.1) Volumetric Laboratory Ware of in-house standards

All volumetric glass ware and polymethylpentene (PMP) ware used were gravimetrically calibrated. Plastic volumetric flasks were gravimetrically calibrated at the temperature of use within 0 to 4 K.

Volumetric flasks

Volumetric flasks of Class quality (Class A) are used because their nominal tolerances are 0.05% or less over the size ranges likely to be used in this work. Class A flasks are made of borosilicate glass, and the standard solutions were transferred to plastic bottles as quickly as possible after they are made up to volume and well mixed in order to prevent excessive dissolution of silicate from the glass. High quality plastic (polymethylpentene, PMP, or polypropylene) volumetric flasks were gravimetrically calibrated and used only within 0 to 4 K of the calibration temperature.

The computation of volume contained by glass flasks at various temperatures other than the calibration temperatures were done by using the coefficient of linear expansion of borosilicate crown glass.

Because of their larger temperature coefficients of cubical expansion and lack of tables constructed for these materials, the plastic volumetric flasks were gravimetrically calibrated over the temperature range of intended use and used at the temperature of calibration within 0 to 4 K. The weights obtained in the calibration weightings were corrected for the density of water and air buoyancy.

Pipettes and pipettors

All pipettes have nominal calibration tolerances of 0.1% or better. These were gravimetrically calibrated in order to verify and improve upon this nominal tolerance.

(5.2) Reagents, general considerations

Specifications

For nitrate standard, "potassium nitrate 99.995 suprapur" provided by Merck, CAS No. 7757-91-1, was used.

For phosphate standard, "potassium dihydrogen phosphate anhydrous 99.995 suprapur" provided by Merck, CAS No. 7778-77-0, was used.

For nitrite standard, "sodium nitrate" provided by Wako, CAS No. 7632-00-0, was used. And assay of nitrite was determined according JIS K8019 and assays of nitrite salts were 98.04%. We use that value to adjust the weights taken.

For the silicate standard, we use "Silicon standard solution SiO₂ in NaOH 0.5 mol/l CertiPUR" provided by Merck, CAS No. 1310-73-2, of which lot number is HC75 1838 is used. The silicate concentration is certified by NIST-SRM3 150 with the uncertainty of 0.5%.

Ultra pure water

Ultra pure water (MilliQ water) freshly drawn was used for preparation of reagents, higher concentration standards and for measurement of reagent and system blanks.

Low-Nutrient Seawater (LNSW)

Surface water having low nutrient concentration was taken and filtered using 0.45 µm pore size membrane filter. This water is stored in 20 liter cubitainer with paper box. The concentrations of nutrient of this water were measured carefully in Jul2008.

(5.3) Concentrations of nutrients for A, B and C standards

Concentrations of nutrients for A, B and C standards are set as shown in [Table 3.4.1](#). The C standard is prepared according recipes as shown in [Table 3.4.2](#). All volumetric laboratory tools were calibrated prior the cruise as stated in chapter (i). Then the actual concentration of nutrients in each fresh standard was calculated based on the ambient, solution temperature and determined factors of volumetric lab. wares.

The calibration curves for each run were obtained using 6 levels, C-1, C-2, C-3, C-4, C-S and C-6. For the 10 stations from station 233 to station 245, we used only five levels, from C-1 to C-5 because silicate concentration of C-6 for these stations might be higher rather than target concentration. For the 19 runs, we used only five levels because nutrients concentration of one of the RMs was outlier.

Table 3.4.1: Nominal concentrations of nutrients for A, B and C standards.

	A	B	C-1	C-2	C-3	C-4	C-S	C-6
NO ₃ (μM)	45000	900	AS	BJ	AX	BE	AZ	55
NO ₂ (μM)	4000	20	AS	BJ	AX	BE	AZ	1.2
SiO ₂ (μM)	36000	2880	AS	BJ	AX	BE	AZ	170
PO ₄ (μM)	3000	60	AS	BJ	AX	BE	AZ	3.6

Table 3.4.2: Working calibration standard recipes.

C Std.	B-1 Std.	B-2 Std.
C-6	30ml	30ml

B-1 Std.: Mixture of nitrate, silicate and phosphate
 B-2 Std.: Nitrite

(5.4) Renewal of in-house standard solutions.

In-house standard solutions as stated in (iii) were renewed as shown in Table 3.4.3(a) to (c).

Table 3.4.3(a): Timing of renewal of in-house standards.

NO ₃ , NO ₂ , SiO ₂ , PO ₄	Renewal
A-1 Std. (NO ₃)	maximum 1 month
A-2 Std. (NO ₂)	maximum 1 month
A-3 Std. (SiO ₂)	commercial prepared solution
A-4 Std. (PO ₄)	maximum 1 month
B-1 Std. (mixture of NO ₃ , SiO ₂ , PO ₄)	8 days
B-2 Std. (NO ₂)	8 days

Table 3.4.3(b): Timing of renewal of in-house standards.

C Std.	Renewal
C-6 Std. (mixture of B-1 and B-2 Std.)	24 hours

Table 3.4.3(c): Timing of renewal of in-house standards.

Reduction estimation	Renewal
D-1 Std.(7200 μ M NO ₃)	when A-1 Std. renewed
43/ μ M NO ₃	when C Std. renewed
47/ μ M NO ₂	when C Std. renewed

(6) Reference material of nutrients in seawater

To get the more accurate and high quality nutrients data to achieve the objectives stated above, huge numbers of the bottles of the reference material of nutrients in seawater (hereafter RMNS) are prepared (Aoyama et al., 2006, 2007, 2008). In the previous world wide expeditions, such as WOCE cruises, the higher reproducibility and precision of nutrients measurements were required (Joyce and Corry, 1994). Since no standards were available for the measurement of nutrients in seawater at that time, the requirements were described in term of reproducibility. The required reproducibility was 1%, 1 to 2%, 1 to 3% for nitrate, phosphate and silicate, respectively. Although nutrient data from the WOCE one-time survey was of unprecedented quality and coverage due to much care in sampling and measurements, the differences of nutrients concentration at crossover points are still found among the expeditions (Aoyama and Joyce, 1996, Mordy et al., 2000, Gouretski and Jancke, 2001). For instance, the mean offset of nitrate concentration at deep waters was 0.5 μ mol kg⁻¹ for 345 crossovers at world oceans, though the maximum was 1.7 μ mol kg⁻¹ (Gouretski and Jancke, 2001). At the 31 crossover points in the Pacific WHP one-time lines, the WOCE standard of reproducibility for nitrate of 1% was fulfilled at about half of the crossover points and the maximum difference was 7% at deeper layers below 1.6°C in potential temperature (Aoyama and Joyce, 1996).

(6.1) RMNSs for this cruise

RMNS lots AS, BJ, AX, BE and AZ, which cover full range of nutrients concentrations in the western North Pacific Ocean are prepared. 160 sets of AS, BJ, AX, BE and AZ are prepared.

Three hundred ten bottles of RMNS lot BI and 200 bottles of RMNS lot AV are prepared for MR09Oi. Lot BI was used at 99 stations from 14 to 120 and lot AV was used at 158 stations from 121 to 288, respectively. These RMNS assignment were completely done based on random number. The RMNS bottles were stored at a room in the ship, REAGENT STORE, where the temperature was maintained around 24°C.

(6.2) Assigned concentration for RMNSs

We assigned nutrients concentrations for RMNS lots AS, BJ, AX, BE, AZ, BI and AV as shown in Table 3.4.4.

Table 3.4.4: Assigned concentration of RMNSs.

	Nitrate	Phosphate	Silicate	Nitrite
AS*	0.11	0.077	1.58	0.02
BJ*	7.74	0.628	31.04	0.02
AX**	21.42	1.619	58.06	0.35
BE*	36.70	2.662	99.20	0.03
	42.36	3.017	133.93	0.03
BI*	41.36	2.576	147.51	0.02
AV**	33.36	2.516	154.14	0.10

* The value in the Table is result of measurement on 6 January, 2009.

** The value in the Table is result of measurement on 7 October, 2007.

(6.3) The homogeneity of RMNSs

The homogeneity of lot AV and AZ used in MR0901 cruise and analytical precisions are shown in Table 3.4.5. These are for the assessment of the magnitude of homogeneity of the RMNS bottles those are used during the cruise. As shown in Table 3.4.5 homogeneity of RMNS lot AV and AZ for nitrate, phosphate and silicate are the same magnitude of analytical precision derived from fresh raw seawater in January 2009.

Table 3.4.5: Homogeneity of lot AV and AZ derived from simultaneous 297 samples measurements and analytical precision onboard R/V Mirai in MRO901.

	Nitrate CV%	Phosphate CV%	Silicate CV%
AV	0.09	0.12	0.08
AZ	0.13	0.15	0.08
Precision	0.08	0.10	0.07

AV: N=297 AZ: N=244

We can see history of homogeneity of several lots of RMNS as shown in Table 3.4.6. The homogeneity of phosphate in old lots such as lot AH and K were relatively larger than those of recent lots, BI and BC. The homogeneities of nitrate and silicate, we also see progress from lot K to recent lots.

Table 3.4.6: History of homogeneity of lot BI and previous lots derived from simultaneous 30 samples measurements and analytical precision onboard R/V Mirai in January 2009.

	Nitrate CV%	Phosphate CV%	Silicate CV%
BI	0.19	0.21	0.08
BC*	0.22	0.32	0.19
AH*	0.39	0.83	0.13
K*	0.3	1.0	0.2
Precision	0.18	0.14	0.07

* Table 3.4.5 in WHP P01, P14 REVISIT DATA BOOK (Kawano et al. 2009)

(6.4) Comparability of RMNSs during the periods from 2003 to 2009

Cruise-to-cruise comparability has examined based on the results of the previous results of RMNSs measurements obtained among cruises, and RMNS international comparison experiments in 2003 and 2009. The uncertainties for each value were obtained similar method described in 7.1 in this chapter at the measurement before each cruise and inter-comparison study, shown as precruise and intercomparison, and mean of uncertainties during each cruise, only shown cruise code, respectively. As shown in Table 3.4.7, the nutrients concentrations of RMNSs were in good agreement among the measurements during the period from 2003 to 2009. For the silicate measurements, we show lot numbers and chemical company names of each cruise / measurement in the footnote. As shown in Table 3.4.7, there shows less comparability among the measurements due to less comparability among the standard solutions provided by chemical companies in the silicate measurements.

Table 3.4.7 (a): Comparability for nitrate.

$\mu\text{mol kg}^{-1}$

Cruise / Lab.	Nitrate RM Lots													
	AH	unc.	AZ	unc.	BA	unc.	AX	unc.	AV	unc.	BC	unc.	BE	unc.
2003														
2003intercomp_repeorted	35.23	0.06					21.39							
MR03-K04 Leg1	35.25													
MR03-K04 Leg2	35.37													
MR03-K04 Leg4	35.37													
MR03-K04 Leg5	35.34													
2005														
MR05-02			42.30		0.07	0.02	21.45	0.07	33.35	0.06	40.70	0.06		
MR05-05_1 precruise	35.65	0.05	42.30	0.10	0.07	0.00	21.41	0.01	33.41	0.02	40.76	0.03		
MR05-05_1			42.33		0.07	0.01	21.43	0.05	33.36	0.05	40.73	0.85		
MR05-05_2 precruise			42.33		0.08	0.00	21.39	0.02	33.36	0.05	40.72	0.03		
MR05-05_2			42.34		0.07	0.01	21.44	0.05	33.36	0.05	40.73	0.06		
MR05-05_3 precruise			42.35		0.06	0.00	21.49	0.01	33.39	0.01	40.79	0.01		
MR05-05_3			42.36		0.07	0.01	21.44	0.04	33.37	0.05	40.75	0.05		
2006														
2006intercomp			42.24	0.04	0.04	0.00	21.40	0.02	33.32	0.03	40.63	0.04		
2003intercomp_revisit	35.40	0.03												
2007														
MR07-04_1 precruise	35.74	0.03			0.07	0.00	21.59	0.02	33.49	0.03	40.83	0.03		
MR07-04_2 precruise	35.80	0.01			0.08	0.00	21.60	0.01	33.47	0.01	40.92	0.02		
MR07-04					0.08	0.01	21.41	0.06	33.38	0.05	40.77	0.05		
MR07-06_1 precruise	35.61	0.02			0.07	0.00	21.44	0.01	33.43	0.02	40.79	0.02		
MR07-06_2 precruise	35.61	0.04			0.06	0.00	21.43	0.02	33.54	0.04	40.79	0.05		
MR07-06_1					0.08	0.01	21.44	0.03	33.41	0.05	40.81	0.04		
MR07-06_2					0.09	0.01	21.44	0.03	33.39	0.06	40.81	0.04		
2008														
2008intercomp_report					0.08	0.00	21.44	0.02						
2006intercomp_revisit			42.27	0.04	0.07	0.00	21.47	0.02	33.34	0.03				
2003intercomp_revisit	35.35	0.04												
2009														
MR09-01_0 precruise			42.36	0.02	0.07	0.00	21.43	0.01	33.42	0.02	40.81	0.02	36.70	0.02
MR09-01_1			42.42	0.06	0.11	0.01	21.51	0.04	33.53	0.04	40.82	0.11	36.74	0.04
MR09-01_2			42.43	0.05			21.54	0.03	33.53	0.03			36.74	0.03
INSS stability test_1	35.76	0.22			0.08	0.01	21.49	0.02	33.45	0.03				

Table 3.4.7 (b): Comparability for phosphate.

$\mu\text{mol kg}^{-1}$

Cruise / Lab.	Phosphate													
	AH	unc.	AZ	unc.	BA	unc.	AX	unc.	AV	unc.	BC	unc.	BE	unc.
2003														
2003intercomp	2.141	0.001												
MRO3-K04 Leg1	2.110													
MR03-K04 Leg2	2.110													
MR03-K04 Leg4	2.110													
MR03-K04 Leg5	2.110													
2005														
MR05-02			3.010		0.061	0.010	1.614	0.008	2.515	0.008	2.778	0.010		
MR05-05_1 preruise	2.148	0.006	3.020	0.010	0.045	0.000	1.620	0.001	2.517	0.002	2.781	0.002		
MR05-05_1			3.016		0.063	0.007	1.615	0.006	2.515	0.007	2.778	0.033		
MR05-05_2 preruise			3.015		0.066	0.000	1.608	0.001	2.510	0.001	2.784	0.002		
MR05-05_2			3.018		0.064	0.005	1.614	0.004	2.515	0.005	2.782	0.006		
MR05-05_3 preruise			3.020		0.060	0.000	1.620	0.001	2.517	0.002	2.788	0.002		
MR05-05_3			3.016		0.061	0.004	1.618	0.005	2.515	0.004	2.779	0.008		
2006														
2006intercomp			3.018	0.002	0.071	0.000	1.623	0.001	2.515	0.001	2.791	0.001		
2003intercomp_revisit	2.141	0.001												
2007														
MR07-04_1 preruise	2.140	0.002			0.062	0.000	1.620	0.001	2.512	0.002	2.782	0.002		
MR07-04_2 preruise	2.146	0.002			0.056	0.000	1.620	0.001	2.517	0.002	2.788	0.002		
MR07-04_2 preruise	2.146	0.002			0.056	0.000	1.620	0.001	2.517	0.002	2.788	0.002		
MR07.04					0.066	0.004	1.617	0.005	2.513	0.004	2.781	0.007		
MR07.06_1 preruise	2.144	0.001			0.066	0.000	1.617	0.001	2.517	0.001	2.790	0.001		
MR07.06_2 preruise	2.146	0.002			0.067	0.000	1.620	0.001	2.517	0.002	2.789	0.002		
MR07.06_1					0.064	0.004	1.620	0.003	2.515	0.003	2.783	0.005		
MR07.06_2					0.066	0.004	1.619	0.005	2.515	0.003	2.785	0.006		
2008														
2008intercomp_report					0.068	0.000	1.615	0.005						
2006intercomp_revisit			3.014	0.008	0.065	0.000	1.627	0.005	2.513	0.007				
2003intercomp_revisit	2.131	0.006												
2009														
MR09-01_0 preruise			3.017	0.001	0.074	0.000	1.619	0.001	2.520	0.001	2.790	0.001	2.662	0.001
MR09-01_1			3.019	0.005	0.072	0.002	1.623	0.004	2.528	0.003	2.783	0.004	2.668	0.005
MR09-01_2			3.018	0.004			1.625	0.003	2.527	0.003			2.668	0.003
INSS stability test_1	2.134	0.008			0.069	0.001	1.606	0.001	2.512	0.003				

Table 3.4.7 (C): Comparability for silicate.

$\mu\text{mol kg}^{-1}$

Cruise / Lab.	Silicate													
	AH		AZ		BA		AX		AV		BC		BE	
	unc.	unc.	unc.	unc.	unc.	unc.	unc.	unc.	unc.	unc.	unc.	unc.	unc.	unc.
2003														
2003intercomp *	130.51	0.20												
MRO3-K04 Leg1 **	132.01													
MR03-K04 Leg2 **	132.26													
MR03-K04 Leg4 **	132.28													
MR03-K04 Leg5 **	132.19													
2005														
MR05-02 [#]			133.69		1.61	0.05	58.04	0.11	153.92	0.19	155.93	0.19		
MR05-05_1 precruise ^{##}	132.49	0.13	133.77	0.02	1.51	0.00	58.06	0.03	153.97	0.09	15.65	0.09		
MR05-05_1 ^{##}			133.79		1.59	0.07	58.01	0.12	154.01	0.26	156.08	0.36		
MR05-05_2 precruise ^{##}			133.78		1.58	0.00	57.97	0.04	154.07	0.09	156.21	0.10		
MR05-05_2 ^{##}			133.88		1.59	0.06	58.00	0.09	154.05	0.16	156.14	0.15		
MR05-05_3 precruise ^{##}			134.02		1.57	0.00	58.05	0.05	154.07	0.14	156.11	0.14		
MR05-05_3 ^{##}			133.79		1.60	0.05	57.98	0.09	153.98	0.18	156.08	0.13		
2006														
2006intercomp ^s			133.83	0.07	1.64	0.00	58.20	0.03	154.16	0.08	156.31	0.08		
2003intercomp_revisit ^s	132.55	0.07												
2007														
MR07-04_1 precruise ^{\$\$}	133.38	0.06			1.61	0.00	58.46	0.03	154.82	0.07	156.98	0.07		
MR07-04_2 precruise ^{\$\$}	133.15	0.12			1.69	0.00	58.44	0.05	154.87	0.14	156.86	0.14		
MRO7-04 ^{\$\$}					1.62	0.07	58.11	0.11	154.45	0.21	156.62	0.48		
MRO7-06_1 precruise ^{\$\$}	133.02	0.09			1.64	0.00	58.50	0.04	155.06	0.11	156.33	0.11		
MRO7-06_2 precruise ^{\$\$}	132.70	0.07			1.56	0.00	58.25	0.03	154.39	0.08	156.57	0.08		
MRO7-06_1 ^{\$\$}					1.61	0.04	58.13	0.08	154.48	0.13	156.64	0.08		
MRO7-06_2 ^{\$\$}					1.58	0.07	58.04	0.10	154.38	0.16	156.61	0.13		
2008														
2008intercomp [‡]					1.64	0.00	58.17	0.05						
2006intercomp_re [‡]			134.11	0.11	1.65	0.00	58.26	0.05	154.36	0.12				
2003intercomp_re [‡]	132.11	0.11												
2009														
MR09-01_0 precruise [‡]			133.93	0.04	1.57	0.00	58.06	0.02	154.23	0.05	156.16	0.05	99.20	0.03
MR09-01_1 [‡]			133.97	0.11	1.34	0.11	58.15	0.08	154.48	0.09	155.89	0.13	99.24	0.08
MR09-01_2 [‡]			133.96	0.11			58.19	0.08	154.42	0.12			99.23	0.08
INSS stability test_1 ^{‡‡}	132.40	0.35			1.69	0.02	58.18	0.02	154.43	0.09				

List of lot numbers: * Kanto 306F9235; ** Kanto 402F9041; # Kanto 507F9205; ## Kanto 609F9157;
^s Merck 0C551722; ^{\$\$} Merck HC623465; [‡] Merck HC751838; ^{‡‡} HC814662

(7) Quality control

(7.1) Precision of nutrients analyses during the cruise

Precision of nutrients analyses during the cruise was evaluated based on the 9 to 11 measurements, which are measured every 10 to 13 samples, during a run at the concentration of C-6 std. There is exception for the number of the measurements that are used to evaluate analytical precision of silicate at 10 runs from stations 233 to 245 where we evaluate analytical precision based on 6 to 8 measurements. Summary of precisions are shown as shown in [Table 3.4.8](#) and [Figures 3.4.5 to 3.4.7](#), the precisions for each parameter are generally good considering the analytical precisions estimated from the simultaneous analyses of 14 samples in January 2009 as shown in [Table 3.4.6](#). Analytical precisions previously evaluated were 0.18% for nitrate, 0.14% for phosphate and 0.08% for silicate, respectively. During this cruise, analytical precisions were 0.08% for nitrate, 0.10% for phosphate and 0.07% for silicate in terms of median of precision, respectively. Then we can conclude that the analytical precisions for nitrate,

phosphate and silicate were maintained throughout this cruise. The time series of precision are shown in Figures 3.4.5 to 3.4.7.

Table 3.4.8: Summary of precision based on the replicate analyses.

	Nitrate CV%	Phosphate CV%	Silicate CV%
Median	0.08	0.10	0.07
Mean	0.08	0.10	0.08
Maximum	0.18	0.17	0.14
Minimum	0.02	0.04	0.02
N	265	265	263

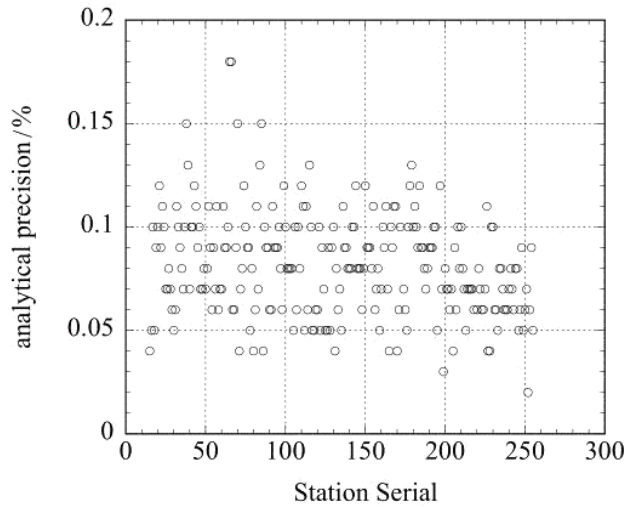


Figure 3.4.5: Time series of precision of nitrate for MRO901.

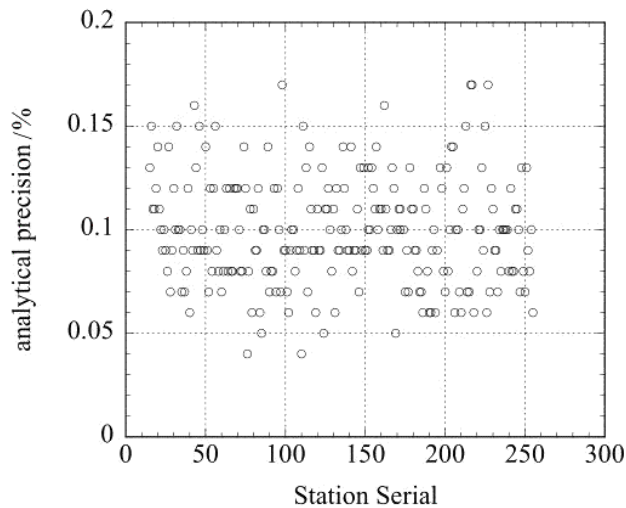


Figure 3.4.6: Time series of precision of phosphate for MRO901

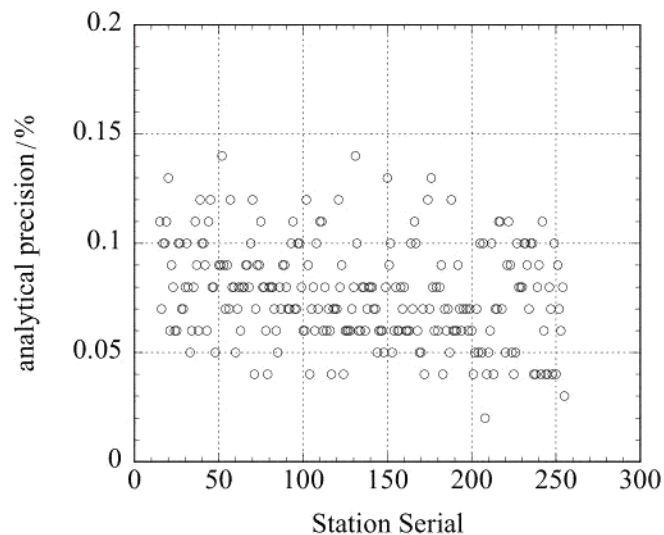


Figure 3.4.7: Time series of precision of silicate for MRO901.

(7.2) Carry over

We can also summarize the magnitudes of carry over throughout the cruise. These are small enough within acceptable levels as shown in Table 3.4.10.

Table 3.4.10: Summary of carry over through out MRO901 cruise.

	Nitrate CV%	Phosphate CV%	Silicate CV%
Median	0.21	0.24	0.20
Mean	0.21	0.23	0.20
Maximum	0.38	0.53	0.33
Minimum	0.03	0.01	0.03
N	237	237	237

(7.3) Dilution for shallower samples by lot AZ.

We decided to dilute 41 samples from shallower layers as shown Table 3.4.11 due to higher nitrite concentration which exceed $2 \mu\text{mol kg}^{-1}$. We add 5.060 ml of lot AZ to 0.504 ml of sample. Therefore, uncertainties of the nutrients concentration of diluted samples were larger compared with non-diluted samples.

Table 3.4.11: Summary of diluted samples.

Station	Pressure (dbar)
29	10, 50, 100, 150, 200, 250, 280
30	10, 50, 100, 150, 200, 250, 300
31	10, 50, 100, 150, 200, 250, 330
32	150, 200, 250, 280
35	280
40	150, 200, 250, 300
41	250,280
43	250,300
46	200,250
51	100
67	100
68	100
143	150
144	150

(7.4) Possible concentration change of lot AV

We found that nutrients concentrations of RM-AV were about 0.5% higher rather than those we assigned before cruise as shown in Table 3.4.4. The reasons of this increase are not clear yet, it might occur depend on the storage history of this RM-AV

(8) Problems/improvements occurred and solutions.

No problem occurred during this cruise.

References

- Aminot, A. and R. Kerouel (1991): Autoclaved seawater as a reference material for the determination of nitrate and phosphate in seawater. *Anal. Chim. Acta*, 248: 277-283.
- Aminot, A. and D.S. Kirkwood (1995): Report on the results of the fifth ICES intercomparison exercise for nutrients in sea water, ICES coop. Res. Rep. Set, 213.
- Aminot, A. and R. Kerouel (1995): Reference material for nutrients in seawater: stability of nitrate, nitrite, ammonia and phosphate in autoclaved samples. *Mar. Chem.*, 49: 221-232.
- Aoyama M. and T.M. Joyce (1996): WHP property comparisons from crossing lines in North Pacific. In Abstracts, 1996 WOCE Pacific Workshop, Newport Beach, California.
- Aoyama, M. (2006): 2003 Intercomparison Exercise for Reference Material for Nutrients in Seawater in a Seawater Matrix, Technical Reports of the Meteorological Research Institute No.50, 91pp, Tsukuba, Japan.
- Aoyama, M., B. Susan, D. Minhan, D. Hideshi, I.G. Louis, H. Kasai, K. Roger, K. Nurit, M. Doug, A. Murata, N. Nagai, H. Ogawa, H. Ota, H. Saito, K. Saito, T. Shimizu, H. Takano, A. Tsuda, K. Yokouchi, and Y. Agnes (2007): Recent Comparability of Oceanographic Nutrients Data: Results of a 2003 Intercomparison Exercise Using Reference Materials. *Analytical Sciences*, 23: 1151-1154.
- Aoyama, M., J. Barwell-Clarke, S. Becker, M. Blum, E.S. Braga, S.C. Coverly, E. Czobik, I. Dahllof, M.H. Dai, G.O. Donnell, C. Engelke, G.C. Gong, G.-H. Hong, D.J. Hydes, M.M. Jin, H. Kasai, R. Kerouel, Y. Kiyomono, M. Knockaert, N. Kress, K.A. Kroglund, M. Kumagai, S. Leterme, Y. Li, S. Masuda, T. Miyao, T. Moutin, A. Murata, N. Nagai, G. Nausch, M.K. Ngirchchol, A. Nybakk, H. Ogawa, J. van Ooijen, H. Ota, J.M. Pan, C. Payne, O. Pierre-Duplessix, M. Pujo-Pay, T. Raabe, K. Saito, K. Sato, C. Schmidt, M. Schuett, T.M. Shammon, J. Sun, T. Tanhua, L. White, E.M.S. Woodward, P. Worsfold, P. Yeats, T. Yoshimura, A.

- Youenou, J.Z. Zhang (2008): 2006 Intercomparison Exercise for Reference Material for Nutrients in Seawater in a Seawater Matrix, Technical Reports of the Meteorological Research Institute No. 58, 104pp.
- Gouretski, V.V. and K. Jancke (2001): Systematic errors as the cause for an apparent deep water property variability: global analysis of the WOCE and historical hydrographic data REVIEW ARTICLE, Progress in Oceanography, 48: Issue 4, 337-402.
- Grasshoff, K., M. Ehrhardt, K. Kremling et al. (1983): Methods of seawater analysis. 2nd rev. Weinheim: Verlag Chemie, Germany, West.
- Joyce, T. and C. Corry (1994): Requirements for WOCE hydrographic programmed data reporting. WHPO Publication, 90-1, Revision 2, WOCE Report No. 67/91.
- Kawano, T., H. Uchida and T. Doi (2009): WHP P01, P14 REVISIT DATA BOOK, (Ryoin Co., Ltd., Yokohama).
- Kirkwood, D.S. (1992): Stability of solutions of nutrient salts during storage. Mar. Chem., 38: 151-164.
- Kirkwood, D.S., A. Aminot and M. Perttita (1991): Report on the results of the ICES fourth intercomparison exercise for nutrients in sea water. ICES coop. Res. Rep. Set, 174.
- Mordy, C.W, M. Aoyama, L.I. Gordon, G.C. Johnson, R.M. Key, A.A. Ross, J.C. Jennings and J. Wilson (2000): Deep water comparison studies of the Pacific WOCE nutrient data set. Eos Trans-American Geophysical Union. 80 (supplement), 0S43.
- Murphy, J. and J.P. Riley (1962): Analytica chim. Acta 27, 31-36.
- Uchida, H. and M. Fukasawa (2005): WHP P6, A10, 13/14 REVISIT DATA BOOK Blue Earth Global Expedition 2003 1, 2, (Aiwa Printing Co., Ltd., Tokyo).

3.5 Chlorofluorocarbons (CFCs)

July 31, 2010

(1) Personnel

Ken'ichi Sasaki	(MIO, JAMSTEC)
Katsunori Sagishima	(MWJ)
Yuichi Sonoyama	(MWJ)
Shoko Tatamisashi	(MWJ)
Hideki Yamamoto	(MWJ)

(2) Introduction

Chlorofluorocarbons (CFCs) are completely man-made compounds that are chemically and biologically stable gasses in the environment. The CFCs have accumulated in the atmosphere since 1930's (Walker et al., 2000) and the atmospheric CFCs can slightly dissolve in sea surface water by air-sea gas exchange. The dissolved CFCs concentrations in sea surface water should have changed year by year and then penetrate into the ocean interior by water circulation. Three chemical species of CFCs, namely CFC-11 (CC13F), CFC-12 (CC12F2) and CFC-113 (CPA), dissolved in seawater are useful as the transient tracers for the ocean circulation with times scale on the order of several decades. In these cruises, we determined concentrations of CFCs dissolved in seawater on board.

(3) Apparatus

Dissolved CFCs were measured by a typical method modified from the original design of Bullister and Weiss (1988). A developed purging and trapping system was attached to gas chromatograph (GC-14B: Shimadzu Ltd) having an electron capture detector (ECD-14: Shimadzu Ltd). Cold trap columns were 1/16 stainless steel tubing packed with 5 cm of 100/120 mesh Porapak T. A pre-column and a main columns were Silica Plot capillary column

[i.d.: 0.53 mm, length: 8 m, film thickness: 6 gm] and a complex capillary column (Pola Bond-Q lid.: 0.53 mm, length: 7 m, film thickness: 10 gm) followed by Silica Plot li. d.: 0.53 mm, length: 22 m, film thickness: 6 gm)], respectively.

(4) Shipboard measurement

(4.1) Sampling

Before every CTD cast, the water sampler was cleaned by diluted acetone to remove any oils which could cause contaminations of CFCs. Seawater sub-samples were collected from 12 liter Niskin bottles into 250 ml glass bottles. The bottles had been filled with pure nitrogen gas before the sampling. The two times bottle volumes of seawater sample were overflowed. The bottles filled with seawater were kept in water bathes roughly controlled on the sample temperature. The CFC concentrations were determined within 12 hrs.

In order to confirm CFC concentrations of standard gases and their stabilities and also to check CFC saturation levels in sea surface water with respect to overlying air, CFC mixing ratios in the background air were periodically analyzed. Air samples were continuously led into the Environmental Research Laboratory using 10 mm OD Dekaron® tubing. The end of the tubing was put on a head of the compass deck and another end was connected onto an air pump in the laboratory. The tubing was relayed by a T-type union which had a small stop cock. Air samples were collected from the flowing air into a 200 ml glass cylinder attached on the cock during running ship from a station to next station. Average mixing ratios of the atmospheric CFC-11, CFC-12 and CFC113 are 242.6 ± 6.3 ppt, 530.4 ± 7.6 ppt, and 76.2 ± 5.4 ppt, respectively.

(4.2) Analysis

Constant volume of sample water (50 ml) was taken into the purging & trapping system. Dissolved CFCs were extracted by nitrogen gas purge. The sample gases were dried by magnesium perchlorate desiccant and concentrated on a trap column cooled to c -45°C. Following 8 minutes extraction, the trap column was isolated by valve switching and heated electrically to 140°C within 1.5 minutes to desorb CFCs. The trap column was connected to GC and CFCs led into the pre-column. The gasses were roughly separated on the pre-column. When required compounds were eluted, the pre-column was switched onto cleaning line and flushed back by counter flow of pure nitrogen gas. The compounds which were sent onto main column were separated further and detected by an electron capture detector (ECD). Retention times of compounds were around 1.5, 4.5 and 11.5 minutes for CFC-12, -11 and -113, respectively. Temperature of an analytical column and a detector was 95 and 240°C. Pure nitrogen gas (99.99995) was further purified by a molecular sieve 13X gas filter and was used for analyses. Mass flow rates of nitrogen gas were 10, 27, 20 and 120 ml/min for carrier, detector make up, back flush and sample purging gasses, respectively. Gas loops whose volumes were 1, 3 and 10 ml were used for introducing standard gases into the analytical system. Calibration curves were made every several days and standard gas analysis using large loop (10 ml) were performed more frequently to monitor change in the detector sensitivity. The standard gasses had been made by Japan Fine Products co. Ltd. Standard gas cylinder numbers used in cruises were listed in [Table 3.5.1](#). Cylinder of CPB30524 was used as reference gas. Precise mixing ratios of the standard gasses were calculated by gravimetric data. The standard gases used in this cruise have not been calibrated to SIO scale standard gases yet because SIO scale standard gasses is hard to obtain due to legal difficulties for CFCs import into Japan. The data will be corrected as soon as possible when we obtain the standard gasses.

(5) Quality control

(5.1) Main problems on the shipboard analysis

A large and broad peak was interfered determining CFC-113 peak area for samples collected from surface layer (several hundred meters depth). Retention time of the interfering peak was around 3% shorter than that of CFC-113. The peak of compound interfering CFC-113 determination could not be completely separated from the peak of CFC-113 by our analytical condition. We tried to split these peaks on chromatogram analysis and give flag "4". In the case of the interfering peak completely covering the CFC-113 peak, we could not determine CFC-113 peak area and give flag "5".

(5.2) Blanks

CFCs concentrations in deep water which was one of oldest water masses in the ocean were low but not zero for CFC-11 and -12. Average concentrations of CFC-11, 12 in the deep water were 0.003 ± 0.001 , 0.008 ± 0.001 pmol kg^{-1} ($n= 1500$), respectively. These values were assumed as sampling blanks which was contaminations from Niskin bottle and/or during sub-sampling and were subtracted from all data. Significant blank was not found in CFC-113 measurements.

(5.3) Precisions

The analytical precisions were estimated from replicate sample analyses (610 pairs for CFC-12, 609 pairs for CFC-11 and 401 pairs for CFC-113). The replicate samples were basically collected from two or three sampling depths which is around 100, 400 and 600 m depths in every stations. Precisions of CFCs are less than ± 0.010 pmol kg^{-1} or 0.6% for CFC-11 (whichever is greater), ± 0.006 pmol kg^{-1} or 0.8% for CFC-12 (whichever is greater), and ± 0.010 pmol kg^{-1} for CFC-113, respectively.

References

Bullister, J.L and R. E Weiss (1998): Determination of CC13F and CC12F2 in seawater and air. *Deep Sea Research*, 35, 839-853.

Table 3.5.1: Standard gas cylinder list.

Cylinder No.	CFC Concentrations (pptv).		
	CFC-11	CFC-12	CFC-113
CPBO3O13	300	159	30.1
CPB19294	299	159	30.1
CPB28545	293	163	29.9
CPB30524	300	159	30.2

3.6 Dissolved Inorganic Carbon (C_T)

December 4, 2010

(1) Personnel

Akihiko Murata (RIGC/JAMSTEC)
Minoru Kamata (MWJ)
Yoshiko Ishikawa (MWJ)
Yasuhiro Arie (MWJ)

(2) Objectives

Concentrations of CO_2 in the atmosphere are now increasing at a rate of 1.9 ppmv y^{-1} due to human activities such as burning of fossil fuels, deforestation, cement production, etc. It is an urgent task to estimate as accurately as possible the absorption capacity of the oceans against the increased atmospheric CO_2 , and to clarify the mechanism of the CO_2 absorption, because the magnitude of the predicted global warming depends on the levels of CO_2 in the atmosphere, and because the ocean currently absorbs $1/3$ of the 6 Gt of carbon emitted into the atmosphere each year by human activities.

In the cruise (MR09-01, revisit of WOCE P21 line) using the R/V Mirai, we were aimed at quantifying how much anthropogenic CO₂ is absorbed in the Pacific Ocean. For the purpose, we measured CO₂-system properties such as dissolved inorganic carbon (C_T), total alkalinity (A_T), pH and underway pCO₂.

In this section, we describe data on C_T obtained in the cruise in detail.

(3) Apparatus

Measurements of C_T were made with two total CO₂ measuring systems (systems-A and -B; Nippon ANS, Inc.), which are slightly different from each other. The systems comprise of a seawater dispensing system, a CO₂ extraction system and a coulometer (Model 5012, UIC Inc.).

The seawater dispensing system has an auto-sampler (6 ports), which takes seawater from a 300 ml borosilicate glass bottle and dispenses the seawater to a pipette of nominal 21 ml volume by a PC control. The pipette is kept at 20°C by a water jacket, where water from a water bath set at 20°C is circulated.

CO₂ dissolved in a seawater sample is extracted in a stripping chamber of a CO₂ extraction system by adding phosphoric acid (10% v/v). The stripping chamber is approx. 25 cm long and has a fine frit at the bottom. The acid is added to the stripping chamber from the bottom of the chamber by pressurizing an acid bottle for a given time to push out a right amount of acid. The pressurizing is made with nitrogen gas (99.9999%). After the acid is transferred to the stripping chamber, a seawater sample kept in a pipette is introduced to the stripping chamber by the same method as in adding an acid. The seawater reacted with phosphoric acid is stripped of CO₂ by bubbling the nitrogen gas through a fine fit at the bottom of the stripping chamber. The CO₂ stripped in the stripping chamber is carried by the nitrogen gas (140 ml min⁻¹ for the systems A and B) to the coulometer through a dehydrating module. For the system A, the module consists of two electric dehumidifiers (kept at 1 -2°C) and a chemical desiccant (Mg(ClO₄)₂). For the system B, it consists of three electric dehumidifiers with a chemical desiccant.

(4) Shipboard measurement

(4.1) Sampling

All seawater samples were collected from depth with 12 liter Niskin bottles basically at every other stations. The seawater samples for C_T were taken with a plastic drawing tube (PFA tubing connected to silicone rubber tubing) into a 300 ml borosilicate glass bottle. The glass bottle was filled with seawater smoothly from the bottom following a rinse with a seawater of 2 full, bottle volumes. The glass bottle was closed by a stopper, which was fitted to the bottle mouth gravimetrically without additional force.

At a chemical laboratory on the ship, a headspace of approx. 1% of the bottle volume was made by removing seawater with a plastic pipette. A saturated mercuric chloride of 100 μl was added to poison seawater samples. The glass bottles were sealed with a greased (Apiezon M, M&I Materials Ltd) ground glass stopper and the clips were secured. The seawater samples were kept at 4°C in a refrigerator until analysis. A few hours just before analysis, the seawater samples were kept at 20°C in a water bath.

(4.2) Analysis

At the start of each leg, we calibrated the measuring systems by blank and 5 kinds of Na₂CO₃ solutions (nominally 500, 1000 1500, 2000, 2500 μmol kg⁻¹). As it was empirically known that coulometers do not show a stable signal (low repeatability) with fresh (low absorption of carbon) coulometer solutions. Therefore we measured 2% CO₂ gas repeatedly until the measurements became stable. Then we started the calibration.

The measurement sequence such as system blank (phosphoric acid blank), 2% CO₂ gas in a nitrogen base, seawater samples (6) was programmed to repeat. The measurement of 2% CO₂ gas was made to monitor response of coulometer solutions (from UIC, Inc.). For every renewal of coulometer solutions, certified reference materials (CRMs, batch 92 and a small number of batch 79) provided by Prof. A. G. Dickson of Scripps Institution of Oceanography were analyzed. In addition, in-house reference materials (RM) (batch QRM Q20 and Q19 for systems A and B, respectively) were measured at the initial, intermediate and end times of a coulometer solution's lifetime.

The preliminary values were reported in a data sheet on the ship. Repeatability and vertical profiles of C_T based on raw data for each station helped us check performances of the measuring systems.

In the cruise, we finished all the analyses for C_T on board the ship. As we used two systems, we had not encountered such a situation as we had to abandon the measurement due to time limitation.

(5) Quality control

We conducted quality control of the data after return to a laboratory on land. With calibration factors, which had been determined on board a ship based on blank and 5 kinds of Na_2CO_3 solutions, we calculated C_T of CRM (batches 92 and 79), and plotted the values as a function of sequential day, separating legs and the systems used. There were no statistically-significant trends of CRM measurements.

Based on the averages of C_T of CRM, we re-calculated the calibration factors so that measurements of seawater samples become traceable to the certified value of batches 92. We did use the measured results of batch 79 because of a small number of measurements.

Temporal variations of RM measurements for one coulometer solution are shown in Fig. 3.6.1. From this figure, it is evident that RM measurements had a linear trend of ~ 3 to $\sim 7 \mu\text{mol kg}^{-1}$, implying that measurements of seawater samples also have the trend. The trend was also found in temporal changes of 2% CO_2 gas measurements. The trend seems to be due to "cell age" change (Johnson et al., 1998) of a coulometer solution.

Considering the trends, we adjusted measurements of seawater samples so as to be traceable to the certified value of batch 92.

Finally we surveyed vertical profiles of C_1 . In particular, we examined whether systematic differences between measurements of the systems A and B existed or not. Then taking other information of analyses into account, we determined a flag of each value of C_1 .

The average and standard deviation of absolute values of differences of C_T analyzed consecutively were 0.8 and 0.7 $\mu\text{mol kg}^{-1}$ ($n=211$), and 0.6 and 0.6 $\mu\text{mol kg}^{-1}$ ($n=165$), for legs 1 and 2, respectively. The combined values were 0.7 and 0.7 $\mu\text{mol kg}^{-1}$ ($n=376$).

Reference

Johnson, K.M., A.G. Dickson, G. Eiseheid, C. Goyet, P. Guenther, R.M. Key, F.J. Millero, D. Purkerson, C.L. Sabine, R.G. Schottle, D.W.R. Wallace, R.J. Wilke and C.D. Winn (1998): Coulometric total carbon dioxide analysis for marine studies: assessment of the quality of total inorganic carbon measurements made during the US Indian Ocean CO_2 survey 1994-1996, *Mar. Chem.*, 63, 21-37.

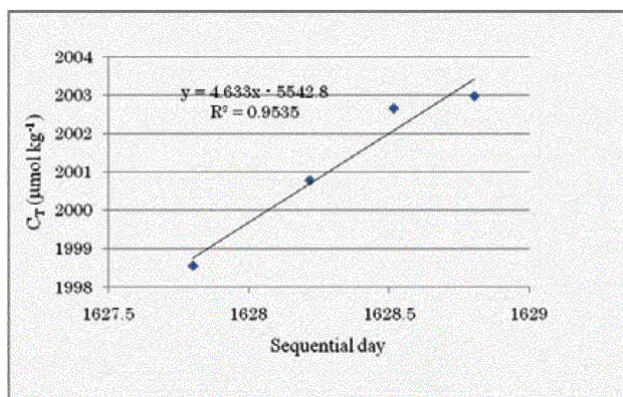


Figure 3.6.1: Distributions of RM measurements as a function of sequential day for Stns. 279 and 282 during MR09-01.

3.7 Total Alkalinity (A_T)

December 4, 2010

(1) Personnel

Akihiko Murata (RIGC/JAMSTEC)
Tomonori Watai (MWJ)
Yoshiko Ishikawa (MWJ)
Ayaka Hatsuyama (MWJ)

(2) Objectives

Concentrations of CO_2 in the atmosphere are now increasing at a rate of 1.9 ppmv y^{-1} due to human activities such as burning of fossil fuels, deforestation, cement production, etc. It is an urgent task to estimate as accurately as possible the absorption capacity of the oceans against the increased atmospheric CO_2 , and to clarify the mechanism of the CO_2 absorption, because the magnitude of the predicted global warming depends on the levels of CO_2 in the atmosphere, and because the ocean currently absorbs 1/3 of the 6 Gt of carbon emitted into the atmosphere each year by human activities.

In the cruise (MR09-01, revisit of WOCE P21 line) using the R/V Mirai, we were aimed at quantifying how much anthropogenic CO_2 is absorbed in the Pacific Ocean. For the purpose, we measured CO_2 -system properties such as dissolved inorganic carbon (C_T), total alkalinity (A_T), pH and underway pCO_2 .

In this section, we describe data on A_T obtained in the cruise in detail.

(3) Apparatus

Measurement of A_T was made based on spectrophotometry using a custom-made system (Nippon ANS, Inc.). The system comprises of a water dispensing unit, an auto-burette (765 Dosimat, Metrohm), and a spectrophotometer (Cary 50 Bio, Varian), which are automatically controlled by a PC. The water dispensing unit has a water-jacketed pipette and a water-jacketed titration cell. The spectrophotometer has a water-jacketed quartz cell, length and volume of which are 8 cm and 13 ml, respectively. To circulate sample seawater between the titration and the quartz cells, PFA tubes are connected to the cells.

A seawater of approx. 42 ml is transferred from a sample bottle (borosilicate glass bottle; 130 ml) into the water-jacketed (25°C) pipette by pressurizing the sample bottle (nitrogen gas), and is introduced into the water-jacketed (25°C) titration cell. The seawater is circulated between the titration and the quartz cells by a peristaltic pump to rinse the route. Then, Milli-Q water is introduced into the titration cell, and is circulated in the same route twice to rinse the route. Next, a seawater of approx. 42 ml is weighted again by the pipette, and is transferred into the titration cell. The weighted seawater is introduced into the quartz cell. Then, for seawater blank, absorbances are measured at three wavelengths (750, 616 and 444 nm). After the measurement, an acid titrant, which is a mixture of approx. 0.05 M HCl in 0.65 M NaCl and bromocresol green (BCG) is added (approx. 2.1 ml) into the titration cell. The seawater + acid titrant solution is circulated for 6 minutes between the titration and the quartz cells, with stirring by a stirring tip and bubbling by wet nitrogen gas in the titration cell. Then, absorbances at the three wavelengths are measured again.

Calculation of A_T was made by the following equation:

$$A_T = (-[\text{H}^+]_T V_{SA} + M_A V_A) / V_S,$$

where M_A is the molarity of the acid titrant added to the seawater sample, $[\text{H}^+]_T$ is the total excess hydrogen ion concentration in the seawater, and V_S , V_A and V_{SA} are the initial seawater volume, the added acid titrant volume,

and the combined seawater plus acid titrant volume, respectively. $[H^+]_T$ is calculated from the measured absorbances based on the following equation (Yao and Byrne, 1998):

$$pH_T = -\log[H^+]_T = 4.2699 + 0.002578(35-S) + \log((R-0.00131)/(2.3148-0.1299R)) - \log(1-0.001005S),$$

where S is the sample salinity, and R is the absorbance ratio calculated as:

$$R = (A_{616} - A_{750}) / (A_{444} - A_{750}),$$

where A_i is the absorbance at wavelength i nm. The HCl in the acid titrant was standardized (0.049983 M, 0.049982 M) on land.

(4) Shipboard measurement

(4.1) Sampling

All seawater samples were collected from depth using 12 liter Niskin bottles basically at every other stations. The seawater samples for A_T were taken with a plastic drawing tube (PFA tubing connected to silicone rubber tubing) into borosilicate glass bottles of 130 ml. The glass bottle was filled with seawater smoothly from the bottom after rinsing it with a seawater of half a or a full bottle volume. A few hours before analysis, the seawater samples were kept at 25°C in a water bath.

(4.2) Analysis

We analyzed reference materials (RM), which were produced for C_T measurement by JAMSTEC, but were efficient also for the monitor of A_T measurement. In addition, certified reference materials (CRM, batches 92, certified value = 2201.91 $\mu\text{mol kg}^{-1}$, respectively) were also analyzed periodically to monitor systematic differences of measured A_T . The reported values of A_T were set to be traceable to the certified value of the batch 92.

The preliminary values were reported in a data sheet on the ship. Repeatability calculated from replicate samples and vertical profiles of A_T based on raw data for each station helped us check performance of the measuring system.

In the cruise, we finished all the analyses for A_T on board the ship. We did not encounter so serious problems as we had to give up the analyses. However, we experienced some malfunctions of the system during the cruise, which are listed in the followings:

At the early stage of the 1st leg, we found malfunction of the instrument such as showing different A_T values by different quantities of acid titrant added. The malfunction was attributed to the light source of spectrophotometer. After the light source was changed to a new one, the malfunction was resolved.

(5) Quality control

Temporal changes of A_T , which originate from analytical problems, were monitored by measuring A_T of CRM.

We found no abnormal measurements during the cruises.

After making the measured values of A_T comparable to CRM, we examined vertical profiles of A_T . Then taking other information of analyses into account, we determined a flag of each value of A_T .

The average and standard deviation of absolute values of differences of A_T analyzed consecutively were 0.5 and 0.5 $\mu\text{mol kg}^{-1}$ ($n = 200$), and 0.6 and 0.5 $\mu\text{mol kg}^{-1}$ ($n = 165$) for legs 1 and 2, respectively. The combined values were calculated to be 0.5 and 0.5 $\mu\text{mol kg}^{-1}$ ($n = 365$).

Reference

Yao, W. and R. H. Byrne (1998): Simplified seawater alkalinity analysis: Use of linear array spectrometers. Deep-Sea Research 145, 1383-1392.

3.8 pH (pH_T)

December 10, 2010

(1) Personnel

Akihiko Murata (RIGC/JAMSTEC)
Tomonori Watai (MWJ)
Yoshiko Ishikawa (MWJ)
Ayaka Hatsuyama (MWJ)

(2) Objectives

Concentrations of CO₂ in the atmosphere are now increasing at a rate of 1.9 ppmv y⁻¹ due to human activities such as burning of fossil fuels, deforestation, cement production, etc. It is an urgent task to estimate as accurately as possible the absorption capacity of the oceans against the increased atmospheric CO₂, and to clarify the mechanism of the CO₂ absorption, because the magnitude of the anticipated global warming depends on the levels of CO₂ in the atmosphere, and because the ocean currently absorbs 1/3 of the 6 Gt of carbon emitted into the atmosphere each year by human activities.

In the cruises (MR09-01, revisit of WOCE P21 line) using the R/V Mirai, we were aimed at quantifying how much anthropogenic CO₂ is absorbed in the Pacific Ocean. For the purpose, we measured CO₂-system properties such as dissolved inorganic carbon (C_T), total alkalinity (A_T), pH and underway pCO₂.

In this section, we describe data on pH obtained in the cruise in detail.

(3) Apparatus

Measurement of pH was made by a pH measuring system (Nippon ANS, Inc.), which adopts spectrophotometry. The system comprises of a water dispensing unit and a spectrophotometer (Carry 50 Scan, Varian).

Seawater is transferred from borosilicate glass bottle (300 ml) to a sample cell in the spectrophotometer.

The length and volume of the cell are 8 cm and 13 ml, respectively, and the sample cell was kept at 25.00 ± 0.05°C in a thermostated compartment. First, absorbances of seawater only are measured at three wavelengths (730, 578 and 434 nm). Then an indicator is injected and circulated for about 4 minutes, to mix the indicator and seawater sufficiently. After the pump is stopped, the absorbances of seawater + indicator are measured at the same wavelengths.

The pH is calculated based on the following equation (Clayton and Byrne, 1993):

$$pH = pK_2 + \log \left(\frac{A_1/A_2 - 0.00691}{2.2220 - 0.1331(A_1/A_2)} \right) \quad (1),$$

where A₁ and A₂ indicate absorbances at 578 and 434 nm, respectively, and pK₂ is calculated as a function of water temperature and salinity.

(4) Shipboard measurement

(4.1) Sampling

All seawater samples were collected from depth with 12 liter Niskin bottles basically at every other stations. The seawater samples for pH were taken with a plastic drawing tube (PFA tubing connected to silicone rubber tubing)

into a 300 ml borosilicate glass bottle, which was the same as used for C_T sampling. The glass bottle was filled with seawater smoothly from the bottom following a rinse with a sea water of 2 full, bottle volumes. The glass bottle was closed by a stopper, which was fitted to the bottle mouth gravimetrically without additional force.

A few hours just before analysis, the seawater samples were kept at 25°C in a water bath.

(4.2) Analysis

For an indicator solution, m-cresol purple (2 mM) was used. The indicator solution was produced on board a ship, and retained in a 1000 ml DURAN® laboratory bottle. We renewed an indicator solution 3 times when the headspace of the bottle became large, and monitored pH or absorbance ratio of the indicator solution by another spectrophotometer (Carry 50 Scan, Varian) using a cell with a short path length of 0.5 mm. In most indicator solutions, the absorbance ratios of the indicator solution were kept mostly between 1.4 and 1.6 by adding acid or alkali solution appropriately.

It is difficult to mix seawater with an indicator solution sufficiently under no headspace condition. However, by circulating the mixed solution with a peristaltic pump, a well-mixed condition came to be attained rather shortly, leading to a rapid stabilization of absorbance. We renewed a TYGON® tube of a peristaltic pump periodically, when a tube deteriorated.

Absorbances of seawater only and seawater + indicator solutions were measured 11 times each, and the last value was used for the calculation of pH (Eq. 1).

The preliminary values of pH were reported in a data sheet on the ship. Repeatability calculated from replicate samples and vertical profiles of pH based on raw data for each station helped us check performance of the measuring system.

We finished all the analyses for pH on board the ship. We did not encounter so serious a problem as we had to give up the analyses. However, we sometimes experienced malfunctions of the system during the cruise.

(5) Quality control

It is recommended that correction for pH change resulting from addition of indicator solutions is made (DOE, 1994). To check the perturbation of pH due to the addition, we measured absorbance ratios by doubling the volume of indicator solutions added to a same seawater sample. We corrected absorbance ratios based on an empirical method (DOE, 1994), although the perturbations were small. [Figure 3.8.1](#) illustrates an example of perturbation of absorbance ratios by adding indicator solutions.

We surveyed vertical profiles of pH. In particular, we examined whether systematic differences between before and after the renewal of indicator solutions existed or not. Then taking other information of analyses into account, we determined a flag of each value of pH. The reported values, which are the total scale, were set to the values at 25°C by the CO₂ system calculation using data for pH and C_T with K1, K2 from Mehrbach et al. (1973) refit by Dickson and Millero (1987).

The average and standard deviation of absolute values of differences of pH analyzed consecutively were 0.0005 and 0.0004 pH unit (n = 266), and 0.0004 and 0.0004 pH unit (n = 205) for legs 1 and 2, respectively. The combined values were 0.0004 and 0.0004 pH unit (n = 471).

References

- Clayton T.D. and R.H. Byrne (1993): Spectrophotometric seawater pH measurements: total hydrogen ion concentration scale calibration of m-cresol purple and at-sea results. *Deep-Sea Research*, 40, 2115-2129.
- Dickson A.G. and E.J. Millero (1987): A Comparison of the equilibrium constants for the dissociation of carbonic acid in seawater media. *Deep-Sea Research*, 34, 1733-1743.
- DOE (1994): Handbook of methods for the analysis of the various parameters of the carbon dioxide system in sea water, version 2, A.G. Dickson & C. Goyet, eds. (unpublished manuscript).
- Mehrbach, C., C.H. Culberson, J.E. Hawley, and R.M. Pytkowicz (1973): Measurement of the apparent dissociation constants of carbonic acid in seawater at atmospheric pressure. *Limnology and Oceanography*, 18, 897-907.

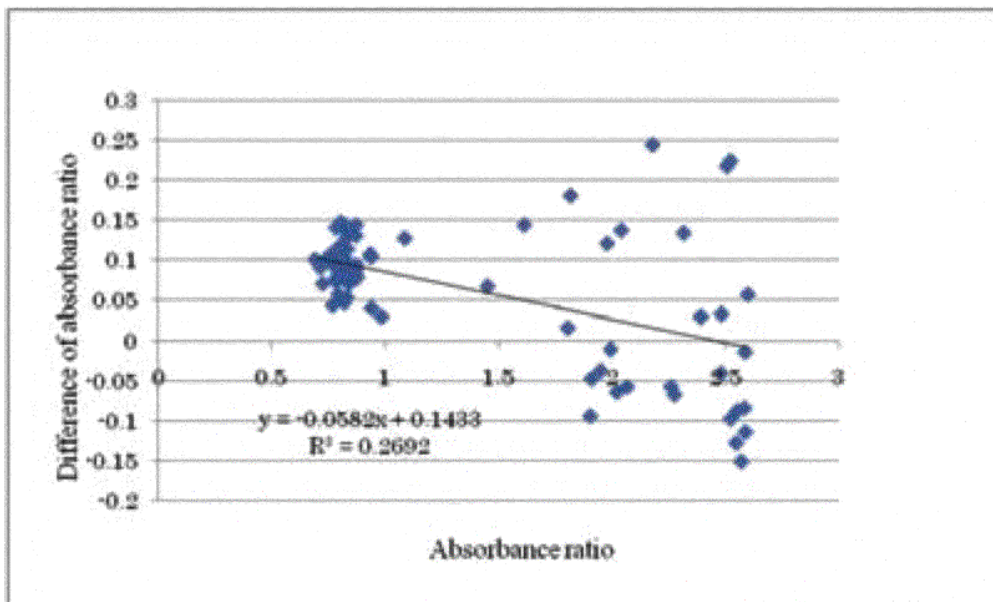


Figure 3.8.1: Perturbation of absorbance ratios by adding indicator solutions. The line was determined by the method of least squares.

3.9 LADCP

November 1, 2010

(1) Personnel

Shinya Kouketsu	(JAMSTEC)
Hiroshi Uchida	(JAMSTEC)
Katsurou Katsumata	(JAMSTEC)
Toshimasa Doi	(JAMSTEC)

(2) Overview of the equipment

An acoustic Doppler current profiler (ADCP) was integrated with the CTD/RMS package. The lowered ADCP (LADCP), Workhorse Monitor WHIM300 (Teledyne RD Instruments, San Diego, California, USA), which has 4 downward facing transducers with 20-degree beam angles, rated to 6000 m. The LADCP makes direct current measurements at the depth of the CTD, thus providing a full profile of velocity. The LADCP was powered during the CTD casts by a 50.4 volts rechargeable Ni-Cd battery pack. The LADCP unit was set for recording internally prior to each cast. After each cast the internally stored observed data was uploaded to the computer on-board. By combining the measured velocity of the sea water and bottom with respect to the instrument, and shipboard navigation data during the CTD cast, the absolute velocity profile can be obtained (e.g., Visbeck, 2002).

The instrument used in this cruise was as follows.

Teledyne RD Instruments, WHIM300

S/N 11853 (CPU firmware vet 50.32, vet 50.35, with pressure sensor)

S/N 8484 (CPU firmware vet 50.32, vet 50.35)

S/N 1512 (CPU firmware vet 50.35)

(3) Data collection

In this cruise, data were collected with the following configuration.

Bin size: 8 m

Number of bins: 14

Pings per ensemble: 1

Ping interval: 1 sec

At the following stations, the CTD cast was carried out without the LADCP, because maximum pressure was beyond the pressure-proof of the LADCP (6000 m). Station P21-200

(4) Data collection problems

We changed the instruments many times due to various troubles. The log of changing instruments is as follows.

Station P21-120: from S/N 11853 (firmware vet 50.32) to S/N 8484 (firmware vet 50.32)

Station P21-132: from S/N 8484 (firmware vet 50.32) to S/N 8484 (firmware vet 50.35)

Station P21-141: from S/N 8484 (firmware vet 50.35) to S/N 11853 (firmware vet 50.35)

Station P21-174: from S/N 11853 (firmware vet 50.35) to S/N 1512 (firmware vet 50.35)

Station P21-181: from S/N 1512 (firmware vet 50.35) to S/N 11853 (firmware vet 50.35)

Station P21-182: from S/N 11853 (firmware vet 50.35) to S/N 1512 (firmware vet 50.35)

Until the Station 120, data recording was intermittently stopped during a cast due to the firmware (ver. 50.32) bug. Because the beam 2 of S/N 8484 became weak at the Station 139, we changed instruments from S/N 8484 to S/N 11853. The beam 2 of the instrument (S/N 11853) also didn't work well at the Station 173 and the instrument was changed to S/N 1512. Since the beam 3 of the instrument (S/N 1512) became weak at the Station 180, we tried the S/N 11853 again at the Station 181 to compare the echo intensities. Since the instrument of S/N 1512 worked better than S/N 11853, the S/N 1512 was used after the Station 182 (see Fig. 3.9.1).

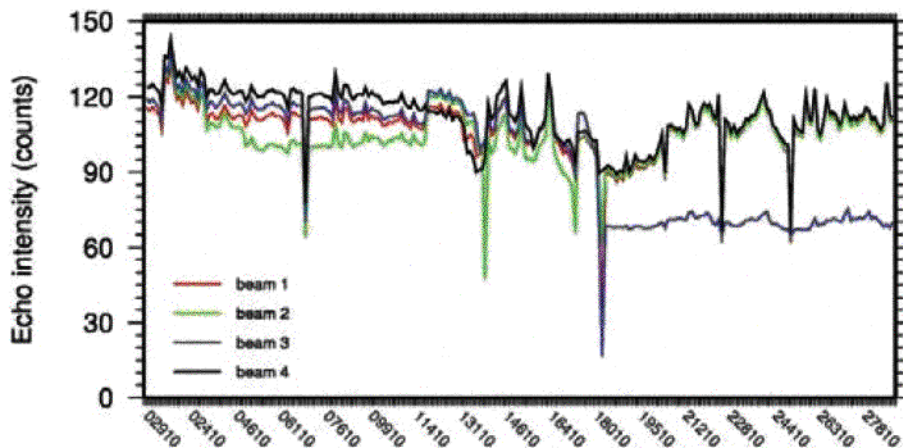


Figure 3.9.1: Cast-averaged echo intensities at 31 bin.

(5) Data process

Vertical profiles of velocity are obtained by the inversion method (Visbeck, 2002). Since the first bin from LADCP is influenced by the turbulence generated by CTD frame, the weight for the inversion is set to 0.1. GPS navigation data and the bottom-track data are used in the calculation of the reference velocities. Shipboard ADCP data averaged for 1 minutes are also included in the calculation. The CTD data are used for the sound speed and depth calculation. The directions of velocity are corrected using the magnetic deviation estimated with International Geomagnetic reference field data.

However, the inversion method doesn't work well due to no-good velocity data due to the instrument problems as well as weak echo intensity at deep layers. So we added a cast flag for each profile. The flag of 5 means that data files for one cast were divided into small files due to firmware bugs provided from RDI. The flag of 6 means that 3 beam solutions were included in the cast.

Reference

Visbeck, M. (2002): Deep velocity profiling using Lowered Acoustic Doppler Current Profilers: Bottom track and inverse solutions. *J. Atmos. Oceanic Technol.*, 19, 794-807.

Water sample parameters:

Number	Parameter	Mnemonic	Mnemonic for expected error
1	Salinity	SALNTY	
2	Oxygen	OXYGEN	
3	Silicate	SILCAT	SILUNC
4	Nitrate	NITRAT	NRAUNC
5	Nitrite	NITRIT	NRIUNC
6	Phosphate	PHSPHT	PHPUNC
7	Freon-11	CFC-11	
8	Freon-12	CFC-12	
12	14Carbon	OELC14	C14ERR
13	13Carbon	OELC13	C13ERR
23	Total carbon	TCARBN	
24	Total alkalinity	ALKALI	
26	pH	PH	
27	Freon-113	CFC113	
28	Carbon Tetrachloride	CCL4	
30	Ammonia	NN4	
31	Methane	CH4	
33	Nitrous oxide	N2O	
34	Chlorophyll a	CHLORA	
41	Particulate Organic Nitrogen	PON	
42	Abundance of bacteria	BACT	
47	Plutonium	PLUTO	PLOTOER
48	Primary Productivity		
64	Incubation		
82	15N-Nitrate	15MO3	
86	Flowcytometry		
88	Nitrogen Fixation	DIAZO	

References

- Aminot, A. and D.S. Kirkwood (1995): Report on the results of the fifth ICES intercomparison exercise for nutrients in sea water, ICES coop. Res. Rep. Set, 213.
- Aminot, A. and R. Kerouel (1991): Autoclaved seawater as a reference material for the determination of nitrate and phosphate in seawater. *Anal. Chim. Acta*, 248: 277-283.
- Aminot, A. and R. Kerouel (1995): Reference material for nutrients in seawater: stability of nitrate, nitrite, ammonia and phosphate in autoclaved samples. *Mar. Chem.*, 49: 221-232.
- Aoyama M. and T.M. Joyce (1996): WHP property comparisons from crossing lines in North Pacific. In Abstracts, 1996 WOCE Pacific Workshop, Newport Beach, California.
- Aoyama, M. (2006): 2003 Intercomparison Exercise for Reference Material for Nutrients in Seawater in a Seawater Matrix, Technical Reports of the Meteorological Research Institute No. 50, 91 pp, Tsukuba, Japan.
- Aoyama, M., B. Susan, D. Minhan, D. Hideshi, I.G. Louis, H. Kasai, K. Roger, K. Nurit, M. Doug, A. Murata, N. Nagai, H. Ogawa, H. Ota, H. Saito, K. Saito, T. Shimizu, H. Takano, A. Tsuda, K. Yokouchi, and Y. Agnes (2007): Recent Comparability of Oceanographic Nutrients Data: Results of a 2003 Intercomparison Exercise Using Reference Materials. *Analytical Sciences*, 23: 1151-1154.
- Aoyama, M., J. Barwell-Clarke, S. Becker, M. Blum, E.S. Braga, S.C. Coverly, E. Czobik, I. Dahllof, M.H. Dai, G.O. Donnell, C. Engelke, G.C. Gong, G.-H. Hong, D.J. Hydes, M.M. Jin, H. Kasai, R. Kerouel, Y. Kiyomono, M. Knockaert, N. Kress, K.A. Kroglund, M. Kumagai, S. Leterme, Y. Li, S. Masuda, T. Miyao, T. Moutin, A. Murata, N. Nagai, G. Nausch, M.K. Ngirchchol, A. Nybakk, H. Ogawa, J. van Ooijen, H. Ota, J.M. Pan, C. Payne, O. Pierre-Duplessix, M. Pujo-Pay, T. Raabe, K. Saito, K. Sato, C. Schmidt, M. Schuett, T.M. Shammon, J. Sun, T. Tanhua, L. White, E.M.S. Woodward, P. Worsfold, P. Yeats, T. Yoshimura, A. Youenou, J.Z. Zhang (2008): 2006 Intercomparison Exercise for Reference Material for Nutrients in Seawater in a Seawater Matrix, Technical Reports of the Meteorological Research Institute No. 58, 104pp.
- Aoyama, M., T. Joyce, T. Kawano and Y. Takatsuki (2002): Standard seawater comparison up to P129. *Deep-Sea Research*, I, Vol. 49, 1103-1114.
- Clayton T.D. and R.H. Byrne (1993): Spectrophotometric seawater pH measurements: total hydrogen ion concentration scale calibration of m-cresol purple and at-sea results. *Deep-Sea Research*, 40, 2115-2129.
- Dickson A.G. and E.J. Millero (1987): A Comparison of the equilibrium constants for the dissociation of carbonic acid in seawater media. *Deep-Sea Research*, 34, 1733-1743.
- Dickson, A. (1996): Determination of dissolved oxygen in sea water by Winkler titration, in WHPO Pub. 91-1 Rev. 1, November 1994, Woods Hole, Mass., USA.
- DOE (1994): Handbook of methods for the analysis of the various parameters of the carbon dioxide system in seawater; version 2. A.G. Dickson and C. Goyet (eds), ORNL/CDIAC-74.
- DOE (1994): Handbook of methods for the analysis of the various parameters of the carbon dioxide system in sea water, version 2, A. G. Dickson & C. Goyet, eds. (unpublished manuscript).
- Downey, N.J., J.M. Stock, R.W. Clayton, and S.C. Cande (2007): History of the Cretaceous Osborn spreading center, *J. Geophys. Res.*, 112, B04102, doi:10.1029/2006JB004550.
- Fukasawa, M., T. Kawano and H. Uchida (2004): Blue Earth Global Expedition collects CTD data aboard Mirai, BEAGLE 2003 conducted using a Dynacon CTD traction winch and motion-compensated crane, *Sea Technology*, 45, 14-18.
- Garcia, H.E. and L.I. Gordon (1992): Oxygen solubility in seawater: Better fitting equations. *Limnol. Oceanogr.*, 37 (6), 1307-1312.
- Goff, J.A., Y. Ma, A. Shah, J.R. Cochran, and J.-C. Sempere (1997): Stochastic analysis of seafloor morphology on the flank of the Southeast Indian Ridge: The influence of ridge morphology on the formation of abyssal hills, *J. Geophys. Res.*, 102, 15,521-15,534.

- Gordon, L.I. and L.B. Jones (1973) The effect of temperature on carbon dioxide partial pressure in seawater. *Mar. Chem.*, 1, 317-322.
- Gouretski, V.V. and K. Jancke (2001): Systematic errors as the cause for an apparent deep water property variability: global analysis of the WOCE and historical hydrographic data REVIEW ARTICLE, *Progress in Oceanography*, 48: Issue 4, 337-402.
- Grasshoff, K., M. Ehrhardt, K. Kremling et al. (1983): *Methods of seawater analysis*. 2nd rev. Weinheim: Verlag Chemie, Germany, West.
- Johnson, K.M., A.G. Dickson, G. Eiseid, C. Goyet, P. Guenther, R.M. Key, F.J. Millero, D. Purkerson, C.L. Sabine, R.G. Schottle, D.W.R. Wallace, R.J. Wilke and C.D. Winn (1998): Coulometric total carbon dioxide analysis for marine studies: assessment of the quality of total inorganic carbon measurements made during the US Indian Ocean CO₂ survey 1994-1996, *Mar. Chem.*, 63, 21-37.
- Joyce, T. and C. Corry (1994): Requirements for WOCE hydrographic programmed data reporting. WHPO Publication, 90-1, Revision 2, WOCE Report No. 67/91.
- Joyce, T., and C. Corry, eds., C. Corry, A. Dessier, A. Dickson, T. Joyce, M. Kenny, R. Key, D. Legler, R. Millard, R. Onken, P. Saunders, M. Stalcup (1994): Requirements for WOCE Hydrographic Programme Data Reporting, WHPO Pub. 90-1 Rev. 2, May 1994 Woods Hole, Mass., USA.
- Kawano, T., H. Uchida and T. Doi (2009): WHP P01, P14 REVISIT DATA BOOK, (Ryoin Co., Ltd., Yokohama).
- Kawano, T., M. Aoyama, T. Joyce, H. Uchida, Y. Takatsuki and M. Fukasawa (2006): The latest batch-to-batch difference table of standard seawater and its application to the WOCE onetime sections, *J. Oceanogr.*, 62, 777-792.
- Kirkwood, D.S. (1992): Stability of solutions of nutrient salts during storage. *Mar. Chem.*, 38: 151-164.
- Kirkwood, D.S., A. Aminot and M. Perttila (1991): Report on the results of the ICES fourth intercomparison exercise for nutrients in sea water. ICES coop. Res. Rep. Set, 174.
- Kizu, S., H. Onishi, T. Suga, K. Hanawa, T. Watanabe, and H. Iwamiya (2008): Evaluation of the fall rates of the present and developmental XCTDs. *Deep-Sea Res I*, 55, 571-586.
- Mackenzie, K.V. (1981): Nine-term equation for the sound speed in the oceans, *J. Acoust. Soc. Am.*, 70 (3), pp 807-812.
- Mehrbach, C., C.H. Culberson, J.E. Hawley, and R.M. Pytkowicz (1973): Measurement of the apparent dissociation constants of carbonic acid in seawater at atmospheric pressure. *Limnology and Oceanography*, 18, 897-907.
- Mordy, C.W., M. Aoyama, L.I. Gordon, G.C. Johnson, R.M. Key, A.A. Ross, J.C. Jennings and J. Wilson (2000): Deep water comparison studies of the Pacific WOCE nutrient data set. *Eos Trans-American Geophysical Union*. 80 (supplement), OS43.
- Murphy, J. and J.P. Riley (1962): *Analytica chim. Acta* 27, 31-36.
- Murray, C.N., J.P. Riley, and T.R.S. Wilson (1968): The solubility of oxygen in Winkler reagents used for determination of dissolved oxygen, *Deep-Sea Res.*, 15, 237-238.
- Nakanishi, M., K. Tamaki, and K. Kobayashi (1992): A new Mesozoic isochron chart of the whole western Pacific Ocean: Paleomagnetic and tectonic implications, *Geophys. Res. Lett.*, 19, 693-696.
- Sea-Bird Electronics (2009): SBE 43 dissolved oxygen (DO) sensor - hysteresis corrections, Application note no. 64-3, 7 pp.
- Searle, R. (1984): GLORIA survey of the East Pacific Rise Near 3.5°S: Tectonic and volcanic characteristics of a fast spreading mid-ocean rise, *Tectonophysics*, 101, 319-344.
- Smith, W.H.F. and D.T. Sandwell (1997): Global seafloor topography from satellite altimetry and ship depth soundings, *Science*, 277, 1956-1962.
- Stramma, L., G.C. Johnson, J. Sprintall, and V. Mohrholz (2008): Expanding Oxygen-Minimum Zones in the Tropical Oceans, *Science*, 320, 655-668.

- Uchida, H. and M. Fukasawa (2005): WHP P6, A10, 13/14 REVISIT DATA BOOK Blue Earth Global Expedition 2003 1, 2, (Aiwa Printing Co., Ltd., Tokyo).
- Uchida, H., K. Ohyama, S. Ozawa, and M. Fukasawa (2007): In situ calibration of the Sea-Bird 9plus CTD thermometer, *J. Atmos. Oceanic Technol.*, 24, 1961-1967.
- Uchida, H., K. Shimada, and T. Kawano (2011): A method for data processing to obtain high quality XCTD data. *J. Atmos. Oceanic Technol.*, accepted.
- Uchida, H., T. Kawano, I. Kaneko, and M. Fukasawa (2008): In situ calibration of optode-based oxygen sensors, *J. Atmos. Oceanic Technol.*, 25, 2271-2281.
- UNESCO (1981): Tenth report of the Joint Panel on Oceanographic Tables and Standards. UNESCO Tech. Papers in Mar. Sci., 36, 25 pp.
- Visbeck, M. (2002): Deep velocity profiling using Lowered Acoustic Doppler Current Profilers: Bottom track and inverse solutions. *J. Atmos. Oceanic Technol.*, 19, 794-807.
- Viso, R.F., R.L. Larson, and R.A. Pockalny (2005): Tectonic evolution of the Pacific-Phoenix-Farallon triple junction in the South Pacific Ocean, *Earth Planet Sci. Lett.*, 233, 179-194.
- Wetzel, R.G. and G.E. Likens (2000): *Limnological Analysis*, 429 pp., Springer, New York, USA.

Figure captions

- Figure 1:** Station locations for WHP P21 revisit cruise with bottom topography based on Smith and Sandwell (1997).
- Figure 2:** Bathymetry measured by Multi Narrow Beam Echo Sounding system.
- Figure 3:** Surface wind measured at 25 m above sea level. Wind data is averaged over 1-hour and plotted every 1 degree in latitude or longitude.
- Figure 4:** Sea surface temperature (SST). Temperature data is averaged over 1-hour.
- Figure 5:** Sea surface salinity (SSS). Salinity data is averaged over 1-hour.
- Figure 6:** Difference in the partial pressure of CO₂ between the ocean and the atmosphere, $\Delta p\text{CO}_2$
- Figure 7:** Surface current at 100 m depth measured by ship board acoustic Doppler current profiler (ADCP).
- Figure 8:** Potential temperature ($^{\circ}\text{C}$) cross section calculated by using CTD temperature and salinity data calibrated by bottle salinity measurements. Vertical exaggeration of the 0-6500 m section is 1000:1. Expanded section of the upper 1000 m is made with a vertical exaggeration of 2500:1.
- Figure 9:** CTD salinity (psu) cross section calibrated by bottle salinity measurements. Vertical exaggeration is same as Figure 8.
- Figure 10:** Absolute salinity (g/kg) cross section calculated by using CTD salinity data. Vertical exaggeration is same as Figure 8.
- Figure 11:** Density (σ_0) (kg/m^3) cross section calculated by using CTD temperature and salinity data. Vertical exaggeration is same as Figure 8.
- Figure 12:** Same as Figure 11 but for σ_4 (kg/m^3).
- Figure 13:** Neutral density γ^n (kg/m^3) cross section calculated by using CTD temperature and salinity data. Vertical exaggeration is same as Figure 8.
- Figure 14:** Cross section of CTD oxygen ($\mu\text{mol/kg}$). Vertical exaggeration is same as Figure 8.
- Figure 15:** Cross section of bottle sampled dissolved oxygen ($\mu\text{mol/kg}$). Data with quality flags of 2 were plotted. Vertical exaggeration is same as Figure 8.

- Figure 16:** Silicate ($\mu\text{mol/kg}$) cross section. Data with quality flags of 2 were plotted. Vertical exaggeration is same as Figure 8.
- Figure 17:** Nitrate ($\mu\text{mol/kg}$) cross section. Data with quality flags of 2 were plotted. Vertical exaggeration is same as Figure 8.
- Figure 18:** Nitrite ($\mu\text{mol/kg}$) cross section. Data with quality flags of 2 were plotted. Vertical exaggeration of the upper 1000 m section is same as Figure 8.
- Figure 19:** Phosphate ($\mu\text{mol/kg}$) cross section. Data with quality flags of 2 were plotted. Vertical exaggeration is same as Figure 3.
- Figure 20:** Dissolved inorganic carbon ($\mu\text{mol/kg}$) cross section. Data with quality flags of 2 were plotted. Vertical exaggeration is same as Figure 8.
- Figure 21:** Total alkalinity ($\mu\text{mol/kg}$) cross section. Data with quality flags of 2 were plotted. Vertical exaggeration is same as Figure 8.
- Figure 22:** pH cross section. Data with quality flags of 2 were plotted. Vertical exaggeration is same as Figure 8.
- Figure 23:** CFC-11 (pmol/kg) cross section. Data with quality flags of 2 were plotted. Vertical exaggeration is same as Figure 8.
- Figure 24:** CFC-12 (pmol/kg) cross section. Data with quality flags of 2 were plotted. Vertical exaggeration is same as Figure 8.
- Figure 25:** CFC-113 (pmol/kg) cross section. Data with quality flags of 2 were plotted. Vertical exaggeration is same as Figure 8.
- Figure 26:** Cross section of current velocity (cm/s) normal to the cruise track measured by LADCP (northward is positive).
- Figure 27:** Difference in potential temperature ($^{\circ}\text{C}$) between results from WOCE (from March to June 1994) and the revisit cruise (from April to June 2009). Red and blue areas show areas where potential temperature increased and decreased in the revisit cruise, respectively. On white areas differences in temperature do not exceed the detection limit of 0.002°C . Vertical exaggeration is same as Figure 8.
- Figure 28:** Difference in salinity (psu) between results from WOCE and the revisit cruise. Red and blue areas show areas where salinity increased and decreased in the revisit cruise, respectively. CTD salinity data with SSW batch correction¹ were used. On white areas differences in salinity do not exceed the detection limit of 0.002 psu. Vertical exaggeration is same as Figure 8.
- Figure 29:** Difference in dissolved oxygen ($\mu\text{mol/kg}$) between results from WOCE and the revisit cruise. Red and blue areas show areas where salinity increased and decreased in the revisit cruise, respectively. CTD oxygen data were used. On white areas differences in dissolved oxygen do not exceed the detection limit of $2 \mu\text{mol/kg}$. Vertical exaggeration is same as Figure 8.

Note

1. As for the traceability of SSW to Mantyla's value, the offset for the batches P123 (WOCE P21) and P150 (the revisit cruise) are -0.0006 and -0.0005 , respectively (Kawano et al, 2006; T. Kawano, personal communication, 2009).

References

- Kawano, T., M. Aoyama, T. Joyce, H. Uchida, Y. Takatsuki and M. Fukasawa (2006): The latest batch-to-batch difference table of standard seawater and its application to the WOCE onetime sections, *J. Oceanogr.*, 62, 777–792.
- Smith, W. H. F. and D. T. Sandwell (1997): Global seafloor topography from satellite altimetry and ship depth soundings, *Science*, 277, 1956–1962.

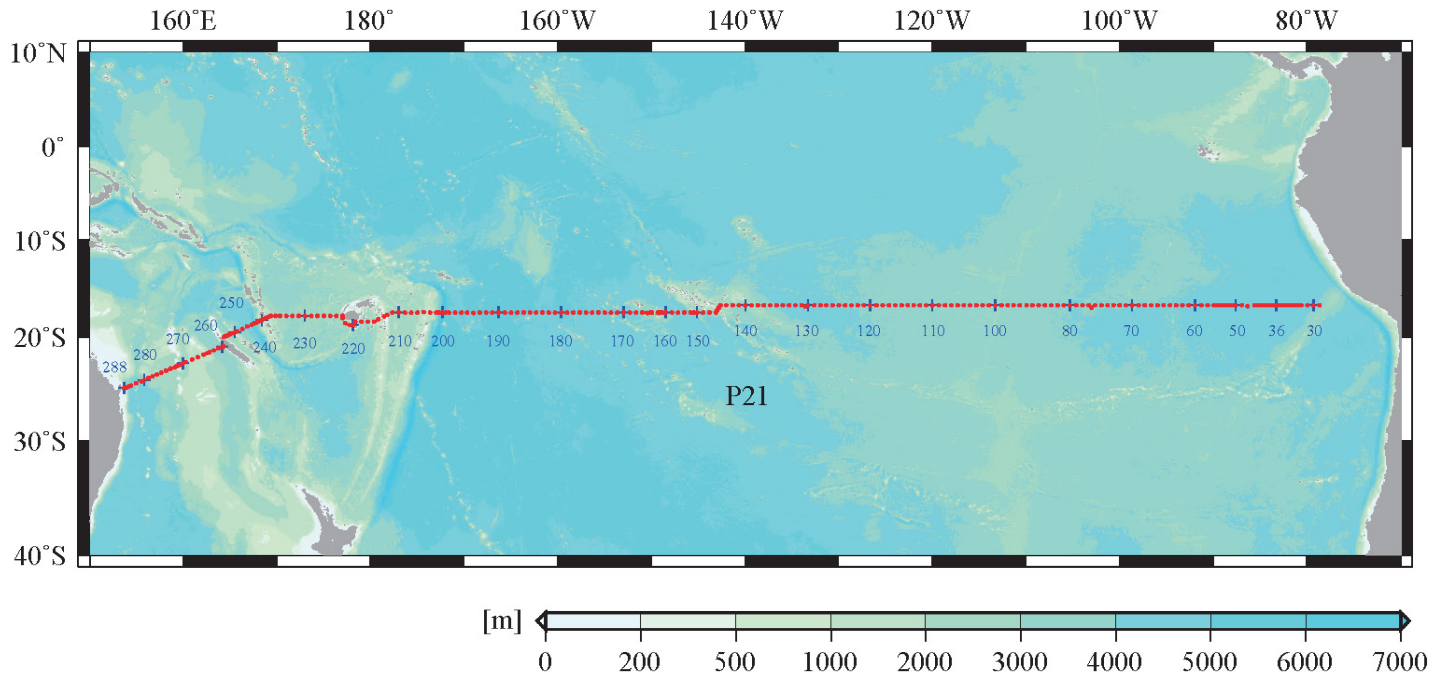


Figure 1: Station locations for WHP P21 revisit cruise with bottom topography based on Smith and Sandwell (1997).

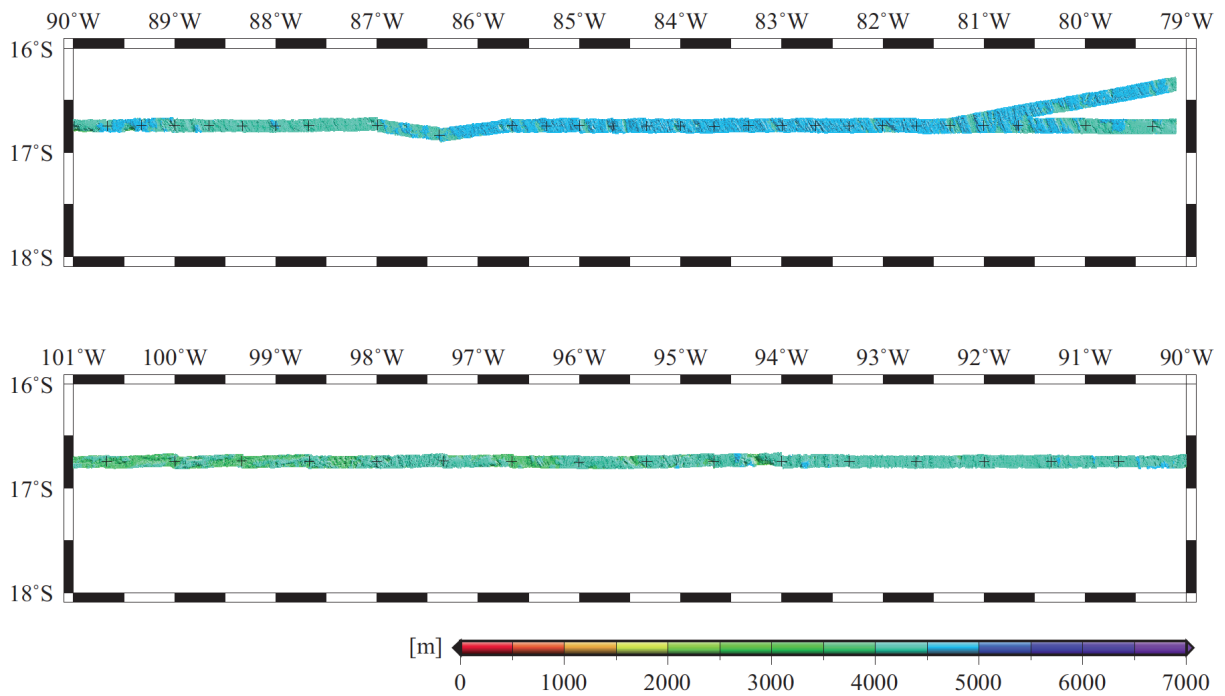


Figure 2.1: Bathymetry measured by Multi Narrow Beam Echo Sounding system.

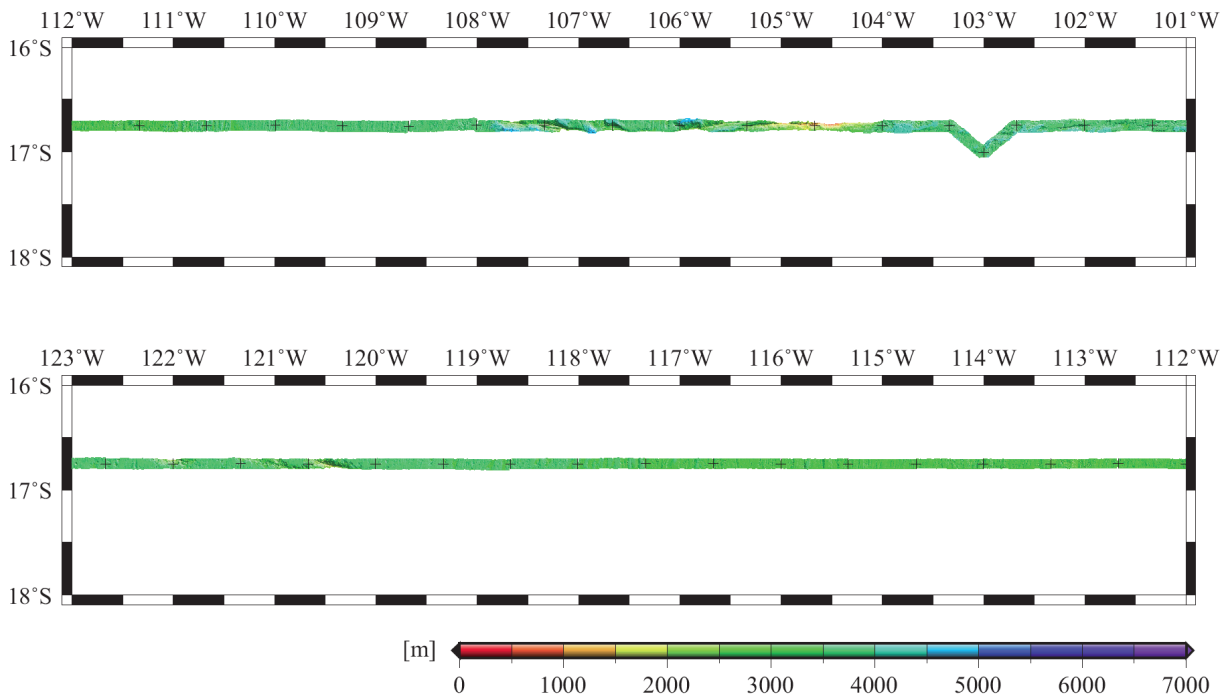


Figure 2.2: Bathymetry measured by Multi Narrow Beam Echo Sounding system.

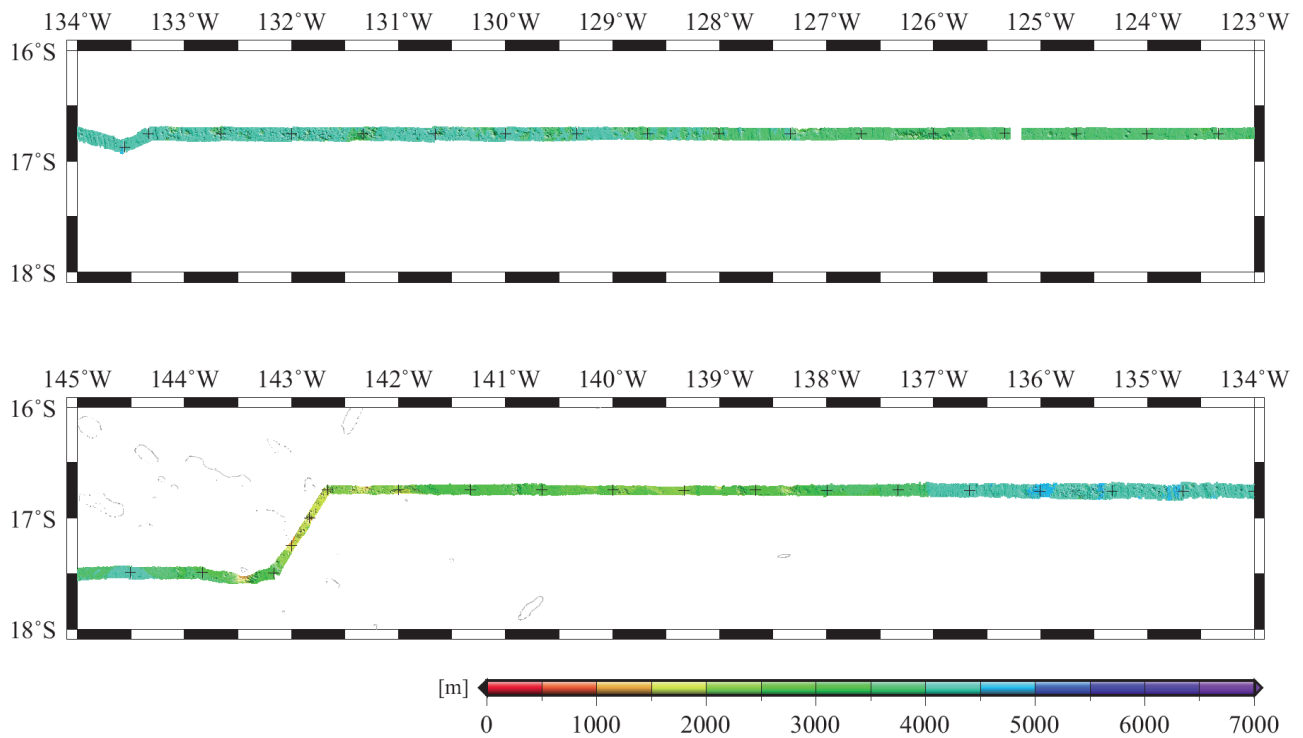


Figure 2.3: Bathymetry measured by Multi Narrow Beam Echo Sounding system.

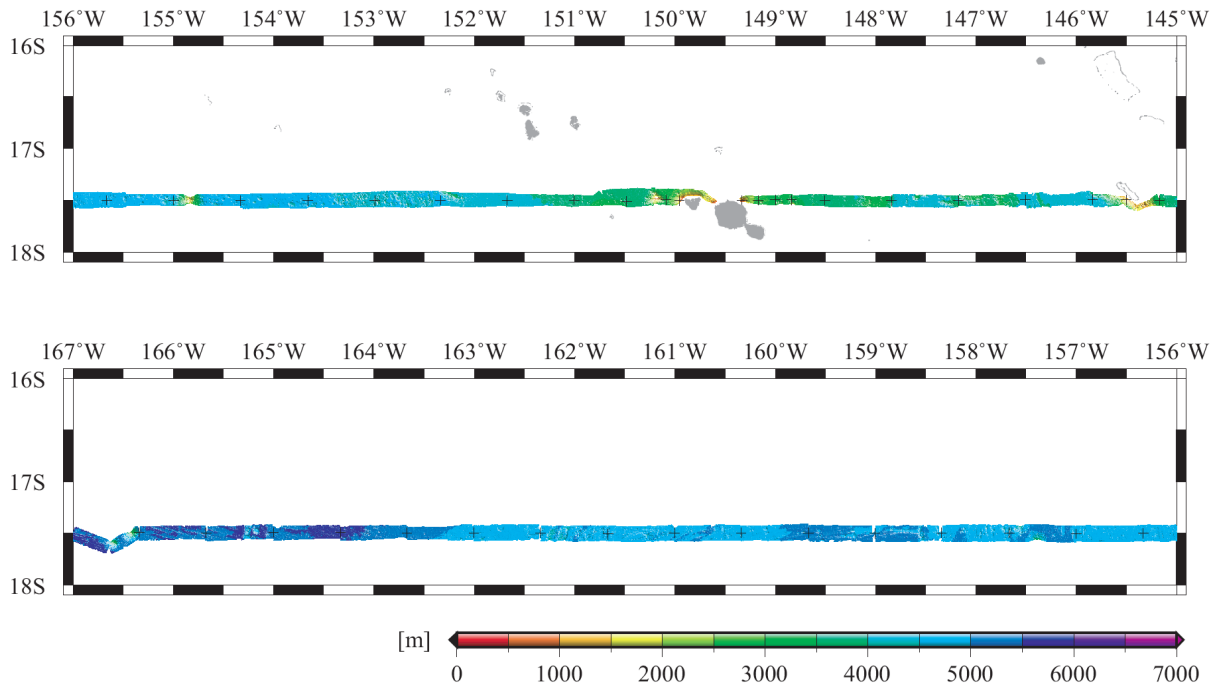


Figure 2.4: Bathymetry measured by Multi Narrow Beam Echo Sounding system.

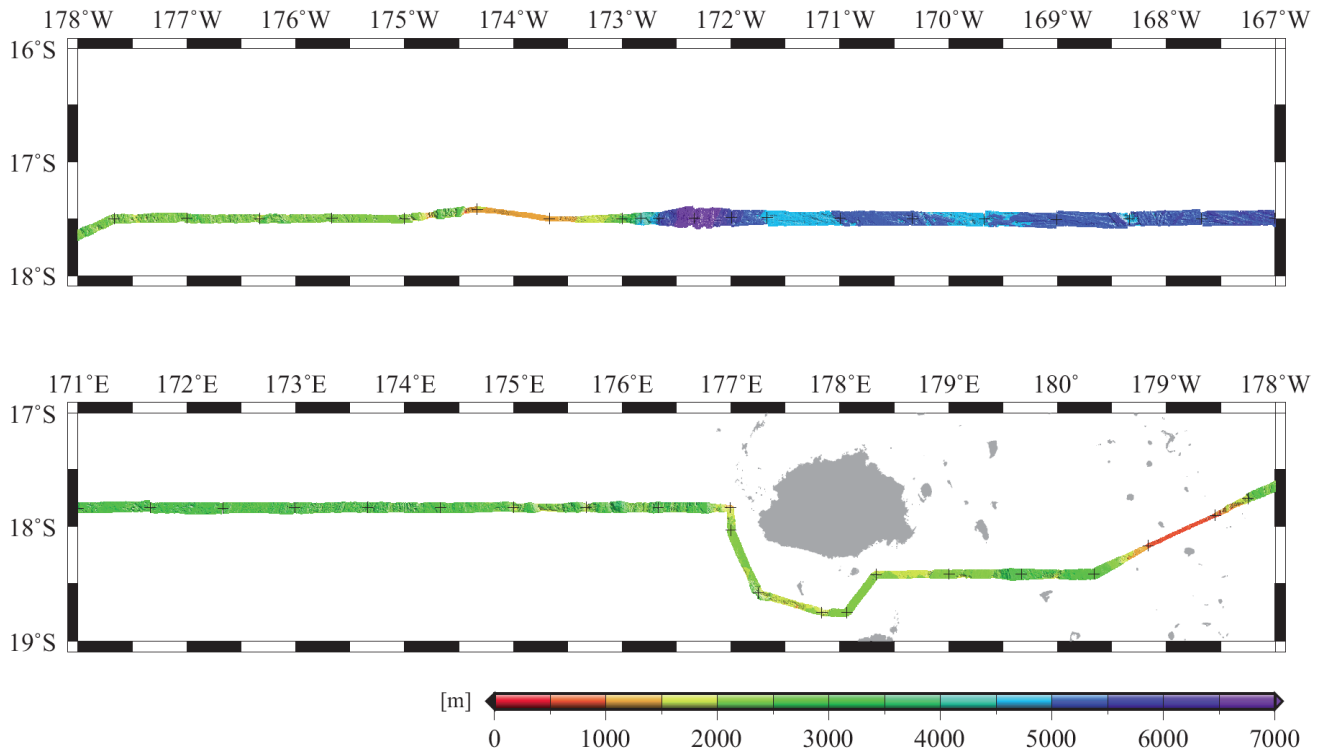


Figure 2.5: Bathymetry measured by Multi Narrow Beam Echo Sounding system.

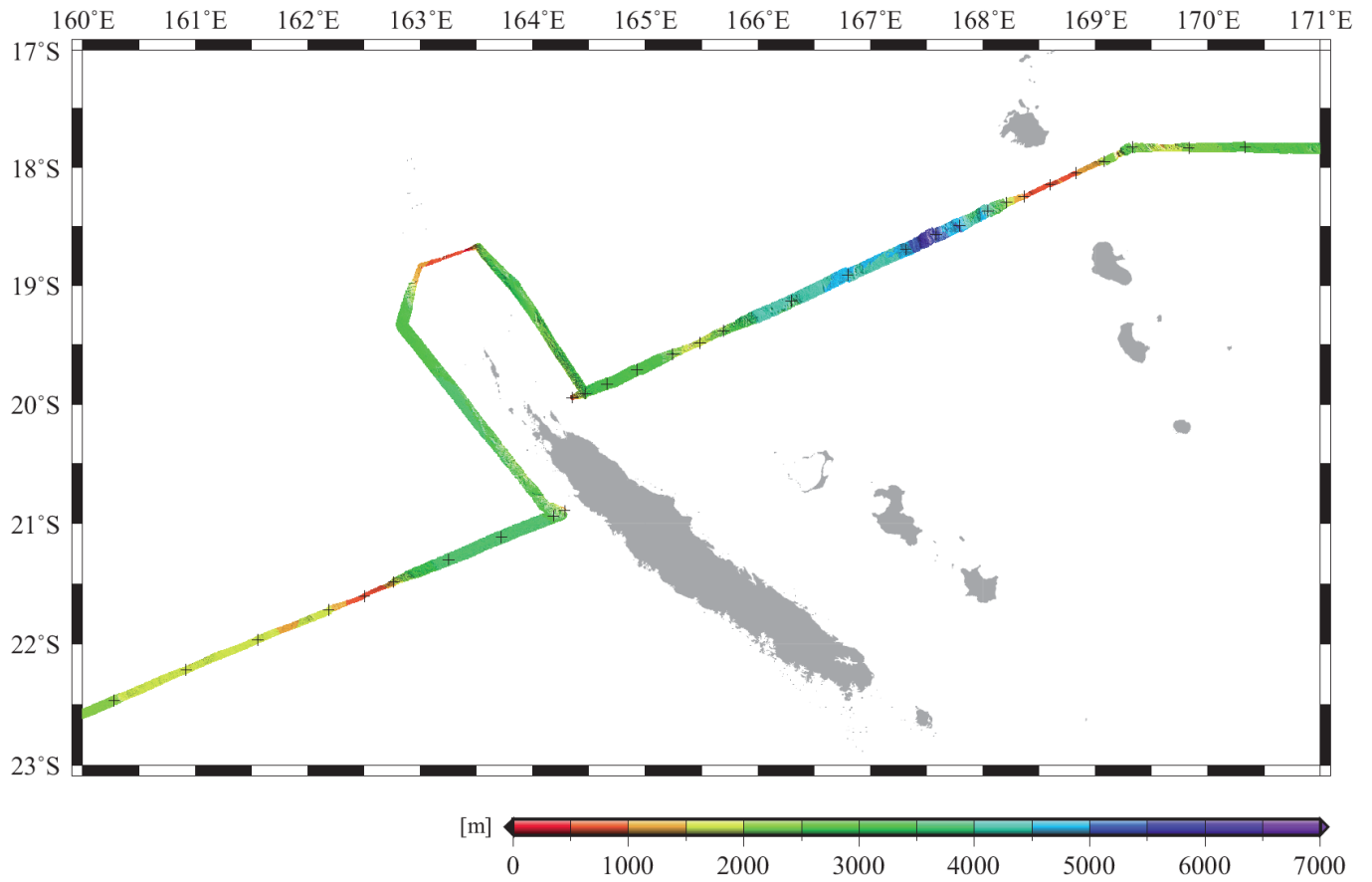


Figure 2.6: Bathymetry measured by Multi Narrow Beam Echo Sounding system.

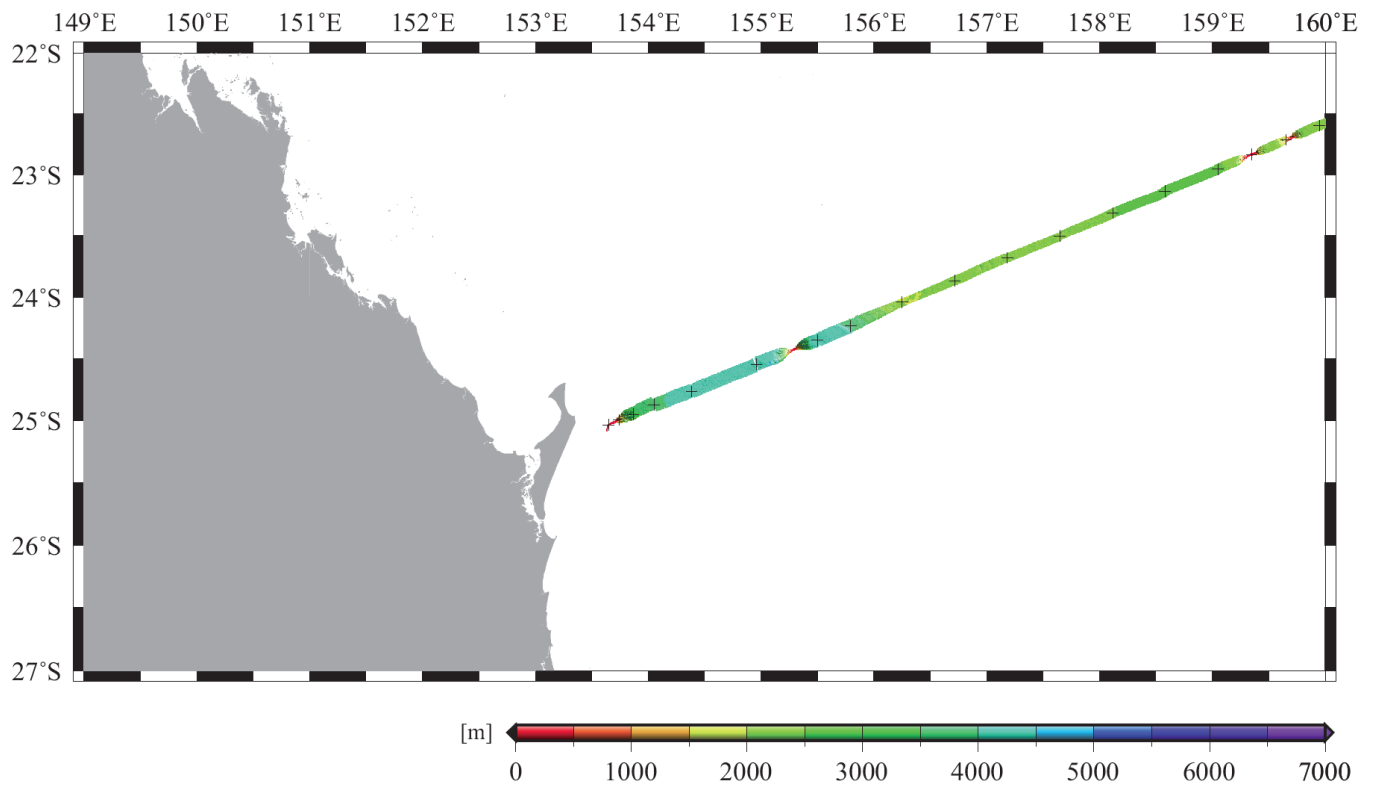


Figure 2.7: Bathymetry measured by Multi Narrow Beam Echo Sounding system.

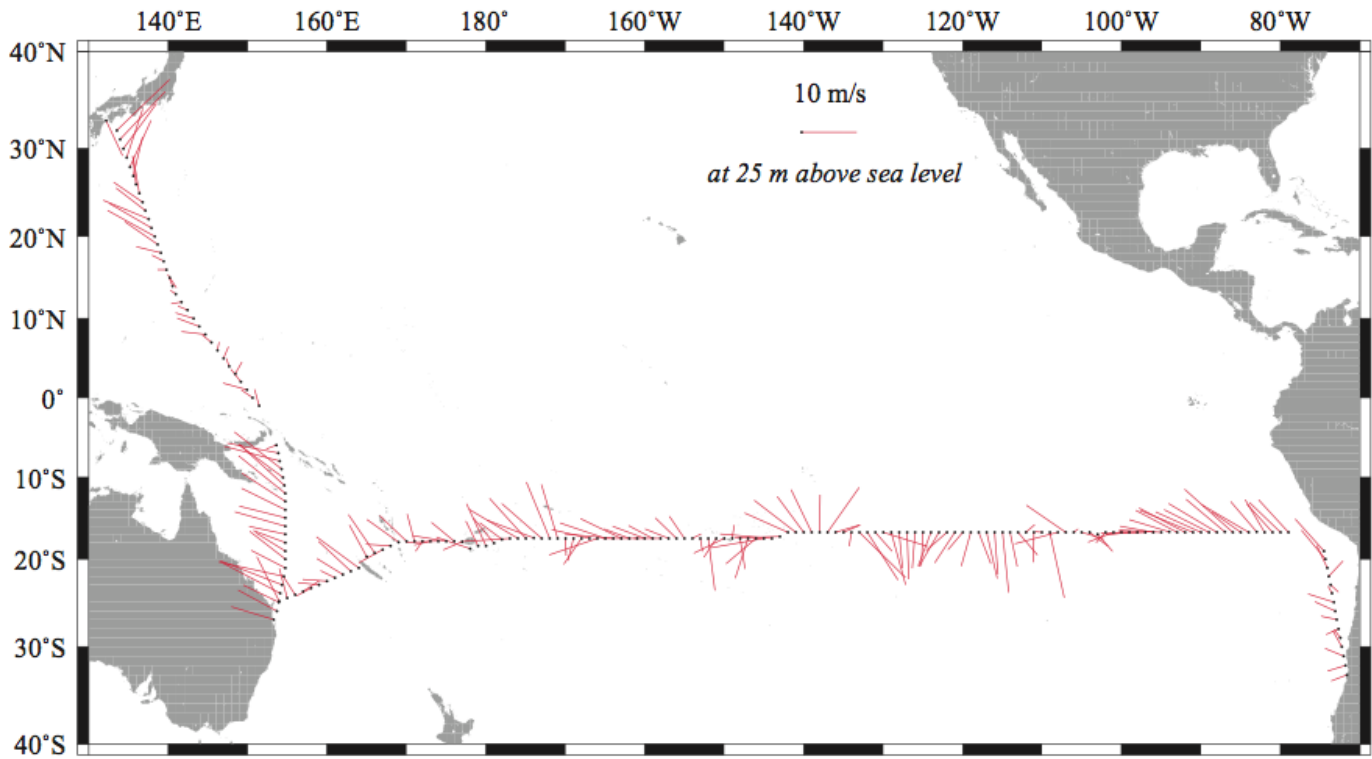


Figure 3: Surface wind measured at 25 m above sea level. Wind data is averaged over 1-hour and plotted every 1 degree in latitude or longitude.

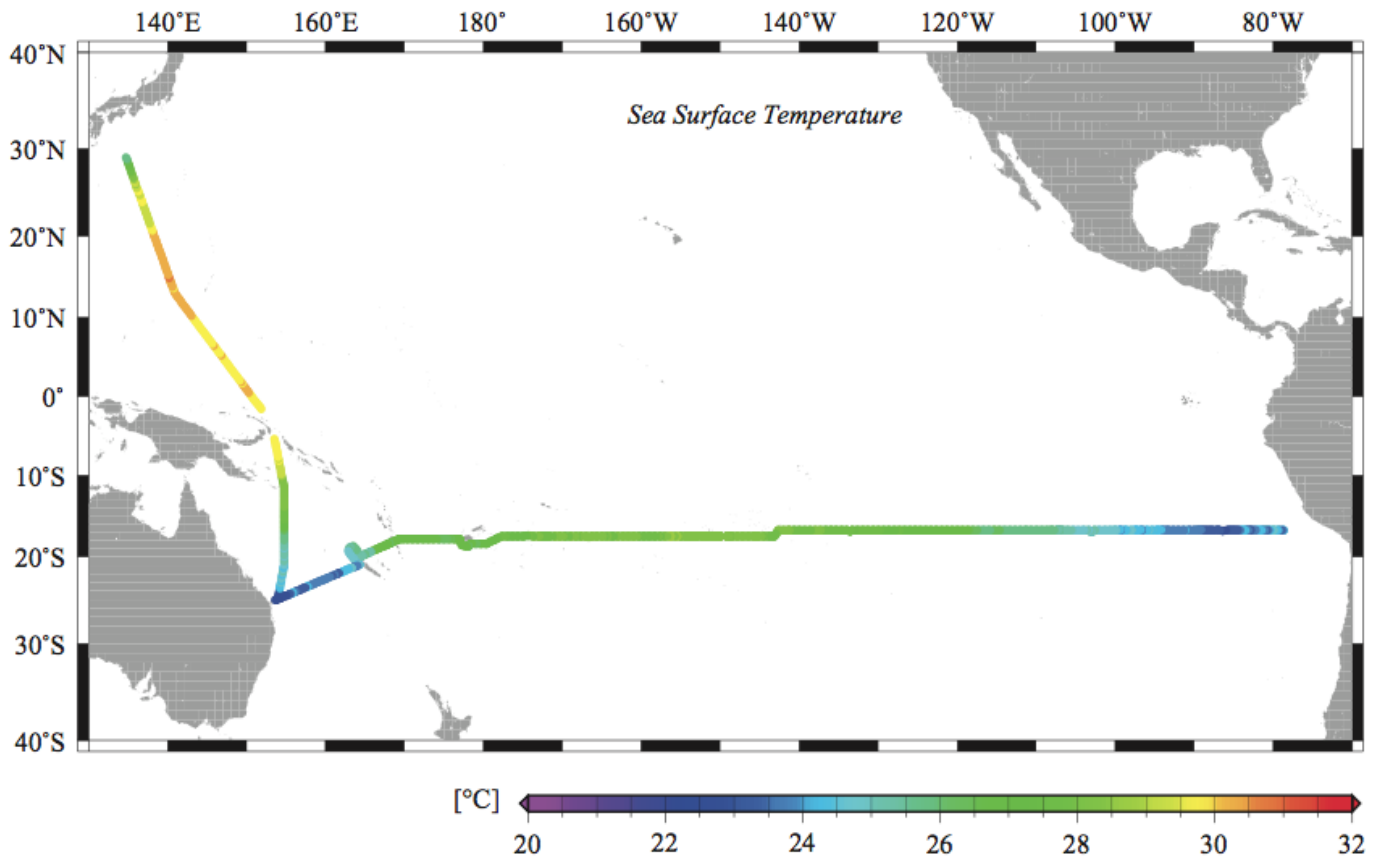


Figure 4: Sea surface temperature (SST). Temperature data is averaged over 1-hour.

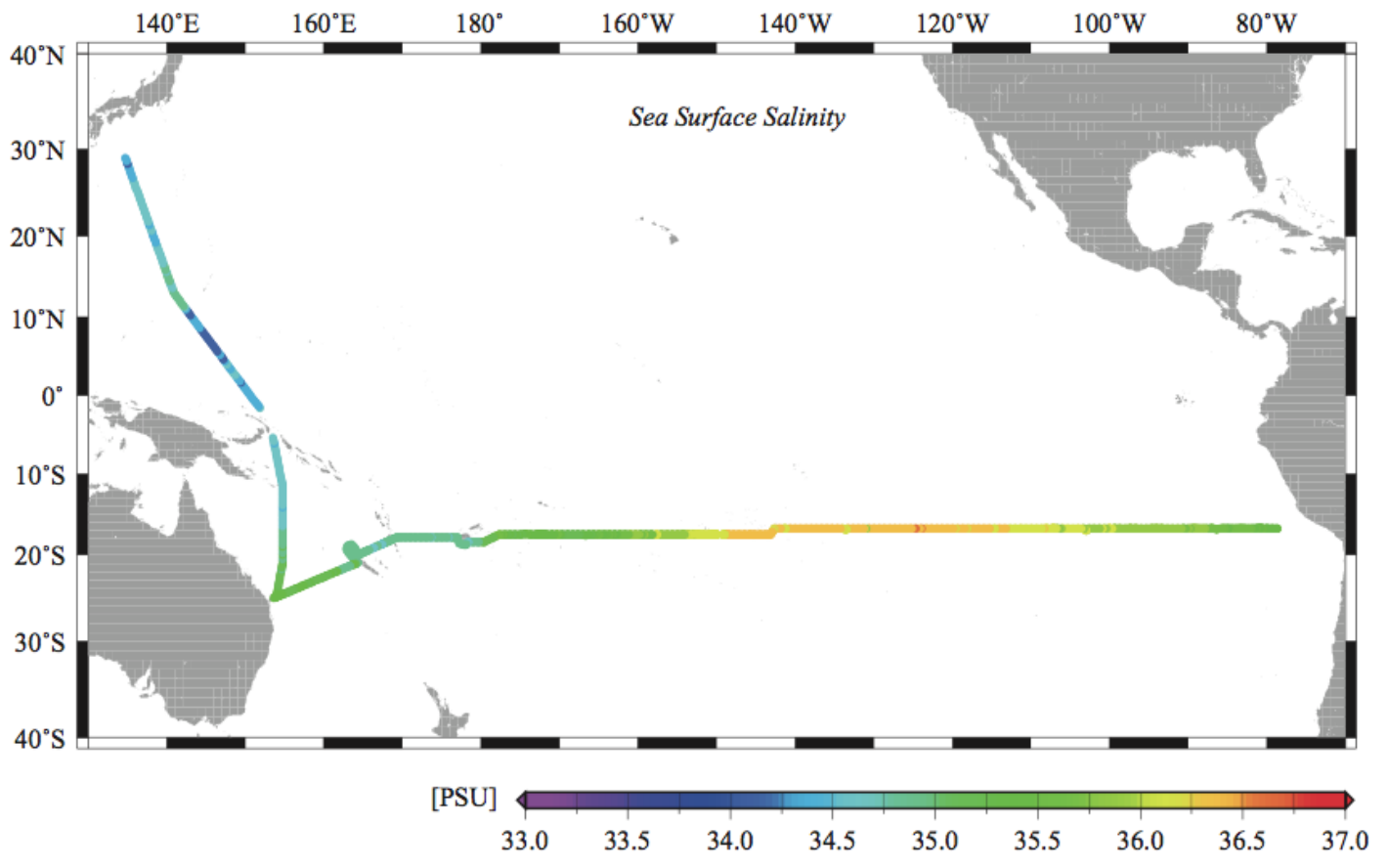


Figure 5 Sea surface salinity (SSS). Salinity data is averaged over 1-hour.

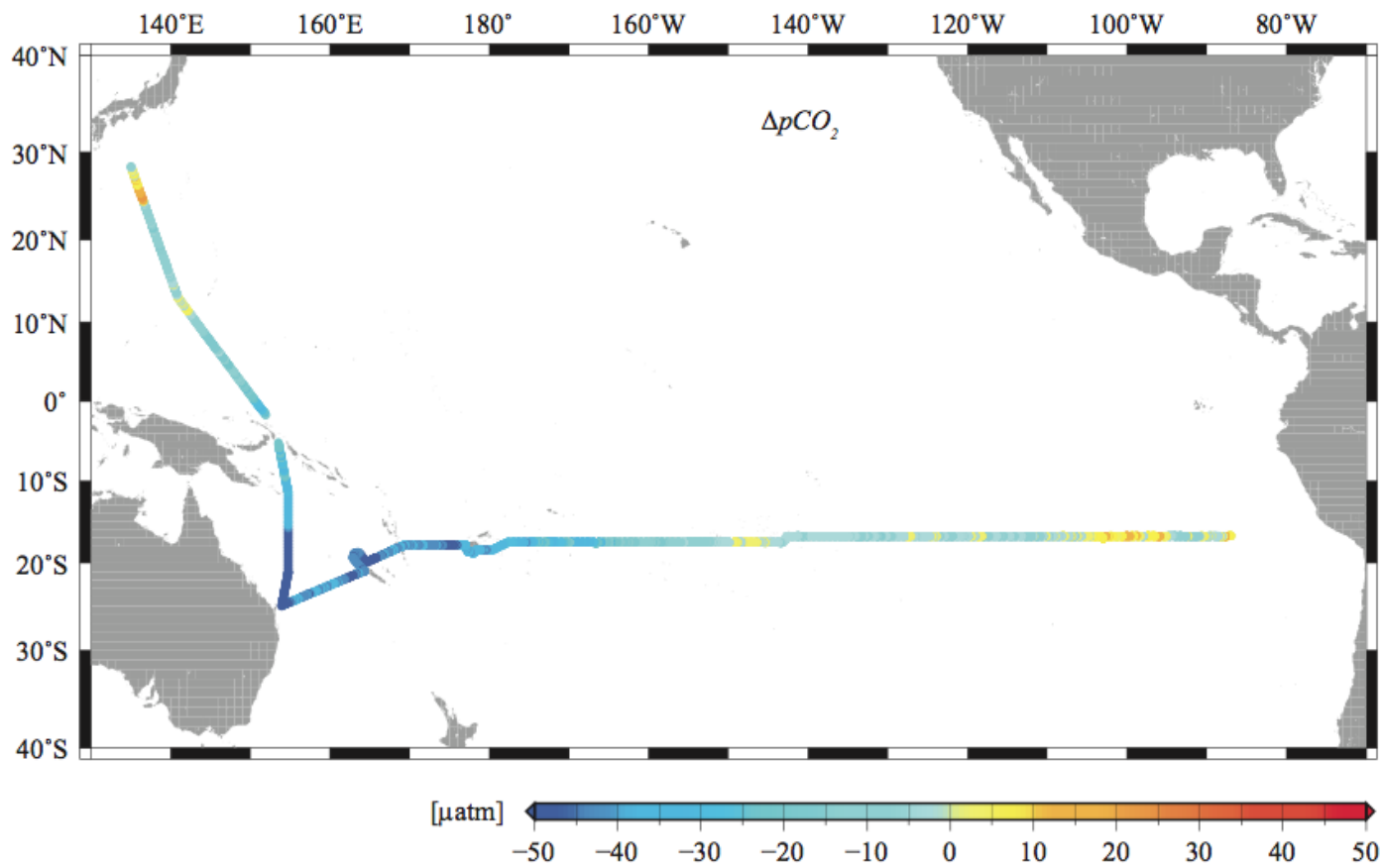


Figure 6: Difference in the partial pressure of CO₂ between the ocean and the atmosphere, ΔpCO_2

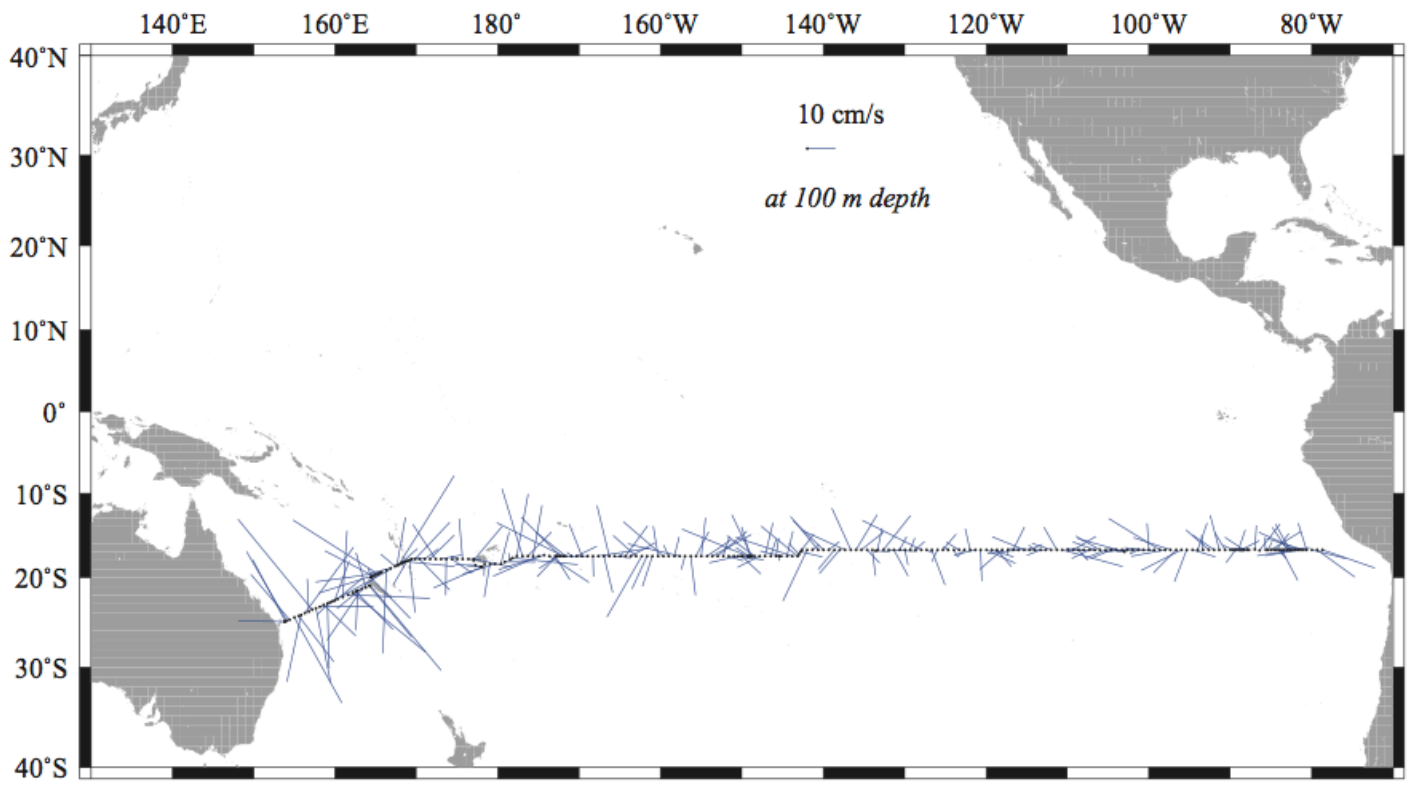


Figure 7: Surface current at 100 m depth measured by ship board acoustic Doppler current profiler (ADCP).

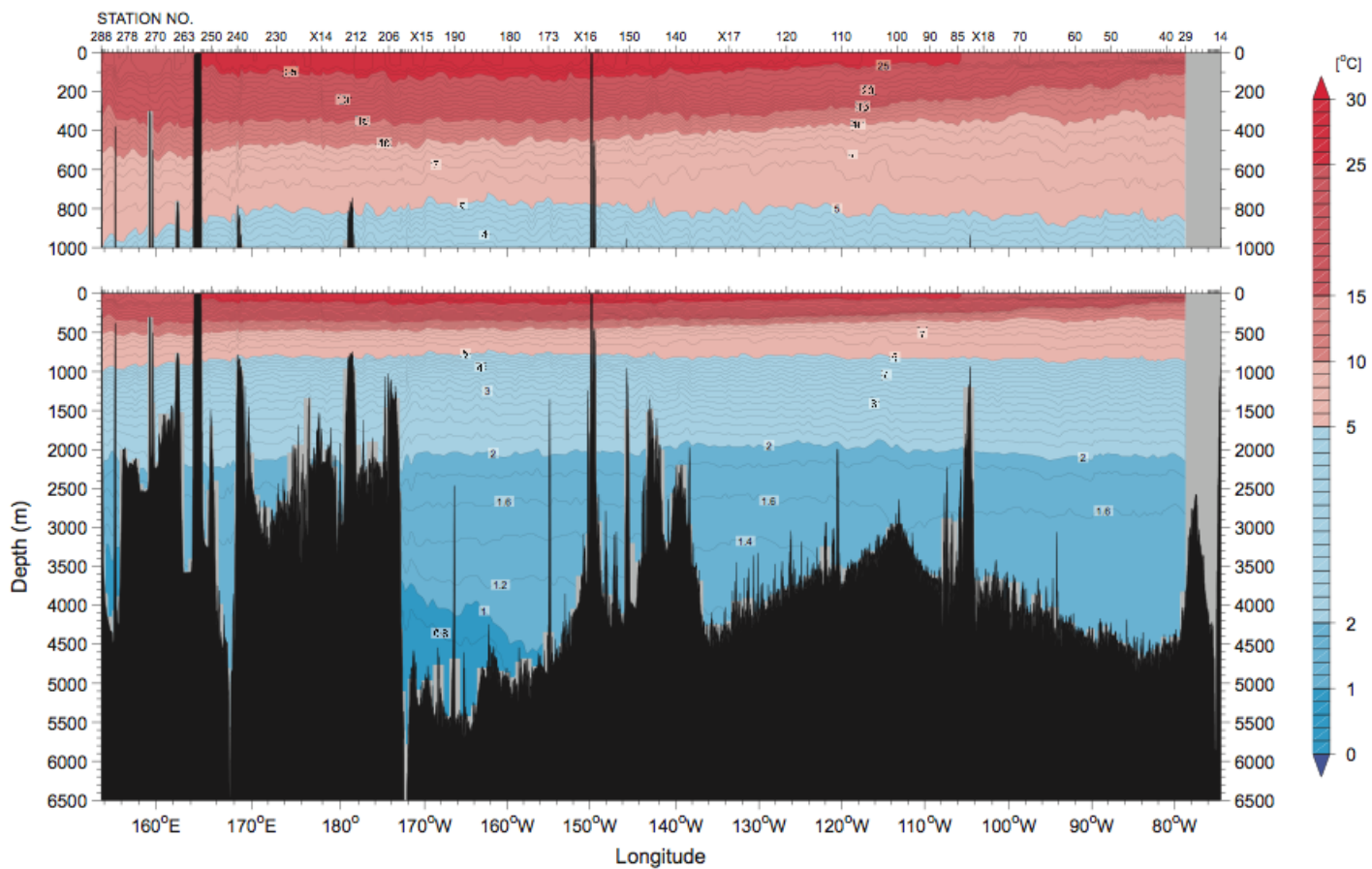


Figure 8: Potential temperature ($^{\circ}\text{C}$) cross section calculated by using CTD temperature and salinity data calibrated by bottle salinity measurements. Vertical exaggeration of the 0-6500 m section is 1000:1. Expanded section of the upper 1000 m is made with a vertical exaggeration of 2500:1.

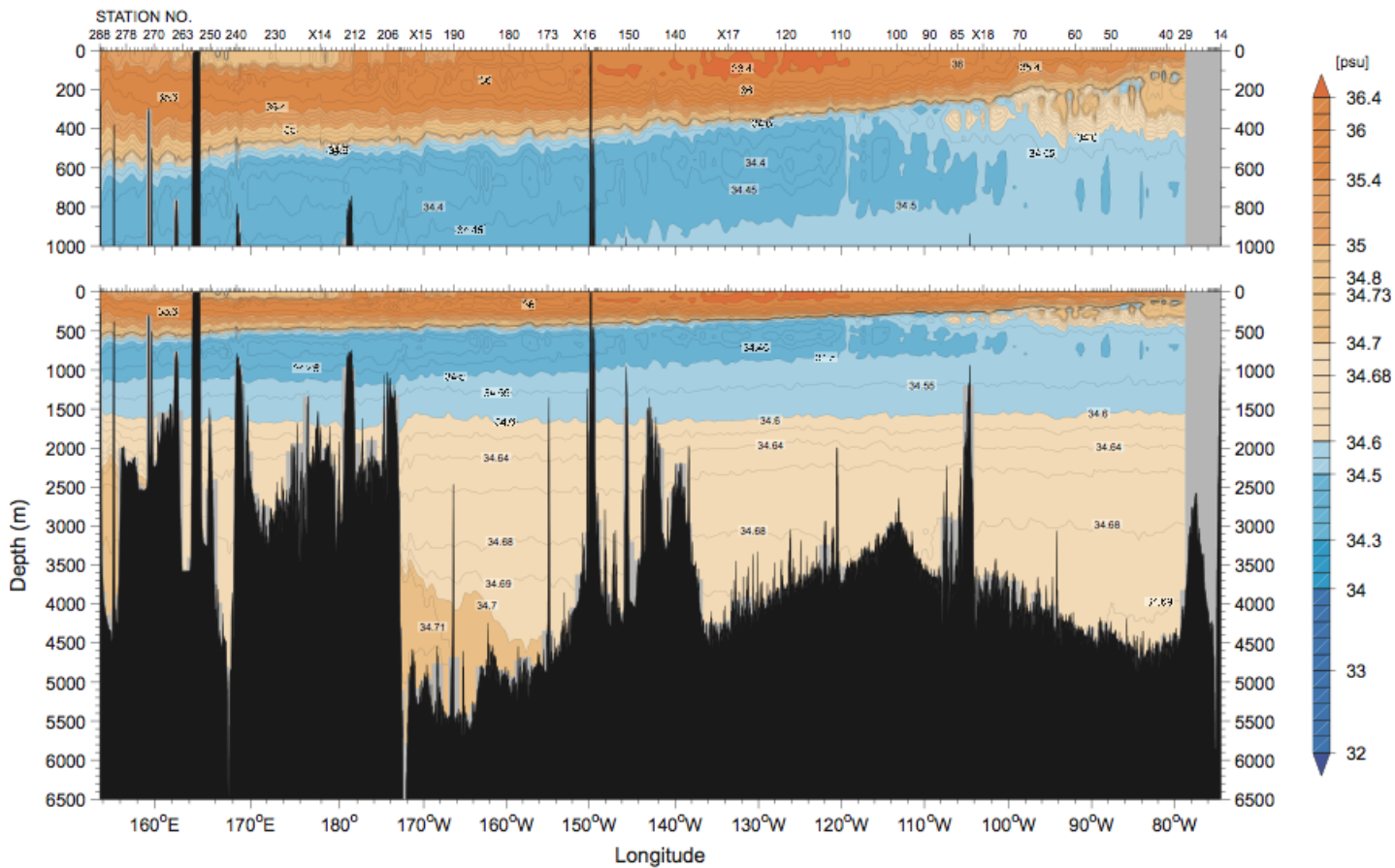


Figure 9: CTD salinity (psu) cross section calibrated by bottle salinity measurements. Vertical exaggeration is same as Figure 8.

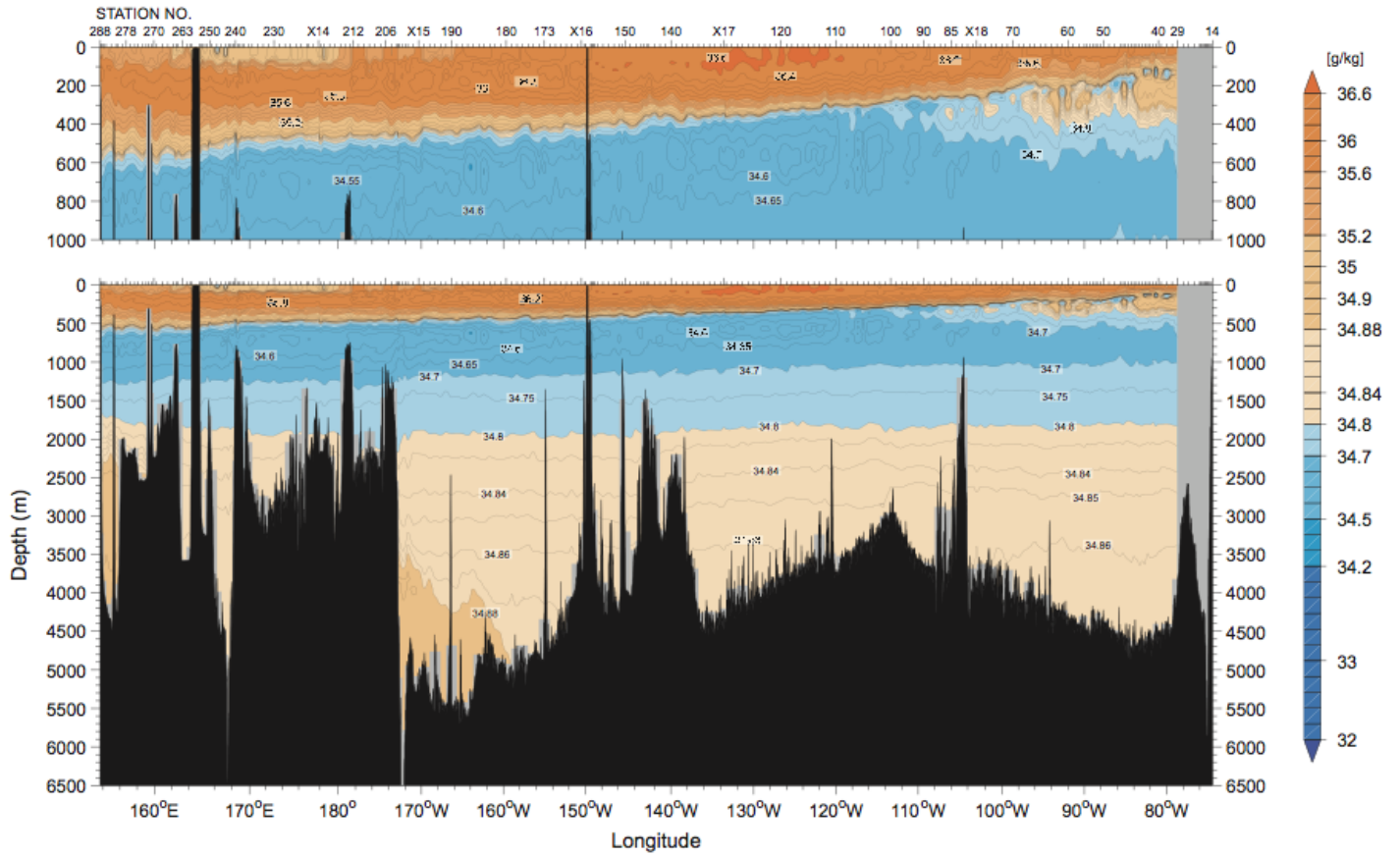


Figure 10: Absolute salinity (g/kg) cross section calculated by using CTD salinity data. Vertical exaggeration is same as [Figure 8](#).

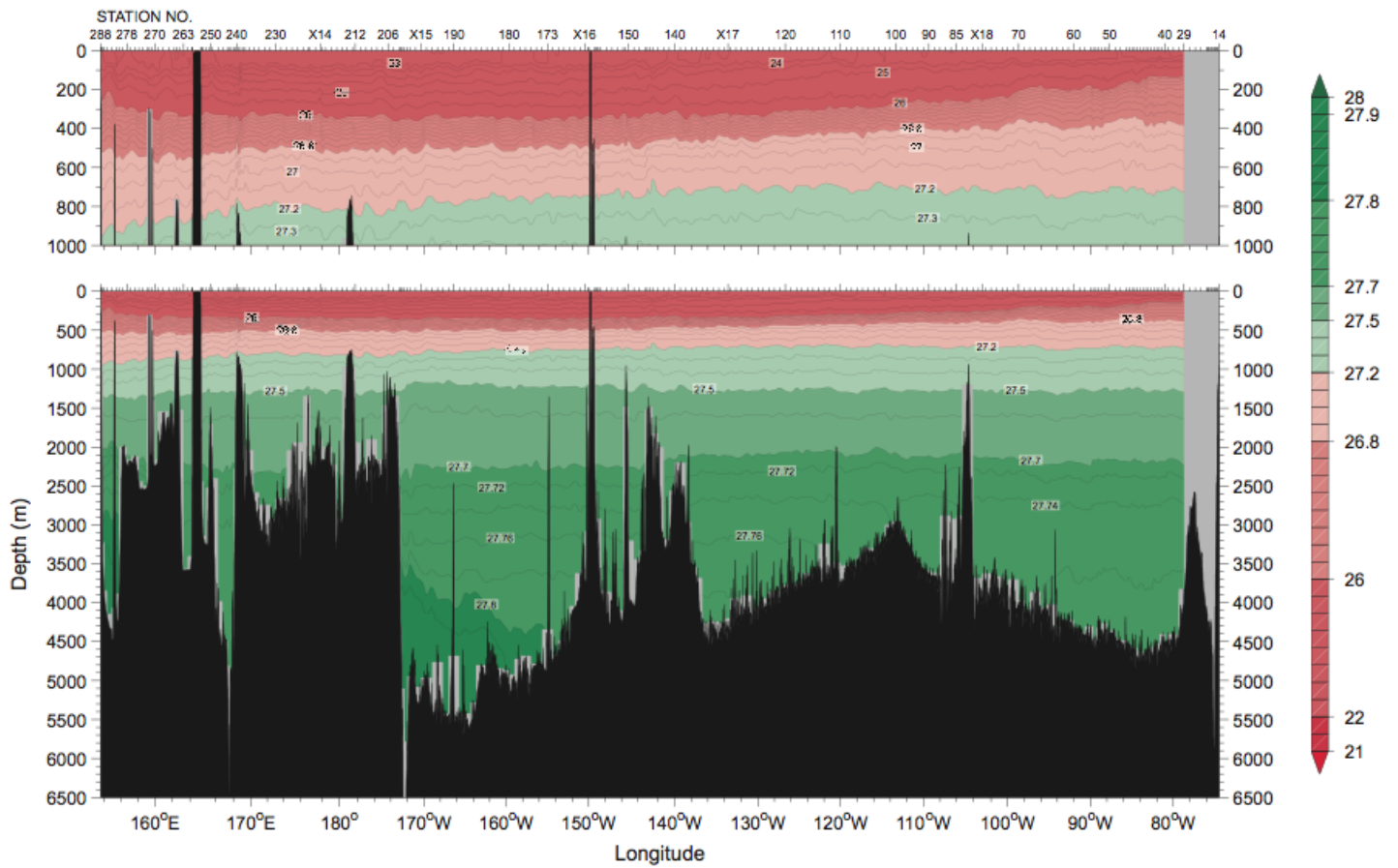


Figure 11: Density (σ_0) (kg/m^3) cross section calculated by using CTD temperature and salinity data. Vertical exaggeration is same as [Figure 8](#).

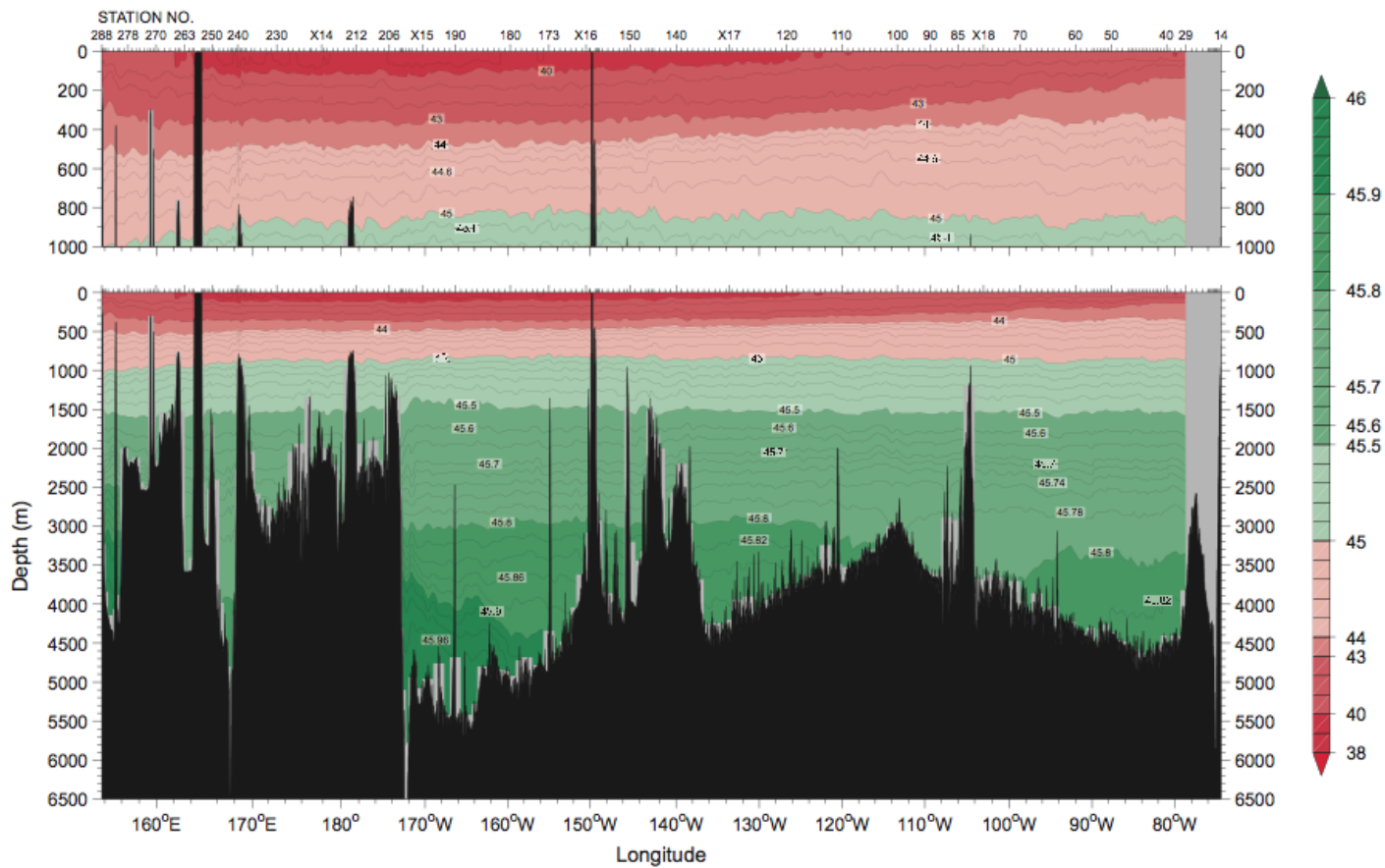


Figure 12: Same as [Figure 11](#) but for σ_4 (kg/m^3).

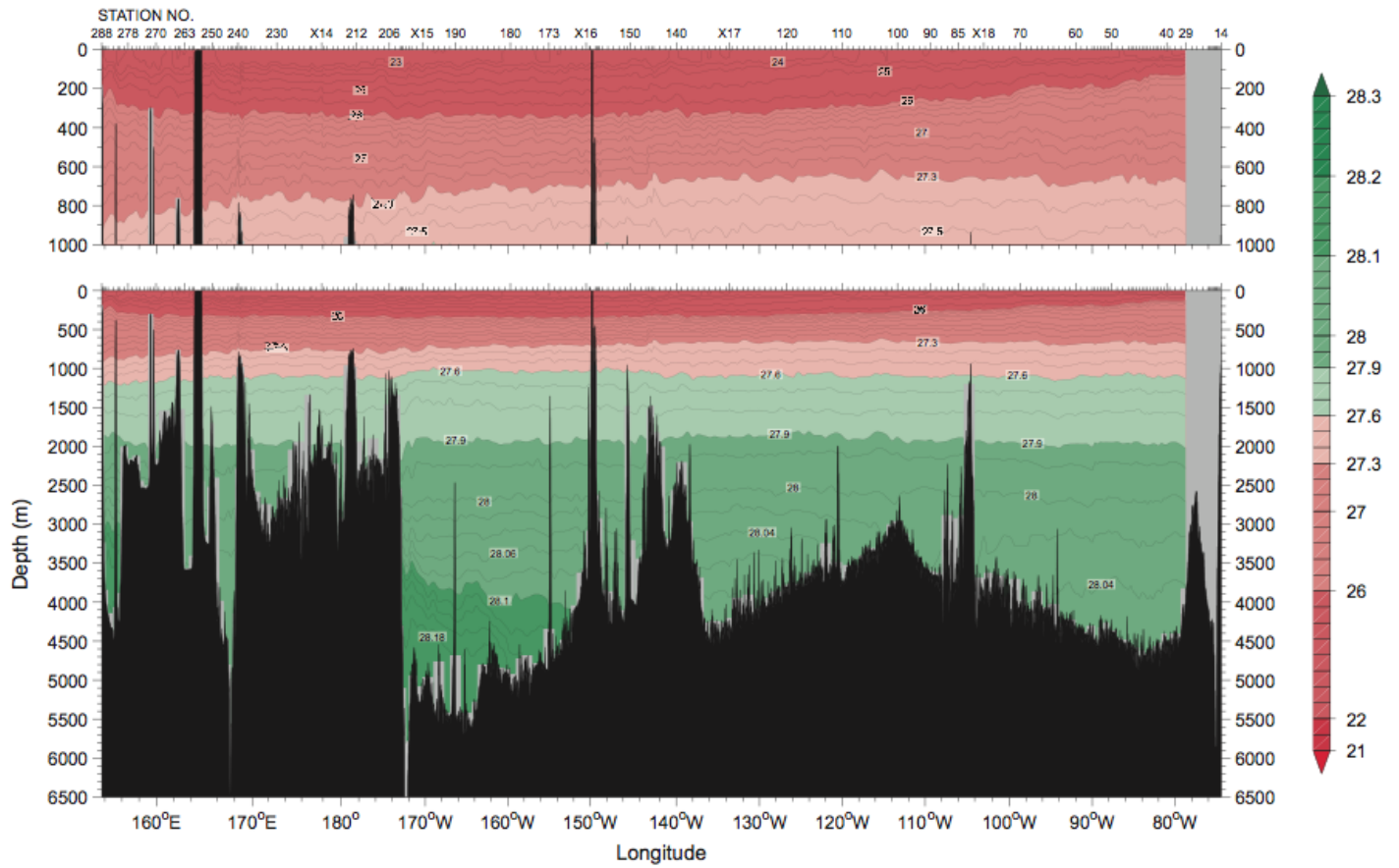


Figure 13: Neutral density γ^n (kg/m^3) cross section calculated by using CTD temperature and salinity data. Vertical exaggeration is same as [Figure 8](#).

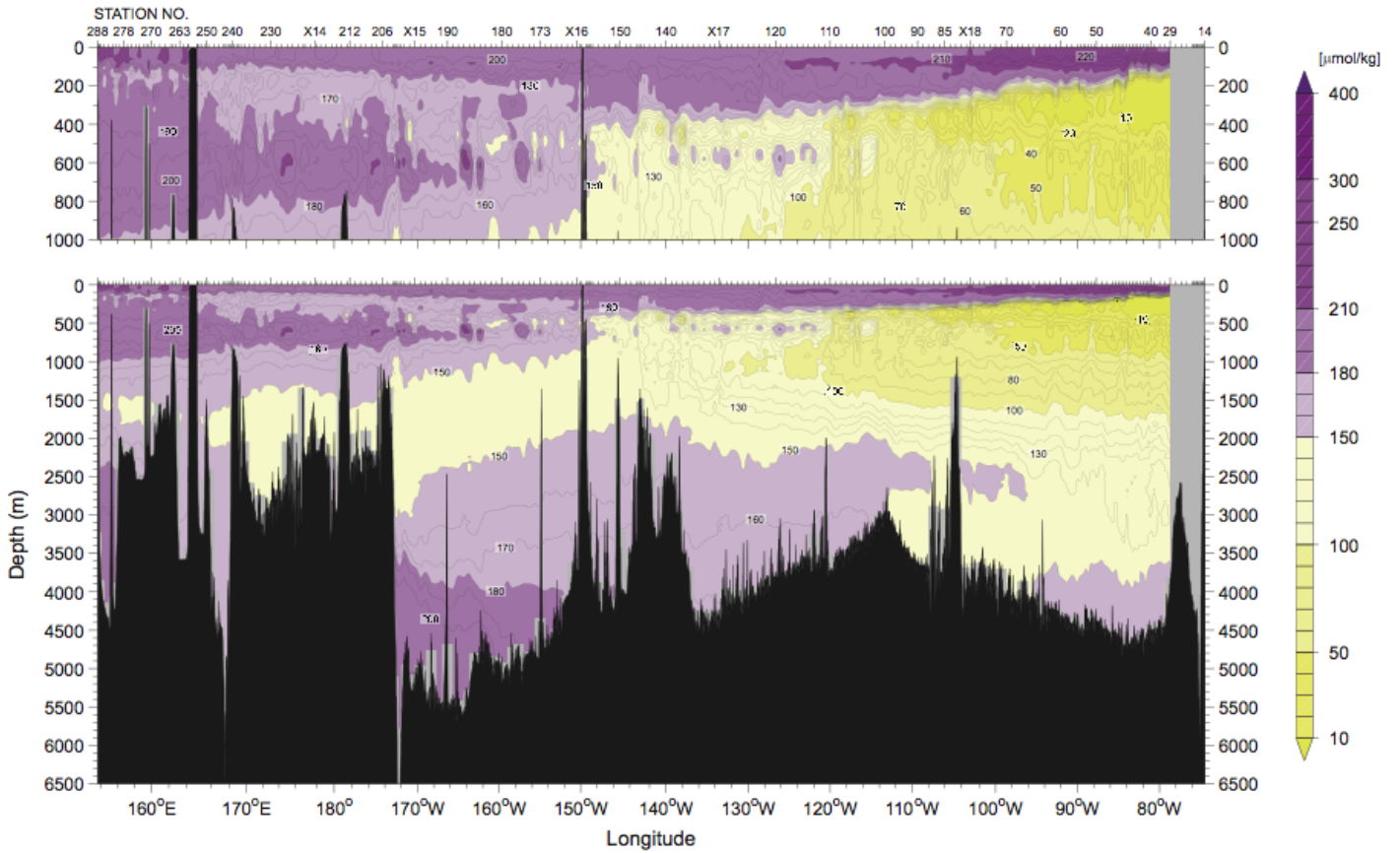


Figure 14: Cross section of CTD oxygen ($\mu\text{mol/kg}$). Vertical exaggeration is same as [Figure 8](#).

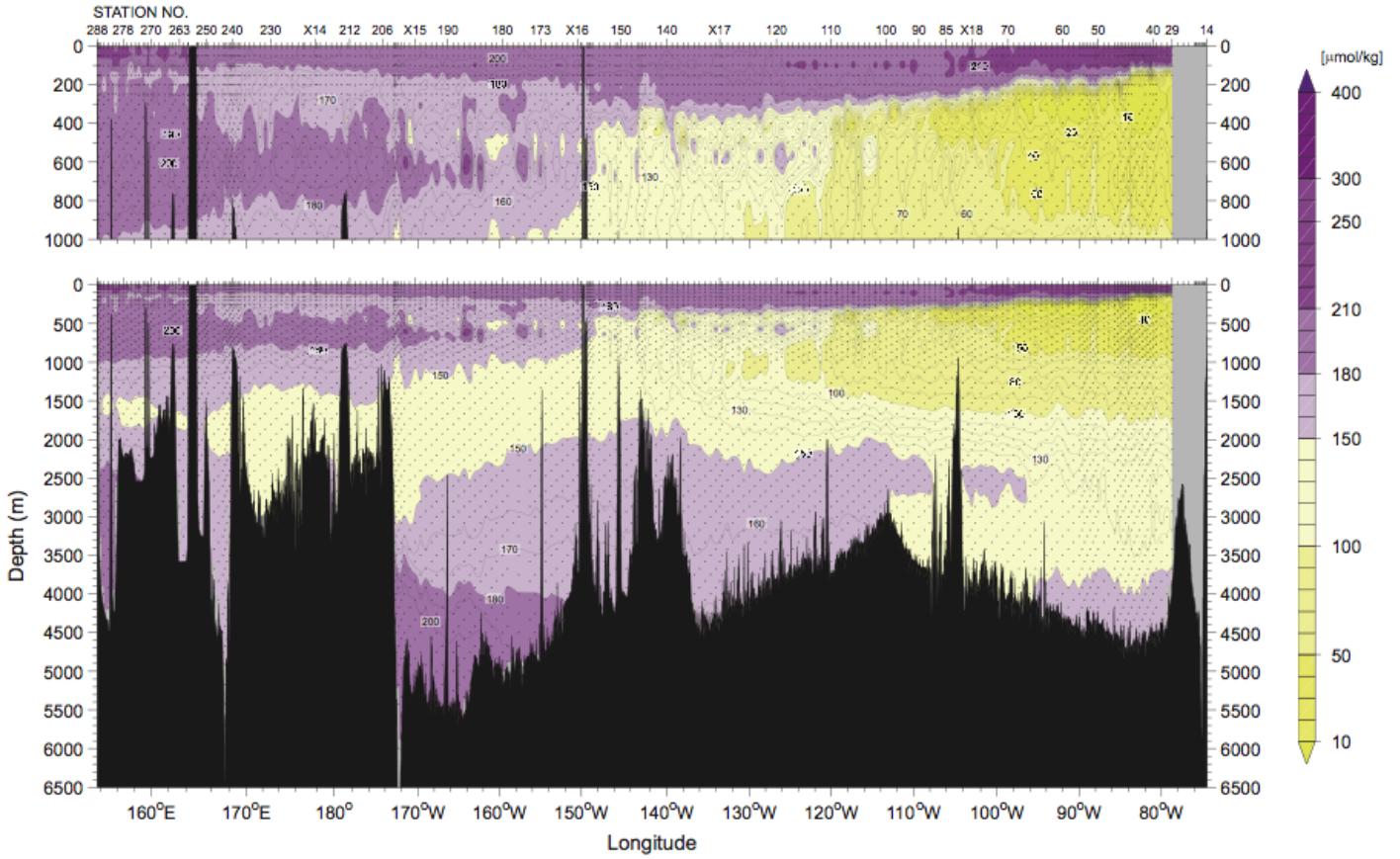


Figure 15: Cross section of bottle sampled dissolved oxygen ($\mu\text{mol/kg}$). Data with quality flags of 2 were plotted. Vertical exaggeration is same as [Figure 8](#).

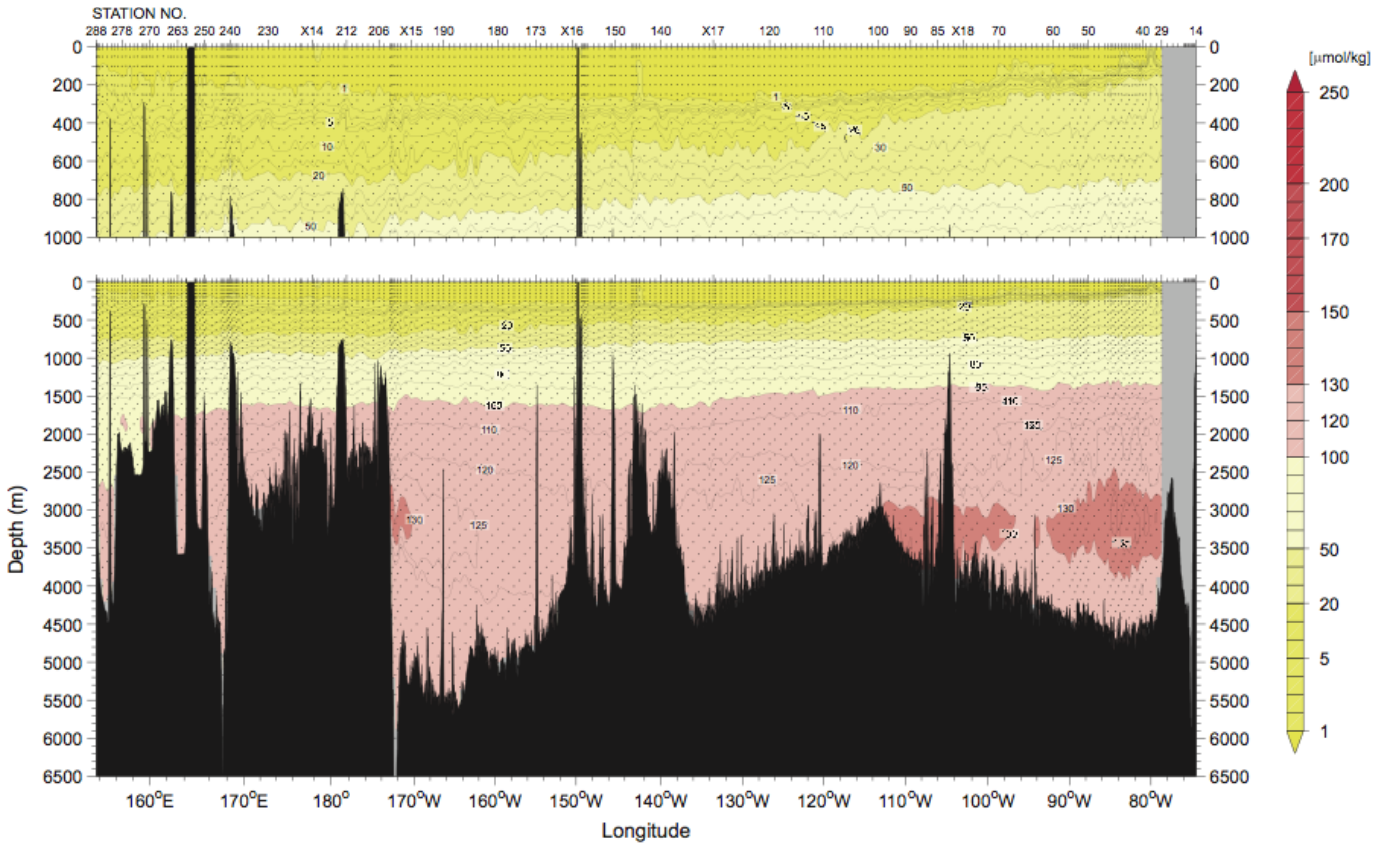


Figure 16: Silicate ($\mu\text{mol/kg}$) cross section. Data with quality flags of 2 were plotted. Vertical exaggeration is same as [Figure 8](#).

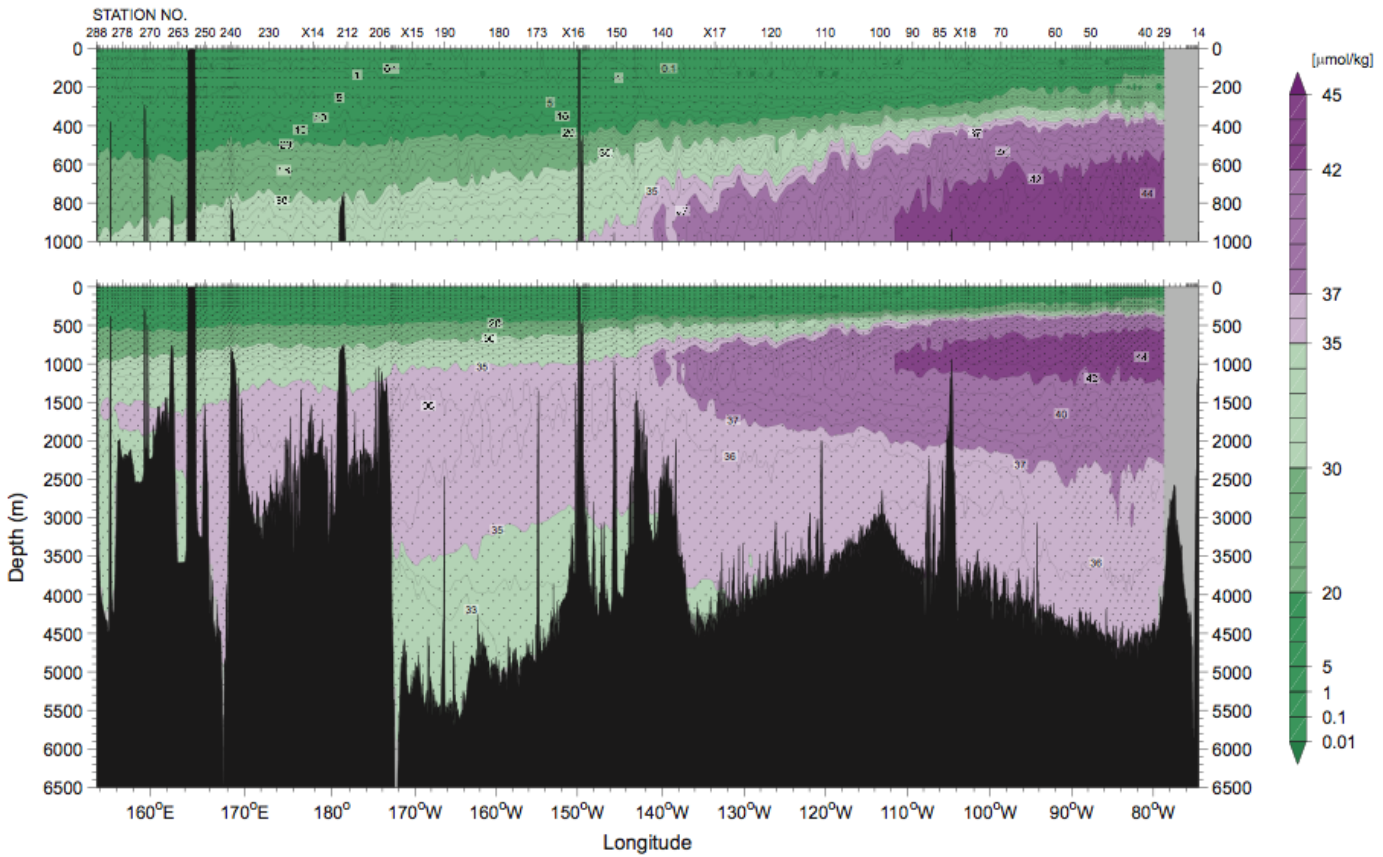


Figure 17: Nitrate ($\mu\text{mol/kg}$) cross section. Data with quality flags of 2 were plotted. Vertical exaggeration is same as [Figure 8](#).

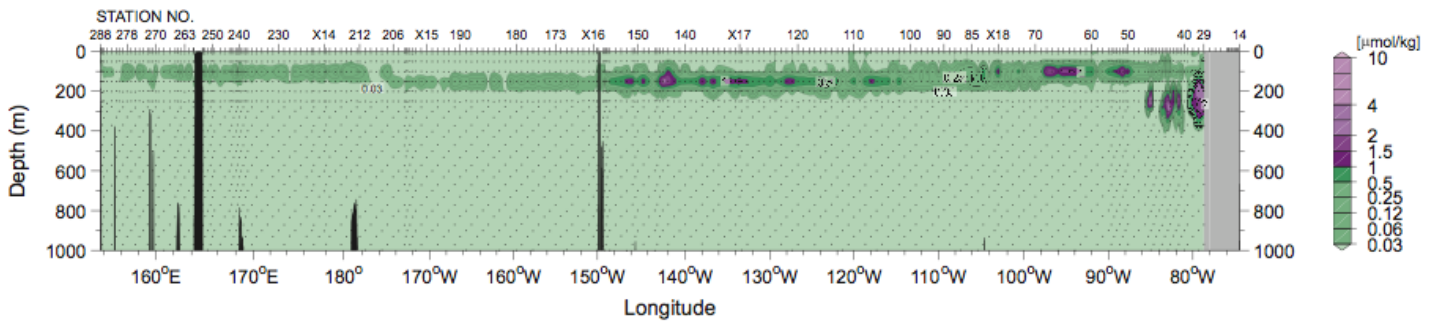


Figure 18: Nitrite ($\mu\text{mol/kg}$) cross section. Data with quality flags of 2 were plotted. Vertical exaggeration of the upper 1000 m section is same as [Figure 8](#).

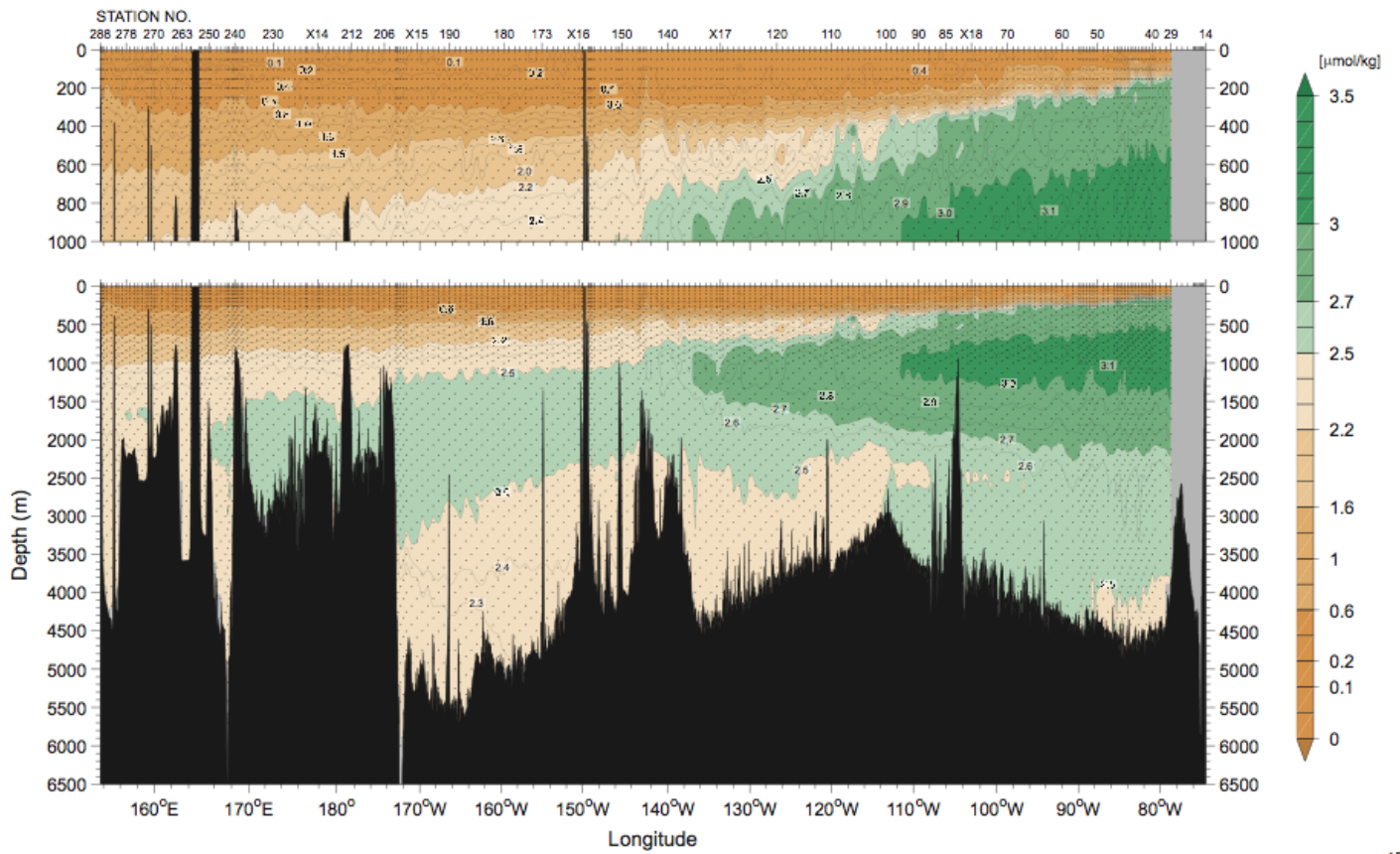


Figure 19: Phosphate ($\mu\text{mol/kg}$) cross section. Data with quality flags of 2 were plotted. Vertical exaggeration is same as [Figure 8](#).

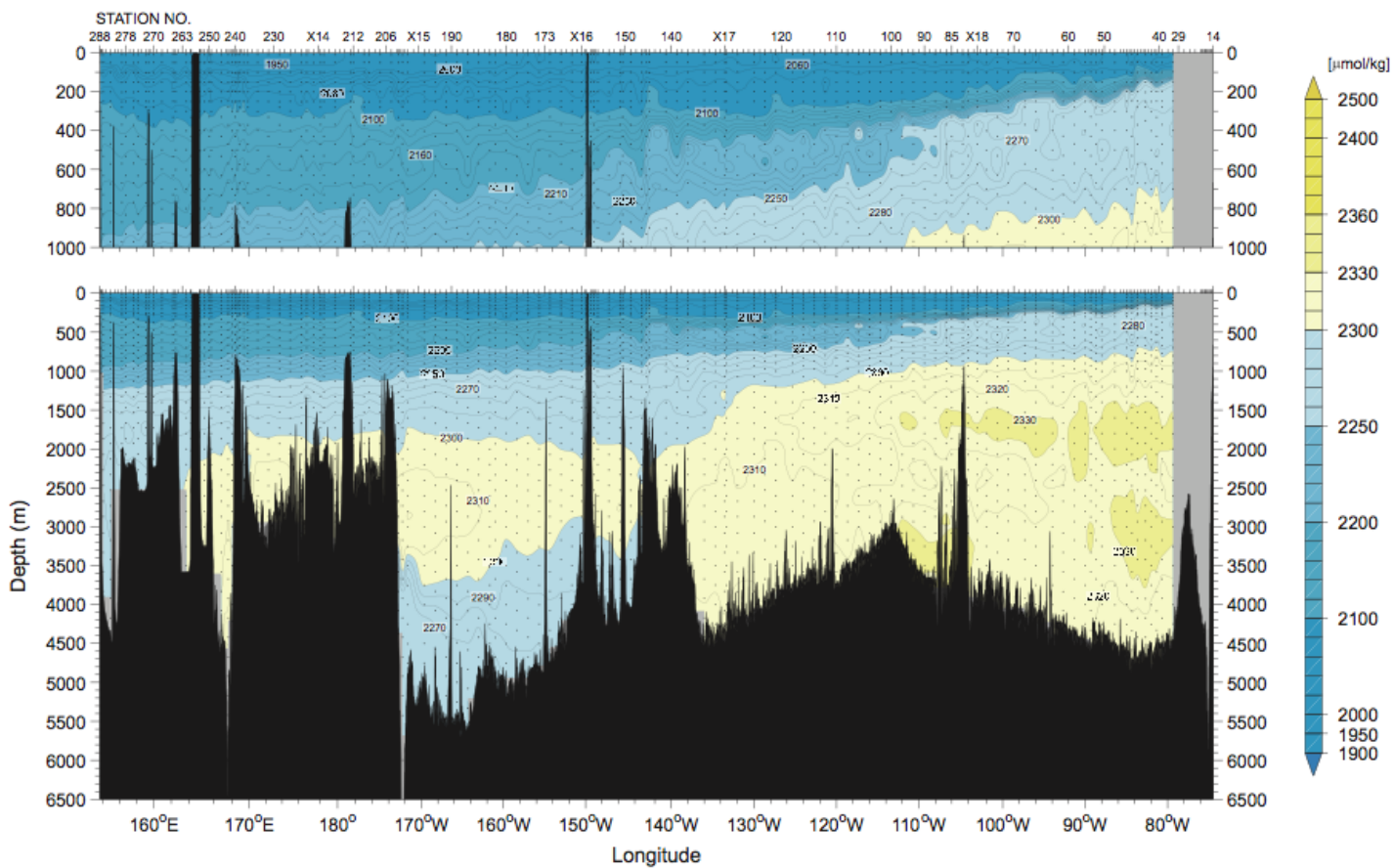


Figure 20: Dissolved inorganic carbon ($\mu\text{mol/kg}$) cross section. Data with quality flags of 2 were plotted. Vertical exaggeration is same as [Figure 8](#).

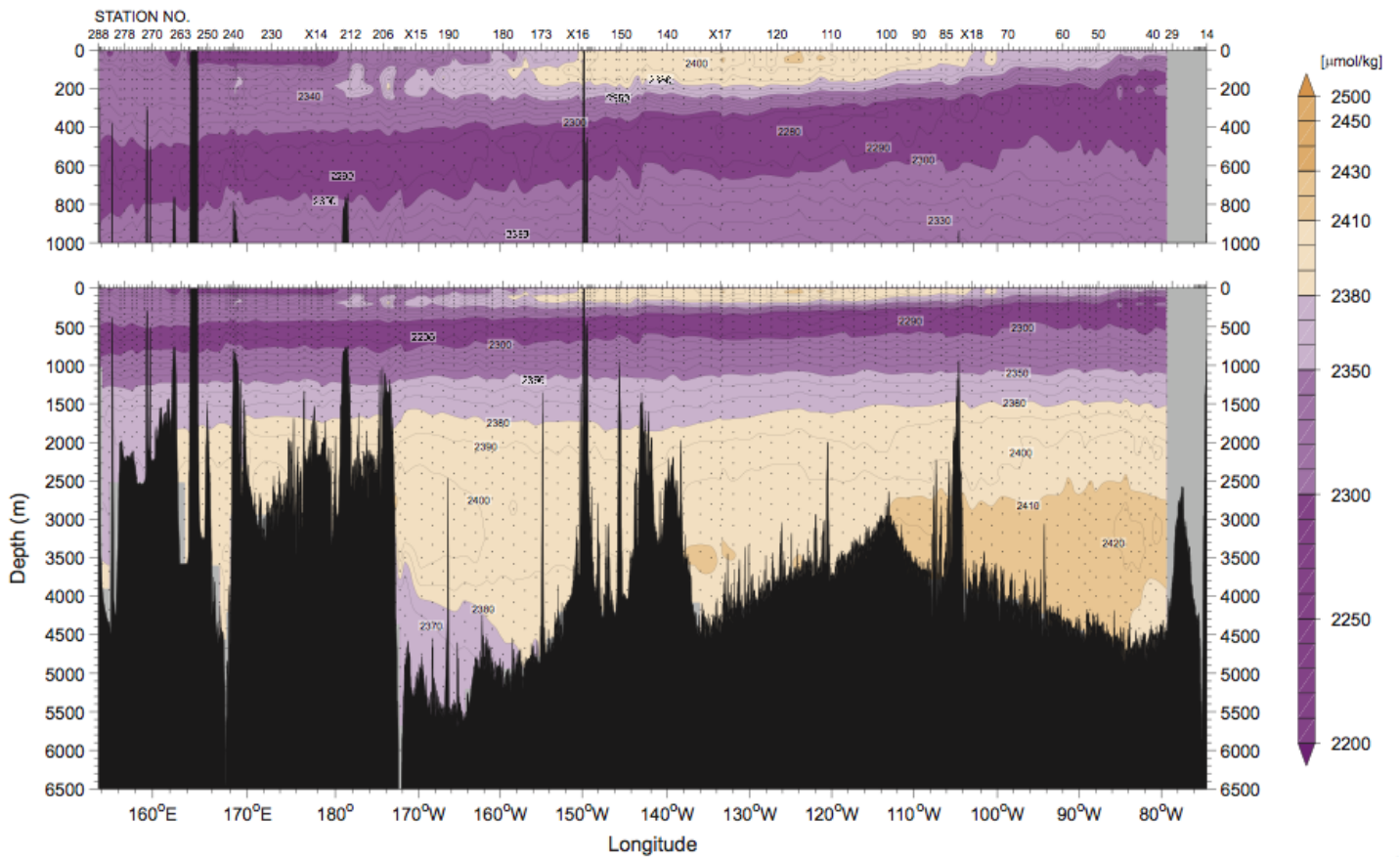


Figure 21: Total alkalinity ($\mu\text{mol/kg}$) cross section. Data with quality flags of 2 were plotted. Vertical exaggeration is same as [Figure 8](#).

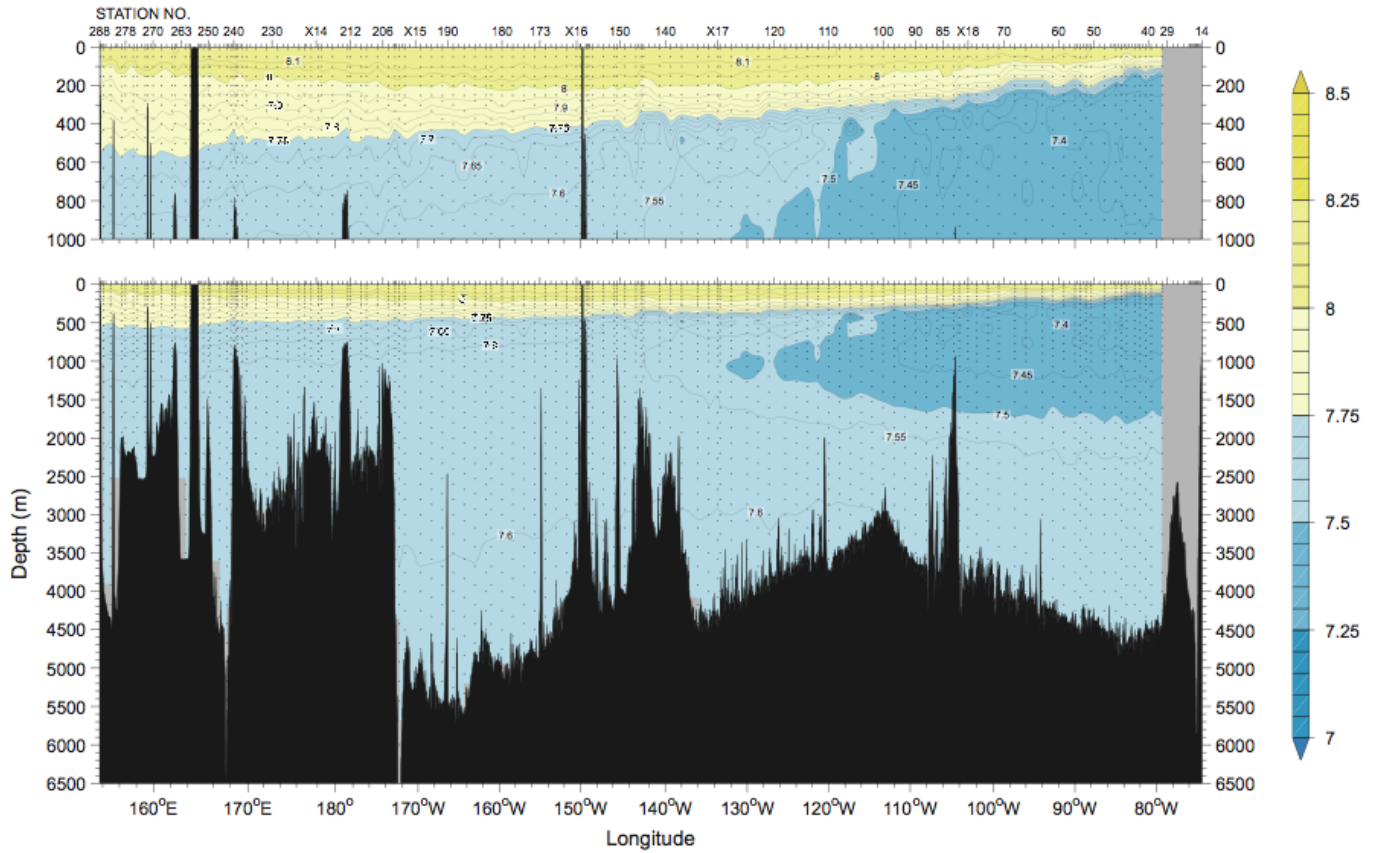


Figure 22: pH cross section. Data with quality flags of 2 were plotted. Vertical exaggeration is same as [Figure 8](#).

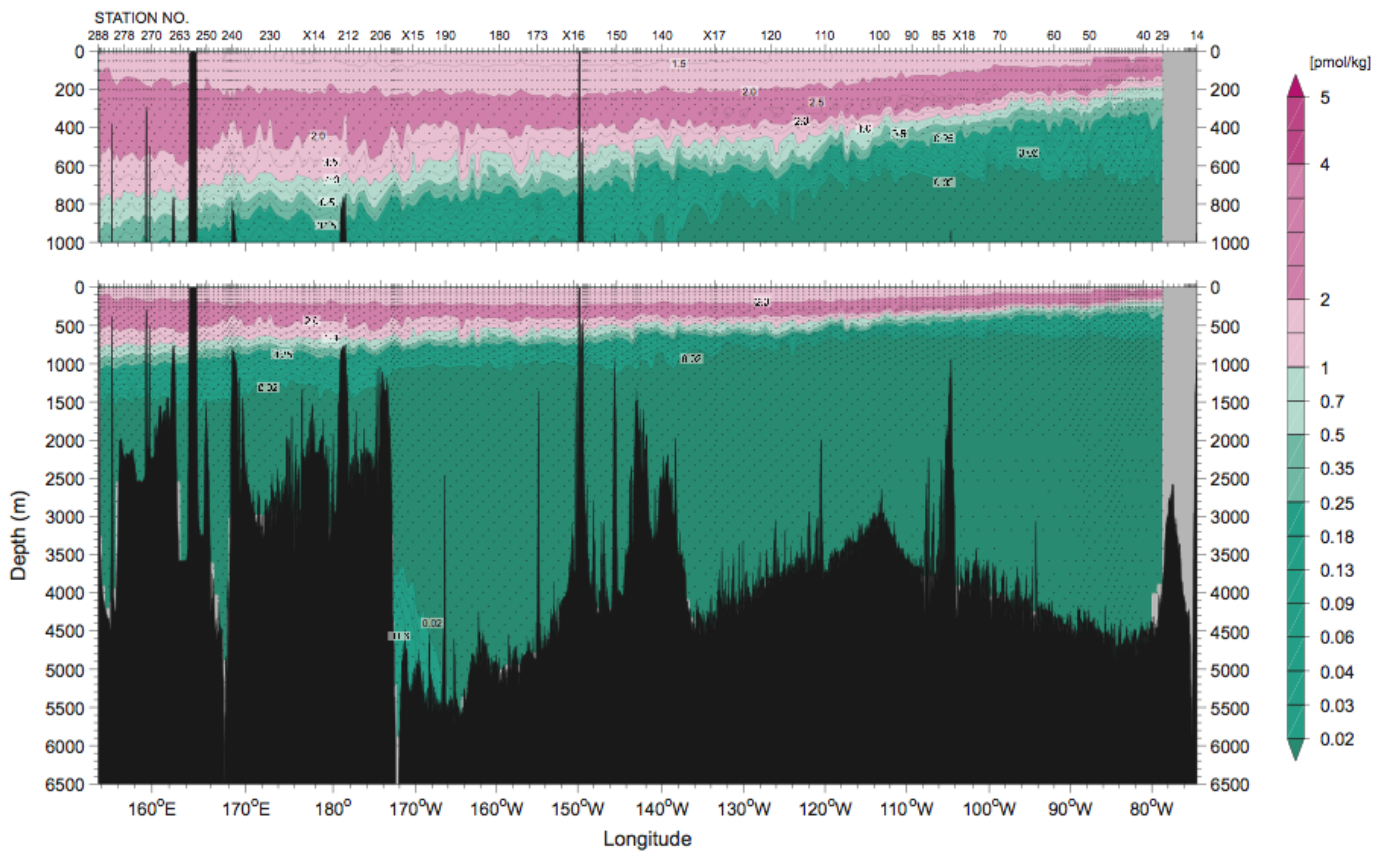


Figure 23: CFC-11 (pmol/kg) cross section. Data with quality flags of 2 were plotted. Vertical exaggeration is same as Figure 8.

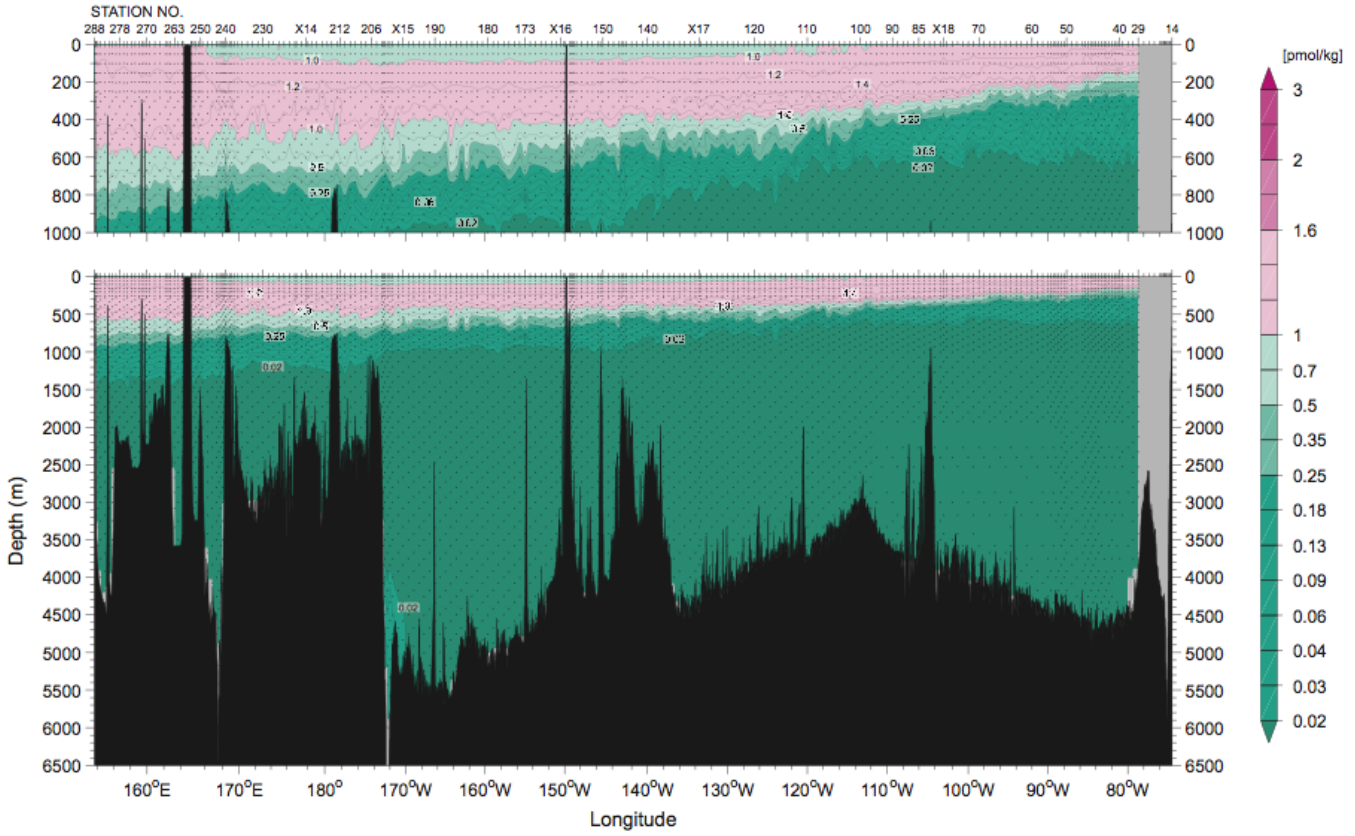


Figure 24: CFC-12 (pmol/kg) cross section. Data with quality flags of 2 were plotted. Vertical exaggeration is same as Figure 8.

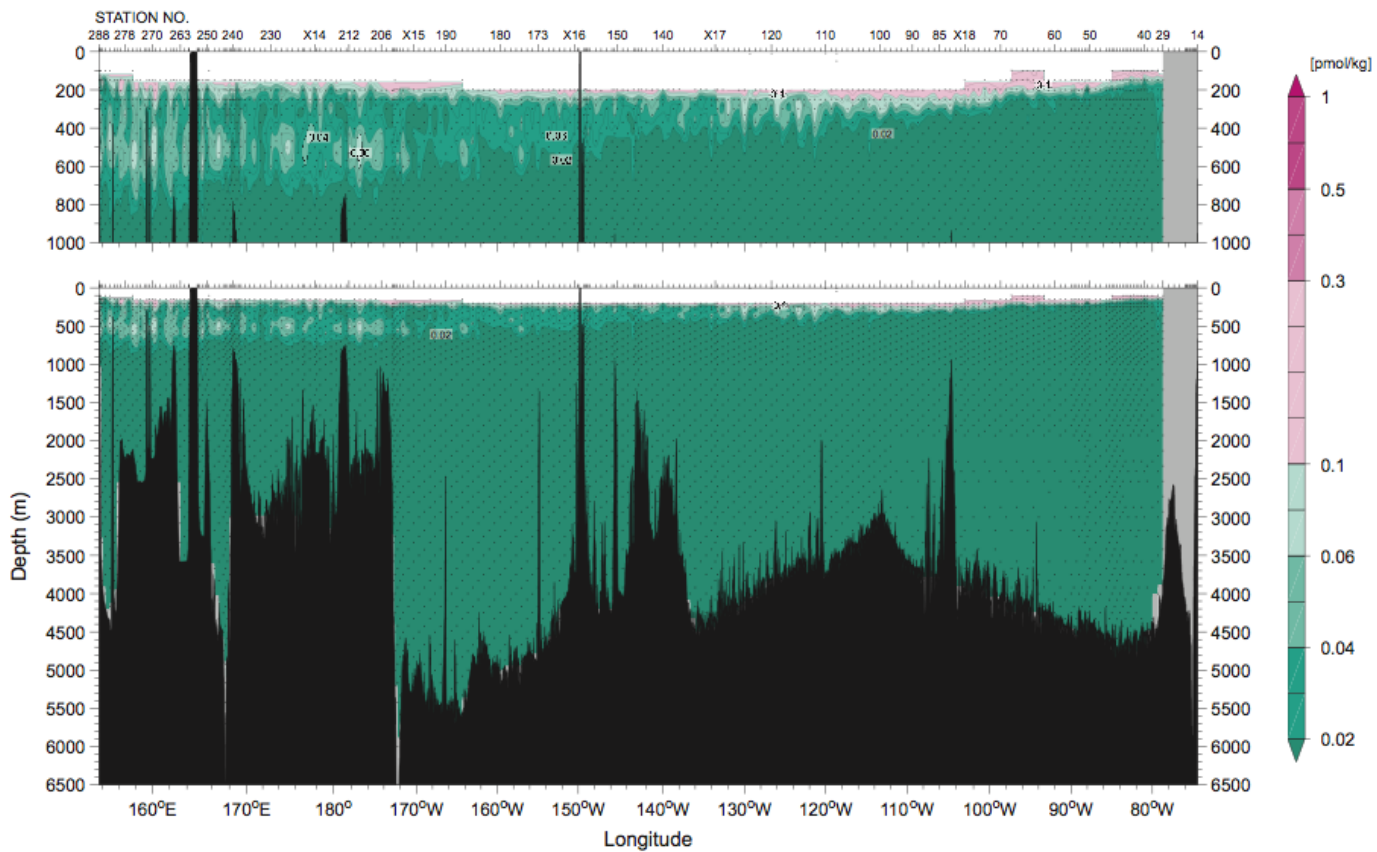


Figure 25: CFC-113 (pmol/kg) cross section. Data with quality flags of 2 were plotted. Vertical exaggeration is same as Figure 8.

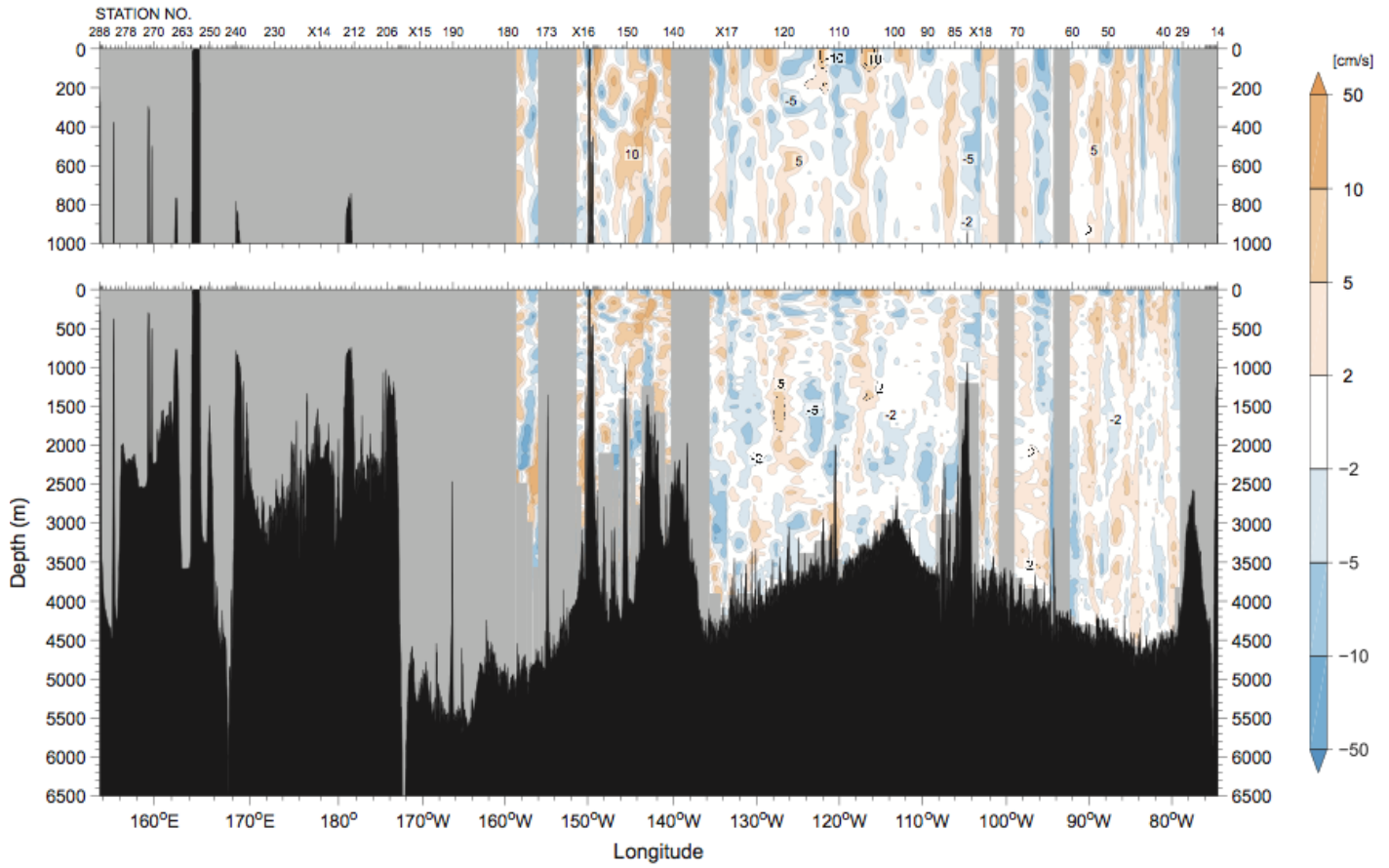


Figure 26: Cross section of current velocity (cm/s) normal to the cruise track measured by LADCP (northward is positive).

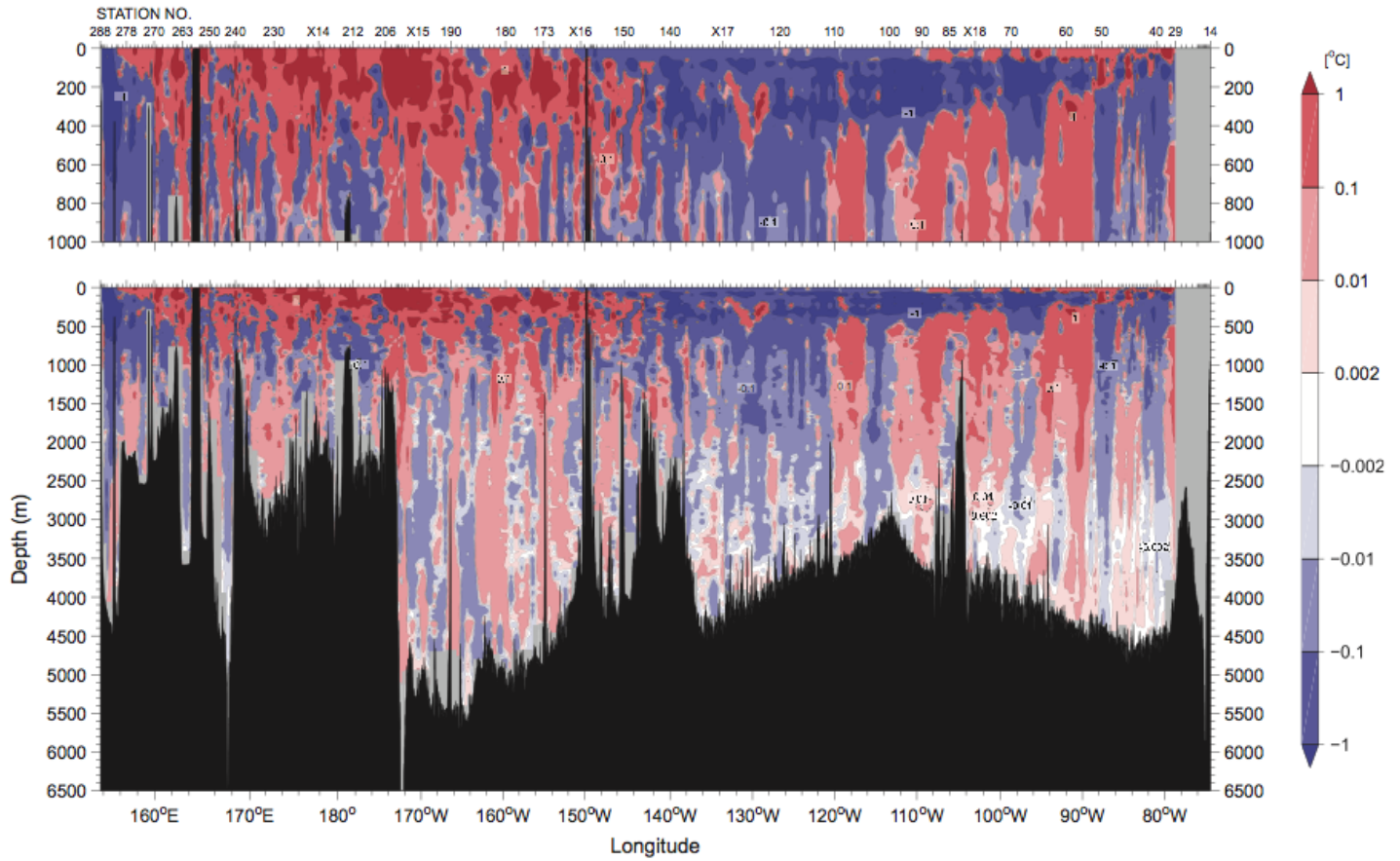


Figure 27: Difference in potential temperature ($^{\circ}\text{C}$) between results from WOCE (from March to June 1994) and the revisit cruise (from April to June 2009). Red and blue areas show areas where potential temperature increased and decreased in the revisit cruise, respectively. On white areas differences in temperature do not exceed the detection limit of 0.002°C . Vertical exaggeration is same as [Figure 8](#).

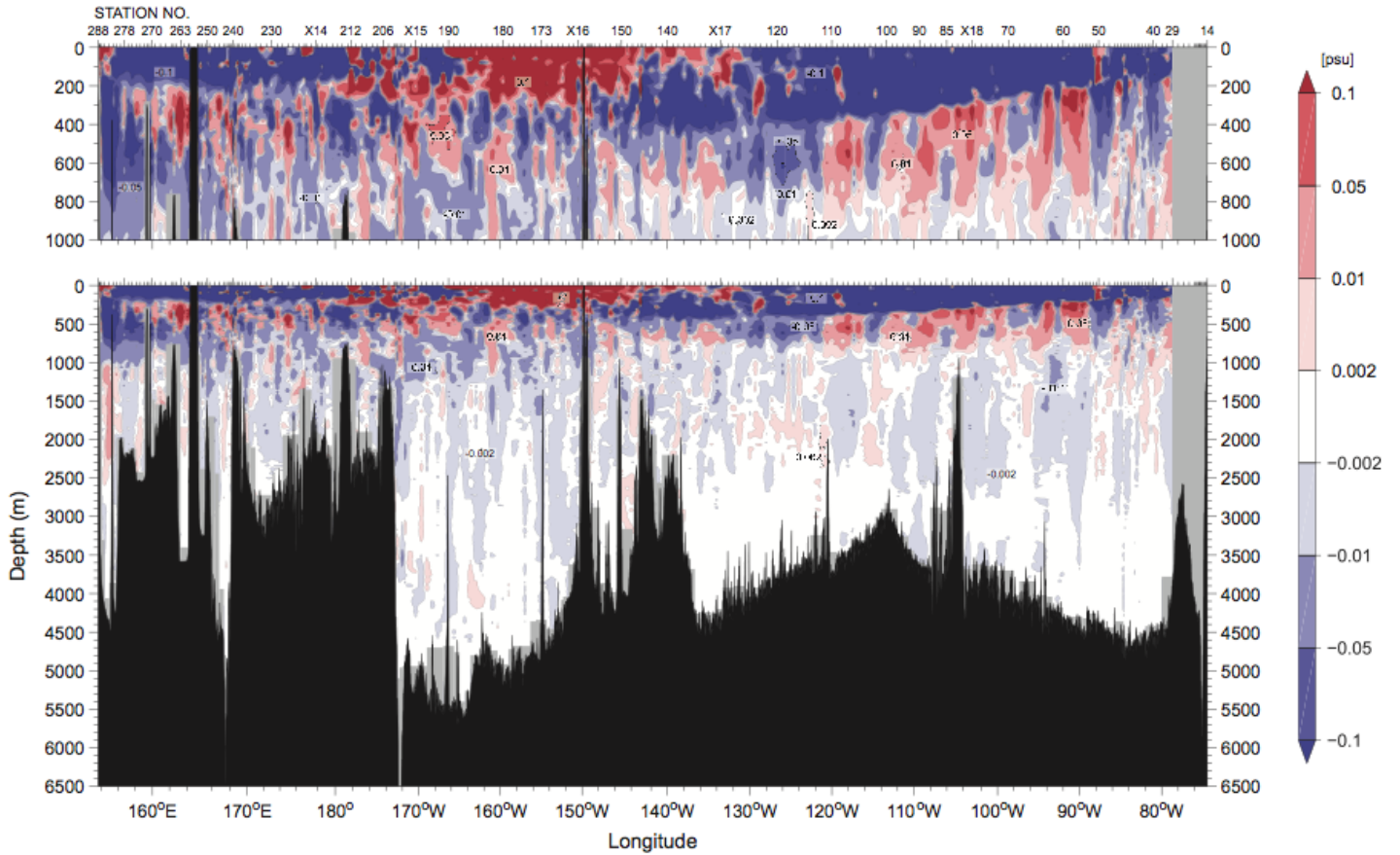
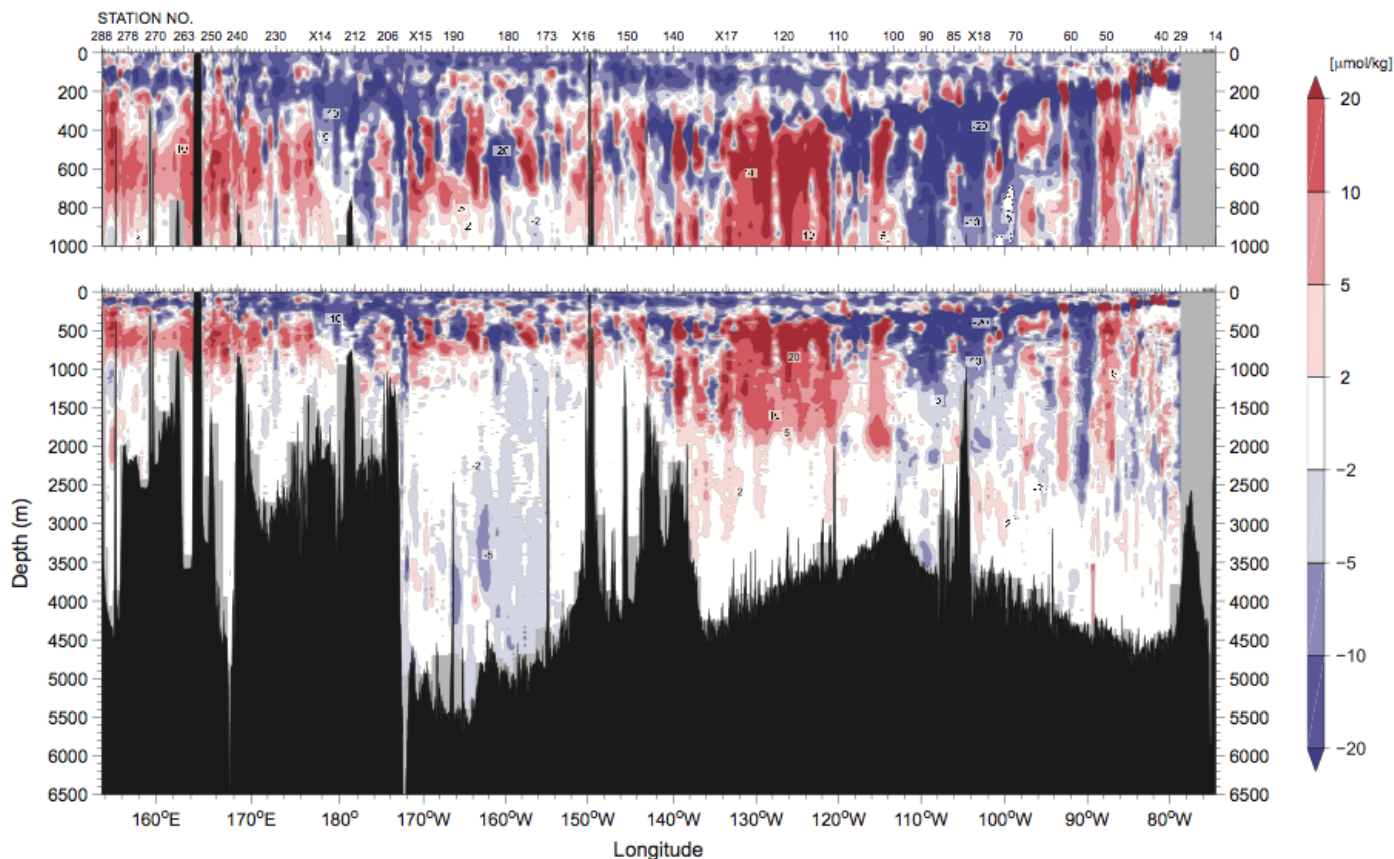


Figure 28: Difference in salinity (psu) between results from WOCE and the revisit cruise. Red and blue areas show areas where salinity increased and decreased in the revisit cruise, respectively. CTD salinity data with SSW batch correction1 were used. On white areas differences in salinity do not exceed the detection limit of 0.002 psu. Vertical exaggeration is same as Figure 8.



173

Figure 29: Difference in dissolved oxygen ($\mu\text{mol/kg}$) between results from WOCE and the revisit cruise. Red and blue areas show areas where salinity increased and decreased in the revisit cruise, respectively. CTD oxygen data were used. On white areas differences in dissolved oxygen do not exceed the detection limit of $2 \mu\text{mol/kg}$. Vertical exaggeration is same as Figure 8.

CCHDO Data Processing Notes

Event Date	Contact	Data Type	Event	Summary
2010-05-27	<i>Uchida, Hiroshi</i>	CTD/SUM	Submitted	Exchange & WOCE files Public
2010-08-12	<i>Berys, Carolina</i>	CTD/BTL/SUM	Website Update	added to "as received"
ArchiveHLY031bottledata.xls bottle file submitted by Jerry Kappa on 2010-03-24 and HLY031CTDO.zip CTD files submitted by Kelly Falkner on 2010-04-08 available under 'Preliminary/Unprocessed', unprocessed by CCHDO.				
49NZ20090410_wct_without_peru.zip CTD files in WOCE format, 49NZ20090410_ct1_without_peru.zip CTD files in Exchange format, and 49NZ20090410_sum_without_peru.txt station summary file submitted by Uchida Hiroshi on 2010-05-27, and MR09-01_leg1-3_all.pdf cruise report submitted by Jerry Kappa on 2010-08-12 available under 'Preliminary/Unprocessed', unprocessed by CCHDO.				
2010-08-12	<i>Fields, Justin</i>	Cruise Report	Website Update	added to "as received"
2011-09-19	<i>Uchida, Hiroshi</i>	BTL/Cruise Report	Submitted	Ready to go online